

LITHOSTRATIGRAPHY AND PETROGRAPHY OF UPPER SANTA FE GROUP
DEPOSITS IN THE NORTHERN ALBUQUERQUE BASIN, NEW MEXICO

by

Nathalie Nicole Brandes

Thesis

Submitted in Partial Fulfillment of the
Requirement for the Degree of

Master of Science in Geology

The New Mexico Institute of Mining and Technology
Socorro, New Mexico

July 2002

ABSTRACT

Recent geologic mapping in the northern Albuquerque Basin near Albuquerque, Rio Rancho, Zia Pueblo, and San Felipe Pueblo, New Mexico suggests that facies of the upper Santa Fe Group are locally differentiable. Integration of these maps with paleocurrent data and studies of sand and gravel petrography supports the differentiation of these facies. Previous petrographic studies in the area concentrated on sand petrography. However, this study shows that gravel petrography is key to differentiating the facies of the upper Santa Fe Group.

Stratigraphic sections were measured in Pliocene and early Pleistocene deposits and sand and gravel samples were collected at different locations in the northern Albuquerque Basin in order to understand the lithologic character of the Arroyo Ojito and Sierra Ladrones formations. Deposits of the Arroyo Ojito Formation constitute the fluvial facies of the ancestral Rio Jemez/Guadalupe, Rio Puerco, and Rio San Jose that drained sedimentary, crystalline, and volcanic rocks exposed along the western and northwestern margins of the basin. Deposits of the Sierra Ladrones Formation are divided into axial fluvial (ancestral Rio Grande) deposits and piedmont deposits derived from basin margin uplifts. The ancestral Rio Grande drained areas dominated by crystalline and volcanic rocks. Piedmont streams drained crystalline and sedimentary rocks.

Arroyo Ojito Formation gravels are typically moderately to poorly sorted, occur in horizontally stratified, laterally discontinuous beds and are primarily composed of volcanic tuff and fine-grained red granite with subordinate Pedernal chert, sandstone, and basalt. Ancestral Rio Grande gravels are generally moderately to well sorted, occur in thin, planar to cross-stratified beds, and are composed of rounded to well rounded metaquartzites and diverse igneous clasts. Granite and sedimentary clasts are relatively sparse. Piedmont gravels contain abundant sedimentary clasts, especially limestone, and coarse-grained pink porphyritic granite deposited in horizontally stratified, clast and matrix supported beds.

Sand composition of all lithofacies ranges from subarkose and arkose to feldspathic litharenite. Arroyo Ojito Formation sands are subarkose to lithic arkose and occur in planar stratified to low angle cross stratified beds. Arroyo Ojito Formation sands contain more chert and granite grains than the ancestral Rio Grande deposits. Ancestral Rio Grande sands were deposited in planar stratified to trough cross stratified beds and contain abundant volcanic grains. Volcanic grains are rare to nonexistent in piedmont sands in the study area. Piedmont sands were deposited in planar stratified to low angle and trough cross stratified beds. Paleocurrents for the ancestral Rio Grande deposits are dominantly to the south. Paleoflow in the Arroyo Ojito Formation was south-southeast, whereas piedmont paleoflow was generally to the west.

The results of this study show that the three lithofacies assemblages in the northern Albuquerque basin can be confidently differentiated by integrating studies of stratigraphy, gravel and sand petrography, and paleocurrents.

ACKNOWLEDGEMENTS

This study was supported in part by a Research Assistantship at the New Mexico Bureau of Geology and Mineral Resources under the direction of Sean Connell. Additional support was provided through a research grant awarded by the New Mexico Geological Society. I thank the Pueblo of Zia and Mr. Peter Pino for facilitating access to Zia tribal lands. I also thank the Pueblo of San Felipe and Mr. Michael Romero for facilitating access to San Felipe tribal lands. Sean Connell, Dave Love, and Dan Koning kindly shared their unpublished stratigraphic sections and geologic mapping. I also thank Bill McIntosh, Lisa Peters, and Nelia Dunbar for sharing their unpublished dates and geochemical correlations on tephra and lava flows. Glen Jones prepared the shaded relief map (Fig. 4). Sean Connell kindly provided paleocurrent vector data measured from geologic maps and many digital graphics files of figures used in this study. Virgil Lueth greatly helped with the identification of many clasts.

My gratitude is also extended to the members of my committee, Sean Connell, Peter Mozley, and David Johnson for their excellent advice and guidance through the course of this project.

My thanks must also go to my husband, Paul Brandes, for enduring many hot desert days helping me measure stratigraphic sections, and offering the moral support I needed while writing this thesis. I owe a great debt of gratitude to my parents, Ronald and Renate

Derrick, who have supported me in every way to pursue my dreams and my career in geology. Lastly, I must thank my friends, Lisa Majkowski, Doug Taylor, Amy and James Mathis, Theresa Boracci, and Tony Perrault. They were always there to listen to my ideas, complaints, and frustrations, and always offered the support I needed to complete this project.

TABLE OF CONTENTS

| | Page |
|---|------|
| Abstract..... | ii |
| Acknowledgements..... | iv |
| Table of Contents..... | vi |
| List of Tables..... | xi |
| List of Figures..... | xii |
| | |
| Introduction..... | 1 |
| Purpose..... | 1 |
| Approach..... | 2 |
| Geologic Setting and Previous Work..... | 3 |
| Stratigraphic Nomenclature..... | 16 |
| Introduction..... | 16 |
| Pre-Santa Fe Group..... | 16 |
| Santa Fe Group..... | 22 |
| Lower Santa Fe Group..... | 25 |
| Tanos and Blackshare Formations..... | 25 |
| Abiquiu Formation..... | 25 |
| Zia Formation..... | 26 |

| | |
|---|----|
| Upper Santa Fe Group..... | 28 |
| Sierra Ladrones Formation..... | 30 |
| Arroyo Ojito Formation..... | 31 |
| Methods..... | 34 |
| Location and Accessibility..... | 34 |
| Field Observations..... | 35 |
| Petrography and Texture..... | 37 |
| Lithofacies and Lithofacies Assemblages..... | 41 |
| Measured Stratigraphic Sections..... | 44 |
| Introduction..... | 44 |
| Arroyo Ojito Formation (Western Margin Lithofacies Assemblage)..... | 48 |
| General Character..... | 48 |
| Measured Sections..... | 52 |
| Sierra Ladrones Formation..... | 62 |
| Ancestral Rio Grande Lithofacies Assemblage..... | 62 |
| Eastern Margin Piedmont Lithofacies Assemblage..... | 69 |
| Summary..... | 74 |
| Petrography..... | 76 |
| Introduction..... | 76 |
| Gravel Composition..... | 76 |
| Introduction..... | 76 |
| Western Margin Lithofacies Assemblage..... | 88 |
| Ancestral Rio Grande Lithofacies Assemblage..... | 90 |

| | |
|--|-----|
| Eastern Margin Piedmont Lithofacies Assemblage..... | 91 |
| Lithofacies Assemblages and Gravel Composition..... | 92 |
| Sand Composition..... | 96 |
| Lithofacies Assemblages and Sand Composition..... | 109 |
| Western Margin Lithofacies Assemblage (Arroyo Ojito Formation)..... | 109 |
| Ancestral Rio Grande Lithofacies Assemblage (Sierra Ladrones Formation) | 110 |
| Eastern Piedmont Lithofacies Assemblage (Sierra Ladrones Formation)..... | 111 |
| Comparison to Previous Studies..... | 112 |
| Surface Samples..... | 112 |
| Subsurface Samples (Drillhole Cuttings)..... | 112 |
| Summary..... | 117 |
| Discussion..... | 119 |
| Sand Data..... | 119 |
| Depositional Environments..... | 121 |
| Provenance..... | 126 |
| Gravel..... | 126 |
| Sand..... | 127 |
| Drainage Evolution..... | 129 |
| Implications for Future Studies..... | 131 |
| Conclusions..... | 132 |
| References..... | 135 |

| | |
|--|-----|
| Appendix A: Stratigraphic sections..... | 148 |
| A1: Marillo measured section..... | 149 |
| A2: Zia measured section..... | 152 |
| A3: San Felipe Pueblo measured section..... | 159 |
| A4: Tonque Arroyo measured section..... | 162 |
| A5: San Felipe Gravel Quarry measured section..... | 164 |
| A6: Arroyo San Francisco measured section..... | 167 |
| A7: Red Cliffs measured section..... | 169 |
| A8: Loma Colorado de Abajo measured section..... | 171 |
| A9: Cat Mesa measured section..... | 173 |
| A10: Isleta Upper Powerline measured section..... | 176 |
| A11: Hell Canyon Wash measured section..... | 178 |
| Appendix B: Gravel Data..... | 182 |
| B1: Detrital modes of gravel from the Arroyo Ojito Formation..... | 182 |
| B2: Detrital modes of gravel ancestral Rio Grande..... | 184 |
| B3: Detrital modes of gravel eastern piedmont..... | 186 |
| B4: Percent normalized detrital parameters of gravel, Arroyo Ojito Formation..... | 187 |
| B5: Percent normalized detrital parameters of gravel, ancestral Rio Grande..... | 189 |

| | |
|--|-----|
| B6: Percent normalized detrital parameters of gravel, eastern piedmont..... | 191 |
| B7: Recalculated parameters of the western margin..... | 192 |
| B8: Recalculated parameters of the ancestral Rio Grande..... | 193 |
| B9: Recalculated parameters of the eastern piedmont..... | 194 |
| Appendix C: Sand Data..... | 195 |
| C1: Detrital modes of medium grained sand for the western margin lithofacies assemblage..... | 195 |
| C2: Detrital modes of medium grained sand for the ancestral Rio Grande lithofacies assemblage..... | 197 |
| C3: Detrital modes of medium grained sand for the eastern piedmont lithofacies assemblage..... | 198 |
| C4: Percent normalized parameters for the western margin, ancestral Rio Rio Grande, and eastern piedmont lithofacies assemblages..... | 199 |
| C5: Recalculated parameters for the western margin lithofacies assemblage..... | 202 |
| C6: Recalculated parameters for the ancestral Rio Grande lithofacies Assemblage..... | 203 |
| C7: Recalculated parameters for the eastern piedmont lithofacies assemblage.. | 204 |
| Appendix D: Gravel and Sand Sample Locations..... | 205 |
| Appendix E: Paleocurrent Data..... | 206 |
| E1: Paleocurrents azimuths measured in this study..... | 206 |
| E2: Paleocurrent azimuths measured from geologic maps..... | 207 |
| E3: Summary of paleocurrent statistics..... | 208 |

LIST OF TABLES

| | page |
|--|------|
| Table 1: Detrital components of medium-grained sand and sandstone..... | 38 |
| Table 2: Detrital components of pebble and cobble gravel..... | 40 |
| Table 3: Summary of lithofacies..... | 42 |
| Table 4: Summary of major characteristics of the western-margin lithofacies assemblage..... | 45 |
| Table 5: Summary of major characteristics of the ancestral Rio Grande lithofacies assemblage..... | 46 |
| Table 6: Summary of major characteristics of the piedmont lithofacies assemblage..... | 47 |
| Table 7: Recalculated detrital parameters for gravel..... | 78 |
| Table 8: Mean and standard deviation of pebble and cobble composition..... | 78 |
| Table 9: Recalculated detrital parameters for medium-grained sand..... | 105 |
| Table 10: Mean and standard deviation for medium-grained sand..... | 105 |

LIST OF FIGURES

| | page |
|---|------|
| Figure 1: Location of the Rio Grande rift and Albuquerque Basin..... | 4 |
| Figure 2: Schematic diagram of sedimentation in half graben basins of the Rio Grande rift..... | 6 |
| Figure 3: Schematic drawing of contributory drainage of the Albuquerque Basin..... | 9 |
| Figure 4: Sample locations within the Albuquerque Basin..... | 10 |
| Figure 5: QFL diagram of very fine to medium grained sand..... | 11 |
| Figure 6: QFL diagram illustrating the results of previous studies..... | 14 |
| Figure 7: Schematic stratigraphic column..... | 17 |
| Figure 8: QFL diagram illustrating composition of various sandstone deposits..... | 19 |
| Figure 9: Comparison of stratigraphic nomenclature used in the northern Albuquerque Basin..... | 24 |
| Figure 10: Photograph of thickly bedded white ash of unit 1 of the Marillo stratigraphic section..... | 49 |
| Figure 11: Photograph of conglomerate beds in the Ceja Member..... | 51 |
| Figure 12: Rose diagram of paleocurrents from the western fluvial lithofacies assemblage..... | 52 |
| Figure 13: Composite stratigraphic column of the Marillo-Zia stratigraphic section..... | 54 |
| Figure 14: San Felipe Pueblo stratigraphic section | 55 |
| Figure 15: Photograph of cemented and laminated sandstone of the Arroyo Ojito Formation | 58 |
| Figure 16: Photograph of vaguely bedded and mottled sandstone in the Loma Barbon Member | 59 |

| | |
|--|----|
| Figure 17: Photograph of subhorizontal and subvertical rhizoconcretions in a well cemented bed of the Loma Barbon Member of the ArroyoOjito Formation... | 60 |
| Figure 18: Photographs of thinly bedded mudstone and sandstone in the Loma Barbon Member of the Arroyo Ojito Formation..... | 61 |
| Figure 19: Photograph of clast supported, thickly bedded, pebble and cobble gravel of ancestral Rio Grande deposits in the Sierra Ladrones Formation..... | 64 |
| Figure 20: Stratigraphic fence constructed across part of the southern Santo Domingo sub-basin of the northern Albuquerque basin at San Felipe Pueblo..... | 65 |
| Figure 21: Rose diagram of paleocurrents from ancestral Rio Grande deposits in the Sierra Ladrones Formation..... | 67 |
| Figure 22: Photograph of ancestral Rio Grande sand in unit 2 of the San Felipe Pueblo Gravel Quarry section..... | 69 |
| Figure 23: Photograph of eastern margin piedmont deposits of the Sierra Ladrones Formation at the Red Cliffs stratigraphic section..... | 71 |
| Figure 24: Rose diagram of paleocurrents from the eastern margin lithofacies assemblage of the Sierra Ladrones Formation..... | 72 |
| Figure 25: Photograph of weakly cemented, trough cross-bedded pebbly sand in eastern margin piedmont deposits of the Sierra Ladrones Formation..... | 73 |
| Figure 26: Ternary diagram of quartz, feldspar, and lithic fragments of pebble and cobble gravels..... | 79 |
| Figure 27: Lithic fragment plot showing metamorphic fragments, volcanic fragments, and sedimentary fragments..... | 80 |
| Figure 28: Bivariate plot of chert and metaquartzite gravel in western, axial, and eastern piedmont lithofacies assemblages..... | 81 |
| Figure 29: Ternary diagram of chert, metaquartzite, and sedimentary gravel..... | 82 |
| Figure 30: Ternary diagram of chert, metaquartzite, and volcanic gravel..... | 83 |
| Figure 31: Ternary diagram of chert, metaquartzite, and plutonic and metamorphic gravel..... | 84 |
| Figure 32: Ternary diagram of chert, granite, and volcanic clasts..... | 85 |

| | |
|---|-----|
| Figure 33: Bivariate plot of quartz and chert versus Pedernal chert..... | 93 |
| Figure 34: Ternary diagram of volcanic, sedimentary, and plutonic-metamorphic clasts..... | 95 |
| Figure 35: Photomicrograph of a stained feldspar grain..... | 98 |
| Figure 36: Photomicrograph of a granite grain..... | 99 |
| Figure 37: Photomicrograph of volcanic grain with a potassium feldspar phenocryst and granular groundmass..... | 100 |
| Figure 38: Photomicrograph of seriate volcanic grains..... | 101 |
| Figure 39: QFL diagram of medium-grained sand..... | 102 |
| Figure 40: Ternary diagram of lithic fragments of medium grained sand..... | 104 |
| Figure 41: Photomicrograph of a chert grain..... | 106 |
| Figure 42: Ternary diagram of medium grained sand illustrating the relationship among chert, granite, and volcanic grains..... | 107 |
| Figure 43: Photomicrograph of opaque grains in eastern piedmont deposits..... | 108 |
| Figure 44: Graphical log of the Matheson Park monitoring well, illustrating sample locations..... | 114 |
| Figure 45: Graphical log of the Metropolitan Detention Center, well illustrating sample locations..... | 115 |
| Figure 46: Ternary plot of water supply and groundwater monitoring wells in the Albuquerque area..... | 116 |
| Figure 47: Ternary diagram of medium grained sand and plate tectonic settings..... | 120 |
| Figure 48: Ternary diagram of lithic fragments of medium grained sand and plate tectonic settings..... | 122 |

INTRODUCTION

Purpose

The principal purpose of this study was to document the stratigraphy and petrography and potential for compositional correlation of western-margin, axial-river and eastern-margin deposits of the upper Santa Fe Group in the northern part of the Albuquerque Basin. Another major goal of this study was to provide useful definitions of the character and variations among mapped deposits in the northern part of the Albuquerque Basin. Delineation of these lithofacies assemblages can aid in ongoing geologic mapping of the basin. The development of descriptive petrofacies for sand and sandstone can constrain sediment dispersal patterns, which can aid in the understanding of the Pliocene-Pleistocene paleogeography of the basin, as well as provide constraints on hydrostratigraphically significant deposits in the subsurface. The influence of sediment recycling associated with basin-margin faults was also examined using gravel composition. Furthermore, results of this study can be used as a base line to trace fluvial systems into the southern end of the basin, which has only been partially mapped to date, and to differentiate major lithofacies assemblages in the subsurface using cuttings from numerous drill-holes in the Albuquerque area.

Previous petrographic studies in the Albuquerque Basin focused primarily on the sand fraction of the Santa Fe Group (Lozinsky, 1988; Lozinsky, 1994; Beckner, 1996; Large and Ingersoll, 1997). This report illustrates the usefulness of integrating sand and gravel petrography within a defined stratigraphic framework.

Approach

This study used a multi-parameter approach, which integrated petrographic (gravel and sand fraction), paleocurrent, and stratigraphic data collected in the field. These data are supplemented by paleocurrent data from geologic maps available from the New Mexico Bureau of Geology and Mineral Resources (Connell et al., 1995; Cather et al., 1997; Connell, 1998; Cather and Connell, 1998) and unpublished stratigraphic sections (S.D. Connell and D.W. Love, unpubl. data).

Gravel and sand were studied in order to document lithofacies and lithofacies assemblages that could be extended throughout the Albuquerque Basin. Lithofacies were described mainly to provide provisional interpretations of depositional environments and general lithologic character of basin-fill deposits of the Santa Fe Group in the Albuquerque Basin. Comparisons of gravel and sand composition also document variations among significantly different grain sizes. Delineation of gravel composition is a useful discriminator among lithofacies assemblages, especially because it is easier than sand to differentiate in the field.

Numerous investigators have used gravel deposits in basin analysis (e.g., Colburn et al., 1989). However, few integrated studies of sand and gravel petrography have been

conducted (e.g., Lane, 1989). In the northern Albuquerque Basin, petrographic studies of the upper Santa Fe Group have concentrated on the sand fraction. This study integrated both sand and gravel petrography in order to better document the character and distribution of upper Santa Fe Group sediments in the northern part of the Albuquerque Basin.

Paleocurrent data were obtained at study sites and combined with paleocurrent vector data from a number of geologic maps of the northern Albuquerque Basin (Connell et al., 1995, 1998a, 1999; Cather et al., 1997; Cather and Connell, 1998; 2000; Connell, 1998; Koning et al., 1998; Koning and Personius, *in press*). The paleocurrent data constrain possible transport directions and sediment dispersal patterns and thus can be used to support petrographic descriptions. Collection of paleocurrent data is also useful for groundwater studies because fluids tend to follow paleoflow directions in fluvial sediments (Davis et al., 1993; Mozley and Davis, 1996). Discrimination of preferential flow paths can aid in the development of regional groundwater-flow models.

Geologic Setting and Previous Work

The Albuquerque Basin is one of the largest basins of the Rio Grande rift (Fig. 1), a chain of linked asymmetric and half-graben basins that extends from north-central Colorado, south through New Mexico into western Texas and northern Mexico (Hawley, 1978; Chapin and Cather, 1994). The Rio Grande rift is divided into three sectors, each with distinctive geological characteristics (Chapin, 1988). From Leadville, Colorado, north to the Wyoming border, the rift is a wide zone of extensional faulting without

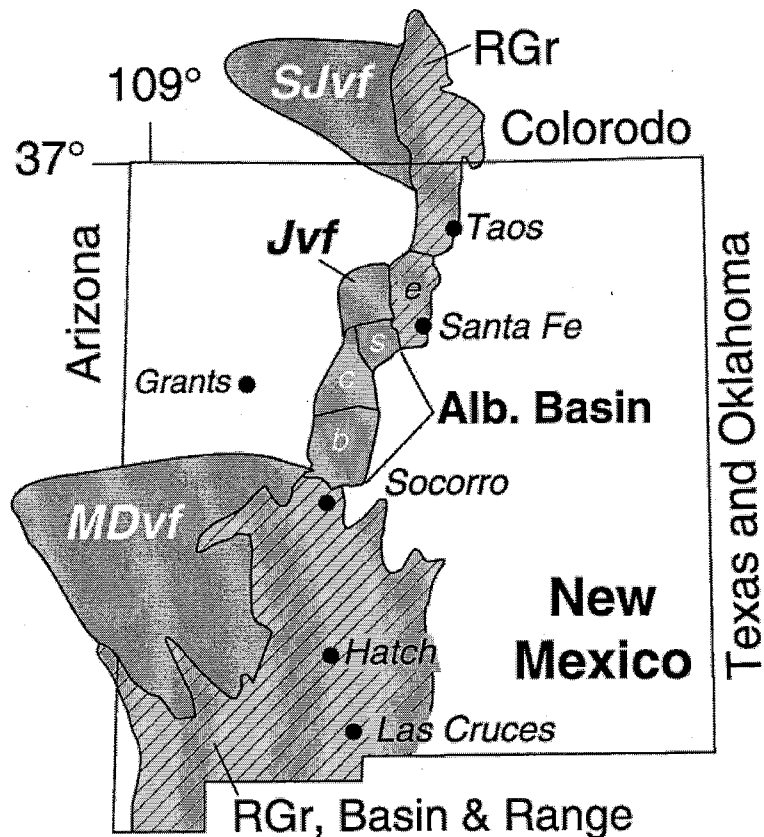


Figure 1. Location of the Rio Grande rift (RGr) and Albuquerque Basin, illustrating major features of the region: the San Juan Volcanic Field (SJvf), Jemez Volcanic Field (Jvf), and Mogollon-Datil Volcanic Field (MDvf). The Socorro Basin bounds the Albuquerque Basin to the south. The Española Basin (e) bounds the Albuquerque Basin to the north. The Albuquerque Basin is subdivided into the Santo Domingo (s), Calabacillas (c), and Belen (b) sub-basins (Grauch et al., 1999). Modified from Woodward et al. (1978).

discrete fault-block basins. From Leadville south to Socorro, New Mexico, the rift consists of discrete *en echelon* axial basins. The southern part of the rift, from Socorro to Chihuahua, Mexico, resembles the southern Basin and Range Province with parallel basins and uplifts (Chapin and Cather, 1994).

The Rio Grande rift formed during three periods of regional extension. During the first period (late Oligocene to middle Miocene, 30 to 18 Ma), broad, shallow, fault-bounded, internally drained basins collected volcanic and alluvial deposits (Chapin, 1979;

Aldrich et al., 1986; Chapin and Cather, 1994; Smith, 2000a). The second period occurred during late Miocene time (10 to 5 Ma) when deep half-graben basins developed and steep, rift-border uplifts formed (Chapin and Seager, 1975; Chapin, 1988). During the third period (Pliocene to Pleistocene, ~5-0.7 Ma), basins of the southern Rio Grande rift filled and became linked by an axial river, the ancestral Rio Grande (Gile et al., 1981; Leeder et al., 1996). Aggradation of Rio Grande axial-fluvial deposits continued until early to middle Pleistocene time, when the ancestral Rio Grande incised into older basin fill and formed the Rio Grande Valley (Gile et al., 1981).

The Albuquerque Basin covers an area of about 5600 km² (Lozinsky, 1994) and is approximately 160 km long and 55 km wide and narrows to about 12 km at the southern end. The Albuquerque Basin lies between the west-tilted Socorro Basin half-graben to the south, and the west-tilted Española Basin to the north. The Albuquerque Basin forms a single physiographic and tectonic feature (Woodward et al., 1978); however, the basin is subdivided into three sub-basins on the basis of regional isostatic gravity (Grauch et al., 1999) and seismic-reflection data (Russell and Snelson, 1994). These sub-basins are, from north to south, the Santo Domingo, Calabacillas, and Belen sub-basins (Fig. 1). The margins of the Albuquerque Basin are faulted and defined by basement uplifts and lower relief footwall uplands. Basement uplifts that define basin margins include the Sandia, Manzano, Los Pinos, and Ladron Mountains. These uplifts are composed of Precambrian granite and metamorphic rocks overlain by upper Paleozoic sedimentary rocks (Kelley, 1977).

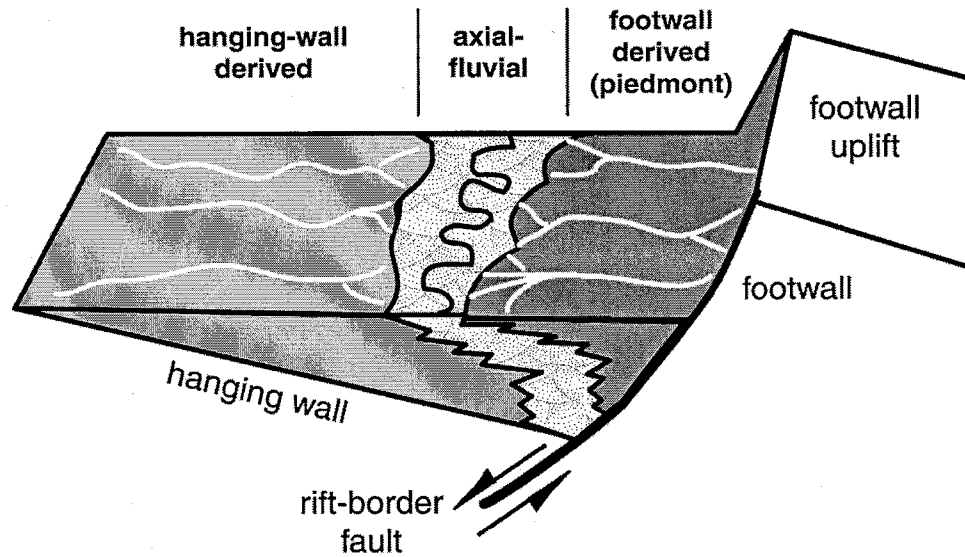


Figure 2. Schematic diagram of sedimentation in half-graben basins of the Rio Grande rift, illustrating relationships among deposits on the hanging wall and footwall with external drainage along an axial river (modified from Mack and Seager, 1990).

In half-graben basins (see Leeder and Gawthorpe, 1987; Rosendahl, 1987) such as the Albuquerque Basin, the direction of basin subsidence shifts through transfer or accommodation zones (Faulds and Varga, 1998). Tectonic subsidence of asymmetric or half-graben basins commonly produces specific geomorphic and structural features, such as the development of footwall uplifts and associated synthetic and antithetic rift-interior faults on the footwall and hanging wall of the basin (Leeder and Jackson, 1993). Half-graben basins with external drainage typically contain three major lithofacies assemblages or fluvial systems tracts (Fig. 2; Leeder and Gawthorpe, 1987; Mack and Seager, 1990; Leeder and Jackson, 1993): relatively long drainages developed on the hanging wall; a central axial river; and fairly short, steep streams draining the footwall.

Recent geologic mapping in the northern part of the Albuquerque Basin, delineates three major fluvially dominated lithofacies assemblages of the Miocene-lower

Pleistocene synrift basin fill of the Rio Grande rift (Hawley et al., 1995; Hawley, 1996; Connell and Wells, 1999; Connell et al., 1999; Maldonado et al., 1999). These lithofacies assemblages correspond to facies distributions found in other half-graben basins (Mack and Seager, 1990; Gawthorpe and Leeder, 2000).

Deposits within the Rio Grande rift are part of the Santa Fe Group (Bryan, 1938; Spiegel and Baldwin, 1963). The Santa Fe Group refers to the synrift volcanic and sedimentary basin fill of the Rio Grande rift (Chapin and Cather, 1994). In the northern Albuquerque Basin, the Santa Fe Group is underlain by the Eocene nonvolcanic Galisteo Formation or the Oligocene volcanic-bearing Espinazo Formation (Kelley, 1977; Ingersoll et al., 1990).

In the Albuquerque Basin, Santa Fe Group strata are up to 4.4 km in thickness and range in age from late Oligocene to Pleistocene (Chapin and Cather, 1994; Lozinsky, 1994). Santa Fe Group deposits do not include deposits that post-date the entrenchment of the Rio Grande and development of the Rio Grande Valley (Spiegel and Baldwin, 1963), which began during early to middle Pleistocene time (Hawley et al., 1969; Chapin and Cather, 1994). In the Albuquerque Basin, delineation of widespread deposition of the Santa Fe Group and younger, inset (post-Santa Fe Group) deposits is ambiguous, principally because of similarities in composition between these two groups of deposits (Connell and Wells, 1999). Recent work in the Albuquerque Basin also suggests the presence of multiple and local stratigraphic tops to the Santa Fe Group that are of different ages, and whose preservation is strongly influenced by the location and activity of intrabasinal normal faults (Connell et al., 2000).

In the Albuquerque Basin of central New Mexico, hanging-wall derived fluvial deposits are assigned to the Arroyo Ojito Formation (Connell et al., 1999). These deposits contain extrabasinal detritus derived from the west. Source areas include the Colorado Plateau, San Juan Basin, Sierra Nacimiento, and southwestern Jemez Mountains (Connell et al., 1999). Axial-fluvial deposits of the ancestral Rio Grande are assigned to the Sierra Ladrones Formation. These deposits contain extrabasinal detritus derived from the north which were transported by the axial-fluvial system originating in northern New Mexico and Colorado (Lambert, 1968; Hawley et al., 1995; Connell et al., 1995; 1998a, b; Connell, 1997, 1998). Piedmont deposits are also assigned to the Sierra Ladrones Formation and contain sediments derived from adjacent footwall uplifts of the Sandia Mountains and eastern basin margin (Hawley et al., 1995; Connell and Wells, 1999).

The Albuquerque Basin is considered a contributory basin (Lozinsky and Hawley, 1991) that acted as a collector for a number of large perennial and intermittent paleo-rivers that merged into a single axial-fluvial system at the southern outlet of the basin, near San Acacia, New Mexico (Fig. 3). The presence of major rivers in the basin was first recognized by Bryan (1938; Bryan and McCann, 1937). Later workers (Lambert, 1968; Kelley, 1977) also recognized the presence of major fluvial systems, but did not differentiate them. Lozinsky (1988, 1994) conducted a petrographic study of the basin fill in the Albuquerque Basin using outcrops and cuttings and core samples from drill-holes. He concluded that much of the basin fill was compositionally variable. This variability was attributed to different extrabasinal sedimentary and volcanic source areas north and west of the Albuquerque Basin and to different locally derived sediments, predominantly composed of metamorphic and plutonic rocks that were derived from nearby rift-flanking

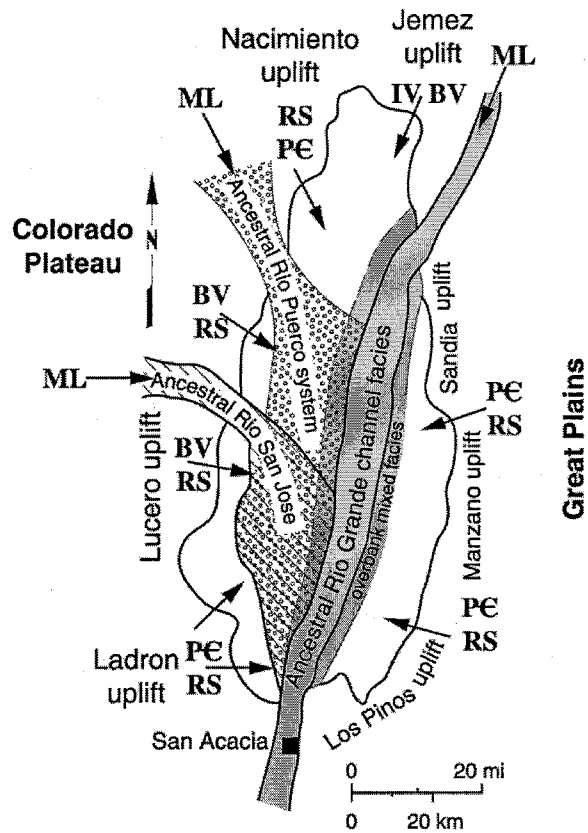


Figure 3. Schematic drawing of contributory drainage of the Albuquerque Basin (Belen and Calabacillas sub-basins) during upper Santa Fe Group deposition (modified from Lozinsky et al., 1991). The Santo Domingo sub-basin is not illustrated on this figure. Arrows indicate source areas and clast types derived from: Precambrian (PE), reworked sedimentary (RS), intermediate volcanic (IV), mafic volcanic (BV), and mixed lithologic composition (ML).

uplifts, such as the Sandia and Manzano Mountains (Kelley, 1977; Hawley et al., 1995; Connell and Wells, 1999). Lozinsky (1994) recognized the following compositional trends in the basin stratigraphy: 1) quartz content tends to decrease and feldspar tends to increase in abundance upsection; and 2) the Santa Fe Group contains more lithic fragments, especially volcanic fragments, than pre-Santa Fe Group deposits, such as the Galisteo Formation; however, volcanic detritus is recognized in Oligocene volcanic and volcanoclastic sediments of the Espinazo Formation and unit of Isleta #2 (Lozinsky, 1988,

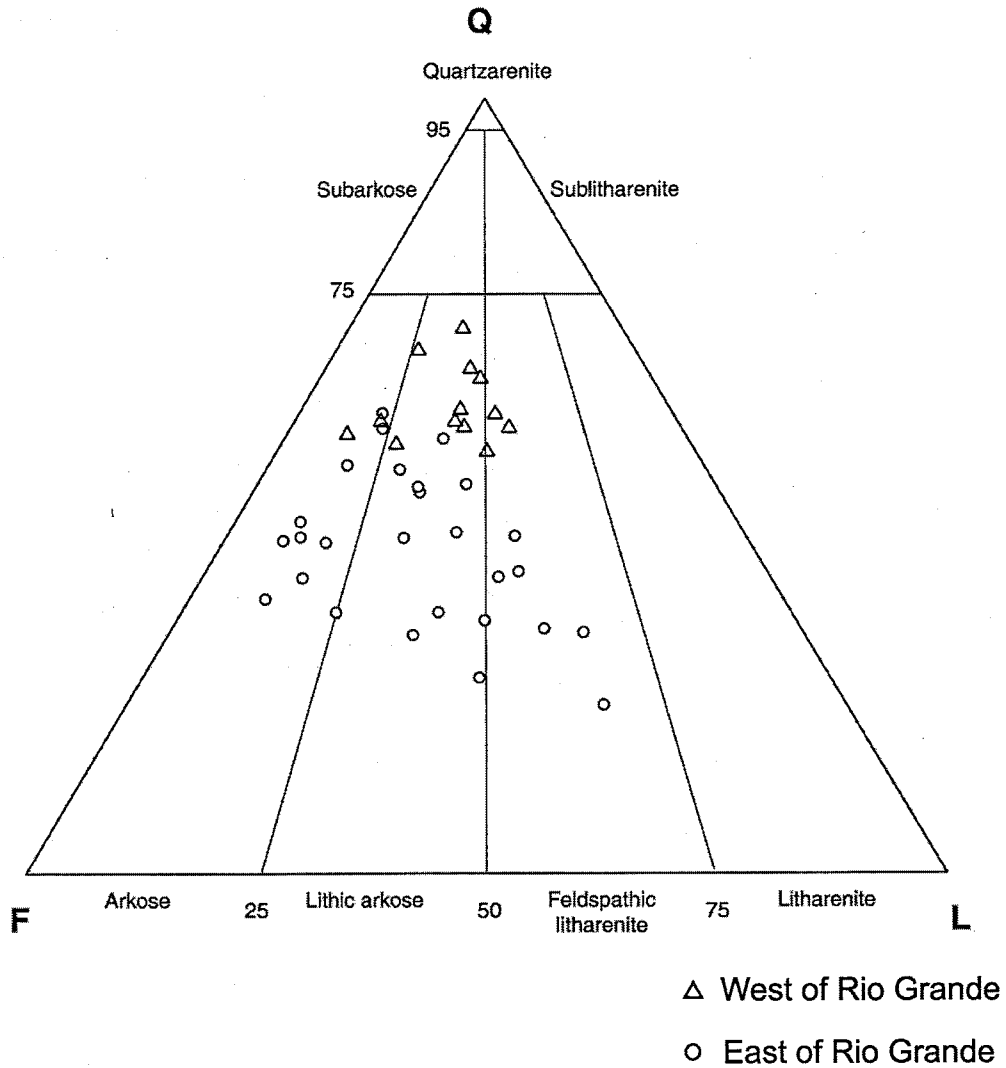


Figure 5. QFL diagram of very fine- to medium-grained sand (Gillentine, 1996), illustrating compositional differences between deposits west of the Rio Grande Valley (triangles, n=13; Cerro Colorado Well #1 and Soil Amendment Facility Well #1; Fig. 4) correlated to the Arroyo Ojito Formation and east of the Rio Grande Valley (circles, n=27; Charles Wells #5 and 6) correlated to the Sierra Ladrones Formation. Deposits contain volcanic detritus, however, the western deposits are slightly more quartz-rich than deposits east of the Rio Grande Valley (Gillentine, 1996). Sandstone compositional fields from Folk (1974).

(1994; Erskine and Smith, 1993). Lozinsky et al. (1991) recognized the influence of source area composition on the stratigraphic architecture of the upper Santa Fe Group (Fig. 3), however, compositional associations among lithofacies were only locally differentiated.

Studies of very fine- to medium-grained sand and sandstone sampled from core and cuttings from four water-supply wells, ranging from about 500-1000 m depth, in the Albuquerque area (Fig. 4) suggest the presence of deposits that were probably derived from different source terrains (Fig. 5; Mozley et al., 1992; Gillentine, 1996; Connell et al., 1998a). Deposits west of the Rio Grande Valley tend to have a greater proportion of quartz than deposits east of the valley (Gillentine, 1996). Deposits along the western margin contain more quartz, suggesting derivation from quartzose sandstone of the adjacent Colorado Plateau (Stone et al., 1983; Gillentine, 1996). Cuttings and core samples from wells on both sides of the Rio Grande Valley contain volcanic detritus (Mozley et al., 1992; Gillentine, 1996), which are not derived from the range-front uplift of the Sandia Mountains (Kelley, 1977), but were probably derived from the San Juan, Latir, and Ortiz volcanic centers of northern New Mexico and southern Colorado (Hawley, 1978; Woodward et al., 1978).

The composition of sand from the four wells studied by Gillentine (1996) differs from the results of a study of medium- to coarse-grained sand and sandstone by Large and Ingersoll (1997) in the northern part of the Albuquerque basin, just north of the wells studied by Gillentine (1996). Large and Ingersoll (1997) differentiated two petrofacies within the Albuquerque Basin. A hypabyssal-intrusive and volcanic dominated succession found in the fault-bounded Hagan embayment on the northeastern margin of

the Albuquerque Basin, which Large (1995) calls the La Bajada petrofacies. The Albuquerque petrofacies of Large and Ingersoll (1997) is a mixed composition assemblage that represents most of the deposits in the Albuquerque Basin. As previously noted, Large and Ingersoll (1997) concluded that the Santa Fe Group exposed in the northern half of the basin are petrographically indistinguishable from one another on the basis of sand composition (Fig. 6). Large and Ingersoll (1997) also concluded that deposits of the Albuquerque Basin (their Albuquerque petrofacies) were partly derived from synrift deposits of the Santa Fe Group in the Española Basin to the north, and from older Santa Fe Group strata exposed along the margins of the Albuquerque Basin. Although the study of Large and Ingersoll (1997) covered much of the northern Albuquerque Basin, several areas were not studied because of access restrictions. Their study of deposits on the Arroyo de las Calabacillas (formerly Sky Village SE) quadrangle and western part of the Cerro Conejo (formerly Sky Village NE) quadrangle was prior to recent geologic mapping (e.g., Cather et al., 1997; Connell et al., 1999). This mapping delineates a number of texturally and compositionally based lithofacies and major intrabasinal faults that cut out much Santa Fe Group section (Cather et al., 1997; Koning et al., 1998; Connell et al., 2001).

Since 1994, geologic mapping of the Albuquerque Basin by the New Mexico Bureau of Geology and Mineral Resources (formerly New Mexico Bureau of Mines and Mineral Resources) and the U.S. Geological Survey resulted in the completion of 26 quadrangle maps (scale of 1:24,000) encompassing over half of the Albuquerque Basin (Connell, 2001). These geologic maps delineate a number of lithofacies in the synrift basin-fill

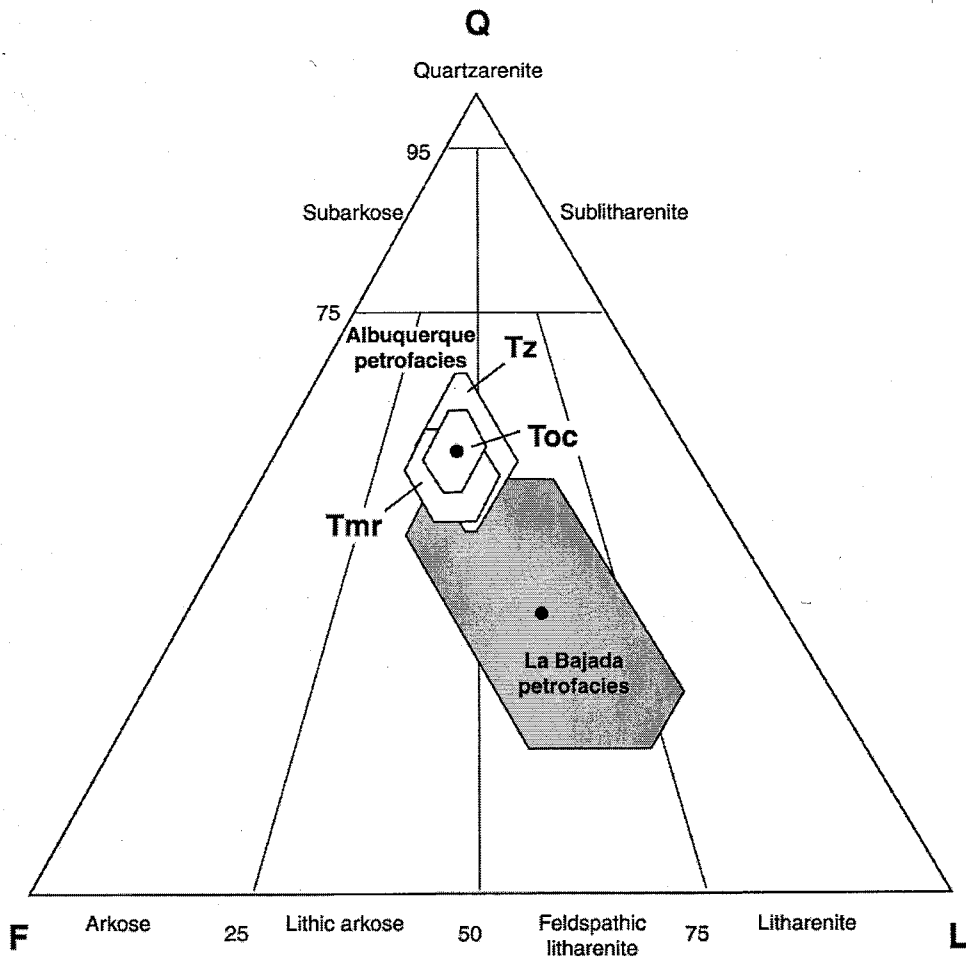


Figure 6. QFL diagram showing results of previous study (Large and Ingersoll, 1997) illustrating means and fields of variation (one standard deviation) of medium- to coarse-grained sand composition using a modification of the Gazzi-Dickinson method. This diagram illustrates the compositional differences between the Albuquerque (white polygons) and La Bajada (gray polygon) petrofacies (Large, 1995; Large and Ingersoll, 1997). The overlap among deposits of the Santa Fe Group, subdivided here into the Zia (Tz), and middle red member (Tmr) of the Santa Fe Formation of Kelley (1977), and Ceja Member (Toc). Sandstone compositional fields from Folk (1974).

of the Santa Fe Group, which comprises the major source of potable groundwater for residents of the basin.

Based on recent geologic mapping, upper Miocene-lower Pleistocene deposits can be differentiated into three relatively distinct lithofacies assemblages (Hawley et al., 1995; Connell and Wells, 1999; Connell et al., 1999; Maldonado et al., 1999; Connell, 2001). Deposits of the western fluvial system are part of the Arroyo Ojito Formation of Connell et al. (1999), which are well exposed along the northwestern portion of the Calabacillas sub-basin. Other units include axial-fluvial deposits of the ancestral Rio Grande, which interfinger with locally derived piedmont detritus shed off of rift-flanking uplifts. The later two units have been included in the Sierra Ladrones Formation by a number of workers (Lucas et al., 1993; Smith and Kuhle, 1998; Connell and Wells, 1999; Smith et al., 2001).

Deposits similar to the Arroyo Ojito Formation have been described by other workers, but have not been universally adopted (e.g. Maldonado et al., 1999; Personius et al., 2000), probably because of presumed ambiguities in the lithologic differentiation of these units among a number of quadrangles. Such apparent ambiguities are probably the result of implementation of an evolving stratigraphic nomenclature in an area that was undergoing intensive mapping by different agencies and geologists during the 1990s.

STRATIGRAPHIC NOMENCLATURE

Introduction

This section presents a summary of the Proterozoic through Pleistocene stratigraphy of the Albuquerque Basin and vicinity in order to provide a framework for understanding potential sources of detritus shed into the basin. A brief summary of pre-rift strata is presented as an overview of the major rock types exposed or encountered in drillholes in and around the study area. This section concludes with an overview of stratigraphy of the Santa Fe Group, mainly to introduce the stratigraphic nomenclature used in this study.

Pre-Santa Fe Group

Pre-rift rocks in the Albuquerque Basin and vicinity range from Proterozoic to Oligocene in age (Fig. 7). Proterozoic rocks include a diverse assemblage of crystalline rocks (mostly granitic, gneiss, aplite, and vein quartz), metasedimentary rocks (mostly metaquartzite and schist), and metavolcanic rocks exposed in Laramide and rift-margin uplifts of the Sandia Mountains, Sierra Nacimiento, Manzanita, Manzano, Los Pinos, and Ladron Mountains (see Kelley and Northrop, 1975; Kelley, 1977; Woodward, 1987). Lower Paleozoic rocks are absent except for limited exposures of Cambrian or

| | | | | |
|----------------------|--|--|--|---|
| CENOZOIC | NEOGENE | Santa Fe Group and post Santa Fe Group | sandstone mudstone conglomerate volcanic | |
| | PALEOGENE | Espinaso Fm unit of Isleta #2 | San Juan volcanic field Mogollon-Datil volcanic field | volcanic & volcaniclastic |
| | | Galisteo Fm Diamond Tail Fm | San Jose Fm Nacimiento Fm Ojo Alamo Ss | sandstone mudstone conglomerate |
| MESOZOIC | CRETACEOUS | Mesaverde Group | | sandstone and shale |
| | | Mancos Shale | | |
| | | Dakota Formation | | |
| | JURASSIC | Morrison Formation | | mostly sandstone and shale |
| | | Summerville Formation | | |
| | | Todilto Formation | | |
| | | Entrada Sandstone | | |
| | TRIASSIC | Petrified Forest Formation | | |
| | | Salitral Formation | | |
| | | Agua Zarca Formation | | |
| Moenkopi Formation | | | | |
| San Andres Formation | | | | |
| PALEOZOIC | PERMIAN | Glorieta Sandstone | | |
| | | Yeso Formation | | |
| | | Abo Formation | | |
| | PENN. | Madera Group | | fossiliferous limestone, chert, conglomerate |
| Sandia Formation | | | | |
| PROT. | granitic, vein quartz, aplitic dikes various schist, gneiss, metavolcanic rocks Ortega quartzite (northern New Mexico) | | granite, quartzite, metamorphic | |

Figure 7. Schematic stratigraphic column illustrating the gross lithologic character of rocks and sediments in the Albuquerque area (modified from Kelley and Northrop, 1975; Woodward, 1987; and Lucas et al., 1999).

Ordovician syenite exposed in the southern Sierra Nacimiento (Woodward, 1987). Mississippian strata are thin or absent in ranges surrounding the study area (Kelley, 1977) and are not discussed. In the Albuquerque Basin, upper Paleozoic sedimentary rocks nonconformably overlie Proterozoic crystalline rocks (Kelley and Northrop, 1975; Woodward, 1987). Pennsylvanian rocks include the Sandia Formation and Madera Group. The Sandia Formation consists of quartz sandstone with interbeds of shale and limestone (Woodward, 1987). The limestone-dominated Madera Group overlies the Sandia Formation and is composed of limestone, with subordinate to minor arkosic sandstone, shale, and conglomerate interbeds. Limestone of the Madera Group is bluish gray to dark gray, fossiliferous (mostly crinoid stems and brachiopod valves), and is locally chert rich (Kelley and Northrop, 1975). Permian rocks exposed along the margins of the Albuquerque Basin include reddish-brown sandstone and shale of the Abo Formation, reddish-yellow sandstone, shale, and gypsiferous beds of the Yeso Formation, light-gray Glorietta Sandstone, and limestone of the San Andres Formation. These rocks represent a wide variety of compositions, including arkosic and quartz arenite sandstone, shale, mudstone, limestone, and gypsum (Kelley and Northrop, 1975; Kelley, 1977; Woodward, 1987). These rock types are generally not very durable (Abbott and Peterson, 1978).

Mesozoic and Paleogene sandstone from the San Juan Basin and eastern Colorado Plateau range from arkose, lithic arkose and subarkose (Fig. 8). Mesozoic strata include shale and sandstone with sparse pebbly sandstone. Deposits are poorly cemented, not very resistant to erosion, and do not produce gravel; however, these sediments could

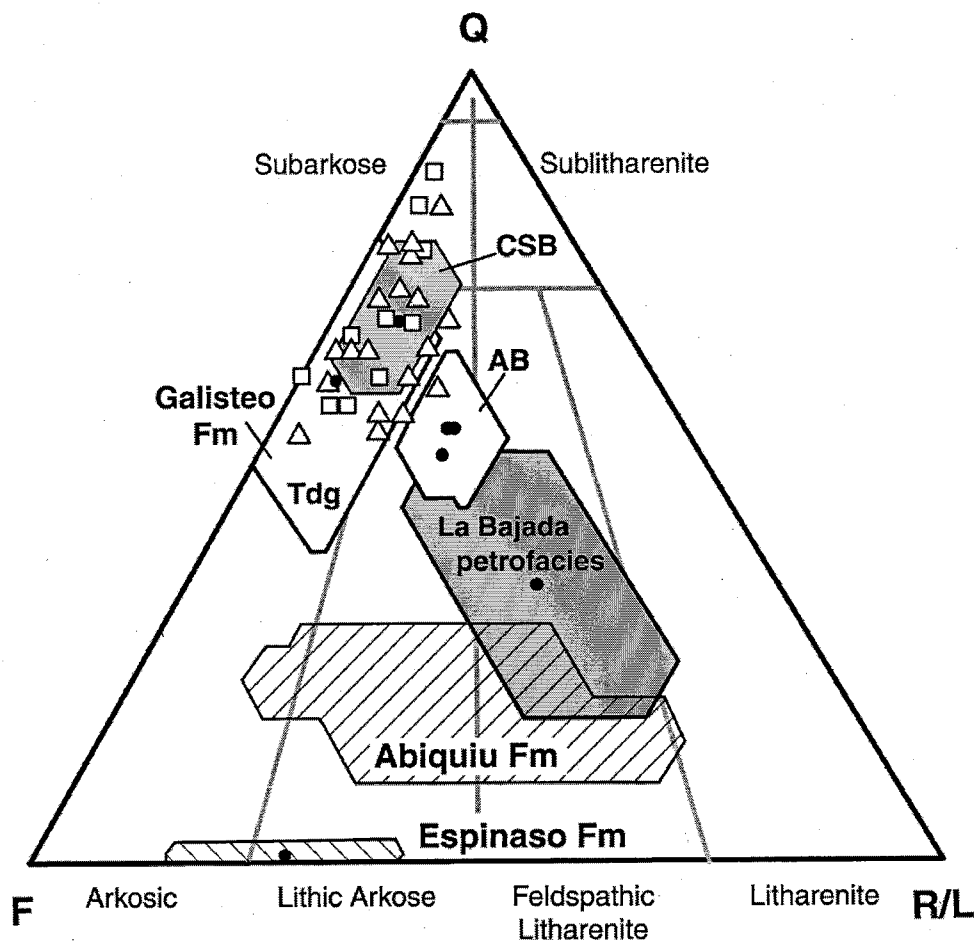


Figure 8. QFL diagram illustrating compositions of various sandstone deposits in the Albuquerque Basin area, including the Espinaso Formation (Kautz et al., 1981) and Galisteo Formation (Gorham, 1979). Squares denote Galisteo Formation at the western margin of the Albuquerque Basin (Lozinsky, 1994). Triangles denote deposits of the unit of Isleta #2 (Lozinsky, 1994). Medium-grained sandstone (n=21) are analyzed in upper Paleozoic to lower Cenozoic deposits exposed along the San Juan Basin and eastern margin of the Colorado Plateau (CSB) using the QFR method of Folk (1974; data taken from Stone et al., 1983). Abiquiu Formation compositions are from the Abiquiu embayment (Moore, 2000). The La Bajada and Albuquerque (AB) petrofacies of Large and Ingersoll (1997) are also shown.

provide a potential source of sand for the Santa Fe Group. With the exception of Proterozoic crystalline rocks and gravelly intervals within the Phanerozoic section, pre-Cenozoic rocks tend to produce little in the way of coarse durable detritus. Notable exceptions include rounded and polished chert and rounded metaquartzite-bearing intervals within upper Paleozoic and Mesozoic strata.

Triassic rocks include the Moenkopi Formation and Chinle Group. The Chinle Group consists of reddish-brown mudstone and sandstone and contains petrified (silicified) wood (Kelley and Northrop, 1975).

Jurassic rocks include the San Rafael Group and the Morrison Formation. The San Rafael Group contains the eolian Entrada Sandstone, limestone and gypsum of the Todilto Formation, and the mudstone and sandstone of the Summerville Formation (Kelley and Northrop, 1975; Woodward, 1987). The Morrison Formation has a variable lithology that includes mudstone, claystone, and sandstone, and contains yellowish-brown to white petrified wood (Kelley and Northrop, 1975).

Cretaceous rocks in the Albuquerque Basin area are exposed north of the Sandia Mountains and on the Colorado Plateau and San Juan Basin (Stone et al., 1983). This includes the Dakota Formation, Mancos Shale, and the Mesa Verde Group. The Dakota Formation is mostly sandstone with minor amounts of shale. The Mancos Shale is a black to gray friable shale. The Mesa Verde Group is an alternating series of shale and sandstone (Kelley and Northrop, 1975). Northwest of the Albuquerque Basin are upper Cretaceous sandstone and shale of the Fruitland Formation and Kirtland Shale (Woodward, 1987).

Paleogene deposits include the Cretaceous-Tertiary Ojo Alamo Sandstone, Paleocene Nacimiento Formation, Eocene San Jose and Galisteo Formations, and Oligocene Espinaso and Abiquiu Formations (Kelley and Northrop, 1975; Gorham and Ingersoll, 1979; Woodward, 1987). The Ojo Alamo Sandstone contains shale interbeds and metaquartzite-bearing pebble lenses. The Nacimiento Formation contains interbedded sandstone and shale. The San Jose Formation includes arkosic sandstone, varicolored shale, and conglomerates (Woodward, 1987).

Eocene and Oligocene deposits exposed along the margins of the Albuquerque Basin include the Espinaso and Galisteo formations. The Galisteo Formation consists mainly of arkosic sandstone and mudstone with minor conglomeratic beds (Gorham and Ingersoll, 1979). The Espinaso Formation is a volcanoclastic apron associated with the Oligocene Ortiz porphyry on the northeastern margin of the basin (Stearns, 1953; Kautz et al., 1981; Erskine and Smith, 1993). Espinaso Formation sandstone contains very little to no quartz (Fig. 8). The Ortiz porphyry belt lies to the northeast of the Albuquerque Basin and supplied volcanic and sub-volcanic detritus into the northeastern part of the basin (Erskine and Smith, 1993; Cather et al., 2000; Connell and Cather, 2001). It is an Oligocene aged group of stocks, laccoliths, sills, and dikes. Volcanic and volcanoclastic deposits derived from the Ortiz porphyry belt are preserved in the Espinaso Formation (Erskine and Smith, 1991).

The unit of Isleta #2 is an informal stratigraphic term applied to 1787-2185 m of upper Eocene-Oligocene strata recognized in at least six deep oil-test wells in the basin (Lozinsky, 1994; May and Russell, 1994). In contrast to the Espinaso Formation, the unit of Isleta #2 is a quartz-rich ($Q=68\pm9\%$; Lozinsky, 1994) succession of purplish-red to

gray, subarkosic, volcanic-bearing sandstone with mudstone interbeds. An ash-flow tuff encountered in the unit's namesake well was K-Ar dated at 36.3 ± 1.8 Ma (May and Russell, 1994), indicating a pre-rift heritage for the unit of Isleta #2.

Santa Fe Group

Cenozoic sedimentary and volcanic deposits associated with the extensional basins of the Rio Grande rift comprise the Santa Fe Group, which is commonly divided into two sub-groups (see Chapin and Cather, 1994). The lower Santa Fe Group records deposition in internally drained basins (bolsons) where streams terminated onto broad alluvial plains or ephemeral to intermittent playa lakes bounded by piedmont deposits derived from emerging basin-margin uplifts (Hawley, 1978; Chapin and Cather, 1994). Upper Santa Fe Group strata record deposition in externally drained basins where perennial streams and rivers associated with the ancestral Rio Grande fluvial system flowed into the southern Rio Grande rift of southern New Mexico. Deposition of the Santa Fe Group ceased during late Pliocene or Pleistocene time, when the Rio Grande began to incise into the earlier aggradational phase of the Santa Fe Group basin fill (Hawley et al., 1969; Gile et al., 1981; Connell et al., 2000).

Hayden (1869) named deposits in Española Basin the "Santa Fe marls." Darton (1922) modified this name to the Santa Fe Formation, and Spiegel and Baldwin (1963) elevated the Santa Fe to group status. Bryan and McCann (1937) proposed a three-part stratigraphy for deposits in the west-central part of the Albuquerque Basin. The lower gray member refers to eolian deposits of the basal Santa Fe Group succession. These are

overlain by the "middle red" member *sensu* Bryan and McCann, 1937), which is overlain by the upper buff member (*sensu* Bryan and McCann, 1937). Spiegel and Baldwin (1963) elevated the Santa Fe to group rank to include deposits associated with the Rio Grande rift and to address complexities in the basin-fill system. Spiegel (1961), Lambert (1968) and Kelley (1977) extended the "middle red" to include a much thicker succession of sediments than Bryan and McCann originally proposed. Kelley (1977) assigned the upper buff member to the Ceja Member of his Santa Fe Formation. Galusha (1966) proposed the Zia Sand Formation and two members (Piedra Parada and Chamisa Mesa) to replace Bryan and McCann's (1937) lower gray member. Gawne (1981) later proposed the Cañada Pilares Member of the Zia Formation. Tedford and Barghoorn (1997) described an upper unnamed member of the Zia Formation for deposits assigned to the middle red member of Bryan and McCann (1937). This upper member of the Zia Formation was subsequently defined as the Cerro Conejo Member by Connell et al. (1999). In addition, Connell et al. (1999) defined the Arroyo Ojito Formation as upper Santa Fe Group deposits derived from the western side of the Albuquerque Basin. The definition of the Arroyo Ojito Formation includes part of the upper buff and middle red members of Bryan and McCann (1937) and the Ceja Member of Kelley (1977). The Arroyo Ojito Formation consists of the Navajo Draw, Loma Barbon, and Ceja members. A summary diagram of Santa Fe Group stratigraphy is presented in Figure 9.

A number of workers studied the biostratigraphy and lithostratigraphy of the Santa Fe Group in the Albuquerque Basin (Bryan and McCann, 1937, 1938; Wright, 1946; Stearns, 1953; Spiegel, 1961; Galusha, 1966; Lambert, 1968; Gawne, 1981; Tedford, 1981; Lozinsky, 1994; Lozinsky and Tedford, 1991; Lucas et al., 1993; Cather et al.,

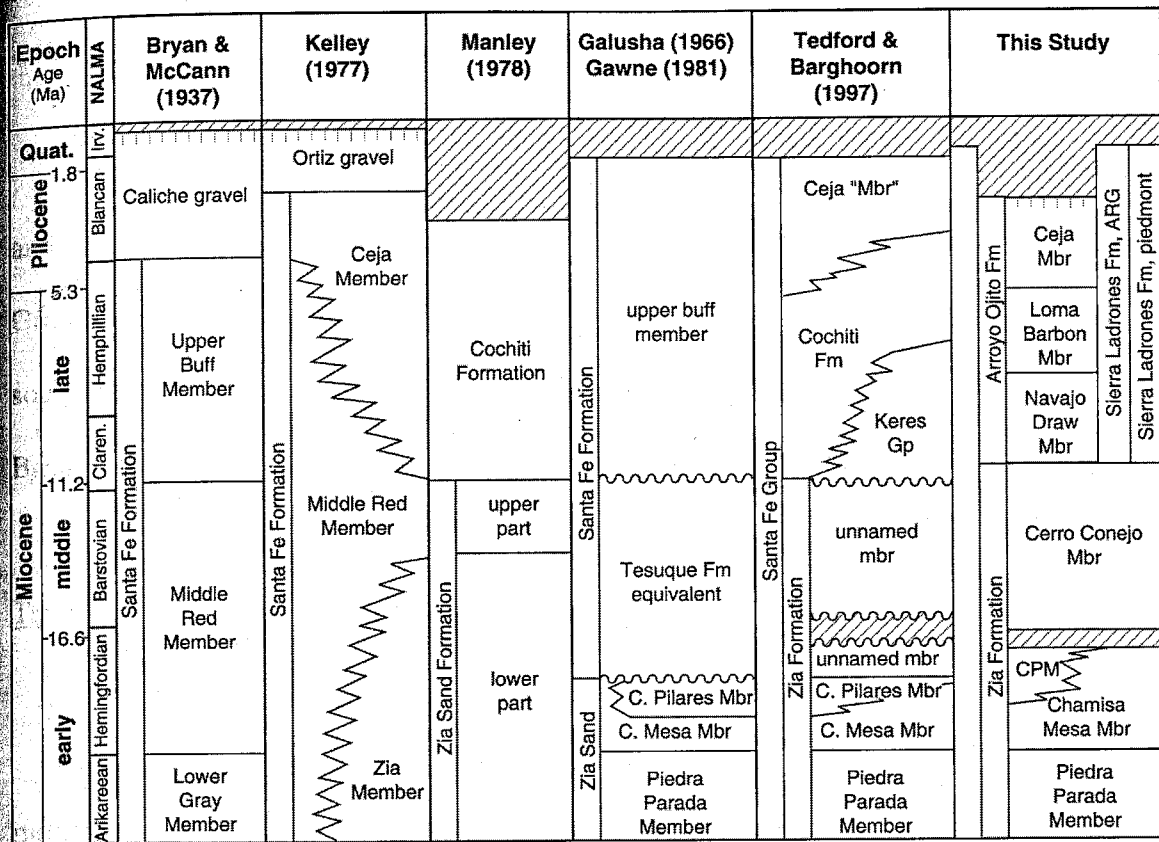


Figure 9. Comparison of stratigraphic nomenclature used in the northern Albuquerque Basin (modified from Connell et al., 1999). The abbreviations CPM and C. Pilares Mbr denote the Cañada Pilares Member of the Zia Formation. The Sierra Ladrones Formation is divided into axial-fluvial Rio Grande (ARG) and piedmont deposits.

1994; Tedford and Barghoorn, 1997; Connell et al., 1995, 1999; Morgan and Lucas, 1999, 2000). Gawne (1981) studied lower Santa Fe Group deposits. Lozinsky (1988, 1994) conducted a petrographic study of Santa Fe Group deposits using well cuttings.

Beckner (1996; Beckner and Mozley, 1998) studied the provenance, diagenetic history, and depositional environments of the Zia Formation, including the upper (Cerro Conejo) member of the Zia Formation. Large (1995; Large and Ingersoll, 1997) studied the petrography of the Santa Fe Group in the northern Albuquerque Basin.

Lower Santa Fe Group

The lower Santa Fe Group ranges from late Oligocene through late Miocene in age and is locally exposed along faulted margins of the Albuquerque Basin. Lower Santa Fe Group sediments in the Albuquerque Basin are assigned to the Popotosa Formation in the southern Albuquerque Basin, the Zia Formation in the northern part of the Albuquerque Basin, and the Tanos and Blackshare formations in the Hagan embayment.

Tanos and Blackshare Formations

The Tanos and Blackshare formations are newly proposed names for well-cemented, moderately tilted conglomerate, sandstone, and mudstone of the lower Santa Fe Group, exposed in the Hagan embayment (Connell and Cather, 2001). These deposits are late Oligocene to Miocene in age and contain volcanic and hypabyssal intrusive rocks that are locally derived from the nearby Ortiz Mountains. These deposits correspond to the volcanic-hypabyssal petrofacies of Large and Ingersoll (1997; La Bajada petrofacies of Large, 1995) and are unconformably overlain by the slightly to nondeformed Plio-Pleistocene Tuerto Gravel of Stearns (1953). These deposits were not studied. A summary of these deposits is given Connell and Cather (2001).

Abiquiu Formation

The Abiquiu Formation is volcanoclastic sandstone and conglomerate derived from the Latir volcanic field, near Taos in northern New Mexico. It is exposed along the

northwestern flank of the Jemez volcanic field and on the crest of the northern Sierra Nacimiento (Smith et al., 1970; Woodward and Timmer, 1979; Woodward, 1987).

Abiquiu Formation sandstone contains abundant feldspar and lithic fragments (Fig. 8) and was deposited by southwest-flowing streams that drained the Latir volcanic field north of Taos, New Mexico (Fig. 2; Smith, 1995; Moore, 2000). The Pedernal chert of Church and Hack (1939) is a black and white chalcedony and chert that is the middle member of the Abiquiu Formation (Moore, 2000). The Pedernal chert is distinctive and commonly forms subangular to angular blocks in gravelly beds of the upper Arroyo Ojito Formation. This distinctive mottled chert is recognized in conglomeratic units of the upper Santa Fe Group. Large and Ingersoll (1997) propose that deposits of the lower Santa Fe Group could represent a compositionally mature counterpart of the Abiquiu Formation and suggest that the northern Albuquerque Basin was connected to the Española Basin prior to late Miocene time. The Abiquiu is Oligocene to Miocene in age (Woodward, 1987). These deposits were not studied.

Zia Formation

The Zia Formation represents a predominantly eolian phase of lower Santa Fe Group deposition in the Calabacillas sub-basin and is exposed along the eastern margin of the Rio Puerco Valley (Caja del Rio Puerco of Bryan and McCann, 1937, 1938) and along the southwestern margin of the Rio Jemez Valley (Rincones de Zia of Galusha, 1966; Tedford, 1981). Bryan and McCann (1937) informally designated the lowermost

sediments as the lower gray member of their Santa Fe Formation, which was subsequently defined as the Zia Formation by Galusha (1966).

The Zia Formation is characterized by massive to cross-stratified, weakly to moderately cemented, well to moderately sorted arkose to feldspathic arenite with scattered thin to medium bedded muddy sandstone and mudstone interbeds (Beckner, 1996; Beckner and Mozley, 1998; Connell et al., 1999; Tedford and Barghoom, 1999). Concretionary zones cemented with coarse-grained poikilotopic calcite crystals (Beckner and Mozley, 1998) are common in the lower members, but decrease in abundance upsection (Connell et al., 1999).

The Zia Formation is subdivided into four members, in ascending stratigraphic order: the Piedra Parada, Chamisa Mesa, Cañada Pilares, and Cerro Conejo members. The Piedra Parada Member consists of basal fluvial conglomerate and sandstone overlain by crossbedded eolian sandstone. The Chamisa Mesa Member includes eolian sandstone and fluviolacustrine mudstone. The Canada Pilares Member is predominantly red claystone with channel sandstone (Galusha, 1966; Gawne, 1981).

The Cerro Conejo Member is the highest member of the Zia Formation and contains very pale-brown to pink and yellowish-red, tabular to cross-bedded, moderately to well sorted sand, with minor thinly bedded mud, and rare very fine-grained pebbly sand. The top of the Cerro Conejo is conformable and interfingers with pale-yellow mudstone of the overlying Navajo Draw Member of the Arroyo Ojito Formation in the Bernalillo NW and Cerro Conejo quadrangles (Koning et al., 1998; Connell et al., 1999; Koning and Personius, *in press*).

The Cerro Conejo Member contains late Barstovian and possible Clarendonian fossils (Tedford, 1981; Tedford and Barghoorn, 1997, 1999) and is overlain by a 10.4 Ma basalt at Chamisa Mesa (K-Ar date of Luedke and Smith, 1978). The upper part of the Cerro Conejo Member contains ashes that have been correlated to the Trapper Creek tephra of Idaho and the northern Basin and Range (Perkins et al., 1998), which range from 10.8-12.17 Ma in parts of the Cerro Conejo Member exposed on the Bernalillo NW and Loma Machette quadrangles section (Connell et al., 1999; Personius et al., 2000; Koning and Personius, *in press*; A. Sarna-Wojcicki, 2000, written commun. to S.D. Connell).

Upper Santa Fe Group

Deposits of the upper Santa Fe Group range from late Miocene to early Pleistocene in age and record deposition by streams and rivers that flowed through externally drained basins (Hawley, 1978; Chapin and Cather, 1994). During this time, the Albuquerque Basin was a large contributory basin (Lozinsky and Hawley, 1991) where large western-margin tributaries, including the ancestral Rio Puerco and Rio San Jose, merged with the ancestral Rio Grande axial-fluvial system.

The upper Santa Fe Group is divided into a number of lithofacies in the Albuquerque Basin, reflecting differences in texture, provenance, and paleoenvironment (Fig. 3; Love and Young, 1983; Lozinsky et al. 1991; Lozinsky and Tedford, 1991; Lucas et al., 1993; Connell et al., 1999; Maldonado et al., 1999; Connell, 2001; Smith et al., 2001). In the northern part of the Albuquerque Basin, three major lithofacies assemblages have been recognized (see Connell and Wells, 1999; Connell et al., 1999; Maldonado et al., 1999;

Smith et al., 2001). These lithofacies assemblages are herein referred to as the western-fluvial, axial-river, and piedmont lithofacies. Gravel of the western-fluvial and axial-fluvial lithofacies is predominantly extrabasinal and contains a mixed assemblage of types, including abundant volcanic and metaquartzite clasts. Piedmont lithofacies are found in association with steep faulted, rift-margin uplifts along the eastern margin. These deposits are locally derived and reflect the lithology of upland drainages, commonly containing limestone, sandstone, and granitic detritus.

These western-fluvial deposits comprise the Arroyo Ojito Formation (Connell et al., 1999) and stratigraphically similar lithofacies to the south (Love and Young, 1983; and Lozinsky and Tedford, 1991). Deposits correlated to the ancestral Rio San Jose, a major tributary to the Rio Puerco, are locally recognized by the presence of rounded Pliocene obsidian that was geochemically correlated to the 2.8-3.3 Ma East Grants Ridge obsidian exposed in the Rio San Jose drainage basin, near Grants, New Mexico (Fig. 1; Love and Young, 1983). This lithofacies assemblage formed by fluvial deposition of ancestral Rio Puerco, Rio Salado, Rio San Jose, and Rio Guadalupe/Jemez fluvial systems.

Axial-fluvial and piedmont deposits are assigned to the Sierra Ladrones Formation (Machette, 1978). Machette defined the Sierra Ladrones Formation from exposures along the front of the Ladron Mountains, about 70-120 km southwest of the study area, at the southwestern margin of the Albuquerque Basin. This unit has been extended throughout much of the Albuquerque Basin (Lucas et al., 1993; Cather et al., 1994; Connell and Wells, 1999; Smith et al., 2001). The axial-fluvial lithofacies form a relatively narrow belt between the western fluvial and piedmont lithofacies. Piedmont deposits interfinger

with western and axial-fluvial deposits near the basin margins (Machette, 1978; Connell and Wells, 1999; Maldonado et al., 1999).

The Cochiti Formation is a succession of volcanic gravel and sand derived from erosion of the Keres Group in the southern Jemez Mountains (Smith and Lavine, 1996).

The Cochiti Formation is partly age correlative to the Loma Barbon and Ceja members and can be differentiated from the Arroyo Ojito Formation by the relative abundance of nonvolcanic clast constituents, such as granite, chert, and quartzite. This unit was not encountered in this study.

Sierra Ladrones Formation

The Sierra Ladrones Formation was defined by Machette (1978) for slightly deformed, coarse-grained interfingering fluvial and basin-margin piedmont deposits that unconformably overlie the Popotosa Formation in the northern Socorro Basin and Belen sub-basin. Through-flowing axial rivers deposited the Sierra Ladrones Formation. The Sierra Ladrones Formation also marked the end of internal drainage that characterized deposition of the Popotosa Formation. These fluvial deposits are typically light-gray to light yellowish-brown, non-cemented to locally cemented, moderately sorted, trough cross stratified sand and gravel with rare muddy interbeds. Deposits typically form channel sand and gravel that interfinger with piedmont deposits derived from basin margin uplifts (Machette, 1978; Connell and Wells, 1999).

The Sierra Ladrones Formation is broadly equivalent to the Plio-Pleistocene Camp Rice and Palomas formations of southern New Mexico (Gile et al., 1981; Lozinsky and

Hawley, 1986), which record deposition of an ancestral Rio Grande beginning around 4.5-5 Ma (Mack et al., 1993, 1996, 1998; Leeder et al., 1996). The base of the ancestral Rio Grande lithofacies is not exposed in the study area, however, quartzite-bearing fluvial gravel is found within the upper Miocene Peralta Tuff Member of the Bearhead Rhyolite (Smith et al., 2001), suggesting that the river was present in the northern part of the basin prior to 6.9 Ma.

The age of the uppermost Sierra Ladrones Formation is constrained by fallout ash from the 1.2 Ma (Izett and Obradovich, 1994) upper Bandelier Tuff, and fluvially transported clasts of the 1.6 Ma (Izett and Obradovich, 1994) lower Bandelier Tuff (Connell et al., 1995; Connell and Wells, 1999; Connell et al., 2001), early Irvingtonian (~1.6-1.2 Ma) fossils (Lucas et al., 1993), and fallout ash from the ~0.66 Ma Lava Creek B ash within inset fluvial and piedmont deposits in the Santo Domingo sub-basin (Smith et al., 2001) and Calabacillas sub-basin (Connell et al., 2001). Thus, Sierra Ladrones Formation deposition ended between about 1.2-0.7 Ma.

Arroyo Ojito Formation

The Arroyo Ojito Formation was proposed for fluvial sediments flowing along the western margin of the Albuquerque Basin (Connell et al., 1999). Deposits of the Arroyo Ojito Formation were derived from the eastern Colorado Plateau, Sierra Nacimiento, and southern Jemez Mountains. Much of the gravel of the Arroyo Ojito Formation is heterolithic, containing a diverse assemblage of volcanic, sedimentary, and plutonic clasts. Conglomeratic parts of this unit commonly contain angular to subrounded red

granite, basalt, sandstone, conglomerate, and angular to subangular cobbles of the Pedernal chert.

The Arroyo Ojito Formation is 437 m thick at the type section between the San Ysidro (Calabacillas fault of Personius et al., 2000) and Zia faults, where it is subdivided into three members (Connell et al., 1999). The Navajo Draw Member is the lowest unit of the Arroyo Ojito Formation and overlies the Cerro Conejo Member of the Zia Formation. At the type section, the Navajo Draw Member is about 230 m thick and overlies the Cerro Conejo Member. The Navajo Draw Member marks a change in depositional environments from the mixed eolian and sand-dominated fluvial system of the Cerro Conejo Member to a more mud- and gravel-dominated fluvial deposition of the Arroyo Ojito Formation. The Navajo Draw Member is a very pale-brown to pale-yellow, lenticular, poorly to moderately sorted, fine- to coarse-grained sand and pebbly sand with minor thin to medium bedded pale-yellow mud. Gravelly beds are mainly clast supported and contain volcanic (mostly intermediate composition) pebbles and subordinate sandstone and brownish-yellow fine chert pebbles, and sparse red granite and Pedernal chert clasts derived from southeast-flowing streams (Connell et al., 1999).

The Loma Barbon Member is the middle unit of the Arroyo Ojito Formation and contains about 200 m of reddish-yellow to strong-brown and yellowish-brown, poorly sorted, sand, pebbly sand, and gravel exposed at the type section (Connell et al., 1999). The Loma Barbon Member contains locally abundant subangular to subrounded pebbles and cobbles of red granite derived from the Sierra Nacimiento. Clast composition becomes increasingly heterolithic up section and Pedernal chert clasts increase in abundance. The Loma Barbon Member is redder than the underlying Navajo Draw

Member; however, the Loma Barbon contains intervals of pale-yellow muddy sand that is similar in color to the Navajo Draw Member. The basal contact is fairly sharp along the Ceja del Rio Puerco, but interfingers with the Navajo Draw Member to the east (Koning and Personius, *in press*). A fallout tephra correlative to the Peralta Tuff Member (6.8-7.0 Ma; Connell et al., 1999; Koning and Personius, *in press*) is present near the middle of the Loma Barbon Member. Axial-fluvial deposits of the uppermost Sierra Ladrones Formation interfinger with and overlie the Loma Barbon Member and similar deposits (Connell et al., 1995). Basalt flows at Santa Ana Mesa (K-Ar date of 2.5 ± 0.3 Ma, Bachman and Mehnert, 1978; $^{40}\text{Ar}/^{39}\text{Ar}$ dates of 1.77-2.58 Ma; New Mexico Geochronological Research Laboratory, W.C. McIntosh, unpubl. data) locally overlie the Loma Barbon Member along the western margin of the Rio Grande Valley, near San Felipe Pueblo, New Mexico.

The Ceja Member (Kelley, 1977) is the uppermost member of the Arroyo Ojito Formation (Connell et al., 1999). Kelley applied the term Ceja to Lambert's (1968) upper buff member type section at El Rincon (Fig. 4) in an attempt to replace the uppermost part of the upper buff member of Bryan and McCann (1937) and Wright (1946). The Ceja Member is 64 m at the type section (Kelley, 1977) and forms an areally extensive pebble to small boulder conglomerate and conglomeratic sandstone beneath the Llano de Albuquerque, a broad mesa between the Rio Puerco and Rio Grande valleys (Fig. 4).

METHODS

Location and Accessibility

Stratigraphic sections were measured on the Pueblo of San Felipe, Pueblo of Zia, and City of Rio Rancho, Sandoval County, New Mexico (Fig. 4). These sites were chosen because they contain mapped and reasonably well dated lithofacies (Cather and Connell, 1998; Koning et al., 1998; Koning and Personius, *in press*). Other localities were sampled near Albuquerque, Rio Rancho, and Isleta Pueblo, New Mexico, principally to document lateral variations among mapped lithofacies assemblages. San Felipe Pueblo is about 40 km north of Albuquerque, and Zia Pueblo is about 50 km northwest of Albuquerque. Access to most of the field sites is by four-wheel drive vehicle or on foot via dirt roads, arroyo floors, and badlands. Access to Zia Pueblo and San Felipe Pueblo tribal lands is restricted and permission for access must be obtained from the tribal governor. To supplement the data taken north of Albuquerque, gravel and sand samples were taken from unpublished stratigraphic sections measured by S.D. Connell and D.W. Love, just south of Albuquerque on the Isleta Pueblo.

The study area encompasses much of the northern part of the Albuquerque Basin (Fig. 4) and includes parts of the southern Santo Domingo, Calabacillas, and northern Belen sub-basins (Fig. 1). Principal study areas and measured stratigraphic sections are

on the Bernalillo NW, San Felipe Pueblo quadrangles (USGS, 7.5-minute, various
vintages). Secondary study areas are on the Albuquerque West, Arroyo de las
Calabacillas (formerly Sky Village SE), Bernalillo, Bernalillo NW, Cerro Conejo
(formerly Sky Village NE), Hubbell Spring, Isleta, La Mesita Negra, Loma Machette,
Los Lunas, The Volcanoes (formerly Volcano Ranch), and Rio Puerco 7.5-minute
quadrangles (Fig. 4).

Field Observations

Seven stratigraphic sections (Appendix A) were measured in upper Santa Fe Group
deposits in the Calabacillas, southern Santo Domingo, and northern Belen sub-basins
between June, 2000 and April, 2001. Three additional stratigraphic sections described by
S.D. Connell and D.W. Love are also included in Appendix A. The base, top, and major
stratigraphic offsets were located using a hand-held 12-channel, non-differentially
corrected, Global Positioning Satellite (GPS) unit. Locations are in Universal Transverse
Mercator coordinates using the North American Datum of 1983 (NAD 83), unless
otherwise noted, and are rounded to the nearest 5 m. Informal units were assigned at
changes in texture or color, or at stratigraphic offsets. Sections were measured with a
Jacob Staff and Abney level, except for the San Felipe Pueblo gravel quarry section,
which was measured using a differentially corrected Global Positioning Satellite system
and a Jacob staff and Abney level. Most of the section at the San Felipe Pueblo gravel
quarry section dips less than 7° and unit thickness was adjusted to reflect this dip.

Colors were described on dry deposits using Munsell (1992) notation. Sedimentary structures and textures were described using methods described in Anstey and Chase (1974), Compton (1985), and Dutro et al. (1989). Sandstone composition was determined using the nomenclature of Folk (1974). Clasts counted ranged between 8 mm and 15 cm. Clast and grain shape were estimated using the descriptions of Powers (1953). Bedding thickness was described using terminology from McKee and Weir (1953).

Gravel and sand samples were collected at selected intervals during description of stratigraphic sections (Appendix B and C). In loose deposits, gravel composition was determined from clast counts on sieved pebble concentrates greater than 8 mm in diameter, mainly to limit compositional variations and uncertainty in identifying smaller pebbles (e.g., Howard, 1993). In well-cemented exposures, such as those encountered in the piedmont lithofacies assemblage, gravel was counted in the outcrop by counting the number of clasts exposed in one square meter. Sand was sampled in weakly cemented units, mainly because most of the ancestral Rio Grande deposits of the Sierra Ladrones Formation and much of the Arroyo Ojito Formation are poorly cemented. Only limited exposures of cemented or concretionary sandstone are present in upper Santa Fe Group deposits (Beckner and Mozley, 1998; Connell et al., 1999). In addition to outcrop samples, cuttings from wells drilled through known stratigraphic units were also studied. The locations of sample sites are listed in Appendix D.

Paleocurrent directions were determined primarily from imbrications on prismoidal gravel (Appendix E); a few measurements of cross-bed orientation and channel geometry were made. Imbrication measurements were made using a Brunton compass on gently dipping beds (less than 7° inclination), so stratal rotation was not necessary to correct for

paleocurrent directions. Paleocurrent data were also compiled from geologic maps of the study area. Equal area paleocurrent roses were constructed using a computer program called *Rosy* for Macintosh operating systems (version 2.1, Eachran, 1991), which is available through Rockware of Golden, Colorado. This application computes the vector mean and confidence angle and calculates the normalized resultant of the normalized vector mean (R; Appendix E; Eachran, 1991). R-values of data with large dispersion are near a value of 0. Data with small dispersions are close to a value of 1.

Petrography and Texture

Sand was prepared for microscopic analysis using the following procedures. Calcium-carbonate cement was removed using a 0.5 N sodium acetate solution with a pH of 4. Clays were deflocculated with sodium hexametaphosphate solution. Medium-grained (0.50-0.25 mm) sand was extracted from sand samples using standard testing sieves. Thin sections were impregnated with epoxy and stained with sodium cobaltinitrite solution to identify potassium feldspar. Modal composition of 70 thin sections was determined using a Swift Model F automated point counter and a Nikon binocular polarizing microscope (Table 1, Appendix C1, C2, C3). Grain counting was done under plane-polarized and cross-polarized light at 10-times magnification. Four-hundred grains were counted per thin section using a modified version of the Gazzi-Dickinson method (Gazzi, 1966; Dickinson, 1970), where the detrital components of medium-grained sand was described in order to minimize compositional variations due to grain-size differences among different deposits (Ingersoll et al., 1984). Modal categories counted include

Table 1. Detrital components of medium-grained sand and sandstone.

| Abbreviation | Description |
|---------------------------------|---|
| Framework | |
| Qm | Monocrystalline quartz |
| Qp | Polycrystalline quartz |
| P | Plagioclase |
| K | Potassium feldspar |
| Gn | Granite |
| Qv | Quartz phenocrysts in volcanic grain |
| Pv | Plagioclase phenocrysts in volcanic grain |
| Vg | Volcanic groundmass |
| Qs | Quartz in sedimentary rock fragment |
| Qc | Chert |
| Fs | Feldspar in sedimentary rock fragment |
| S | Sedimentary rock fragment |
| Non Framework | |
| M | Mica |
| Opq | Opaque |
| U | Unknown |
| Additional Abbreviations | |
| N _f | Total framework grains |
| N _l | Total lithic grains |

monocrystalline quartz (Qm), polycrystalline quartz (Qp), plagioclase feldspar (P), potassium feldspar (K), granitic rock fragments (gn), quartz phenocrysts within volcanic grains (Qv), plagioclase phenocrysts within volcanic grains (Pv), volcanic rock groundmass (Vg), quartz within a sedimentary rock fragment (Qs), chert (Qc), feldspar within a sedimentary rock fragment (Fs), carbonate rock fragments (Sc), and matrix of a sedimentary rock fragment (S). Only grains directly under the crosshairs of the microscope were counted. If, for instance, a volcanic grain containing both groundmass and a plagioclase phenocryst was in the field of view, only the portion under the crosshairs was counted (i.e. if the phenocryst was under the crosshairs, a plagioclase phenocryst grain (Pv) was recorded, but if the groundmass was under the crosshairs a

volcanic groundmass grain (Vg) was counted). Ternary diagrams were constructed using the program *Ternplot* written for Macintosh operating systems.

Gravel clasts were cleaned using a solution of 0.5 N sodium acetate (pH 4) to remove excess calcium-carbonate cement from clast surfaces in order to facilitate identification and classification (Table 2). Modal composition of 40 samples was determined by visual examination and identification of hand specimens. The abundance of each component was determined from counts that varied from 163 to 858 clasts per sample; sample sizes were mostly between 200 and 500 clasts. Gravel sizes ranged from 8 mm to about 15 cm maximum clast diameter. Boulders were observed in the field, but not included in counts. Unidentified (unknown) clasts constituted only a small proportion of the samples (<1% by counting) and do not provide any important information. Thus, unknown (U) gravels were not included in the recalculated parameters (Appendix D).

Cuttings from a water supply and a groundwater monitoring well were also studied. Drillhole cuttings were taken at 10-ft (3 m) intervals during drilling and are archived at the Library of Subsurface Data, New Mexico Bureau of Geology and Mineral Resources in Socorro, New Mexico. The locations of drillhole samples (Appendix C) refer to depth of the top of the sampled interval, in feet below land surface, for a given hole. For example, a sample taken from the 790-800 ft (241-244 m) interval (below land surface) in the Matheson Park monitoring well (MAT) is designated as MAT0790.

Table 2. Detrital components of pebble and cobble gravel. Volcanic constituents include porphyritic, hypabyssal-intrusive and volcanic rocks of the Ortiz Mountains.

| Clast type and symbol | Description |
|--|---------------------------------|
| <i>Quartzite and Chert</i> | |
| Qq | Total quartz and quartzite |
| Q | White quartz |
| Qw | White quartzite |
| Qp | Pink to red quartzite |
| Qg | Gray quartzite |
| Qb | Brown quartzite |
| Ql | Bluish-gray quartzite |
| Qc | Total chert |
| Qcb | Brown chert |
| Qcg | Gray chert |
| Qcr | Red chert |
| Qcp | Pedernal chert |
| Qcl | Black chert |
| <i>Volcanic</i> | |
| Vtg | Gray tuff |
| Vtt | Tan tuff, commonly porphyritic |
| Vtw | White tuff |
| Vtr | Red tuff |
| Vb | Basalt (black) |
| Va | Andesite (greenish color) |
| Vr | Rhyolite (reddish color) |
| <i>Sedimentary</i> | |
| Ssg | Gray sandstone |
| Ssr | Reddish-brown sandstone |
| Ssy | Yellowish-brown sandstone |
| Sir | Red and reddish-brown siltstone |
| Sc | Conglomerate |
| Sw | Petrified wood |
| Sl | Limestone, commonly bluish-gray |
| <i>Plutonic and metamorphic</i> | |
| PMgr | Red granitic |
| PMgw | White granitic |
| PMgp | Pink granitic |
| PMn | Gneiss and foliated granitic |
| PMs | Schist |
| PMd | Diabase (black) |
| <i>Unidentified</i> | |
| U | Unknown |

Lithofacies and Lithofacies Assemblages

The lithofacies codes are modified from Miall (1996) and are used to better understand the variation of depositional styles in the stratigraphic sections. Each lithofacies is considered to represent a particular depositional process (Table 3).

Lithofacies assemblages are defined herein as groups of lithofacies that commonly occur together in a specific part of the basin. They are distinguished primarily by grain size and include gravelly (G), sandy (S), and muddy (F) divisions. Secondary divisions for gravels include clast-supported (c) or matrix-supported (m); stratification (planar, p; trough, t), angularity (well rounded, w; subrounded, s) and sorting (well sorted, w; bimodal, b; poorly sorted, p). Secondary divisions for sand and mud are defined on the basis of sedimentary structures.

Five gravel lithofacies are present in the study area. Rounded gravels occur in two lithofacies. The first lithofacies contains rounded clast-supported gravel and has thick planar bedding and is defined as Gcprw. The clasts are well sorted and locally imbricated. The second lithofacies contains rounded, clast-supported gravel and thick trough cross beds, which commonly cut into older beds both horizontally and vertically. Clasts are well sorted. This lithofacies is defined as Gctrw. Clast supported gravels are also present as deposits composed of subrounded clasts. Clast supported subrounded gravels with planar bedding, bimodal clasts sizes (i.e. abundant pebbles with subordinate cobbles and boulders), and common imbrication are defined as Gcpsb. A similar lithofacies, defined

Table 3. Summary of lithofacies (modified from Miall, 1996).

| Lithofacies Code | Description | Interpretation |
|-------------------------|--|---|
| Gravel | | |
| Gcprw | Gravel, clast supported, planar bedding, rounded, well sorted, locally imbricated. | Longitudinal bedform channel |
| Gcpsb | Gravel, clast supported, planar bedding, subrounded, mostly bimodal clast sizes, commonly imbricated. | Longitudinal bedform channel |
| Gcpsp | Gravel, clast supported, planar bedding, subrounded, poorly sorted, commonly imbricated. | Longitudinal bedform channel |
| Gctrw | Gravel, clast supported, trough cross bedding, commonly scoured base; vertically and horizontally cuts into older beds, well rounded, well sorted. | Channel fill |
| Gmisp | Gravel, matrix supported, vague bedding, subrounded, poorly sorted. | Hyperconcentrated or debris flow |
| Sand | | |
| Sp | Sand, planar bedding, very fine to very coarse grained. | Upper flow regime plane bed flow |
| Sl | Sand, low angle (<15°) cross stratification, fine to very coarse grained. | Low relief bar migration |
| St | Sand, trough cross bedding, fine to very coarse grained, commonly pebbly. | Migration of channels and/or dunes |
| Si | Sand, vague bedding, very fine to coarse grain size, rhizoconcretions. | Bioturbated |
| Sr | Sand with rhizoconcretions, very fine to coarse grain size. | Relative stability and vegetative growth |
| SFp | Sand with mud interbeds, internal planar bedding of sand. | Waning flood |
| SFl | Sand with mud interbeds, sand show internal low angle (<15°) cross stratification in sand. | Waning flood |
| Fines | | |
| Fp | Mud (silt and clay), planar bedding. | Floodplain |
| Fi | Mud (silt and clay), indistinct bedding, commonly contains rhizoconcretions. | Bioturbated |
| Fr | Mud (silt and clay) with rhizoconcretions. | Relative stability allowing for vegetative growth |
| P | Calic (calcium-carbonate) paleosol. | Landscape stability |

Gcsp, includes clast supported, planar bedded gravel that is poorly sorted and commonly imbricated. The fifth type of gravel lithofacies encountered in the field area consists of vaguely bedded, matrix supported gravel. Clasts are subrounded and poorly sorted. This lithofacies is defined as Gmisp.

Seven sand lithofacies are recognized in the study area. Fine- to very fine-grained, planar bedded sand is designated as lithofacies Sp. Fine- to very coarse-sand with low angle cross stratification ($<15^\circ$) is defined as Sl. Trough cross stratified sand is St. Sand in the St lithofacies ranges from fine- to very coarse-grained and commonly contains small pebbles. The fourth lithofacies type is very fine- to coarse-grained sand with indistinct bedding, commonly associated with sand containing scattered rhizoconcretions ($<5\%$ of bed). This vaguely bedded sand is lithofacies Si. Sand with abundant rhizoconcretions is designated lithofacies Sr. Planar bedded sands and interbedded muds are lithofacies SFp. Sand and mud interbeds also comprise lithofacies SFl, however, in this lithofacies the sand beds show a low angle ($<15^\circ$) of cross stratification.

Three lithofacies in the study area are composed of fine-grained deposits (silt and mud). Planar bedded mud is designated lithofacies Fp. Mud with indistinct bedding and minor rhizoconcretions is identified as lithofacies Fi. Mud with abundant rhizoconcretions is defined as lithofacies Fr. Paleosols were identified in the field area. Paleosols contain calcium-carbonate cement, though the degree of soil development varies.

MEASURED STRATIGRAPHIC SECTIONS

Introduction

In the field area, three distinct lithofacies assemblages were recognized: the western-margin lithofacies assemblage, the ancestral Rio Grande lithofacies assemblage, and the eastern piedmont lithofacies assemblage (Tables 4, 5, and 6). The western-margin lithofacies assemblage is assigned to the Arroyo Ojito Formation. The ancestral Rio Grande and piedmont lithofacies assemblages are part of the Sierra Ladrones Formation. The western-margin assemblage consists predominantly of sands interbedded with muds, planar bedded sands, and clast supported, planar bedded gravels. To the east, the western-margin lithofacies assemblage interfingers with the ancestral Rio Grande lithofacies assemblage. Deposits of the ancestral Rio Grande lithofacies assemblage typically consist of stacks of planar bedded gravels and sands, and sands with low angle cross stratification. Eastward, the ancestral Rio Grande lithofacies assemblage interfingers with deposits of the piedmont lithofacies assemblage. These eastern piedmont deposits are better cemented than the sediments of the other two lithofacies assemblages. Poorly sorted, planar bedded gravel and sand with indistinct bedding are the most common lithofacies in this assemblage.

Table 4. Summary of western-margin lithofacies assemblage.

| Color | Outcrop character & cementation | Dominant lithofacies |
|--|---|--|
| Reddish yellow to very pale brown with pale yellow interbeds | Forms badlands with ledge-forming sandstone and conglomerate; loose; moderately to poorly exposed; locally cemented | Fluvial and eolian. Clast-supported., planar cross stratified gravel (Gcpsb), planar bedded sand (Sp), sand and mud interbeds (SFp), and indistinctly bedded sand (Si). |
| Vertical variations | | |
| Sandstone with interbedded mudstone and gravel; gravel beds 1-5 m thick, 20-80 m lateral extent | Gravel, sand, & mud (%) Gravel: 10-25 Sand: 40-80 Mud: 10-35 | Gravel (decreasing order of abundance) Rounded chert, subrounded volcanics and red granite, rounded sandstone, angular to subrounded Pedernal chert, rounded quartzite |
| Sedimentary structures | | |
| Tabular bedded sandstone with sparse trough cross bedding, Common rhizoconcretions and local paleosols | Paleocurrent directions Southerly to southeasterly | Comments Generally poorly to moderately sorted. Apparent bimodal or polymodal size distribution, where 10-25% cobbles and small boulders are present in pebble and cobble gravels and gravelly sand. Uppermost part of section (Ceja Mbr) is sand and gravelly sand. |

Table 5. Summary of ancestral Rio Grande lithofacies assemblage.

| Color | Outcrop character & cementation | Dominant lithofacies |
|---|--|---|
| Pinkish gray to light gray and yellowish brown | Forms low rounded hills; loose and poorly exposed; commonly uncemented | Fluvial. Clast-supported, trough and planar cross stratified sand and gravel (Gcprw, Gcspb, St); sparse overbank mudstone beds (Fp) |
| Vertical variations | Gravel, sand, & mud (%) | Gravel (decreasing order of abundance) |
| Sand with interbedded sparse mudstone and gravel. | Gravel: 20-50 | Rounded metaquartzite and volcanics with sparse rounded granite and chert and very sparse |
| Gravel beds 1-3 m thick, 5-15 m lateral extent | Sand: 40-80 Mud: 0-10 | Pedernal chert. Sandstone is absent. |
| Sedimentary structures | Paleocurrent directions | Comments |
| Armored mudballs; trough cross stratification of sand and gravel; and thick gravel channel deposits | Southerly to southwesterly | Well to moderately sorted. |

Table 6. Summary of eastern-margin piedmont lithofacies assemblage.

| Color | Gravel, sand, & mud (%) | Dominant lithofacies |
|--|--|---|
| Yellowish-red to reddish-yellow and pale brown | Forms cliffs and steep slopes; uncemented to well cemented | Fluvial and debris flow. Clast- and matrix-supported, vaguely to planar bedded conglomerate (Gcsp, Gmisp) and planar and cross stratified sandstone (Sp, Sl) and bioturbated sandstone (Si, Sr). |
| Vertical variations | | |
| Common fining upward sequences of conglomerate, sandstone, and weakly developed paleosols. | Gravel: 30-60 Sand: 30-70 Mud: 0-10 | Gravel (decreasing order of abundance) Rounded limestone, subrounded to subangular sandstone, subangular pink porphyritic granite; angular white quartz, very sparse, local volcanic (north of Placitas, New Mexico) |
| Gravel beds 1-5 m thick, 10-30 m lateral extent | | |
| Sedimentary structures | | |
| Paleosols, upward-fining sequences, poorly to moderately sorted, clast- and matrix supported, lenticular conglomeratic beds. | Paleocurrent directions Westerly | Comments Poorly sorted. Gravel is typically more angular than in other lithofacies assemblages. Gravel is poorly sorted and has a somewhat bimodal or polymodal size distribution. |

Arroyo Ojito Formation (Western-Margin Lithofacies Assemblage)

General Character

Deposits of the western-margin lithofacies assemblage are assigned to the Arroyo Ojito Formation of Connell et al. (1999). The Arroyo Ojito Formation conformably overlies the Cerro Conejo Member of the Zia Formation at a stratigraphic section measured on the hanging wall of the Zia fault (Marillo-Zia stratigraphic section, Appendix A). The base of the Arroyo Ojito Formation interfingers with the Cerro Conejo Member (Koning and Personius, *in press*), which contains a thickly bedded white ash about 10 m below the upper contact (Fig. 10). This ash was analyzed by N. Dunbar (New Mexico Bureau of Geology and Mineral Resources) and A. Sarna-Wojcicki (U.S. Geological Survey) and is geochemically similar to the Miocene Trapper Creek tephra of the northern Basin and Range/Snake River Plain area (Perkins et al., 1998). Possible correlations include the 12.17 Ma Cougar Point V ash or the 11.31 Ma Aldrich Station ash (A. Sarna-Wojcicki, 2001, personal commun. to S.D. Connell). A slightly younger ash is recognized near highway NM-44 on Santa Ana Pueblo tribal lands. This ash was correlated to the 10.8 Ma ash of the Trapper Creek succession (Personius et al., 2000; Koning and Personius, *in press*). This younger ash was not recognized in the Marillo section.

Deposits of the western-margin lithofacies assemblage have a wide range of colors. Most commonly the deposits are reddish yellow (5YR 6/6 to 7.5YR 6/6), very pale brown

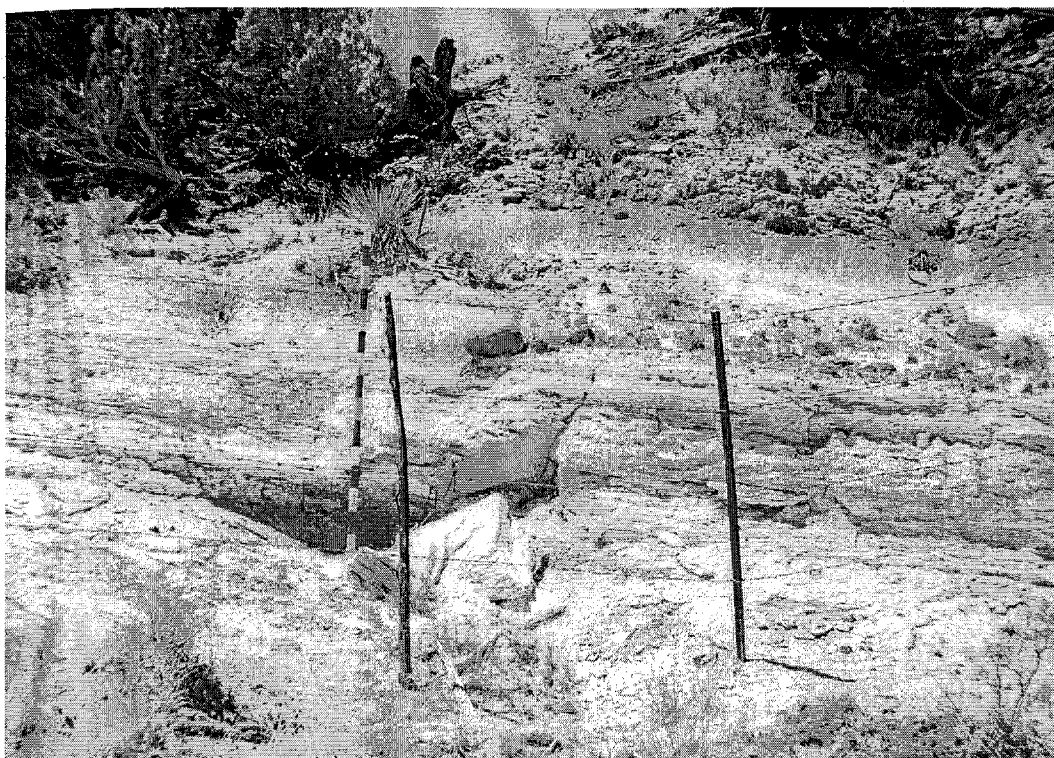


Figure 10. Photograph of thickly bedded white ash of unit 1 of the Marillo section in the upper Cerro Conejo Member of the Zia Formation. This ash, about 10 m below the base of the Arroyo Ojito Formation, has been geochemically correlated to one of the Miocene Trapper Creek tephra (Koning and Personius, *in press*). Jacobs staff is 1.5 m high and divided into 10 cm intervals.

(10YR 8/2 to 10YR 8/4), and pale yellow (2.5Y 7/3 to 2.5Y 7/4). Outcrops of the Arroyo Ojito Formation are locally cemented with calcium-carbonate and commonly form badlands along the edges of the Rio Jemez Valley (Rincones de Zia of Galusha, 1966; Tedford, 1981) and Rio Puerco Valley (Ceja del Rio Puerco of Bryan and McCann, 1937, 1938).

Sand ranges from feldspathic litharenite to arkose, but is mostly lithic arkose and generally very fine- to coarse-grained and poorly to moderately sorted. Subrounded to subangular quartz, feldspar, and volcanic grains are the most common constituents of

western-margin sands. Chert and granite grains, though not the most abundant, are important constituents in differentiating western deposits from the axial-fluvial deposits of the ancestral Rio Grande (see Petrography section).

Gravel beds are sparse in the lower part of the Arroyo Ojito Formation at the Marillo-Zia section and increase in abundance upsection. Gravels of the western-fluvial lithofacies assemblage commonly occur as distinct channels. Gravel tends to be subangular to subrounded in shape, poorly to moderately sorted, clast-supported, and commonly contains abundant pebbles with scattered cobbles and small boulders (Gcpsb, Fig. 11). Gravel beds are typically 1 to 5 m in thickness and extend 20 to 80 m laterally. The base of the gravel beds is commonly undulating with 5 to 10 centimeters of scour into underlying beds. Gravel includes gray porphyritic volcanic rocks of intermediate composition and fine- to medium-grained red granite with subordinate rounded metaquartzite and chert. Chert varies from black, brownish-yellow, to red and includes the distinctive variegated black and white Pedernal chert. Gray and yellowish-brown sandstone clasts are also abundant. Paleocurrents measured from imbricated clasts ($n=116$) trend to the south-southeast at an azimuth of $157\pm 8^\circ$ (Fig. 12). Paleocurrent directions are oblique to the dominantly south-trending Rio Grande Valley and south-flowing deposits of the ancestral Rio Grande (see below). This south-southeast trend in western fluvial deposits is not typical of hanging-wall derived sediments, which commonly flow transverse to the axial river (Fig. 2; Mack and Seager, 1990).



Figure 11. Photograph of conglomerate beds in Ceja Member. Top: Poorly sorted pebble to cobble conglomerate exposed a couple of kilometers south of type section at El Rincon. Dan Koning for scale (~2 m tall). Bottom: Pebble to cobble gravel of lithofacies Gcpsb just south of El Rincon. This deposit contains scattered subangular cobbles of red granite and minor rounded quartzite in an abundant pebble matrix that is scoured into cross bedded sandstone (SI). Lens cap (6 cm diameter) for scale. Photographs courtesy of S.D. Connell.

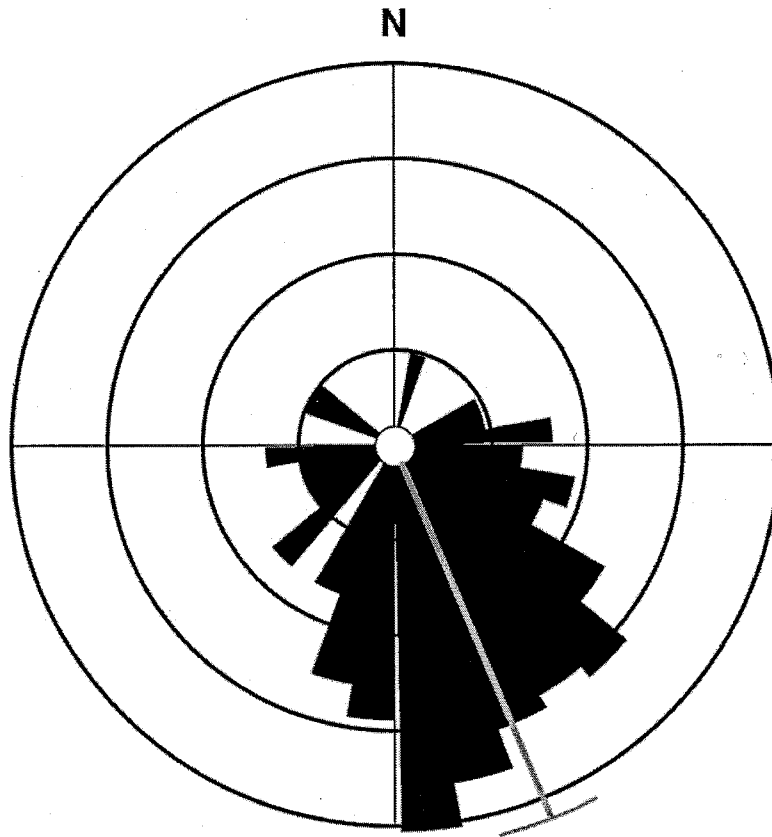


Figure 12. Rose diagram of paleocurrents (n=116, Appendix E) from the western-margin lithofacies assemblage, Arroyo Ojito Formation, indicating a south-southeast paleoflow direction of $157 \pm 8^\circ$. Data was analyzed in 10° intervals.

Measured Sections

The Marillo-Zia stratigraphic section is 449 m thick and was measured in the upper part of the Cerro Conejo Member of the Zia Formation and in the Navajo Draw, Loma Barbon, and Ceja Members of the Arroyo Ojito Formation (Fig. 13). The Marillo-Zia section was measured on the hanging wall of the Zia fault. The Navajo Draw Member in the Marillo-Zia section is 265 m thick tends to have a yellowish color, and contains

sandstone and mudstone beds. The contact between the Cerro Conejo and Navajo Draw members is gradational and interfingering and was chosen at the lowest presence of gravel containing volcanic and sandstone clasts. The Loma Barbon Member is 134 m thick, is reddish yellow to brown, and contains sandstone, mudstone, and conglomerate. The contact between the Navajo Draw and Loma Barbon members is sharp and was chosen at a color change from light gray to light brown. Large boulders, up to 2 m in diameter, are locally present in the Loma Barbon Member. The Ceja Member is 51 m thick at the Marillo-Zia Section. The contact between the Loma Barbon and Ceja members was chosen at an abrupt coarsening in the sediments. The Ceja Member tends to be reddish yellow to light brown and contains sandstone, conglomerate and minor mudstone beds. The top of the stratigraphic section ends at a degraded calcic soil exposed along the northern edge of the Llano de Albuquerque and southern margin of the Rio Jemez Valley. The upper part of the Marillo-Zia section tends to coarsen upwards. This coarsening upwards sequence is recognized at the type section of the Arroyo Ojito Formation (Connell et al., 1999) and also in drillholes in the Albuquerque area (Hawley et al., 1995; Connell et al., 1998a).

A stratigraphic section measured below upper Pliocene basalt flows at Santa Ana Mesa, just south of San Felipe Pueblo (SFP, Appendix A), is 106 m thick and exposes alternating layers of gravel, sand, and mud (Fig. 14). Several beds in the Loma Barbon Member contain rhizoconcretionary intervals, indistinct stratification, mottled colors, and weak soil horizon development. These features indicate bioturbation and paleosol development, suggesting that deposition of the Loma Barbon Member was episodic.

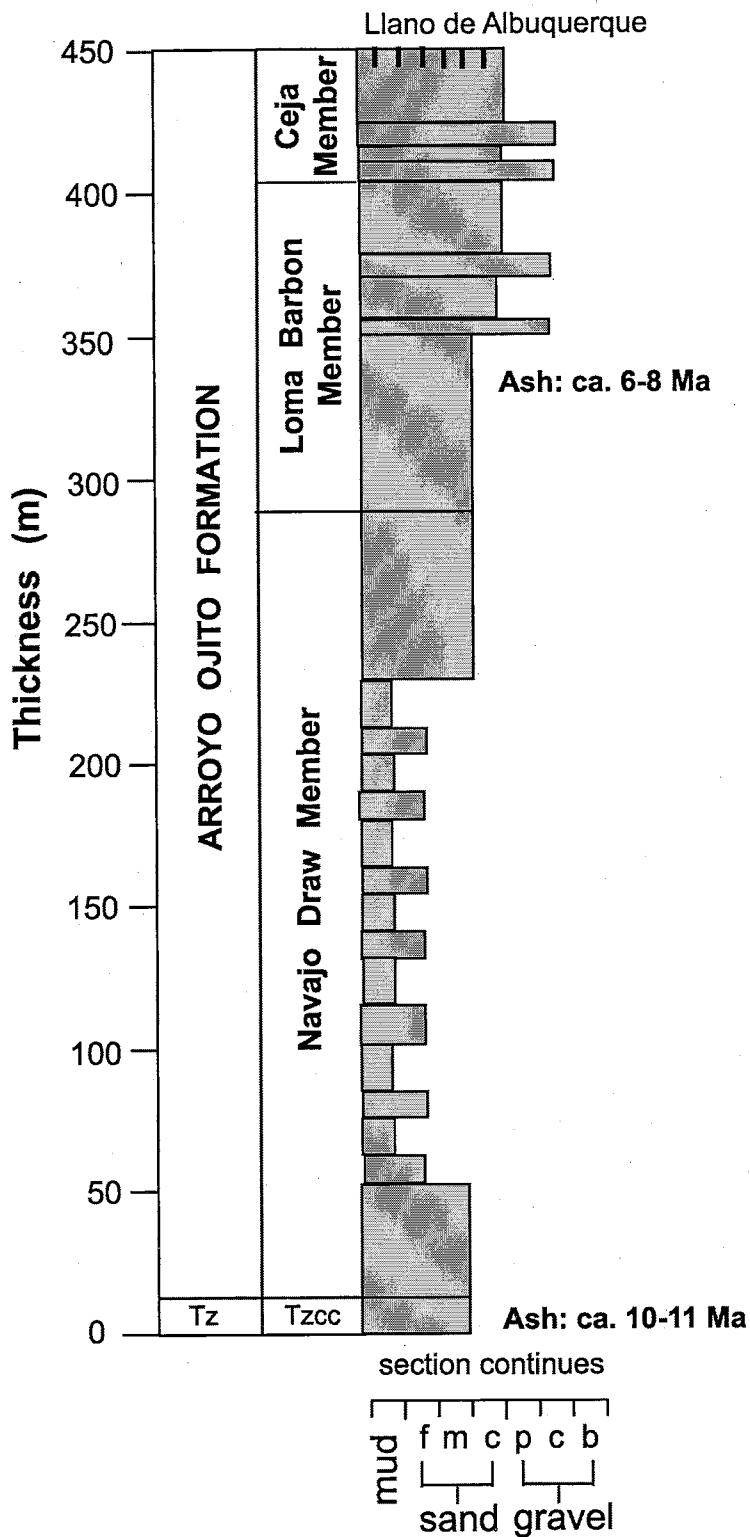


Figure 13. Composite, simplified stratigraphic column of the Marillo-Zia stratigraphic section. The Cerro Conejo Member (Tzcc) of the Zia Formation (Tz) is at the base of the section. Sample locations are noted to the right of the column. Symbols are described in Appendix A.

San Felipe Pueblo Section

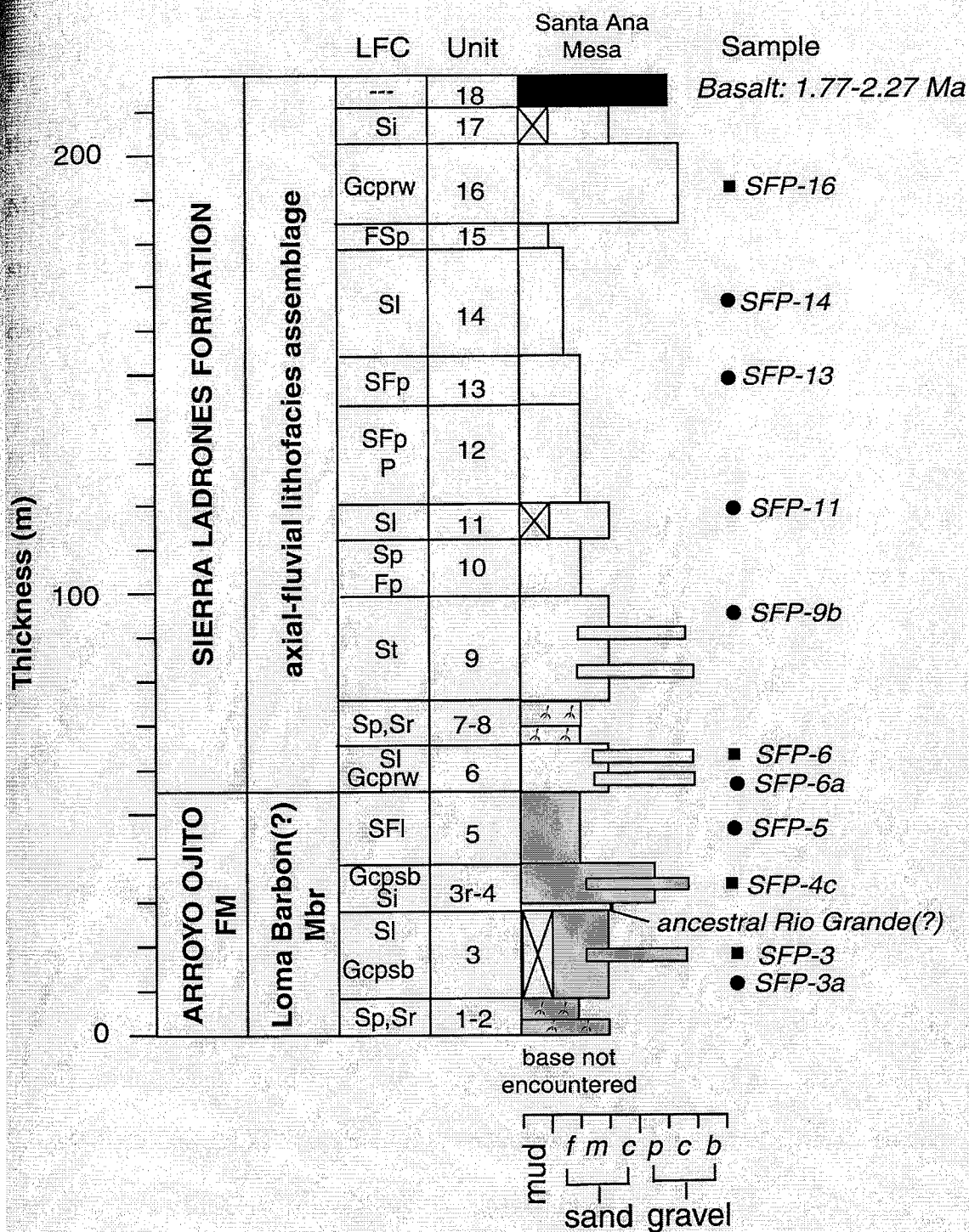


Figure 14. San Felipe Pueblo stratigraphic section, sample locations (Appendix A), and interpretations of lithofacies (Table 3). See Appendix A for explanation of symbols.

A section measured near Rio Rancho High School at Loma Colorado de Abajo (LC, Fig. 4) on the Loma Machette quadrangle is 30 m thick and exposes deposits assigned to the Ceja and Loma Barbon members of the Arroyo Ojito Formation (Appendix A; Morgan and Lucas, 2000). The presence of the pocket gopher *Geomys (Nerterogeomys)* sp. near the top of the Loma Barbon Member indicates a Blancan (Pliocene) age for these deposits (Morgan and Lucas, 2000). Fluvially recycled pumice pebbles are scattered in the lower part of this section. These pumice pebbles may be similar to suites of pumice pebbles recognized in the Isleta Pueblo and near Rio Rancho (Connell et al., 2001). Pumice pebbles associated with the upper part of the western-margin lithofacies assemblage have been dated with only partial success. Some of the $^{40}\text{Ar}/^{39}\text{Ar}$ dates are 3.0 Ma (Maldonado et al., 1999), which supports a Blancan age as determined biostratigraphically by Morgan and Lucas (2000).

Several beds show structures indicative of bioturbation and soil formation, suggesting episodic deposition. Gravels from the Loma Colorado section contain greater amounts of metaquartzite and fewer granitic rocks relative to other sites in the Arroyo Ojito Formation. A possible explanation is that these deposits are near the confluence of the western-margin and ancestral Rio Grande fluvial systems. The larger percentage of metaquartzite gravel could be due to mixing of the two fluvial systems. These samples fall within the standard deviation of Arroyo Ojito gravels, thus, the differences could merely reflect variation within the sample population.

Numerous lithofacies types occur in the western-margin lithofacies assemblage. The dominant lithofacies types include clast supported, planar bedded gravels with an

apparent bimodal clast size distribution (Gcpsb). As discussed previously, these gravels are commonly

1-5 m thick and extend laterally up to 20 to 80 m. Planar bedded sands (lithofacies Sp) are also typical of the western-margin lithofacies assemblage. Thickness of these sands varies from millimeter-scale laminations to beds 1 to 30 cm thick (Fig. 15). The third dominant lithofacies in the western-margin assemblage is interbedded sand and mud beds (lithofacies SFp). These units typically consist of planar stratified, interbedded sand and mud beds 10 to 50 cm thick.

The fifth major lithofacies in the western-margin assemblage is sand with indistinct bedding (lithofacies Si). This lithofacies is massive or contains vague internal laminations with scattered white calcium-carbonate cemented mottles or rhizoconcretions (Fig. 16). Numerous, less common lithofacies also occur in deposits of the western-margin assemblage. Low angle cross-stratified sand (lithofacies Sl) is thinly to thickly bedded and typically has internal laminations (Fig. 15). Low angle cross-stratified sand also occurs interbedded with muds (lithofacies SF1). Interbeds range from 10 to 30 cm in thickness. Lithofacies Sr (Fig. 17) contains 2- to 10-mm diameter rhizoconcretions that typically range up to 40 mm in length. Fine-grained (muddy) sediments include silt and clay that have millimeter scale planar laminations (Fig. 18). These muds are assigned to lithofacies Fp. Mud deposits that are massive or contain indistinct laminations are described as lithofacies Fi. Paleosols (P) typically have a pale color, soil horizons, and are cemented with micritic calcium carbonate and exhibit pedogenic carbonate morphology.

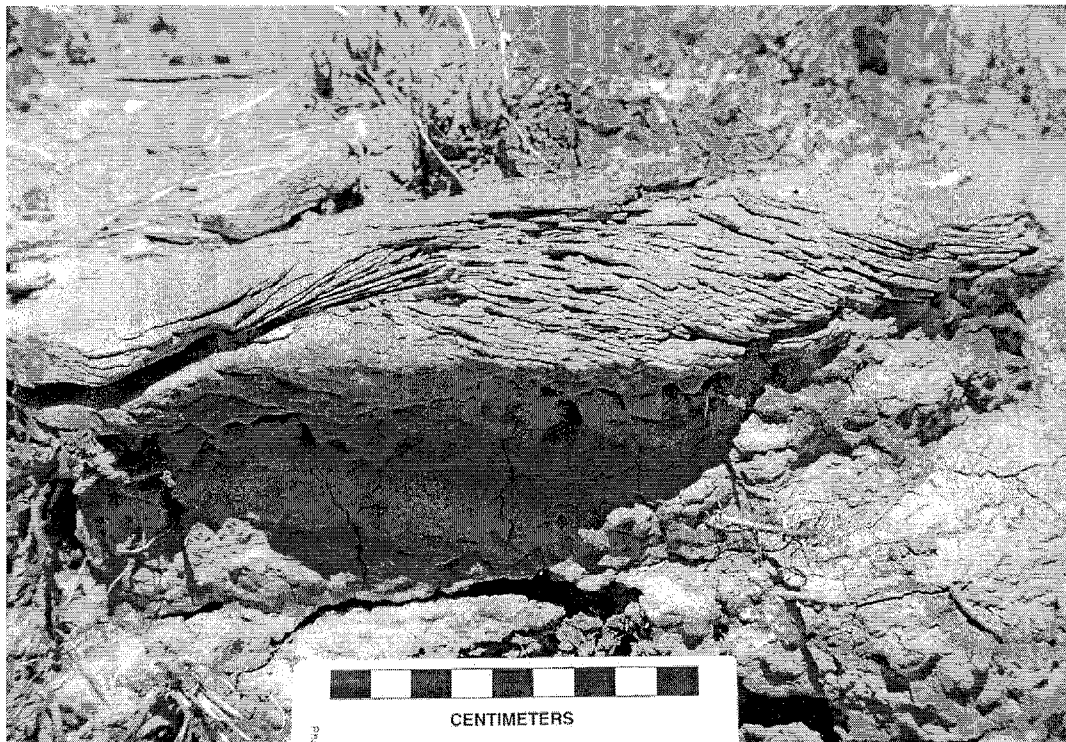
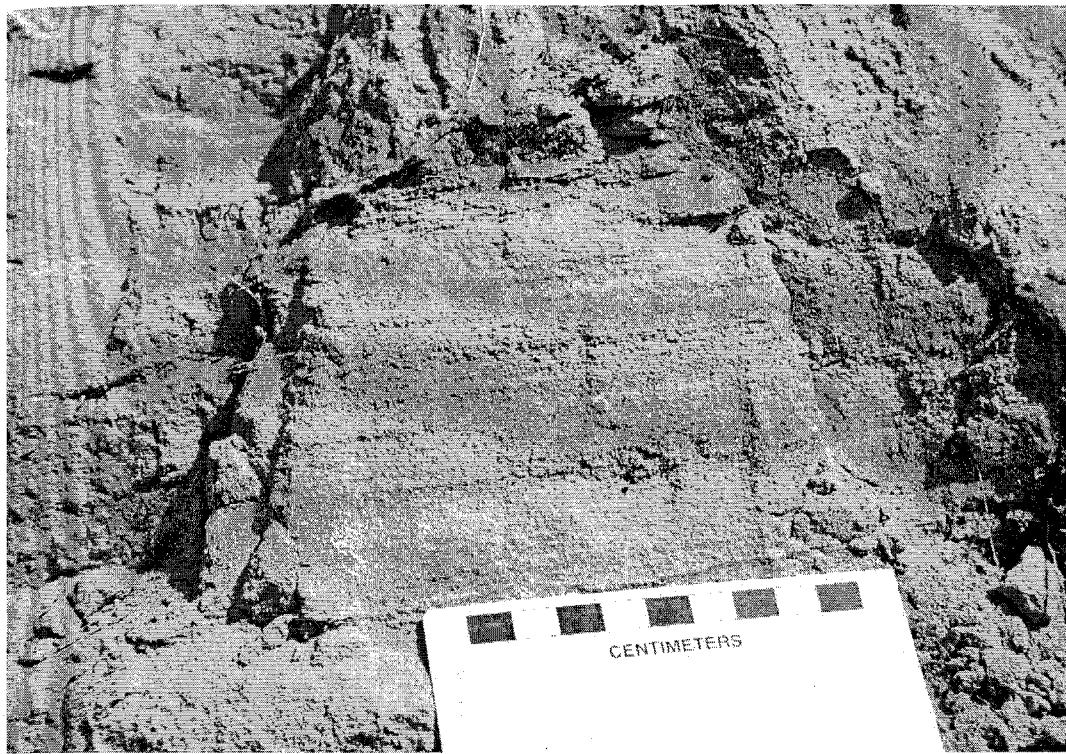


Figure 15. Photographs of cemented and laminated sandstone of the Arroyo Ojito Formation in the Marillo-Zia stratigraphic section. Top: Planar laminated sandstone (Sp) in unit 15. Bottom: Low-angle cross beds (Sl) overlies mottled and bioturbated sandstone (Si) in unit 8.

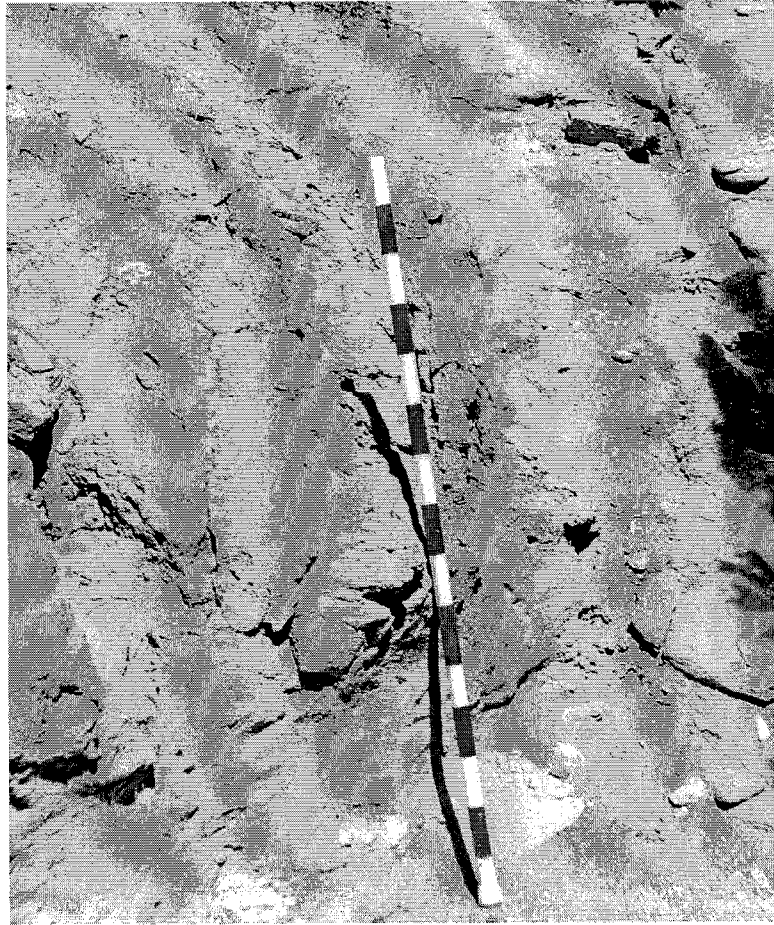


Figure 16. Photograph of vaguely bedded and mottled sandstone (Si) in Loma Barbon Member of the Arroyo Ojito Formation, unit 1 of the San Felipe Pueblo stratigraphic section. Scale is 1.5 m long.

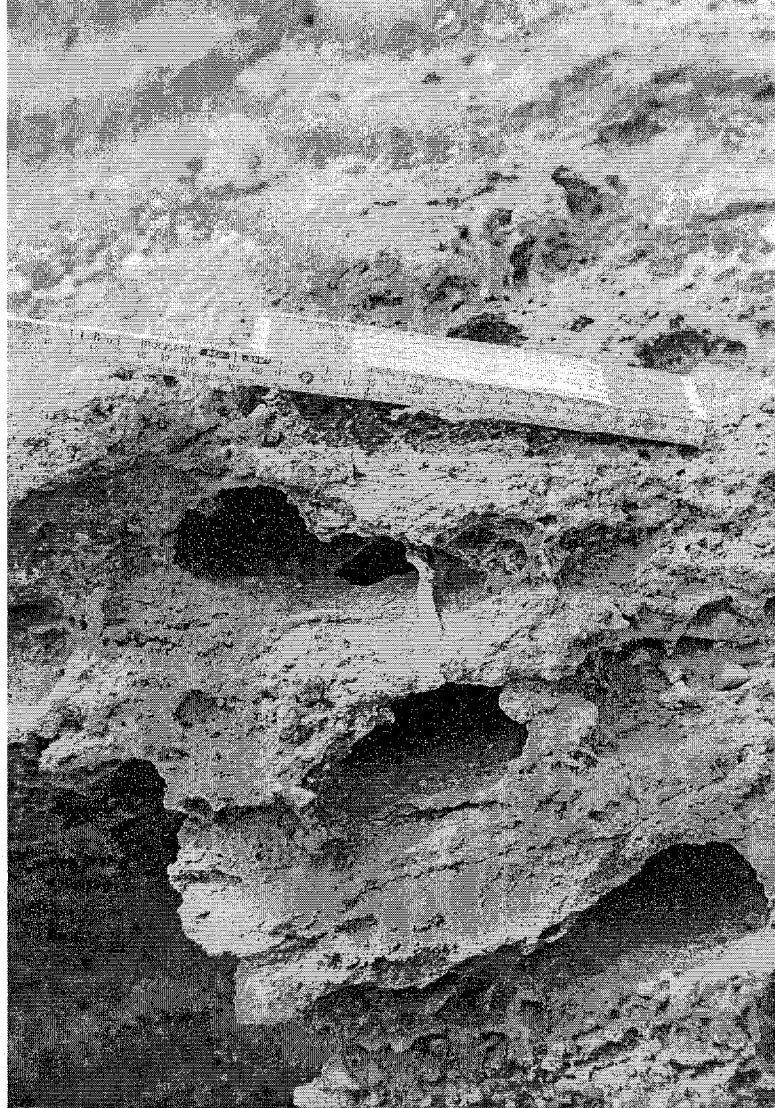


Figure 17. Photograph of subhorizontal and subvertical rhizoconcretions (Sr) in a well cemented bed of the Loma Barbon Member of the Arroyo Ojito Formation, unit 2 of the San Felipe Pueblo stratigraphic section. Scale is 32 cm long.

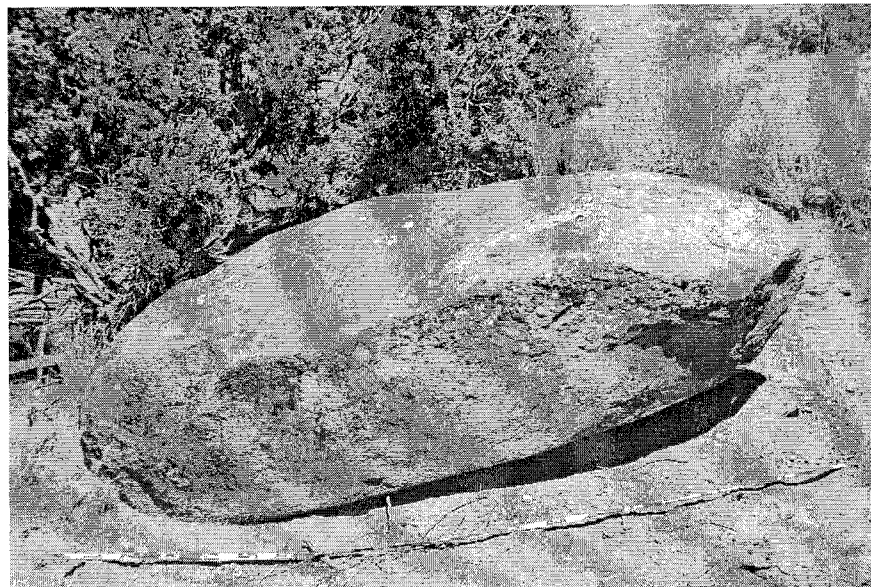
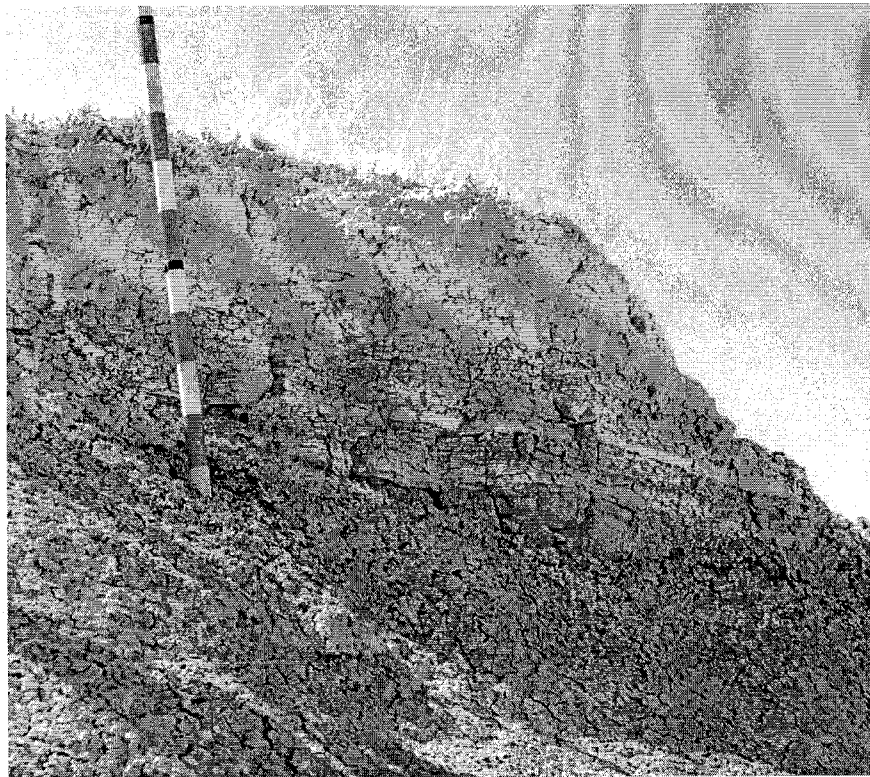


Figure 18. Photographs of thinly bedded mudstone and sandstone (SFp) in the Loma Barbon Member of the Arroyo Ojito Formation (top), unit E of the Marillo stratigraphic section. Scale shows 10 cm striped intervals. Bottom: A 2-m long boulder of arkosic sandstone in the Loma Barbon Member of the Arroyo Ojito Formation. This boulder is about 15-20 km south-southeast of upper Paleozoic-Mesozoic strata exposed along the southern flanks of the Sierra Nacimiento.

The Arroyo Ojito Formation contains a greater proportion of mud (silt and clay) and fewer gravels than the axial-fluvial deposits of the Sierra Ladrones Formation. Rare scattered boulders, up to 2 m in diameter, are found in the Loma Barbon Member along the southern margin of the Rio Jemez Valley (Fig. 18). These boulders are composed of reddish-brown to yellowish-brown quartz rich sandstone. Smaller boulders are composed of rounded sandstone, subrounded to subangular granite, and subangular to angular Pedernal chert.

Sierra Ladrones Formation

Ancestral Rio Grande Lithofacies Assemblage

Deposits of the axial-fluvial Sierra Ladrones Formation (ancestral Rio Grande lithofacies) tend to be grayer than those of the Arroyo Ojito Formation, although pale yellow (2.5Y 8/2 to 5Y 7/3) is a common color. Typical colors are pinkish gray (5YR 6/2 to 5YR 7/2), light gray (10YR 7/2 to 2.5Y 7/2) and yellowish brown (10YR 5/8). The ancestral Rio Grande lithofacies is typically poorly exposed, forming low, rounded hills, whereas the piedmont deposits typically form steeper slopes and are better exposed.

Ancestral Rio Grande deposits are weakly cemented to non-cemented and include gravel and sand with minor mud. Muddy deposits are preserved west of the Rio Grande Valley at San Felipe Pueblo, where they interfinger with sand and pebbly sand of the ancestral Rio Grande. To the east, towards the faulted eastern margin of the basin, mud beds are sparse and the presence of muddy intervals are recognized by the presence of rounded

mudballs within thickly bedded sands. Ancestral Rio Grande deposits include thickly bedded (1-3 m thick), clast-supported, well sorted, planar- and trough-cross stratified gravels (Gcprw and Gctrw), which contain rounded to well rounded and mostly clast supported and open-framework pebbles and cobbles. Gravel beds tend to be thickly bedded and have scoured bases, resulting in preservation of thickly bedded successions of stacked pebble and cobble gravel beds (Fig. 19).

Ancestral Rio Grande deposits contain abundant subrounded volcanic rocks and rounded metaquartzite. Volcanic rocks include a variety of tuffs, tan porphyritic igneous rocks, andesitic, and rhyolitic clasts. Metaquartzite is found in various colors, including a bluish-purple color. Quartz grains are fused together and many of the quartzite clasts show bedding and cross bedding, indicating a sedimentary origin. A likely source of sedimentary quartzite is the Proterozoic Ortega Group of northern New Mexico (Soegaard and Eriksson, 1985); however, petrographic correlations to the Ortega Group were not made.

Stratigraphic sections of the ancestral Rio Grande facies of the Sierra Ladrones Formation were measured within San Felipe Pueblo. These sections were supplemented with data from the Isleta Pueblo (Appendix A). At the San Felipe Pueblo (San Felipe stratigraphic section), the Arroyo Ojito Formation interfingers with axial fluvial deposits of the ancestral Rio Grande (Fig. 20). The Tonque Arroyo section is 36 m thick. Most of the Tonque Arroyo section is measured in ancestral Rio Grande sediments with less than 3 m of eastern-margin piedmont facies sediments at the top of the section. The Tonque Arroyo stratigraphic section is important because a basalt of Santa Ana Mesa volcanic

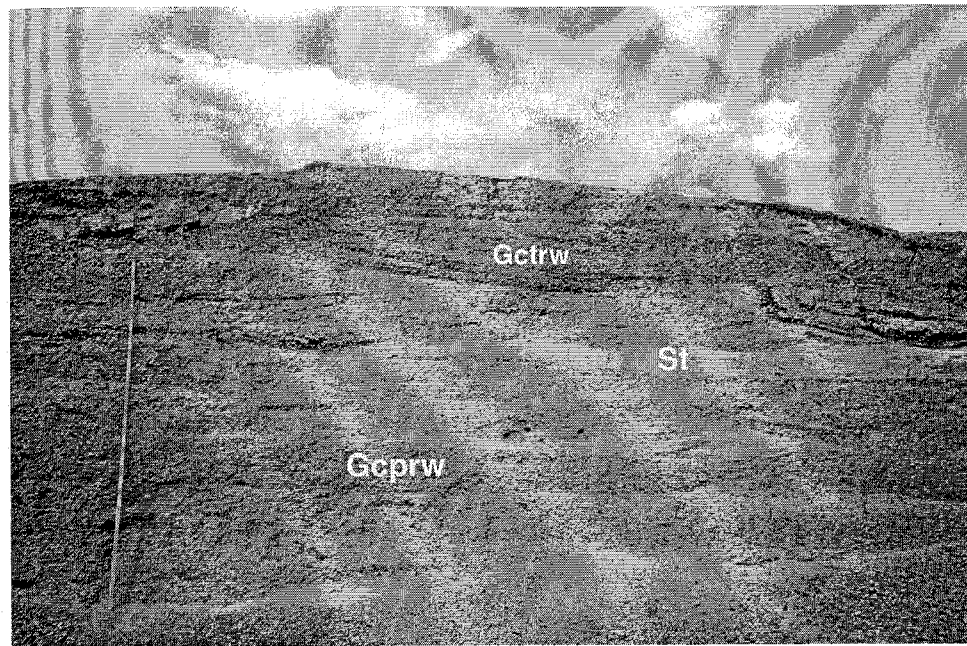


Figure 19. Photographs of clast-supported (mostly open framework), thickly bedded, pebble and cobble gravel of the ancestral Rio Grande deposits of the Sierra Ladrones Formation. Top: 1-3 m thick stacked gravel channels exposed in unit 1 of the San Felipe gravel quarry site (Scale is 7 m high). Photograph courtesy of S.D. Connell. Bottom: Open-framework pebble gravel (Gcprw) beneath 2.58 Ma basalt flow of Santa Ana Mesa exposed in unit 1 of the Tonque Arroyo site (TQA). Note the abundant rounded metaquartzite and volcanic clasts. Hammer is 26 cm long.

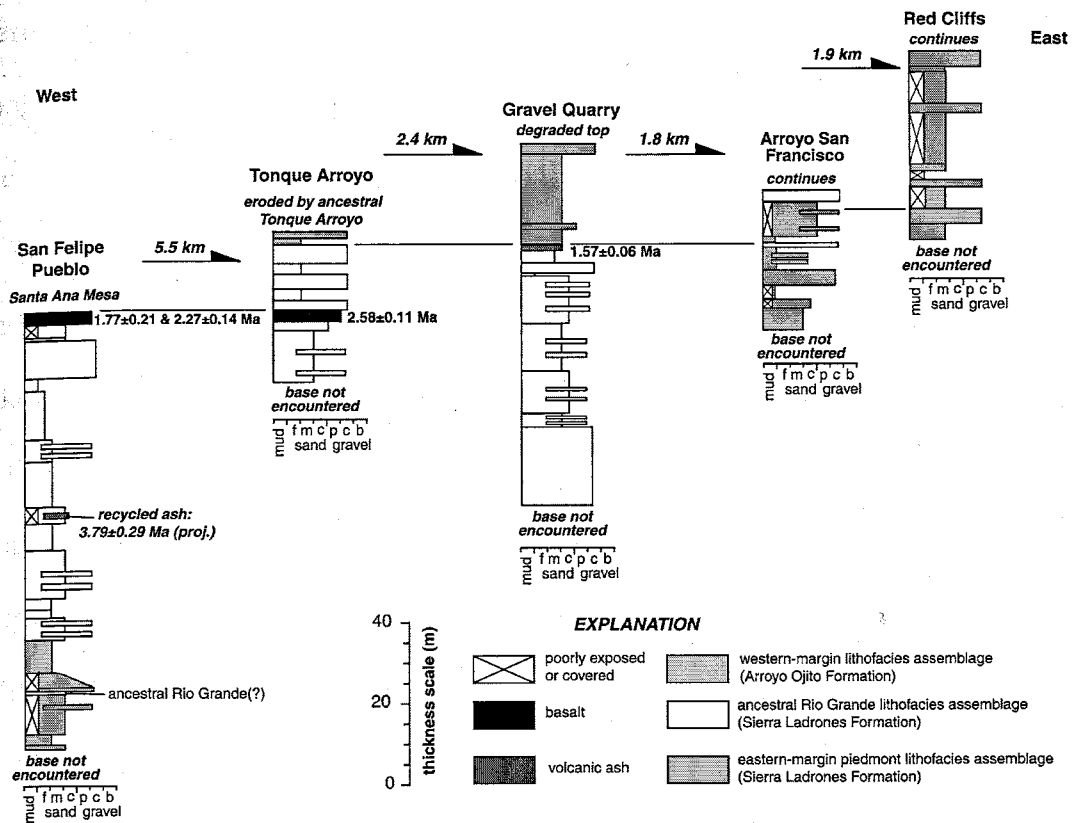


Figure 20. Stratigraphic fence diagram constructed across part of the southern Santo Domingo sub-basin of the northern Albuquerque basin at San Felipe Pueblo, illustrating the interfingering nature of the ancestral Rio Grande deposits with both the western-margin lithofacies assemblage and the eastern piedmont lithofacies assemblage.

field is located in the middle of this section and allows for correlation between this section and the San Felipe section.

A K-Ar date is reported for flows on Santa Ana Mesa at 2.5 ± 0.3 Ma (Bachman and Mehnert, 1978). A sample at the top of Santa Ana Mesa, at the San Felipe Pueblo stratigraphic section, yielded a $^{40}\text{Ar}/^{39}\text{Ar}$ date of 1.77 ± 0.21 Ma (SF-bas3; Cather and Connell, 1998). Other basalt samples taken along the eastern margin of Santa Ana Mesa yielded dates of 2.27 ± 0.14 Ma (SF-bas2) and 2.24 ± 0.22 Ma (SF-bas1; Cather and Connell, 1998). A basaltic lava flow correlated to one of the Santa Ana Mesa flows

interfingers with pebble conglomerate and pebbly sand of the ancestral Rio Grande lithofacies assemblage at the Tonque Arroyo section. This basalt flow yielded a $^{40}\text{Ar}/^{39}\text{Ar}$ date of 2.58 ± 0.11 Ma (NMGRL-51967; Peters, 2001).

The San Felipe Pueblo Gravel Quarry section is 87 m thick. Most of this section consists of ancestral Rio Grande sediments, although 27 m of piedmont facies sediment makes up the top of the section. Thick sequences of stacked gravel beds are exposed at the Gravel Quarry section. In addition, the ash of unit 9 of the gravel quarry section (Appendix A) is geochemically similar to the Cerro Toledo Rhyolite (N. Dunbar, 2000, written commun. to S.D. Connell) and yields a $^{40}\text{Ar}/^{39}\text{Ar}$ age of 1.57 ± 0.06 Ma (NMGRL-9749; W.C. McIntosh, unpubl. data). Ancestral Rio Grande sediments interfinger with piedmont sediments at the Arroyo San Francisco stratigraphic section. This section is 33 m thick and exposes 14 m of ancestral Rio Grande sediments. This stratigraphic section illustrates the interfingering nature of the ancestral Rio Grande and piedmont deposits (Fig. 20).

Plutonic and metamorphic clasts are present in minor quantities (~10%) and include rounded black diabase and subrounded pink coarse-grained and porphyritic granitic pebbles. Clasts of Pedernal chert are relatively rare, commonly subrounded, and smaller in size (typically pebble sized), relative to their abundance in western-margin deposits, which are commonly subangular to angular cobbles and pebbles. Paleocurrents measured from imbricated clasts ($n=39$) trend to the southwest and have an azimuth of $209 \pm 14^\circ$ (Fig. 21). This orientation is consistent with southward transport of an axial river and is similar to the orientation of the modern Rio Grande Valley in the northern part of the

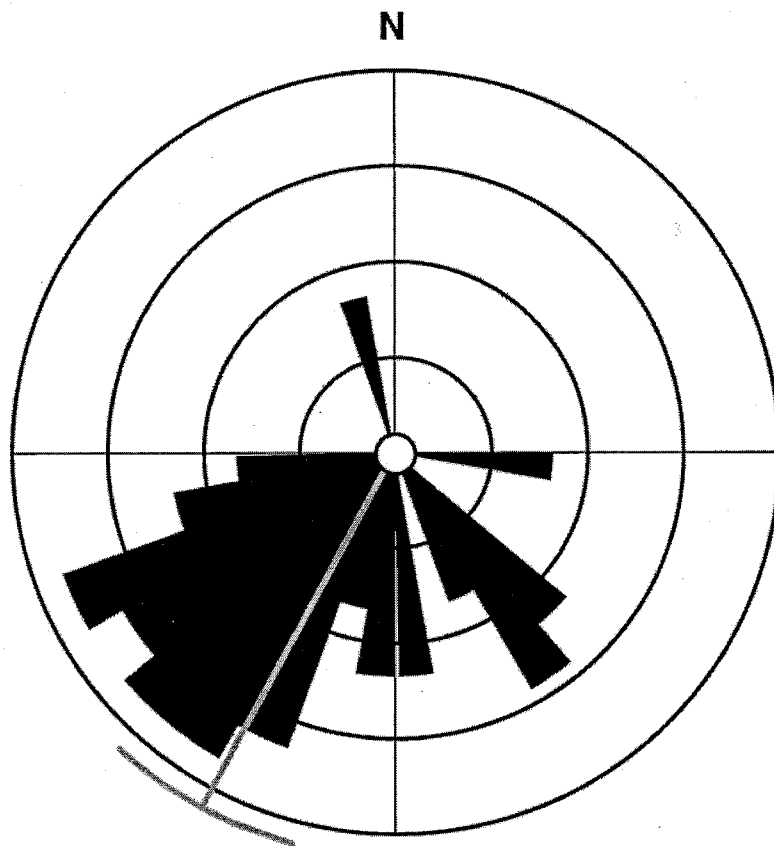


Figure 21. Rose diagram of paleocurrents (n=41) from the ancestral Rio Grande deposits of the Sierra Ladrones Formation (Appendix E) indicating southwest paleoflow direction of $209\pm 14^\circ$. Data was analyzed in 10° intervals.

Albuquerque Basin (Fig. 4). Scatter in the paleocurrent data is most likely due to variations in the stream flow direction at different parts of the river system (Boggs, 1995).

Sand is recognized in a wide variety of lithofacies in the ancestral Rio Grande sediments. Planar laminated sand (Sp), low angle cross laminated sand (Sl), and trough cross laminated sand (St) are found in beds a meter or less thick. Deposits with indistinct bedding (Si) and randomly scattered pebbles throughout the unit are thickly bedded and

bioturbated. Sand is medium to thickly bedded (up to 50 cm thick) and is a common lithofacies in the ancestral Rio Grande deposits. Sand ranges from lithic arkose to feldspathic litharenite and is generally fine to coarse and moderately to well sorted. Quartz, feldspar, and volcanic grains with zoned plagioclase phenocrysts are important constituents. Ancestral Rio Grande sands tend to contain less chert and granite grains than sands of the western-margin lithofacies assemblage (Appendix C).

Metaquartzite gravels commonly mantle slopes giving the deposits a gravelly appearance, however, deposits contain abundant trough-cross bedded sand and gravelly sand. Mud is rare and commonly found as armored mudballs and rounded rip-up clasts in sand and gravel lithofacies (Fig. 22).

Fine-grained deposits in the lithofacies assemblage of the ancestral Rio Grande are sparse. The presence of armored mudballs in several beds (Fig. 22) indicates that mud beds were present, though they are only locally preserved near the western margin of this lithofacies assemblage where it interfingers with the Arroyo Ojito Formation (Fig. 14). The preservation of muddy beds west of the Rio Grande, on the up-dip portion of the Santo Domingo sub-basin, and extensive recycling of mudbeds into mudballs towards the master fault to the east suggests bank instability to the east and possible tectonic control on the preservation of muddy facies, or rapid migration of channel facies (Mack and James, 1993).



Figure 22. Photograph, looking east, of ancestral Rio Grande sand in unit 2 of the San Felipe Pueblo Gravel Quarry section, illustrating cross-stratified sand (St) and a bed of armored mudballs (indicated by the dark arrows). Exposures are about 5 m thick. The northern flank of Sandia Mountains is in background to right. Photograph courtesy of S.D. Connell.

Eastern-Margin Piedmont Lithofacies Assemblage

Two stratigraphic sections were measured in deposits of the eastern-margin piedmont lithofacies assemblage, the Arroyo San Francisco, and Red Cliffs sections (Appendix A). Deposits of the Sierra Ladrones Formation (piedmont lithofacies assemblage) are exposed along the eastern margin of the basin and along the western front of the Sandia Mountains. Deposits of the eastern-margin piedmont lithofacies assemblage tend to be redder than the ancestral Rio Grande or western-margin lithofacies assemblages. Piedmont colors are commonly yellowish red (5YR 5/6), reddish yellow (7.5YR 6/6), and

very pale brown (10YR 7/4). Piedmont lithofacies are commonly well to moderately cemented with calcium-carbonate and tend to form cliffs or steep slopes (Fig. 23).

Gravel of the piedmont lithofacies assemblage crop out in beds up to 5 m thick that extend tens of meters laterally. The base of these gravel beds typically show a few centimeters of scour into the underlying beds. Gravel is subangular to subrounded and poorly sorted (Fig. 23). Clast-supported, planar bedded conglomerate (Gcsp), and matrix-supported, vaguely bedded conglomerate (Gmisp) are common constituents. Bluish-gray limestone and reddish-brown and yellowish-brown quartz-rich and arkosic sandstone are the most abundant clast types; reddish-brown siltstone and gray quartz-rich sandstone are minor components. Plutonic and metamorphic rocks are also present, especially pink, coarse-grained, commonly porphyritic granite and pink gneissic or foliated granitic rocks. Quartz gravel is angular, commonly white, has a vitreous luster, and are probably correlative to numerous vein quartz-dikes that intrude the Sandia granite and Rincon metamorphics (Kelley, 1977). Gray porphyritic volcanic and hypabyssal-intrusive gravel clasts are not common. These volcanic rocks are of intermediate composition and are probably derived from the Ortiz Mountains, which lie on the eastern edge of the Hagan embayment and Santo Domingo sub-basin east of the San Felipe Pueblo study area.

Paleocurrent measurements from imbricated gravels (n=42) indicate a westerly direction of paleoflow having an azimuth of $271 \pm 15^\circ$ (Fig. 24). This flow direction is transverse to the axial-fluvial lithofacies assemblage and supports a local derivation of deposits from the eastern basin margin.

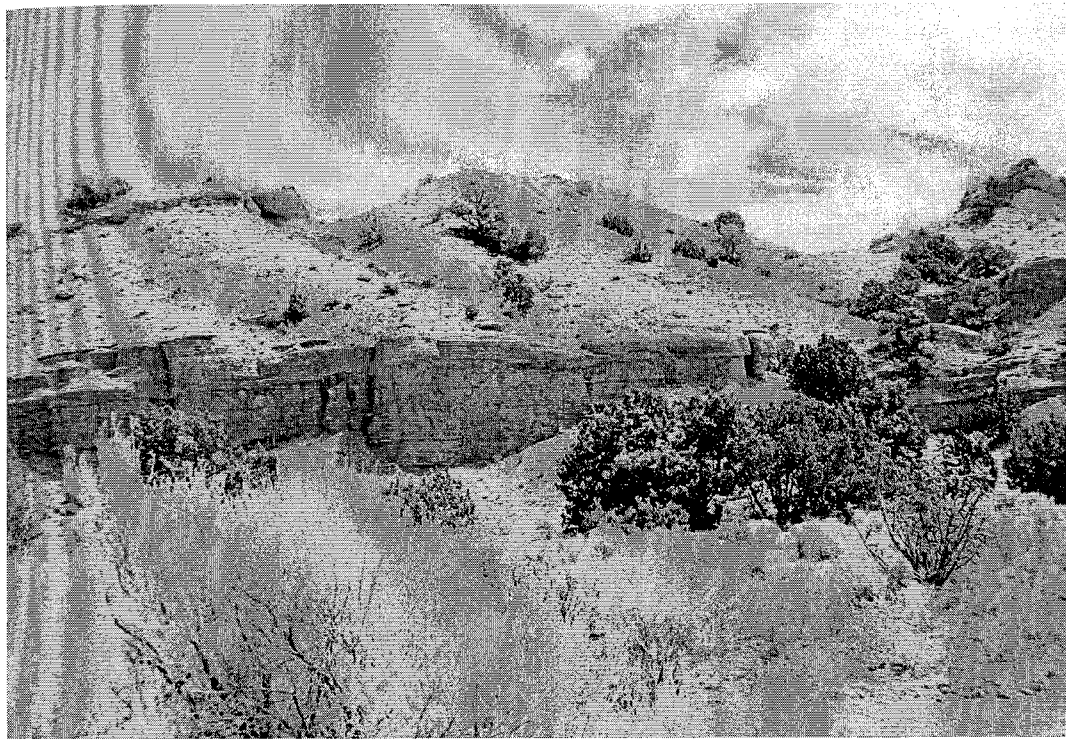


Figure 23. Photographs of eastern-margin piedmont deposits of the Sierra Ladrone Formation at the Red Cliffs stratigraphic section. Top: Cemented piedmont deposits of units 1-4. Piedmont deposits tend to be better cemented and better exposed than the loose and relatively uncemented ancestral Rio Grande deposits. Bottom: Pebble to cobble conglomerate (Gcsp) of unit 2. Note the angularity of the clasts and overall poor sorting of exposures. Jacob staff is divided into 10 cm intervals.

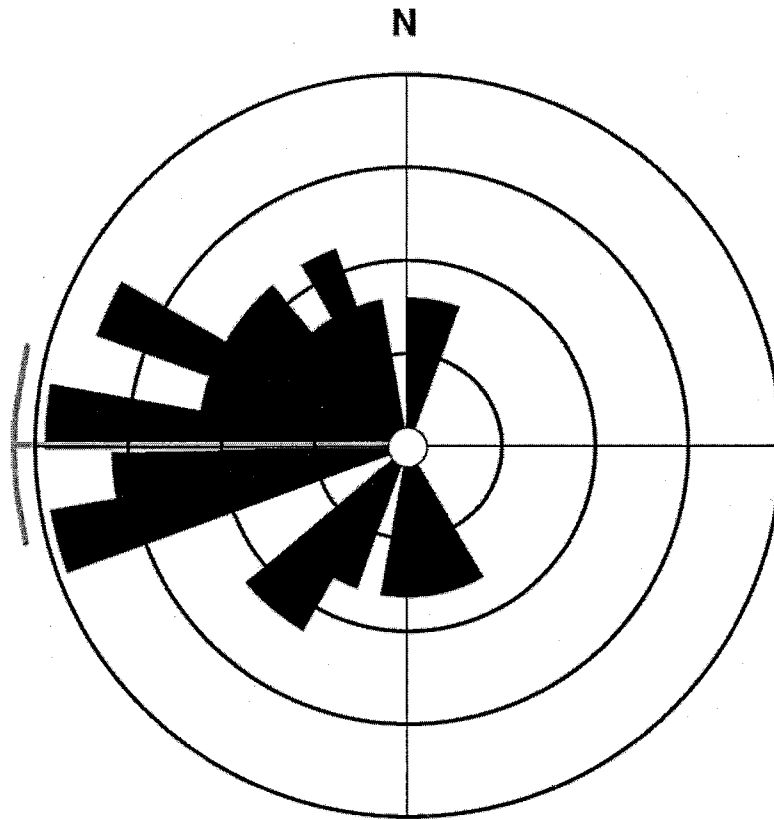


Figure 24. Rose diagram of paleocurrents (n=42) from the eastern-margin piedmont lithofacies assemblage of the Sierra Ladrones Formation (Appendix E) indicating westerly paleoflow direction of $271 \pm 15^\circ$. Data was analyzed in 10° intervals.

Conglomeratic deposits are poorly sorted and resemble textures of the Arroyo Ojito Formation; however, piedmont deposits are commonly better cemented and more angular than the ancestral Rio Grande and western-margin lithofacies assemblages.

Sand beds tend to be about 50 cm thick with internal planar laminations (Sp), low angle cross laminations (Sl), or trough cross laminations (St; Fig. 25). Sandstone exhibiting indistinct bedding with randomly scattered pebbles (Si) or rhizoconcretions (Sr) is common at the tops of fining upward sequences. These fining upward sequences have variable thickness, but are up to 3 m thick. Sandstone up to 50 cm thick with interbedded



Figure 25. Photograph of weakly cemented, trough cross bedded pebbly sand (St) in the eastern-margin piedmont deposits of the Sierra Ladrones Formation, unit 12 of the San Felipe Pueblo gravel quarry stratigraphic section (Appendix A). Hammer is 26 cm long.

centimeter-scale mud beds is assigned to lithofacies SFp where they have planar laminations and SFl where the sand beds exhibit low angle cross laminations. Sands range from lithic arkose, arkose, and subarkose and are generally fine- to very coarse-grained and moderately sorted. Quartz and feldspars are common constituents. Volcanic grains are rare or absent.

Fine-grained (muddy) lithofacies contain silt and clay and include planar bedded muds (Fp), muds with indistinct bedding (Fi), and muds with rhizoconcretions (Fr). Fine-grained beds are up to 30 cm thick and typically form the tops of fining-upward

sequences. Piedmont deposits commonly contain more lithofacies indicative of plant growth and bioturbation (lithofacies Si, Sr, Fi, Fr) than in the ancestral Rio Grande and Arroyo Ojito lithofacies assemblages. Paleosols (lithofacies P) are locally common and typically cap the tops of fining-upwards sequences.

Deposits of the piedmont lithofacies assemblage are dominantly sandy (about 60% sand). However, conglomeratic deposits are also an important constituent, forming approximately 30% of the deposits. Mud is not as prevalent in the piedmont assemblage, forming around 10% of the deposits. Of the three lithofacies assemblages discussed in this study, the piedmont is the best cemented. At least 50% of the deposits are well cemented with the remainder moderately cemented. Conglomerates and medium- to coarse-grained sandstones are generally cemented. Fine-grained sandstones and mudstones are moderately to weakly cemented.

Summary

The western-margin lithofacies assemblage can be recognized on the basis of several features (Table 4). First, the outcrops of this assemblage typically weather into badlands-type topography. Western-margin deposits also contain more muddy sediments than the ancestral Rio Grande and eastern piedmont lithofacies assemblages. Western-margin deposits contain approximately 15% gravel, 60% sand, and 25% mud, although the proportion of gravel units increases up section in the Arroyo Ojito Formation. The dominant lithofacies in the western-margin assemblage include clast supported, planar bedded gravels with a bimodal clast size distribution (Gcpsb), planar bedded sands (Sp), and planar, interbedded sands and muds (SFp). Important, but minor lithofacies

in the western-margin assemblage include sands with rhizoconcretions (Sr) and calcic paleosols (P).

The ancestral Rio Grande lithofacies assemblage crops out as low, rounded gravel covered hills. Sediments of this assemblage are mostly gravel and sand, with minor mud beds found locally at the western margin of this assemblage. The ancestral Rio Grande lithofacies assemblage typically consists of approximately 45% gravel, 50% sand, and 5% mud. The dominant lithofacies of this assemblage includes clast supported, rounded and well sorted, planar bedded gravels (Gcprw). Planar bedded sands (Sp) and sands with low angle cross stratification (Sl) are also typically common. Minor lithofacies that are also present in the ancestral Rio Grande lithofacies assemblage include clast supported, rounded and well sorted, trough cross stratified gravels (Gctrw), trough cross stratified sands (St). Sands with indistinct bedding (Si), sands with rhizoconcretions (Sr), and planar bedded muds (Fp) are present in this lithofacies assemblage as minor constituents.

The piedmont lithofacies assemblage tends to be more cemented than either the ancestral Rio Grande assemblage or the western-margin assemblage. Piedmont deposits typically form cliffs or steep hillslopes. The piedmont lithofacies assemblage typically consists of approximately 35% gravel, 55% sand, and 10% mud. The principal lithofacies in this assemblage are clast supported, subangular to angular, poorly sorted, planar bedded gravels (Gcsp), as well as sands with indistinct bedding (Si). Minor lithofacies in the assemblage include matrix supported, subangular to angular, poorly sorted gravels (Gmisp), planar bedded sands (Sp), sands with trough cross stratification (St) sands with rhizoconcretions (Sr), muds with indistinct bedding (Fi) and calcic soils (P).

PETROGRAPHY

Introduction

Gravel and sand compositions were determined from samples collected at numerous stratigraphic sections, selected localities, and two drillhole sites (Fig. 4). This section presents results of studies of gravel and sand composition and how these data can be used to differentiate western-margin, axial-fluvial, or eastern-margin piedmont lithofacies assemblages. This section concludes with an evaluation of drillhole data and comparisons to a previous study of cuttings and core petrography done in the Albuquerque area by Gillentine (1996)

Gravel Composition

Introduction

The three lithofacies assemblages described in this study have distinct gravel types. The western-margin lithofacies (Arroyo Ojito Formation) contains abundant chert, volcanic, sandstone, and granitic clasts. The ancestral Rio Grande lithofacies of the Sierra Ladrones Formation contains metaquartzite and volcanic rocks with a small proportion of

plutonic and metamorphic clasts and very sparse sedimentary rocks. Gravel of the piedmont lithofacies assemblage of the Sierra Ladrones Formation is dominated by subrounded fossiliferous blue-gray limestone and reddish-brown to yellowish-brown and light-gray quartz-rich sandstone with subordinate angular vein quartz, chert, porphyritic granite, schist, gneiss, and rare intermediate volcanic rocks of intermediate composition (Appendix B).

Comparing modal composition of gravel (Table 7) allows for examination of compositional trends. Gravel from the three lithofacies assemblages is dominantly lithic in nature (Fig. 26). Western-margin assemblage gravels are the most feldspathic, ancestral Rio Grande gravels are dominated by quartz and volcanic lithic detritus, and piedmont deposits contain mostly lithic sedimentary and feldspathic detritus. All three facies contain sparse or nonexistent lithic-metamorphic fragments (Fig. 27). The relative abundance of chert and metaquartzite are important discriminants (Fig. 28), as are proportions of chert and metaquartzite to the sedimentary, volcanic and plutonic-metamorphic fractions of the gravels (Table 8, Figs. 29, 30 and 31). Comparison of chert, granite, and volcanic constituents, an important relationship in the sand fraction, shows distinct, but somewhat overlapping relationships (Fig. 32).

Common gravel constituents of all three lithofacies assemblages include metaquartzite, chert, volcanic, sedimentary rocks, and plutonic and metamorphic rocks. Rounded metaquartzite pebbles and cobbles in the ancestral Rio Grande and western-margin lithofacies assemblages contain fine- to coarse-grained, fused quartz grains, with minor, fine- to medium-grained opaque heavy mineral grains. Metaquartzite gravels commonly exhibit internal sedimentary structures such as planar laminations and cross

Table 7. Recalculated detrital parameters for gravel, percent normalized to total number of clasts counted ($N^* = N-U$). See Table 2 for description of gravel constituents.

| Recalculated Parameter (%) | Constituents |
|----------------------------|---|
| Q | $(Q + Qw + Qp + Qg + Ql + Qcb + Qcg + Qcr + Qcp + Qcl)/N^*$ |
| F | $(PMgr + PMgw + PMgp)/N^*$ |
| L | $(Vtg + Vtt + Vtr + Vb + Va + Vr + Ssg + Ssr + Ssy + Sir + Sc + Sw + Sl + PMn + PMs + PMd)/N^*$ |
| Lm | $(PMn + PMs + PMd)/L$ |
| Lv | $(Vtg + Vtt + Vtr + Vb + Va + Vr)/L$ |
| Ls | $(Ssg + Ssr + Ssy + Sir + Sc + Sw + Sl)/L$ |
| V | $(Vtg + Vtt + Vtw + Vtr + Vb + Va + Vr)/N^*$ |
| S | $(Ssg + Ssr + Ssy + Sir + Sc + Sw + Sl)/N^*$ |
| Pm | $(PMgr + PMgw + PMgp + PMn + PMs + PMd)/N^*$ |
| Qq | $(Q + Qw + Qp + Qg + Ql)/N^*$ |
| Qc | $(Qcb + Qcg + Qcr + Qcp + Qcl)/N^*$ |

Table 8. Mean and standard deviation (1σ) of pebble and cobble composition for the western, axial, and eastern piedmont lithofacies assemblages in the study area (Table 7). Distinguishing relationships denoted by asterisk (*).

| Detrital components | Western (%) | Axial (%) | Eastern (%) |
|---------------------|-------------|-----------|-------------|
| QFL%Q | 23±12 | 31±6 | 11±5 |
| QFL%F | 22±18 | 9±5 | 17±4 |
| QFL%L | 54±14 | 60±7 | 71±6 |
| LmLvLs%Lm* | 0 | 0 | 3±2 |
| LmLvLs%Lv* | 61±13 | 92±4 | 9±8 |
| LmLvLs%Ls* | 36±13 | 3±2 | 87±8 |
| QcQq%Qc* | 15±8 | 1±1 | 3±2 |
| QcQq%Qq* | 9±7 | 30±6 | 9±4 |
| QcQqPm%Qc | 36±19 | 3±2 | 8±5 |
| QcQqPm%Qq | 20±14 | 71±12 | 29±10 |
| QcQqPm%Pm | 44±27 | 26±11 | 63±14 |
| QcQqV%Qc* | 25±12 | 1±1 | 15±1 |
| QcQqV%Qq* | 14±9 | 35±7 | 52±16 |
| QcQqV%V* | 61±17 | 64±8 | 33±24 |
| QcQqS%Qc* | 35±13 | 4±3 | 4±3 |
| QcQqS%Qq* | 19±9 | 91±5 | 12±4 |
| QcQqS%S* | 47±15 | 5±3 | 84±6 |

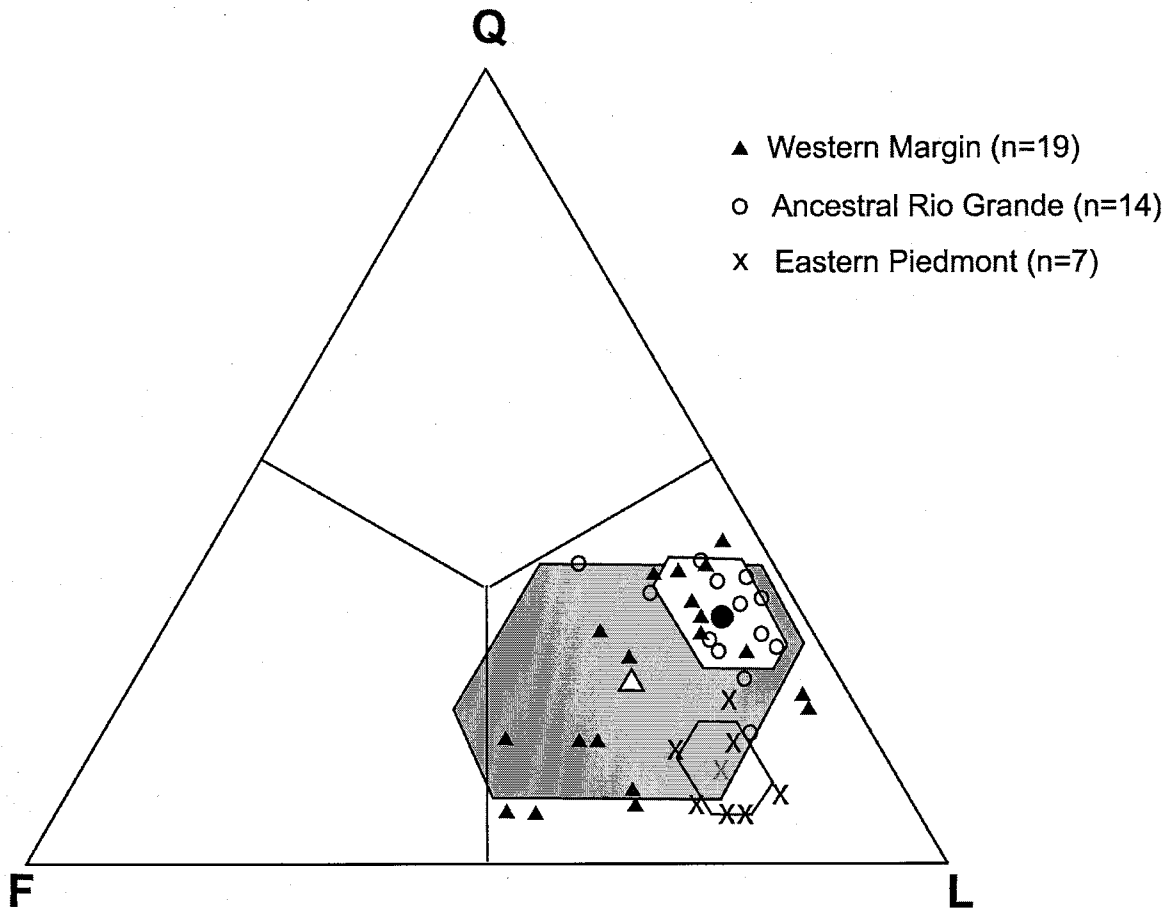


Figure 26. Ternary diagram of quartz, feldspar, and lithic fragments of pebble and cobble gravel, indicating significant compositional overlap among the three lithofacies assemblages. Field of variations (1σ) and mean are noted by polygons and larger symbols.

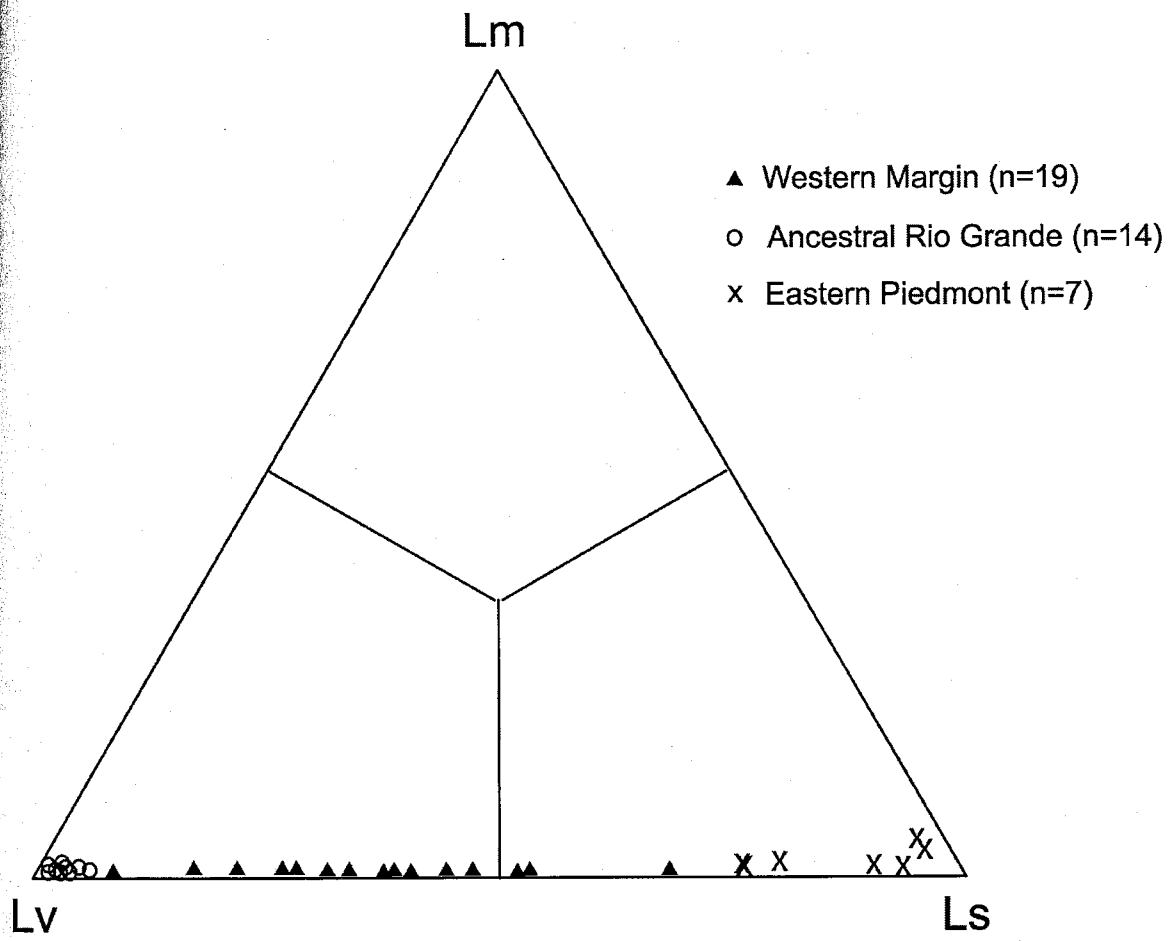


Figure 27. Lithic fragment plot showing metamorphic fragments (Lm), volcanic fragments (Lv), and sedimentary fragments (Ls). The ancestral Rio Grande lithofacies assemblage is dominated by volcanic lithic fragments while the eastern piedmont lithofacies assemblage is predominantly sedimentary lithic fragments. The western-margin lithofacies assemblage contains a mixture of volcanic and sedimentary lithic fragments.

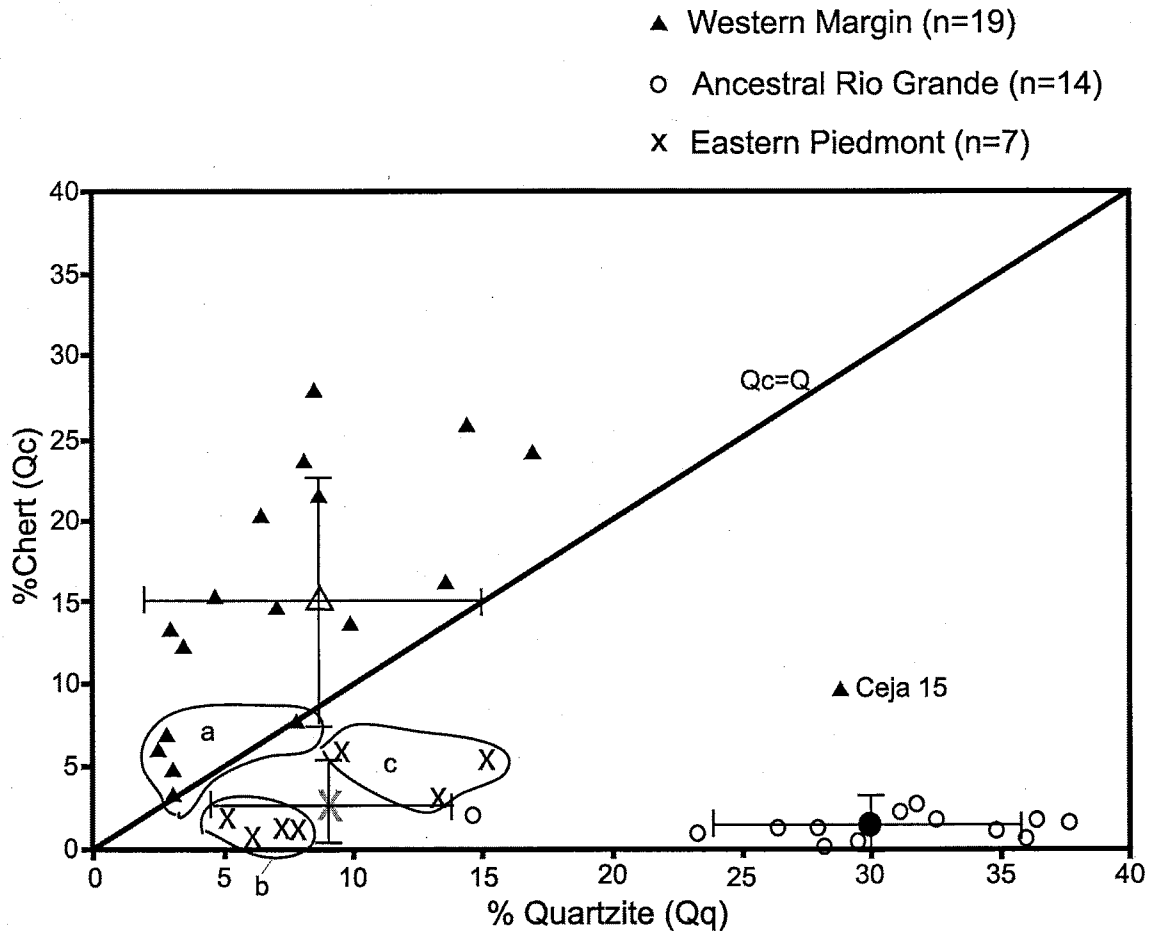


Figure 28. Bivariate plot of chert (Qc) and metaquartzite and quartz (Qq) gravel among the western-margin, axial, and eastern piedmont lithofacies assemblages. The outlier of western-margin lithofacies assemblage from the Ceja 15 locality may represent mixing of the western-margin and ancestral Rio Grande lithofacies or may be caused by local variations in drainage sources. Mean compositions of lithofacies assemblages are denoted by larger symbols. Field *a* encloses samples from the Marillo-Zia section; field *b* encloses samples from the Red Cliffs section; field *c* encloses samples from the San Felipe Pueblo section. This figure illustrates that the ancestral Rio Grande gravels contain a greater proportion of quartzite and little chert, the western-margin gravels contain abundant chert and minor quartzite, and the piedmont gravels contain little chert or quartzite.

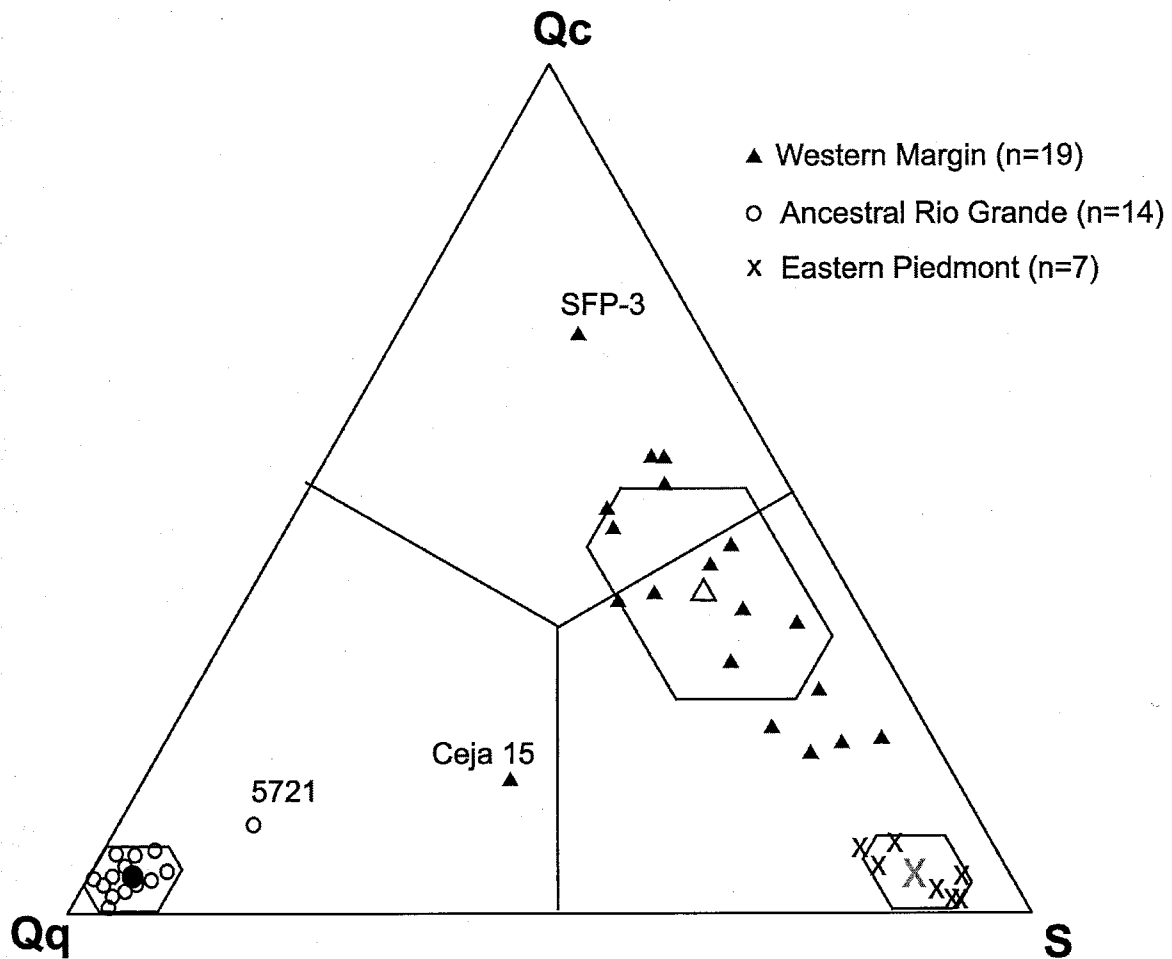


Figure 29. Ternary diagram of chert (Qc), metaquartzite (Qq), and sedimentary (S) gravel. The ancestral Rio Grande lithofacies assemblage contains abundant metaquartzite whereas the piedmont lithofacies assemblage contains mostly sedimentary clasts. The western-margin lithofacies assemblage contains mostly chert and sedimentary gravel. Field of variations (1σ) and means are noted by polygons and larger symbols.

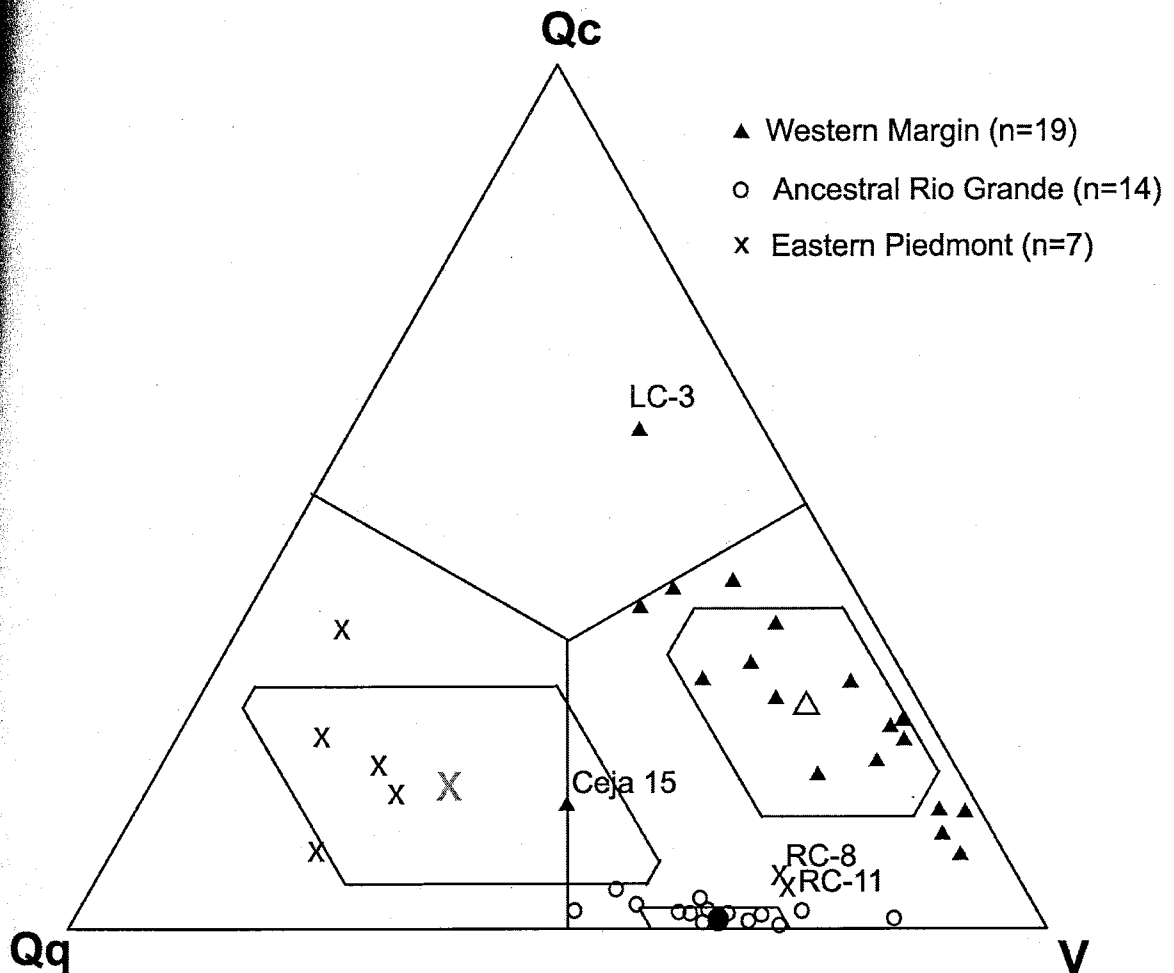


Figure 30. Ternary diagram of chert (Qc), metaquartzite (Qq), and volcanic (V) gravel. The ancestral Rio Grande lithofacies assemblage contains mostly volcanic and metaquartzite clasts whereas the western-margin lithofacies assemblage contains volcanic and chert gravels. The piedmont lithofacies assemblage contains quartzite clasts. Western-margin outliers include a sample from the Loma Colorado stratigraphic section (LC), which may represent mixing with ancestral Rio Grande sediments, and a sample from the Marillo-Zia stratigraphic section, which could be due to local drainage conditions such as source rocks exposed at the time of deposition. The piedmont outliers are from the Red Cliffs stratigraphic section (RC) and may represent mixing with the ancestral Rio Grande and the distal end of the piedmont or an influx of sediment from the Ortiz Mountains. Field of variations (1σ) and means are noted by polygons and larger symbols.

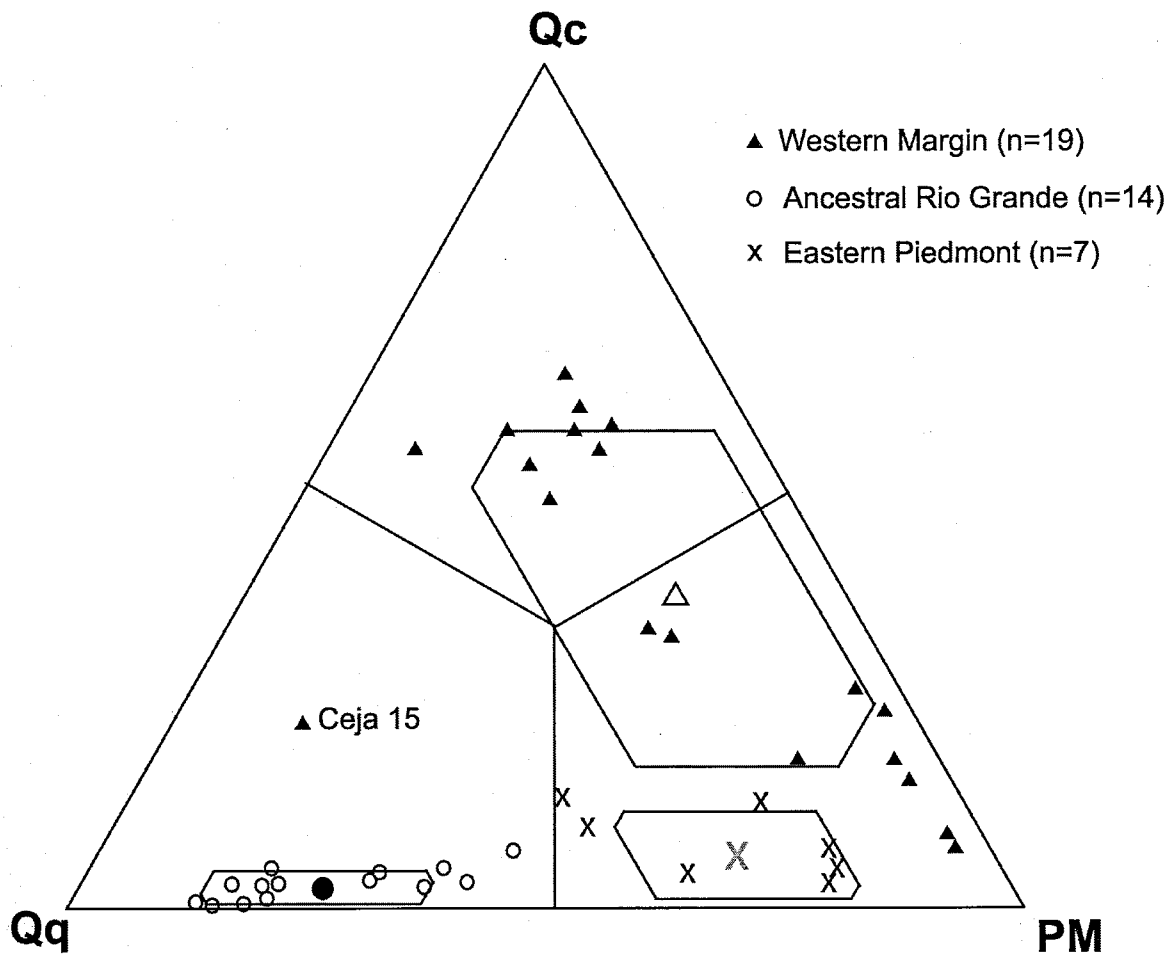


Figure 31. Ternary diagram of chert (Qc), metaquartzite (Qq), and plutonic-metamorphic (Pm) gravel. The ancestral Rio Grande lithofacies assemblage tends to have quartzite and little chert. The piedmont lithofacies assemblage is predominantly composed of plutonic/metamorphic clasts. The western-margin lithofacies assemblage reflects a bimodal composition. Samples collected towards the north tend to have abundant plutonic/metamorphic clasts whereas samples collected to the south tend to have abundant chert clasts. Sample Ceja 15 is an outlier and tends to contain more quartzite than typical western-margin samples. Field of variations (1σ) and means are noted by polygons and larger symbols.

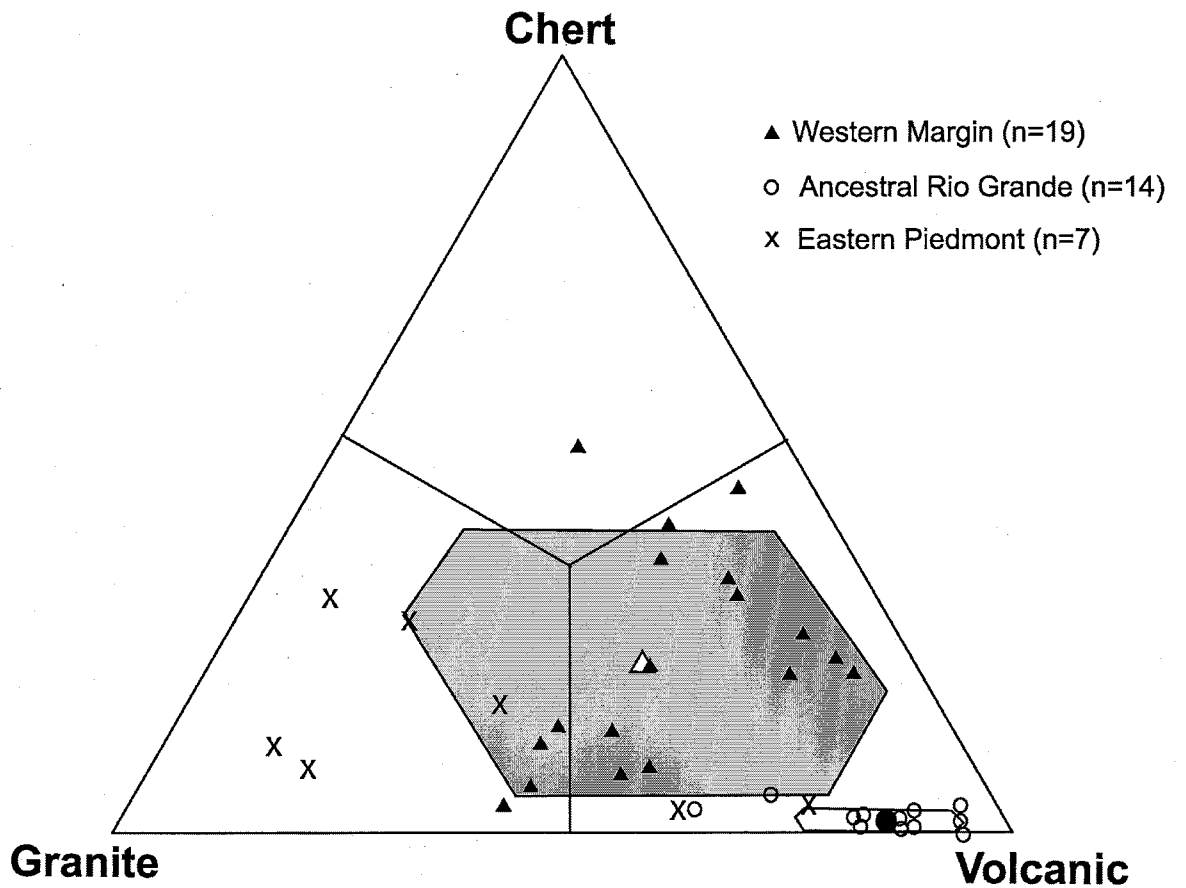


Figure 32. Ternary diagram of chert, granite, and volcanic clasts for gravels in the western, axial, and eastern-piedmont lithofacies assemblages. The ancestral Rio Grande lithofacies assemblage contains abundant volcanic clasts. The western-margin lithofacies assemblage contains volcanic and chert clasts. The piedmont lithofacies assemblage contains mostly granite clasts. Field of variations (1σ) and means for western and axial facies are noted by polygons and larger symbols.

laminations. Metaquartzite gravel is found in various colors, including bluish gray (10B 6/1), weak red (7.5R 4/2), brown (7.5YR 4/3), gray (N5/0), and white (N8/0 to 7.5YR 8/3). Chert gravel includes a wide variety of colors such as brown, gray, red, and black. The Pedernal chert is a distinct white and black banded chalcedony and chert, and is commonly found as angular to subangular pebble- to cobble-sized clasts.

Volcanic clasts are common in many gravels of the study area and are predominantly gray intermediate volcanic rocks with plagioclase phenocrysts. These volcanic rocks are present as pebble sized subrounded to rounded clasts. A distinctive volcanic clast is recognized as subrounded to rounded pebbles with 1 to 4 mm diameter plagioclase phenocrysts in a brown (7.5YR 5/4) aphanitic groundmass. Basalt commonly is present as pebble to cobble sized, subangular to subrounded clasts. These black to dark gray basaltic rocks are generally vesicular and can have fine-grained olivine phenocrysts. Rhyolitic gravel typically consists of reddish-brown to red and subangular to subrounded pebbles with quartz phenocrysts. Andesitic gravel consists of subrounded to rounded pebbles with a greenish-gray groundmass and plagioclase phenocrysts that are up to 1 to 3 mm in diameter. Ancestral Rio Grande deposits contain a slightly higher proportion of andesite and porphyritic tuff gravel than the western-margin lithofacies assemblage.

Sedimentary clasts in the conglomerates studied include siliciclastic and carbonate rocks. Common siliciclastic rocks include yellow and gray quartz-rich sandstone and reddish-brown arkosic sandstone and very sparse siltstone. Minor amounts of conglomerate clasts and silicified wood are also present. Carbonate rocks are dark bluish-gray, locally cherty, limestone that commonly contains fragments of crinoids, bryozoans, and brachiopods.

Plutonic and metamorphic gravels include quartz, granite, gneiss, schist, and diabase gravels. White vein quartz is recognized as pebble sized clasts in the piedmont lithofacies assemblage with a vitreous luster and milky white color. The lack of visible fused grains and sedimentary structures indicates an igneous origin, possibly related to dikes in the Sandia Mountains (Kelley and Northrop, 1975). Granitic rocks are commonly red or pink and fine-grained to porphyritic. Red granitic gravel varies in color from weak red to red (10R 5/4 to 7.5R 4/6) and is a common constituent of the western-margin lithofacies assemblage. Western margin granitic gravels have a phaneritic fine- to medium-grained subhedral granular texture containing abundant potassium feldspar. Red granitic gravel is subangular to subrounded and pebble to cobble sized. Pink granite is light red (7.5R 6/6) and contains large feldspar phenocrysts, which gives this granite a porphyritic texture with subhedral to euhedral microcline phenocrysts in a light to medium gray matrix of quartz, feldspar, and biotite. Pink granite gravels are typically subangular to subrounded pebbles. Gneissic rocks studied contain foliated bands from 1 to 5 cm in thickness. Colors range from light red (7.5R 6/6) to weak red (7.5R 4/4). Muscovite schist pebbles are subangular and rare. Diabase occurs as rounded dark gray pebbles and cobbles with aligned feldspar laths (1 to 3 mm in length) within an aphanitic groundmass.

The large boulders (1 to 2 m in diameter) found in the Loma Barbon Member are quartzose sandstones of probable Permo-Triassic origin. Smaller boulders (<1 m in diameter) include clasts of quartzose sandstones and Pedernal chert.

Western-Margin Lithofacies Assemblage

Metaquartzite and chert gravel make up about one-quarter of the clasts in the western-margin lithofacies assemblage (Table 8). Metaquartzite gravels mainly consist of subrounded to rounded white metaquartzite pebbles, though pebbles of gray and brown metaquartzite are also present. Brownish-yellow, black, and red chert is common in western-margin deposits. Chert clasts are mainly angular to subangular pebbles. Pedernal chert is locally common and is found as subangular to subrounded pebbles and cobbles.

Volcanic detritus makes up 35% of gravels in the western lithofacies assemblage (Table 7; Fig. 30). Most of the volcanic gravels are subangular to subrounded pebbles of gray intermediate volcanic rocks with plagioclase phenocrysts. Basalt is a locally important constituent in western-margin gravels, especially in the Ceja and Loma Barbon members of the Arroyo Ojito Formation.

Sedimentary rocks, mostly sandstone, make up 20% of gravel in western-margin deposits (Table 7; Fig. 29). These clasts are mostly subrounded pebbles of light-gray and yellowish-brown quartzose sandstone. Angular to subangular pebbles of red quartzose to arkosic sandstone are also present. Gravel of the western-margin assemblage contains clasts of red to brown silicified wood that were probably derived from the Chinle Group (Fig. 7; Woodward, 1987).

Plutonic and metamorphic clasts compose about one-fifth of the western-margin gravels (Table 7; Fig. 31). Pink and red granitic rocks are in the western-margin lithofacies assemblages; however, pink granite, especially the porphyritic variety is abundant in the eastern-margin lithofacies assemblage. Pink granite generally is present

as subangular to subrounded pebbles, whereas the red granite occurs as subangular to subrounded pebbles and cobbles that are up to 15 cm in diameter. Gneiss is not common.

At the type section of the Arroyo Ojito Formation, Connell et al. (1999) noted vertical variations in clast composition of member units. They report that the Navajo Draw Member contains abundant volcanic clasts, sandstone, and chert; red granite and Pedernal chert are sparse. In the overlying Loma Barbon Member, red granite is common, with sandstone and volcanic clasts as subordinate constituents. Gravels of the Ceja Member at the Arroyo Ojito type section contain abundant volcanic clasts, especially basalt, with other important clast types being red granite, sandstone, and Pedernal chert. Systematic vertical variations in clast composition were not recognized in the Marillo-Zia section. This finding differs from observations at the type section, which is about 3 km west of the Marillo-Zia section. Few conglomeratic intervals were recognized in the Navajo Draw Member at the Marillo-Zia section, which is in contrast to the thickly bedded conglomerates of the Navajo Draw Member type section. This difference could be the result of basinward fining of deposits and undersampling of gravel in the Marillo-Zia section. Another possible explanation is that Marillo-Zia lies just to the east of the main belt of Navajo Draw Member channel lithofacies.

The composition of sample Ceja 15 as well as the samples from the Loma Colorado stratigraphic section does not fall within the standard deviation of typical western-margin gravels. This could be due to local drainage conditions at the time of deposition. For instance, the fluvial system could have cut through a chert-rich interval, resulting in a larger proportion of chert to be transported. Another possible explanation for the outliers present is possible mixing with sediments of the ancestral Rio Grande.

Ancestral Rio Grande Lithofacies Assemblage

About one-third (~31%) of the gravel in the ancestral Rio Grande lithofacies assemblage is well rounded metaquartzite pebbles and cobbles (Table 7; Figs. 28-31). Chert is rare and consists mostly of brown and gray subrounded pebbles. Subrounded to rounded pebbles of Pedernal chert are also found in the ancestral Rio Grande deposits, but they are quite sparse and commonly smaller and better rounded as compared to the western-margin lithofacies assemblage.

Volcanic grains comprise a little over half (55%) of the clasts in the ancestral Rio Grande gravel (Table 7; Fig. 30). Volcanic gravels are mainly subrounded to rounded pebbles and some cobbles of gray intermediate volcanic rocks. Tan porphyritic volcanic and hypabyssal intrusive gravels are also common and are more abundant than in the western-margin lithofacies assemblage. Basaltic and rhyolitic clasts tend to be less common than intermediate volcanic clasts.

The ancestral Rio Grande deposits contain sparse or no sedimentary clasts. Less than 1% of gravel clasts in the ancestral Rio Grande facies are sedimentary (Table 7; Fig. 29). These gravels are commonly found near the margins of the peripheral lithofacies, suggesting they are locally mixed into the axial-river system from tributary deposits. The sedimentary clasts present are mostly rounded yellow-brown or gray sandstone pebbles.

Ancestral Rio Grande facies gravels contain an average of 11% plutonic and metamorphic clasts (Table 7; Fig. 31). Of these clasts, subrounded pebbles of pink granite

are the most common. Rounded pebbles and cobbles of diabase are also present.

Subrounded to rounded pebbles of gneiss and schist are rare or not present.

Eastern-Margin Piedmont Lithofacies Assemblage

White vein quartz and angular chert make up 12% of gravel in the piedmont facies (Fig. 28). Quartz is generally recognized as milky white subangular pebbles. Chert is found as gray angular to subangular pebbles. Volcanic clasts are rare in the piedmont facies relative to deposits of the western margin and ancestral Rio Grande. An average of 7% of gravel clasts in the piedmont are volcanic (Table 7; Fig. 30). Most of these are subangular to subrounded pebbles of gray intermediate volcanics. There are no volcanic clasts reported from the Sandia Mountains (Kelley and Northrop, 1975). The Ortiz Mountains, located north of the Sandia Mountains and east of the San Felipe Pueblo study area, could provide a source of volcanic and hypabyssal-intrusive detritus (Kelley, 1977).

Sedimentary clasts typically are angular to subangular pebbles and cobbles of gray, commonly fossiliferous limestone. Other sedimentary clasts include angular to subangular pebbles of gray and yellow-brown quartzose sandstone and reddish arkosic sandstone and siltstone, probably derived from Permian rocks along the northern flank of the Sandia Mountains (Connell et al., 1995).

Plutonic and metamorphic rocks compose an average of 19% of piedmont gravels (Table 7; Fig. 31). The majority of these clasts are subangular to subrounded pink

porphyritic granite and gneiss pebbles. Angular to subangular pebbles of schist are also present but are sparse.

Lithofacies Assemblages and Gravel Composition

The three lithofacies assemblages studied have compositions of gravel clasts that can be distinguished in the field (Figs. 28-31). Deposits of the western-margin lithofacies assemblage contain abundant red granite, volcanics, and Pedernal chert, as well as significant amounts of sedimentary rocks. The ancestral Rio Grande facies deposits contains sparse Pedernal chert, whereas in the western-margin lithofacies assemblage Pedernal chert composes a significant percentage of the quartzite and chert fraction (Fig. 33). Gravel of the ancestral Rio Grande deposits is dominated by rounded metaquartzite and volcanic rocks (Table 7, Fig. 30). Eastern piedmont facies in the study area are identified by the paucity of volcanic clasts and the abundance of sedimentary clasts (Fig. 29, Fig 30, Table 7).

The difference among the three facies is the relationship of the relative abundance of quartzite, chert, volcanic, sedimentary, and plutonic and metamorphic rocks (Figs. 29-32). These data indicate that the presence of sedimentary rocks, such as sandstone and limestone, are important in differentiating lithofacies assemblages based on gravel composition.

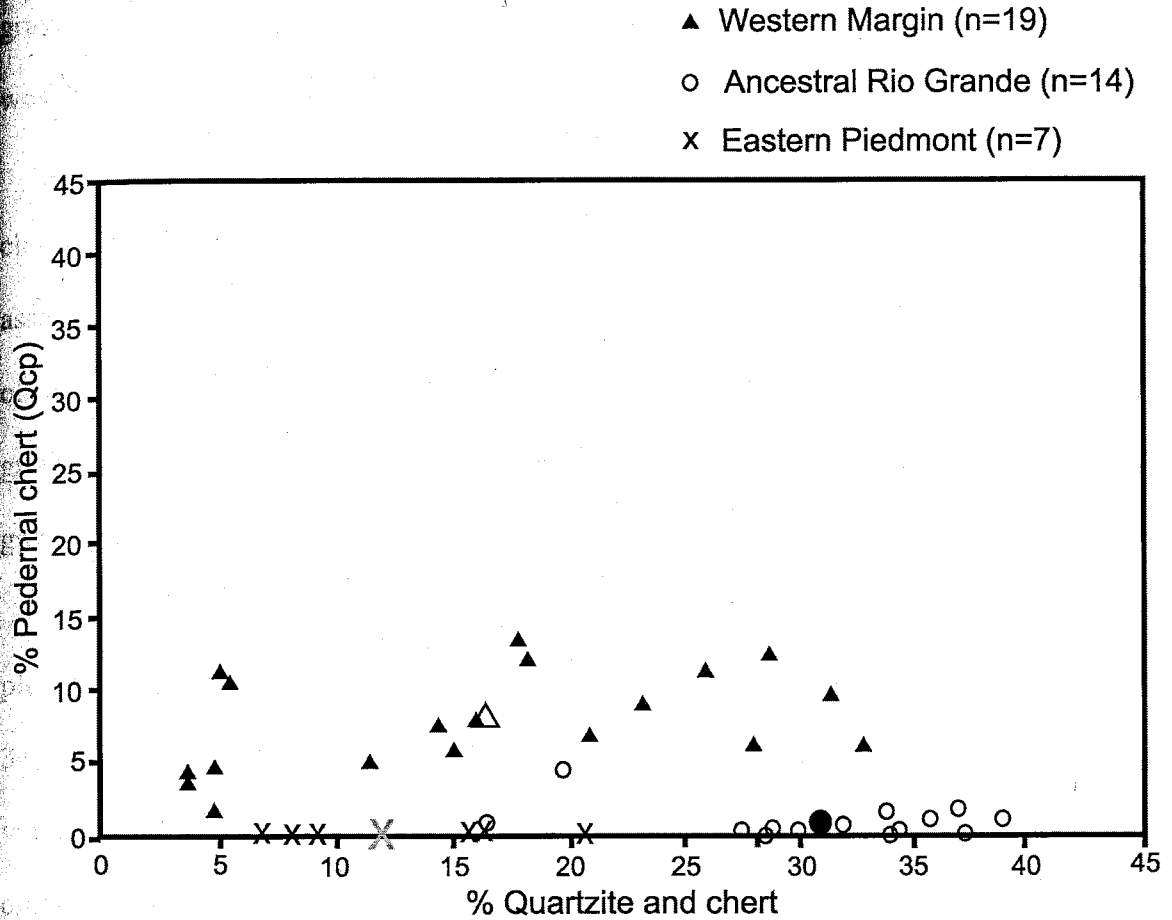


Figure 33. Bivariate plot of quartzite and chert versus Pedernal chert gravel among the western-margin, ancestral Rio Grande, and eastern piedmont lithofacies assemblages. Mean compositions are denoted by larger symbols.

The relative abundance of chert, quartzite, and sedimentary clasts (Fig. 29) shows that the ancestral Rio Grande lithofacies assemblage is primarily quartzite, whereas the piedmont lithofacies assemblage is composed mainly of sedimentary clasts. The western-margin lithofacies assemblage contains abundant chert and sedimentary clasts. The relative abundance of chert, metaquartzite, and volcanic clasts indicate clustering among the three lithofacies assemblages studied (Fig. 30). This compositional clustering of

gravel indicates that the abundance of sedimentary clasts can discriminate between the western-margin and ancestral Rio Grande lithofacies assemblages.

Comparing the relative abundance of chert, quartzite, and plutonic/metamorphic clasts shows bimodality, or two separate clusters of data within each lithofacies assemblage (Fig. 31). This compositional bimodality appears to be related to the position of the sample in the basin. For example, the western-margin lithofacies assemblage subgroup that contains a greater proportion of chert was collected farther south than the subgroup that contains a greater proportion of plutonic/metamorphic clasts (Fig. 31).

The comparison of the relative abundance of volcanic, sedimentary, and plutonic/metamorphic clasts illustrates a distinct trend in the lithofacies assemblages (Fig. 34). This ternary plot shows that ancestral Rio Grande deposits are dominated by volcanic detritus. The piedmont lithofacies assemblage contains abundant sedimentary clasts, minor plutonic/metamorphic clasts, and sparse volcanic clasts. The western-margin lithofacies assemblage contains significant amounts of volcanic, sedimentary, and plutonic/metamorphic clasts, trending towards a central position on the ternary diagram. The most distinctive difference among the three lithofacies assemblages is in the relative abundance of quartzite and chert (Fig. 28). The ancestral Rio Grande lithofacies assemblage contains abundant quartzite with sparse chert. The western-margin lithofacies assemblage contains abundant chert and minor quartzite. The eastern-margin piedmont lithofacies assemblage contains minor amounts of both quartzite and chert, which is consistent with a source area that is lacking in major sources of quartzite and chert.

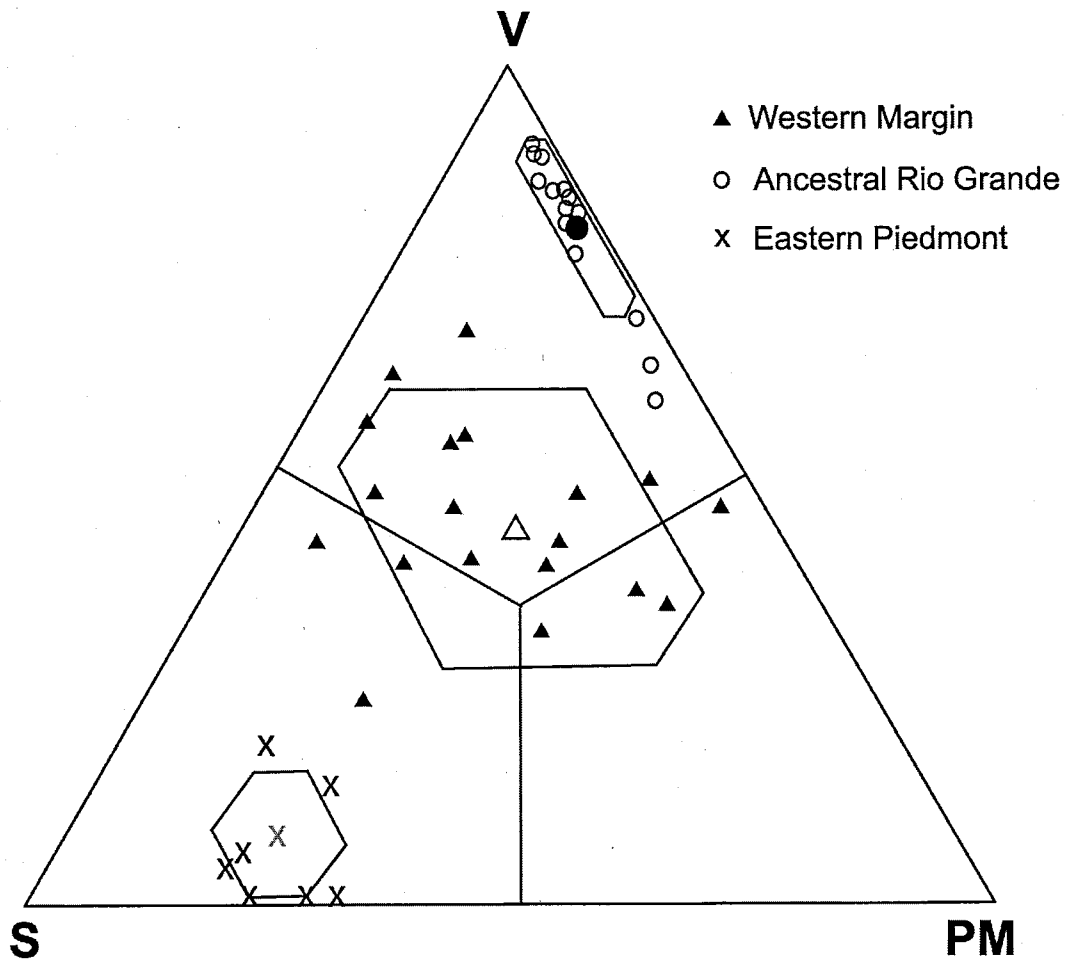


Figure 34. Ternary diagram of volcanic (V), sedimentary (S), and plutonic-metamorphic (Pm) gravel. Field of variations (1σ) and means for western and axial facies are noted by polygons and larger symbols.

The lithofacies assemblages studied include somewhat anomalous gravel compositions. In the western-margin lithofacies assemblage points that are anomalous include the Ceja 15 sample and the LC-3 sample. A possible cause of the anomalous composition of LC-3 and Ceja 15 could occur if granite was temporarily exposed in the drainage headlands. Another possible explanation of these points is that the samples were taken near the paleoconfluence between the western-margin fluvial system and the

ancestral Rio Grande. In this case, the samples would reflect an intermediate composition between the ancestral Rio Grande and western-margin lithofacies. The Ceja 15 sample is intermediate to the ancestral Rio Grande and western-margin lithofacies assemblages (Figs. 28-31).

The different clast assemblages present in the three lithofacies assemblages may reflect clast durability as well as differences in provenance. Though sources for sedimentary clasts are present along the drainage of the ancestral Rio Grande, sedimentary clasts such as sandstone are not as durable as the metaquartzite and volcanic clasts in the river system and are thus quickly eroded (Abbott and Peterson, 1978). The piedmont lithofacies assemblage likely contains the abundant sedimentary clasts since the deposits are close to the source area and the clasts have not undergone as extensive abrasion as in the ancestral Rio Grande fluvial system.

Sand Composition

Quartz (Q), plagioclase (P), potassium feldspar (K) and volcanic lithic grains (Vg) are the most abundant grain type found in sands. Sands are generally fine- to coarse-grained, subangular to well rounded, and poorly to well sorted. Calcium-carbonate is the dominant type of cement. Monocrystalline quartz (Qm) is the most abundant grain type and is recognized by its clear texture and straight extinction. Polycrystalline quartz (Qp) is present in samples and is recognized by undulose extinction. Plagioclase (P) and potassium feldspar (K) are abundant in sand samples of all three lithofacies assemblages. Plagioclase grains are often twinned and a few grains show oscillatory zoning around

grain edges. Potassium feldspar (K) grains exhibit tartan twinning (Fig. 35), non-twinned grains are identified by a yellowish hue from cobaltinitrate staining. Granite grains (gn) are counted with feldspars using the modified Gazzi-Dickinson method and are identified as polymineralic grains containing feldspar (plagioclase or potassium feldspar) and quartz (Fig. 36). Volcanic grains are the most abundant lithic fragment in the medium-grained sand fraction. Several types of volcanic grains are present. Granular and seriate grains are the most common types of volcanic grains, though lathwork grains are also present. Granular volcanic grains contain abundant equigranular microcrystals of quartz and feldspar (Fig. 37). Seriate grains contain feldspar and quartz phenocrysts of varying size in a fine matrix (Fig. 38). Lathwork grains exhibit a texture of interlocking plagioclase laths. These different types of volcanic grains were identified during point counts, but were not counted separately.

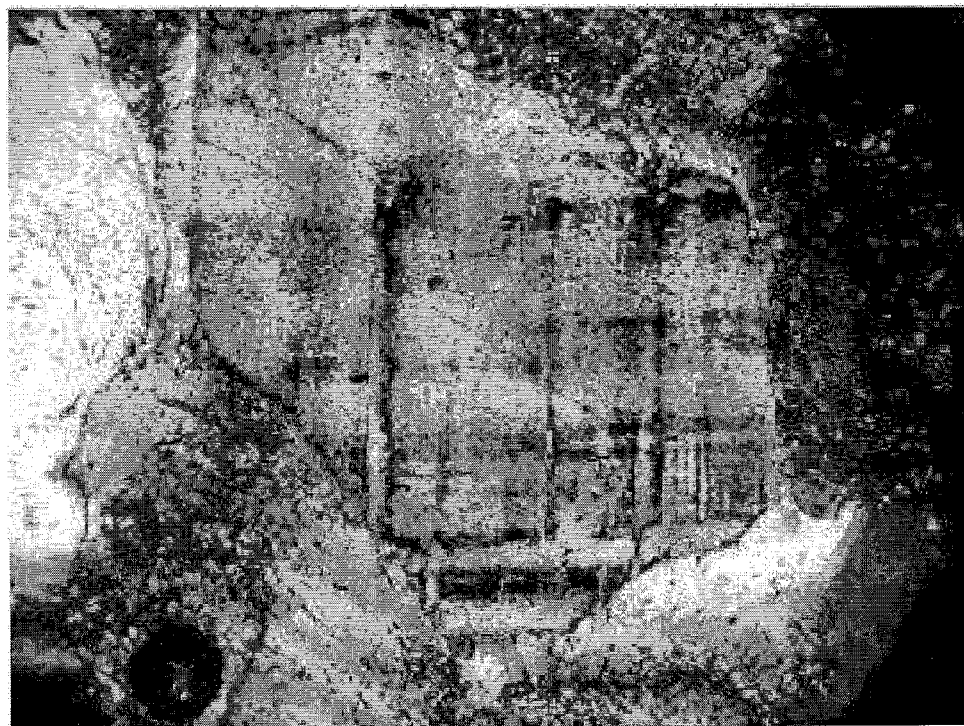
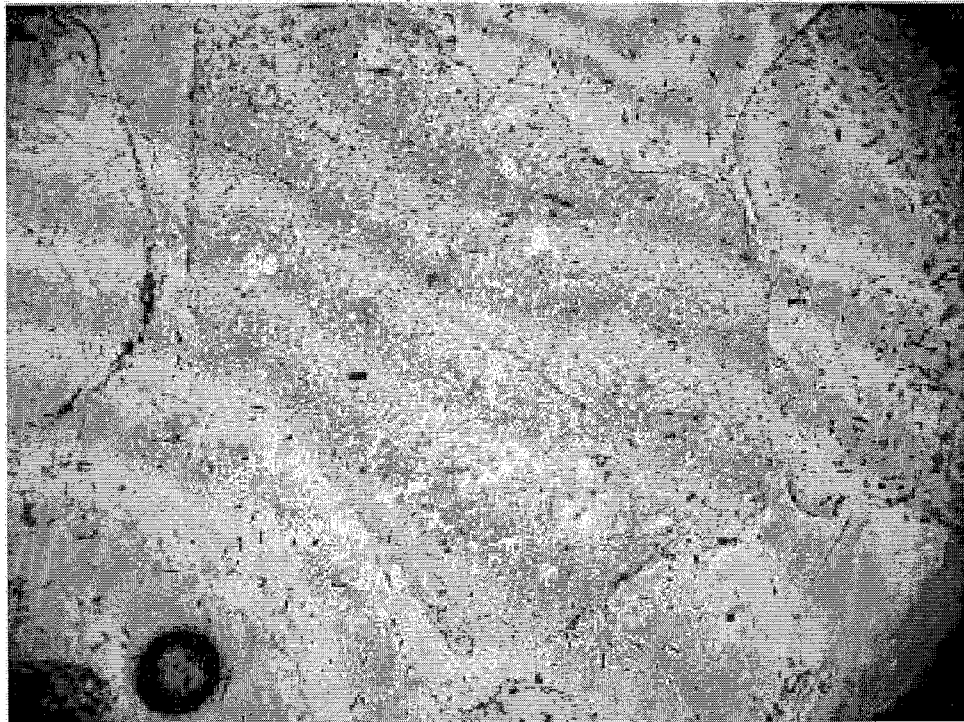


Figure 35. Photomicrographs of a stained potassium feldspar grain illustrating tartan twinning, from ancestral Rio Grande lithofacies assemblage in the San Felipe gravel quarry section, viewed in plane light (top) and cross-polarized light (bottom). Grains are 0.5-0.25 mm in diameter.

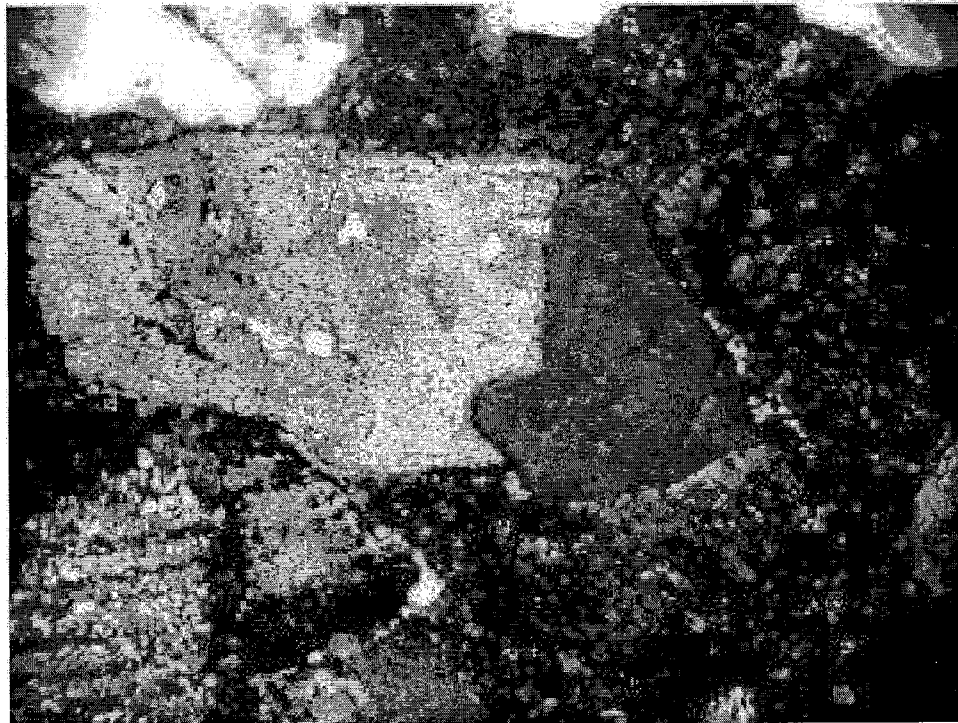


Figure 36. Photomicrographs of a granitic grain consisting of potassium feldspar (left side of grain) and quartz (right side), from 98 m (320 ft) below land surface in the Matheson Park monitoring well (eastern-margin piedmont deposits), viewed in plane light (top) and cross-polarized light (bottom). Grains are 0.5-0.25 mm in diameter.

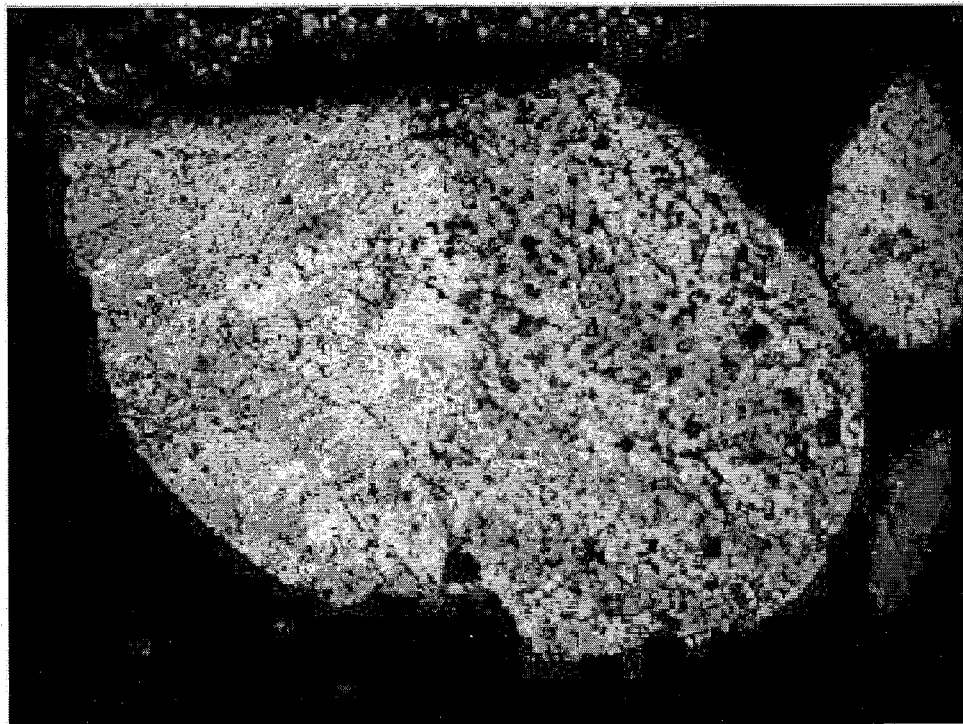
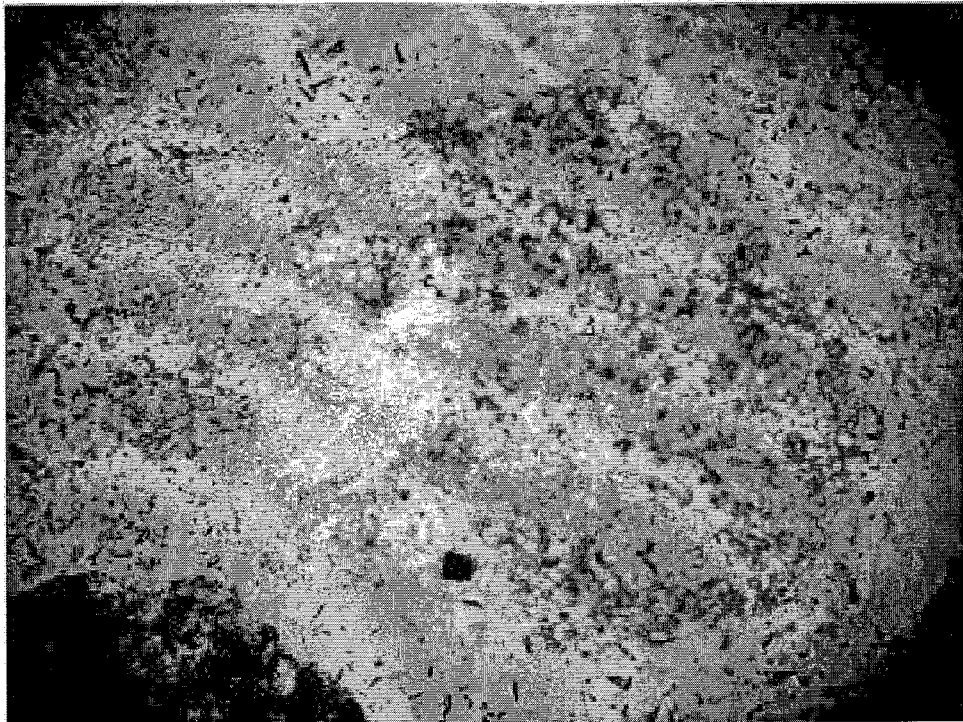


Figure 37. Photomicrographs of a volcanic grain with a potassium feldspar phenocryst on left side and granular groundmass to right side, from the western-margin lithofacies assemblage, unit 18 of the Marillo section, viewed in plane light (top) and cross-polarized light (bottom). Grains are 0.5-0.25 mm in diameter.

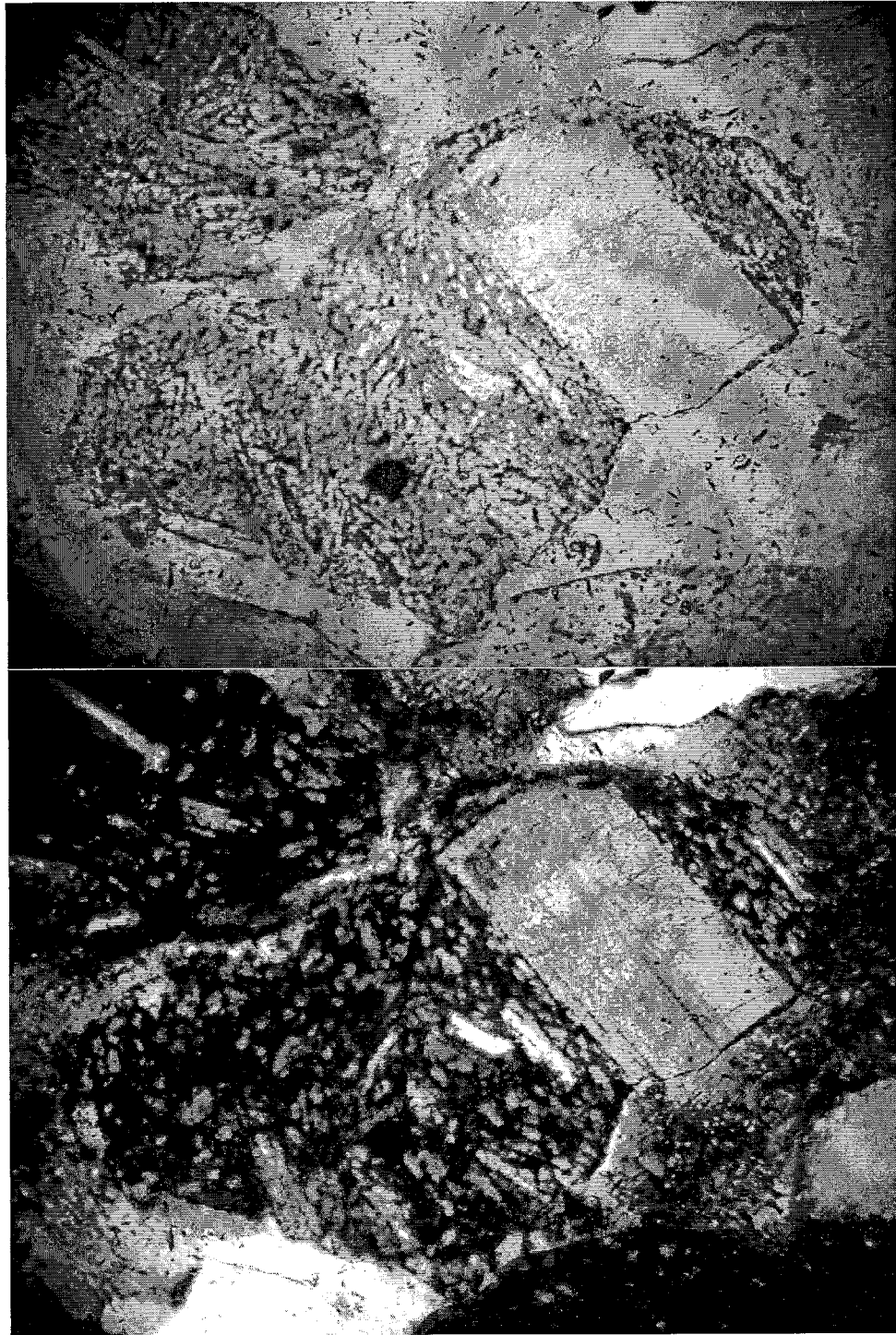


Figure 38. Photomicrographs of seriate volcanic grains, from ancestral Rio Grande lithofacies assemblage in unit 1 of the Tonque Arroyo section, viewed in plane light (top) and cross-polarized light (bottom). Grains are 0.5-0.25 mm in diameter.

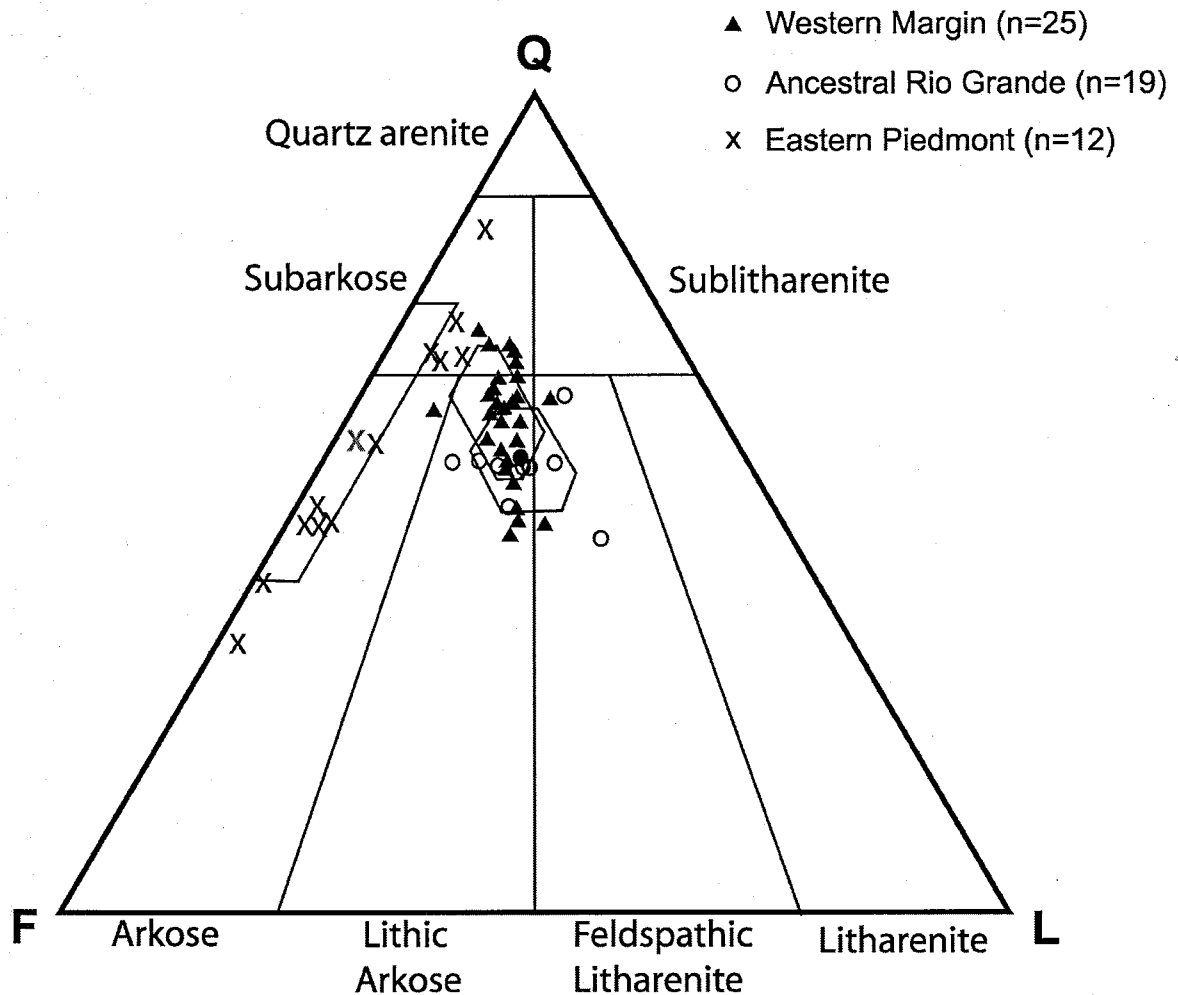


Figure 39. Diagram of quartz (Q), feldspar (F), and lithic (L) fragments of medium-grained sand. Field of variations (1σ) and means for western and axial facies are noted by polygons and larger symbols. Classification of Folk (1974) is used.

The composition of medium-grained sand in this study indicates that these deposits range from subarkose, arkose, lithic arkose, and feldspathic litharenite (Fig. 39). Sands of the western margin and ancestral Rio Grande facies show considerable compositional overlap, although sands of the western-margin lithofacies assemblage tend to contain more quartz (Fig. 39). The most common lithic fragment in each of these facies is volcanic. Eastern-margin piedmont deposits in the study area plot near the quartz-feldspar axis, as these sands tend to have sparse lithic fragments.

The plot of quartz, feldspar, and lithic sand fraction differs from the plot of the gravel fraction in that the sand fraction is more quartz rich (Figs. 26 and 39). This difference can be attributed to the difference in grain size (Ingersoll et al., 1984). For example, a quartzose sandstone pebble is classed as a lithic fragment; however, quartz sand grains are classed as quartz. Transport and weathering processes would also reduce rocks into sand-sized particles of quartz, feldspar and lithic fragments.

The western-margin and ancestral Rio Grande deposits contain a greater amount of lithic fragments than the piedmont deposits. A comparison of lithic grain content shows that the piedmont lithofacies assemblage contains a greater amount of sedimentary lithics than the other two lithofacies assemblages (Fig 40, Table 10). The western-margin lithofacies assemblage and the ancestral Rio Grande lithofacies assemblage contain predominantly volcanic lithic fragments and overlap considerably. Metamorphic rock fragments are absent from all three of the lithofacies assemblages.

A comparison of the relative abundance of chert (Fig. 41), granite, and volcanic grains (Fig. 42) indicates that the western-margin and ancestral Rio Grande lithofacies assemblages are dominated by volcanic grains, the ancestral Rio Grande containing the contains minor amounts of chert. The piedmont lithofacies assemblage contains abundant granite detritus. This clustering indicates that the three lithofacies can be differentiated.

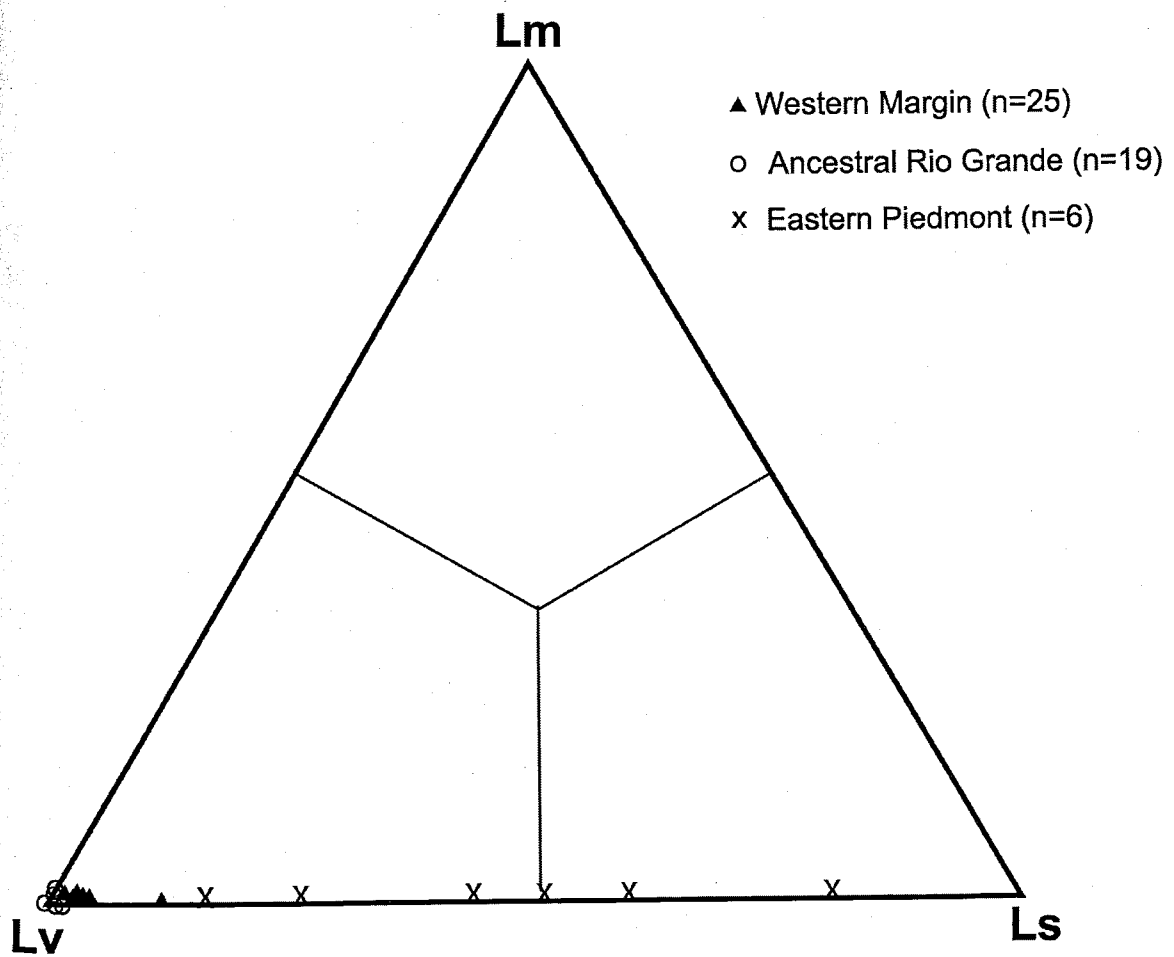


Figure 40. Ternary diagram of lithic fragments of medium-grained sand indicating relationships among metamorphic fragments (Lm), volcanic fragments (Lv), and sedimentary fragments (Ls).

Table 9. Recalculated detrital parameters for medium-grained sand. See Table 1 for description of sand constituents.

| Recalculated Parameter (%) | Constituents |
|-------------------------------|---|
| Q | (Qm + Qp + Qv + Qs + Qc)/total framework grains |
| F | (P + K + gn + Pv + Fs)/ total framework grains |
| L | (Vg + Sc + S)/ total framework grains |
| V | (Vg)/ total lithic fragments |
| S | (Sc + S)/ total lithic fragments |
| Pm | gn |
| gn | Gn |
| Qq | Qm + Qp |
| Qc | Qc |

Table 10. Mean and standard deviations (1σ) for medium-grained sand composition for the three lithofacies assemblages in the study area (Table 9). Distinguishing relationships denoted by asterisk (*).

| Detrital components | Western | Axial | Eastern |
|---------------------|---------|-------|---------|
| QFL%Q | 61±7 | 56±5 | 57±14 |
| QFL%F | 23±4 | 24±3 | 40±16 |
| QFL%L | 16±5 | 20±5 | 3±2 |
| LmLvLs%Lm | 0 | 0 | 0 |
| LmLvLs%Lv | 99±2 | 100±1 | 64±37 |
| LmLvLs%Ls | 1±2 | 0±1 | 21±27 |
| QcgnV%Qc | 16±6 | 7±3 | 9±9 |
| QcgnV%gn | 13±7 | 7±4 | 78±17 |
| QcgnV%V | 70±9 | 87±5 | 13±11 |
| QcQq%Qc | 3±1 | 1±1 | 2±1 |
| QcQq%Qq | 57±7 | 54±5 | 63±13 |
| QcQqPm%Qc* | 5±2 | 2±1 | 2±2 |
| QcQqPm%Qq* | 90±3 | 95±2 | 83±5 |
| QcQqPm%Pm* | 4±2 | 3±1 | 16±5 |
| QcQqV%Qc | 4±2 | 2±1 | 3±2 |
| QcQqV%Qq | 75±7 | 73±6 | 94±3 |
| QcQqV%V | 20±6 | 26±6 | 3±2 |
| QcQqS%Qc | 6±2 | 2±1 | 2±2 |
| QcQqS%Qq | 94±2 | 98±1 | 97±2 |
| QcQqS%S | 0 | 0 | 1±2 |

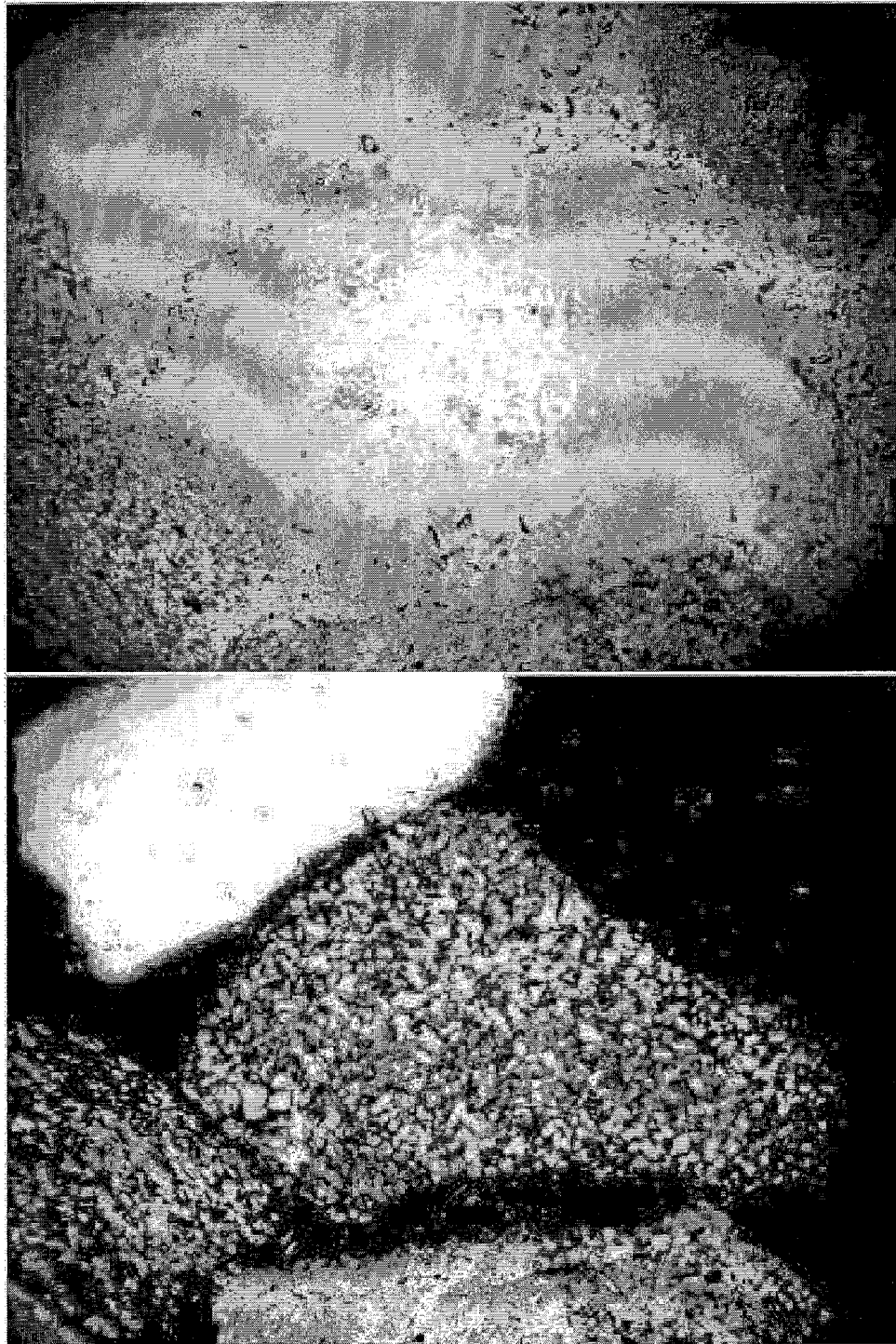


Figure 41. Photomicrographs of chert grain, from unit 18 of the Marillo section, viewed in plane light (top) and cross-polarized light (bottom). Grains are 0.5-0.25 mm in diameter.

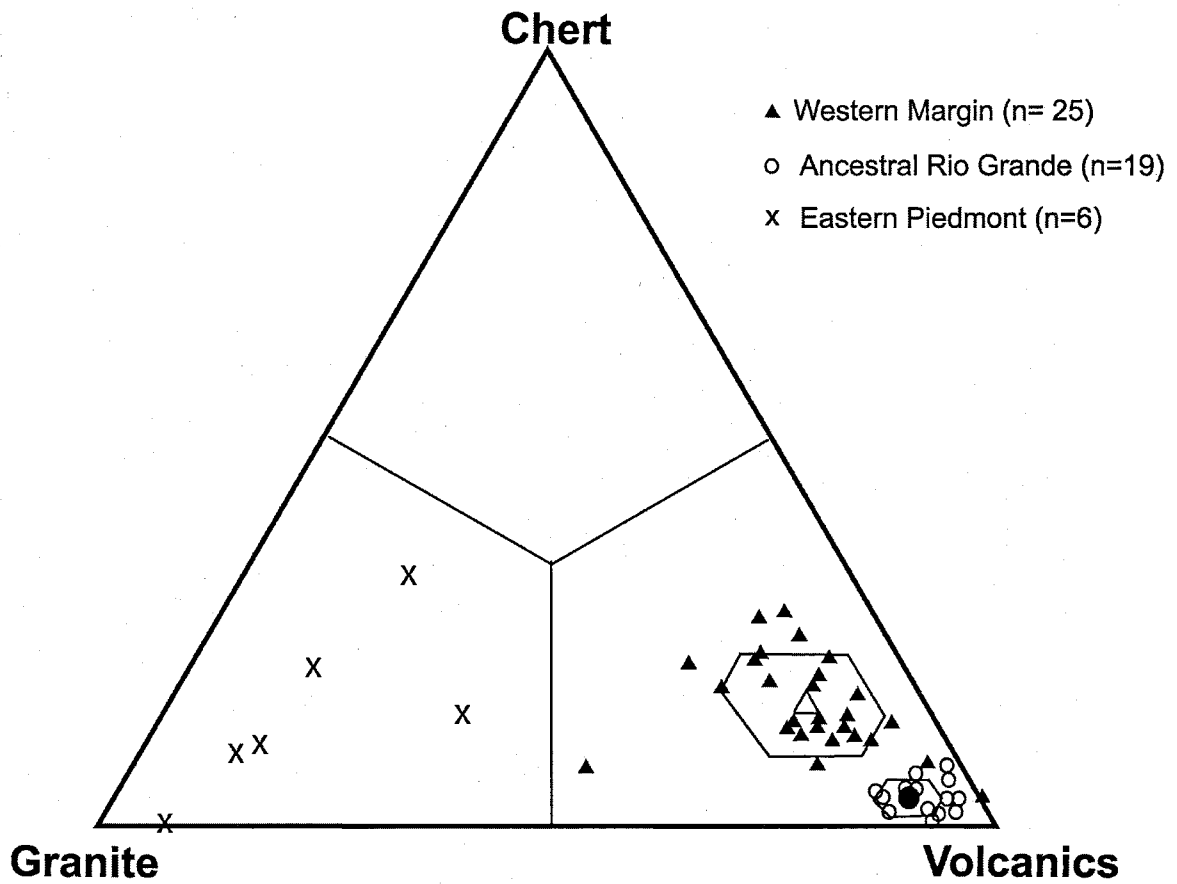


Figure 42. Ternary diagram of medium-grained sand illustrating the relationships among chert, granite, and volcanic fragments. Field of variations (1σ) and mean are noted by polygons and larger symbols. Samples SFP-5 and ER-1 are compositionally similar to ancestral Rio Grande deposits, but are part of the western-margin lithofacies assemblage.

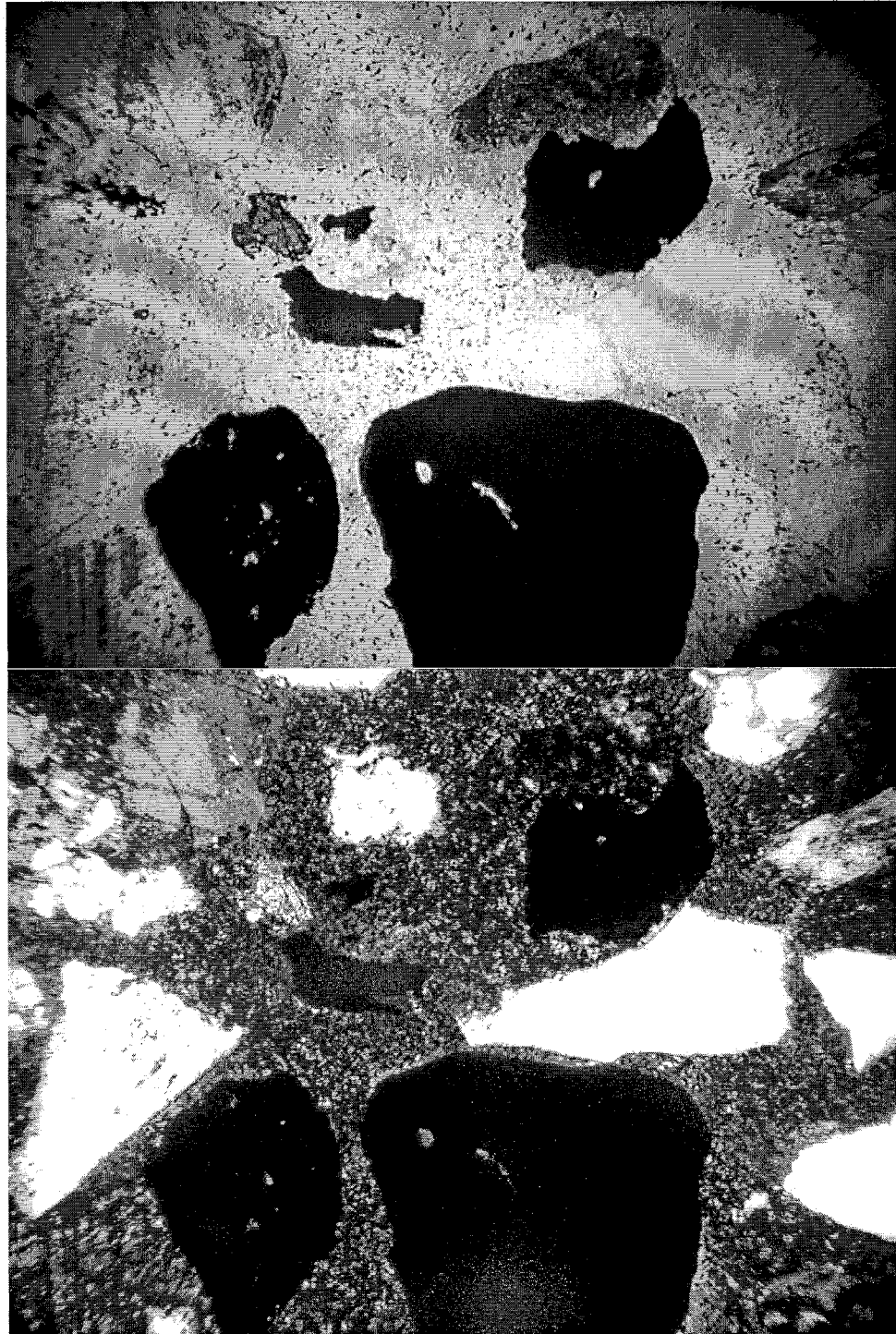


Figure 43. Photomicrographs of opaque grains from eastern-margin piedmont deposits, 82 m (270 ft) below land surface in the Matheson Park monitoring well, viewed in plane light (top) and cross-polarized light (bottom). Grains are 0.5-0.25 mm in diameter.

Opaque minerals (Fig. 43) tend to be more abundant in the piedmont deposits. In point counts of four hundred points per sample, an average of three points were opaque minerals in western margin and ancestral Rio Grande sediments. An average of 2.5% opaque minerals were counted in eastern-piedmont piedmont samples in the study area.

Lithofacies Assemblages and Sand Composition

Comparisons of medium-grained sand shows only slight variation among the three lithofacies assemblages. The similarity in quartz-feldspar-lithic (QFL) content between this study and that of Large and Ingersoll indicates that the sand compositions of Large and Ingersoll are reproducible in this study. The degree of overlap among lithofacies assemblages indicates that quartz-feldspar-lithic relationships are not a sensitive indication of mappable lithofacies assemblages studied here (Fig. 39, Table 10).

Western-Margin Lithofacies Assemblage (Arroyo Ojito Formation)

Sands studied in the Arroyo Ojito Formation are predominantly lithic arkose, with subordinate amounts of subarkose and feldspathic litharenite. Monocrystalline quartz (Qm) is the most abundant mineral grain. Feldspars, both plagioclase (P) and potassium feldspar (K), are also important constituents in the western margin deposits. Volcanic grains are the most abundant lithic fragment in these deposits, accounting for an average of 15% of all grains counted in the samples. Many grains from the western-margin lithofacies assemblage in the study area contain plagioclase and, to a lesser extent, quartz phenocrysts.

Important, but less common constituents of the sand fraction of the western-margin assemblage include granitic and chert grains. Granitic grains typically make up 3% of the medium-grained sand in the Arroyo Ojito Formation. Chert grains also compose about 3% of the western margin-deposits in the study area. Though these are relatively minor constituents, granite and chert are important in distinguishing the western margin deposits from the ancestral Rio Grande deposits. The amount of quartz, feldspar, and volcanic lithic fragments is similar in sediments of both deposits, however, slight differences exist in the minor sand constituents. The western-margin sediments contain slightly more granite and chert grains than the Rio Grande deposits (Fig. 42). At the Marillo-Zia stratigraphic section, systematic vertical variation of sand composition was not noted. This observation is consistent with the clast samples of the section, but different from observations of gravel composition at the type Arroyo Ojito Formation stratigraphic section (Connell et al., 1999).

Ancestral Rio Grande Lithofacies Assemblage (Sierra Ladrones Formation)

Sands that compose the ancestral Rio Grande deposits are lithic arkose and feldspathic litharenite. Compositionally, these sands are similar to those of the Arroyo Ojito Formation. Monocrystalline quartz (Qm) is the most abundant grain in these sands, comprising an average of at least 50% of the sand. Both plagioclase (P) and potassium feldspar (K) are also important constituents. Like the sands of the western margin deposits, volcanic grains are the most abundant lithic fragment, comprising

approximately 17% of the medium sand grains. Plagioclase and quartz phenocrysts are present in many volcanic grains.

Ancestral Rio Grande sands generally do not have as many granite and chert grains as the western margin sands (Fig. 42). Granite grains compose an average of 2% of all the medium-grained sands in the ancestral Rio Grande deposits and chert grains make up about 1% of the sand.

Eastern-Margin Piedmont Lithofacies Assemblage (Sierra Ladrones Formation)

Medium-grained sands of the eastern-margin piedmont in the study area are subarkosic to arkosic in composition. Like the western margin and ancestral Rio Grande deposits, monocrystalline quartz (Qm) is the most abundant grain in piedmont sands, comprising an average of 50% of the deposit. Plagioclase and potassium feldspar are also important constituent, making up approximately 28% of the sands. Granite grains are also important in the piedmont deposits. An average of 9% of the grains in piedmont sands are granite, a larger number than in the other two lithofacies assemblages studied. Also in contrast to the other two lithofacies assemblages, sands of the piedmont do not contain significant amounts of volcanic lithic fragments (Vg). This decrease in the amount of volcanic lithic fragments compared to the ancestral Rio Grande deposits is the easiest way to distinguish the piedmont sands from the ancestral Rio Grande sands (Fig. 42). In addition, the amount of opaque minerals is larger in the piedmont deposits than in western margin or ancestral Rio Grande deposits (Appendix C). The piedmont contains

an average of 3% opaque minerals. Deposits of the Arroyo Ojito Formation and the ancestral Rio Grande both contain less than 0.1% opaque minerals.

Comparison to Previous Studies

Surface Samples

A previous petrographic study in the Albuquerque Basin (Large, 1995; Large and Ingersoll, 1997) concluded that all upper Santa Fe Group sediments in the northern Albuquerque Basin are petrographically indistinguishable from one another and deposits were grouped into their "Albuquerque petrofacies," which contains 53% quartz, 26% feldspathic, and 21% lithic components. These percentages closely resemble the results from the ancestral Rio Grande deposits of this study (Q=5%, F=24%, and L=20%), and are within one standard deviation of the composition of the western-margin lithofacies assemblage. The results of this study show that the eastern piedmont deposits contain 57% Q, 40% F, and 3% L, which does not correlate well with the Albuquerque petrosome of Large (1995) and Large and Ingersoll (1997).

Subsurface Samples (Drillhole Cuttings)

Cuttings from wells drilled in the northern Albuquerque Basin were studied to determine if the three mapped lithofacies assemblages can be differentiated in the subsurface using the medium-grained sand fraction. A previous study by Gillentine

(1996) indicated that sands of different lithofacies were distinguishable from drillhole cuttings.

The composition of medium-grained sand from four wells drilled in the Albuquerque area has been calculated from Gillentine's (1996) data (Fig. 46). The Soil Amendment Facility and Cerro Colorado wells were drilled into western-margin deposits on the west side of the basin (Fig. 4). The Charles 5 and 6 wells were drilled into ancestral Rio Grande deposits and are east of the Rio Grande Valley (Fig. 4). Gillentine did not study samples from wells drilled into the eastern-margin piedmont of the Sandia Mountains.

This report includes a petrographic analysis of well cuttings from the Matheson Park Well (Fig. 44) and Metropolitan Detention Center (Fig. 45). The Matheson Park well is located east of the Rio Grande Valley near the western front of the Sandia Mountains. The Metropolitan Detention Center well is southwest of Albuquerque, near the western margin of the Albuquerque Basin (Fig. 4). Sand examined from these two wells have compositions similar to the surface samples collected at the stratigraphic sections measured in the northern Albuquerque Basin. The Matheson Park well samples contain two distinctive lithofacies (Fig. 44), an upper nonvolcanic-bearing interval assigned to the eastern-margin piedmont lithofacies assemblage, and a lower volcanic-bearing interval that is compositionally similar to the ancestral Rio Grande lithofacies assemblage (Fig. 46). The Metropolitan Detention Center well samples are compositionally similar to the western-margin lithofacies assemblage (Figs. 45-46).

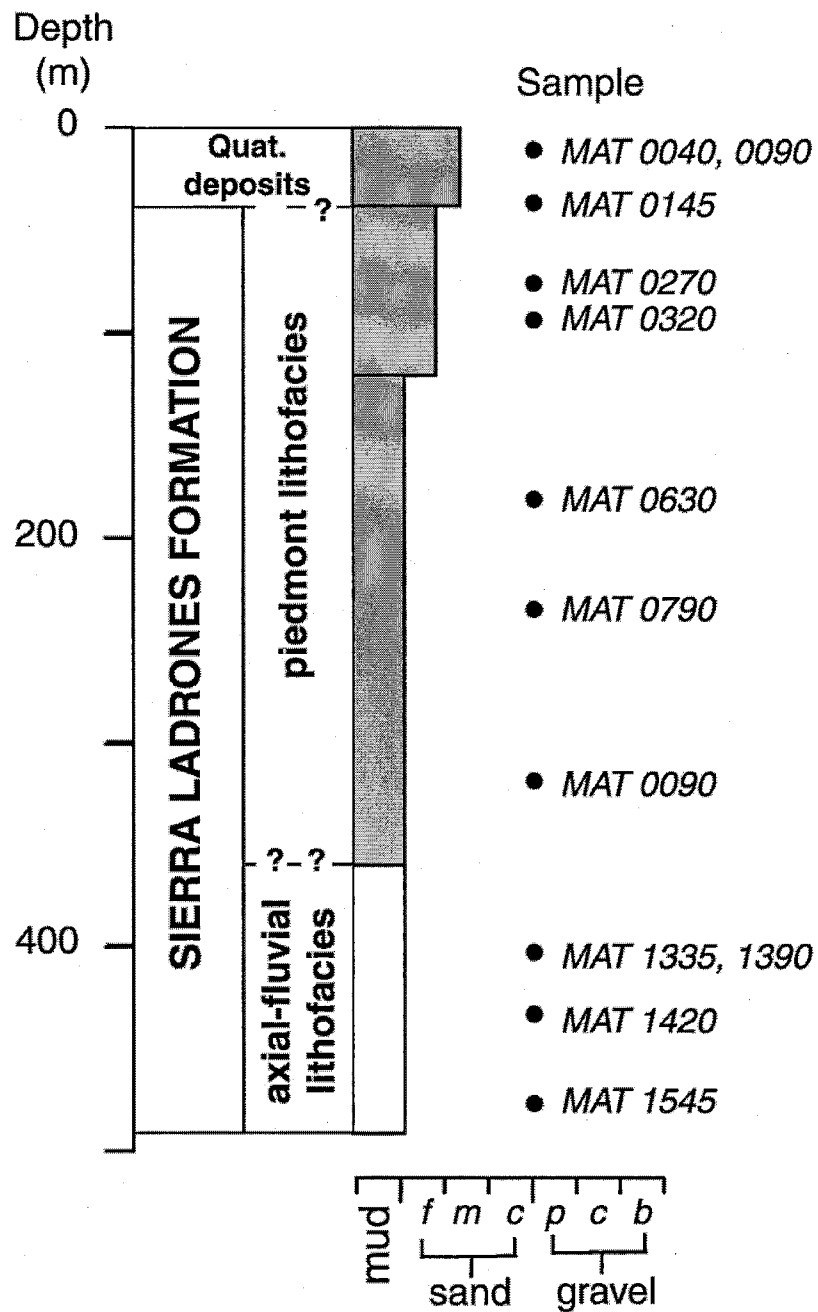


Figure 44. Graphical log of Matheson Park monitoring well, illustrating sample locations. Well was drilled less than 2 km west of the western front of the Sandia Mountains and eastern margin of the Albuquerque Basin. Samples described in Appendix C.

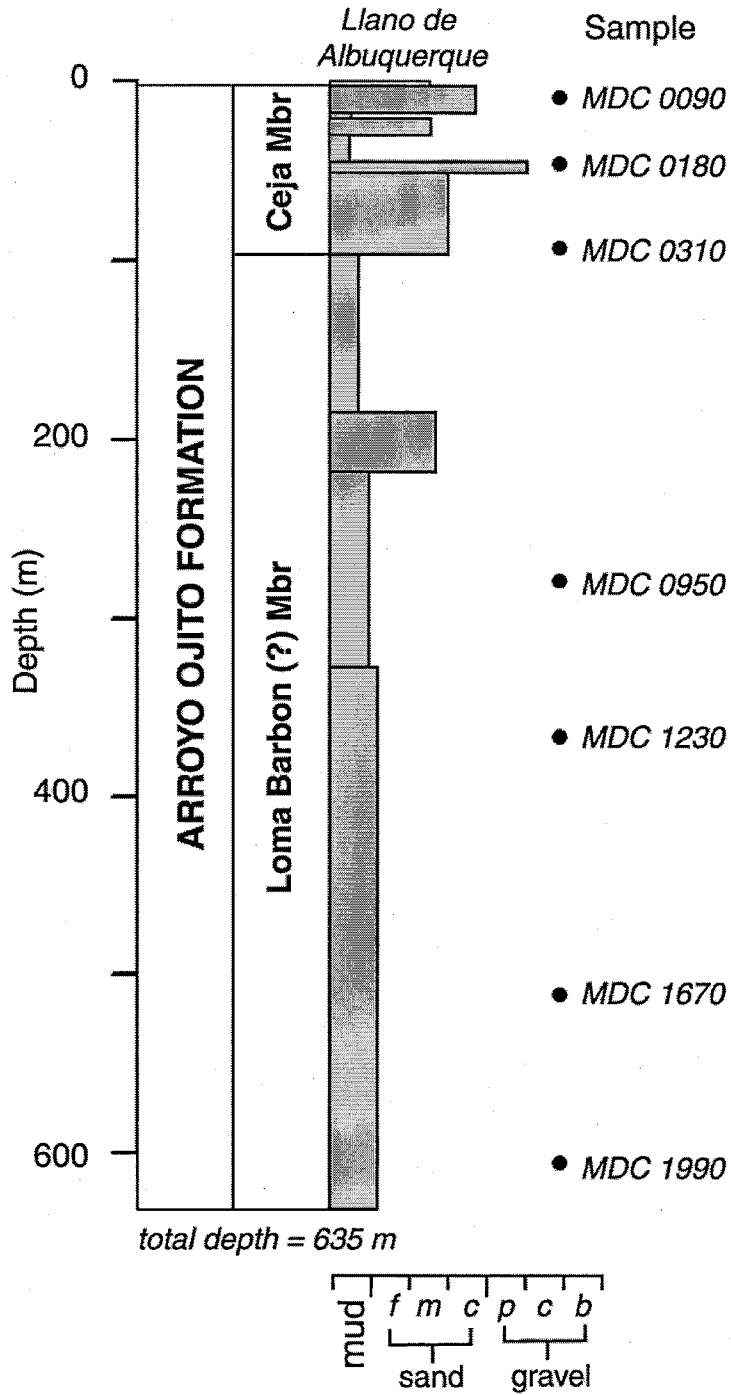


Figure 45. Graphical log of Metropolitan Detention Center well, illustrating sample locations and stratigraphic interpretations. Samples described in Appendix C.

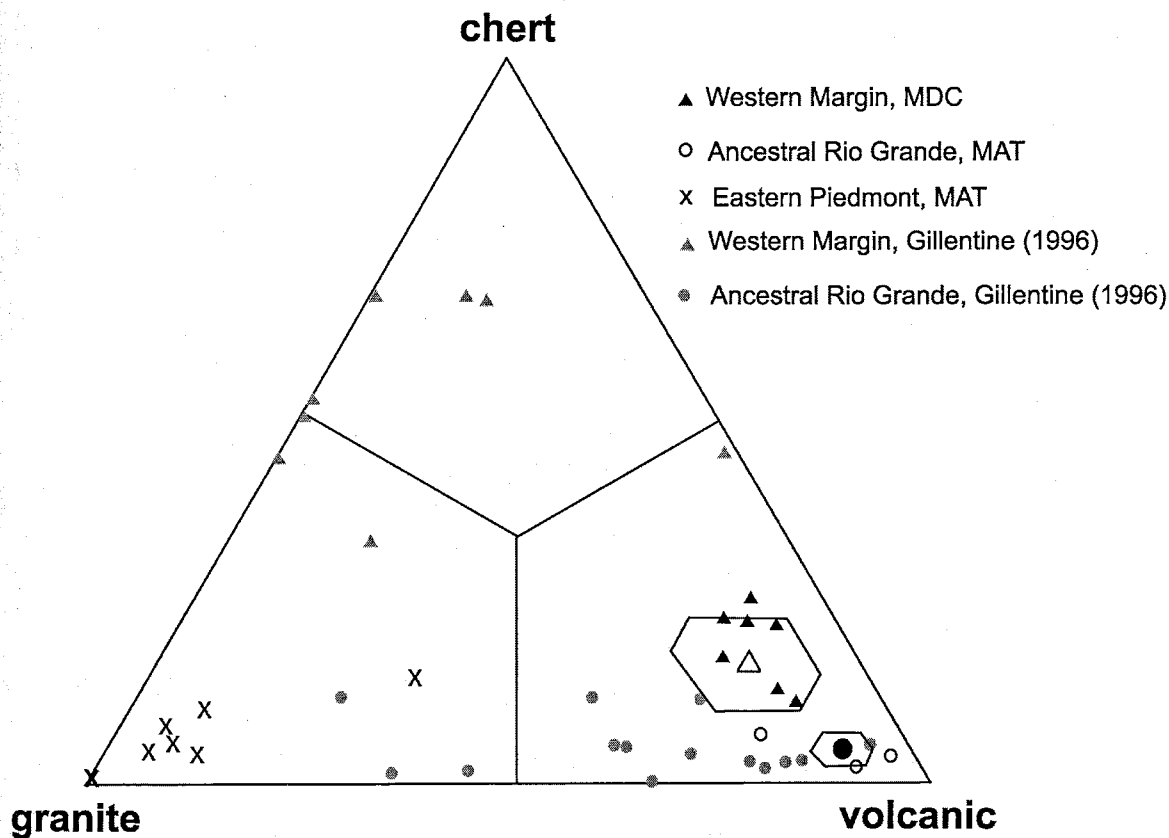


Figure 46. Ternary plot of water supply and groundwater monitoring wells in the Albuquerque area. Medium-grained sand of the Matheson Park (MAT) and Metropolitan Detention Center (MDC) wells (black symbols) are compared to plots of the medium-grained sand fraction analyzed by Gillentine (1996) from the Cerro Colorado #1 (cc1), Soil Amendment Facility #1 (saf), and the Charles #5 and #6 wells (ch5, ch6) (gray symbols). Mean and field of variation (1σ) of surface sandstone samples are noted by polygons and larger symbols. Locations of wells are on Figure 4.

Comparisons of the recalculated data of Gillentine (1996) to drillhole data of this study indicate a number of similarities and differences in detrital composition among lithofacies assemblages. The wells east of the Rio Grande Valley contain abundant volcanic constituents and minor chert and granite, supporting assignment to the Sierra Ladrones Formation. The wells west of the Rio Grande Valley do not favorably compare to the Metropolitan Detention Center well (Fig. 46), but contain abundant chert grains. The abundance of chert grains suggests that Gillentine's (1996) wells west of the Rio Grande correlate to the western-margin lithofacies assemblage; however, the rather large compositional variation among western wells is not known. Variability in the deposits or differences in sampling and grain counting methods could cause scatter in the data. Gillentine visually estimated grain size in core, whereas this study mechanically separated medium-grained sand for study. Although the comparisons between this study and the results of Gillentine are weak, they do support differentiation of lithofacies assemblages; however, additional study is needed to determine the causes of this apparent scatter.

Summary

Gravel deposits of the upper Santa Fe Group in the northern Albuquerque Basin can be used to differentiate among the three lithofacies assemblages present (Tables 7 and 8). Western-margin gravels contain a variety of clasts, including chert, granite, volcanic, and sedimentary pebbles and cobbles. The most distinguishing clasts of the western-margin lithofacies assemblage are Pedernal chert, fine-grained red granite, and gray to yellow

sandstone. Gravel of the ancestral Rio Grande deposits consists mainly of metaquartzite and volcanic clasts. Though Pedernal chert and sedimentary clasts are present in these deposits, they are very sparse. Piedmont gravels are distinguished by the abundance of sedimentary rocks, especially limestone, and the relative lack of volcanic clasts when compared to the other facies.

Sands deposits of the three lithofacies assemblages in the study area are more difficult to differentiate from one another. The western margin sands and ancestral Rio Grande sands contain abundant quartz, feldspar, and volcanic fragments. Western-margin deposits contain a greater proportion of chert than the deposits of the ancestral Rio Grande, however, the composition of these two facies overlap somewhat. Sand of the eastern piedmont contains mainly quartz, feldspar, and granitic fragments. Piedmont sands have little or no volcanic lithic fragments and thus can be distinguished from the other lithofacies assemblages studied.

DISCUSSION

Sand Data

The Gazzi-Dickinson method modal analysis of sandstone was developed primarily to determine sandstone compositions related to specific plate tectonic settings (Dickinson and Suczek, 1979; Ingersoll and Suczek, 1979; Dickinson, 1988). Examination of the proportions of quartz-feldspathic-lithic (QFL) components for sand in the study area, deposits of the western-margin and axial-river assemblages have a recycled orogen provenance, whereas deposits of the eastern-piedmont assemblage have a continental block provenance (Fig. 47). Western-margin and axial-river deposits are derived from the Colorado Plateau and southern Rocky Mountains provinces, which contain cratonic and orogenic rocks (Sloss, 1988) and support derivation from recycled orogens as indicated on Figure 47. Piedmont deposits are derived mostly from the granitic western front of the Sandia Mountains, supporting a continental block provenance (Fig. 47). The QFL analysis has been widely used in studies of sedimentology and stratigraphy. Many of these studies have been conducted in large basins and concerning large-scale sedimentation within tectonic basins. In comparison, the Albuquerque Basin is relatively small, and differentiating provenance using quartz, feldspar, and lithic sand fragments might not be sensitive enough to show variations at this scale. In addition, the source

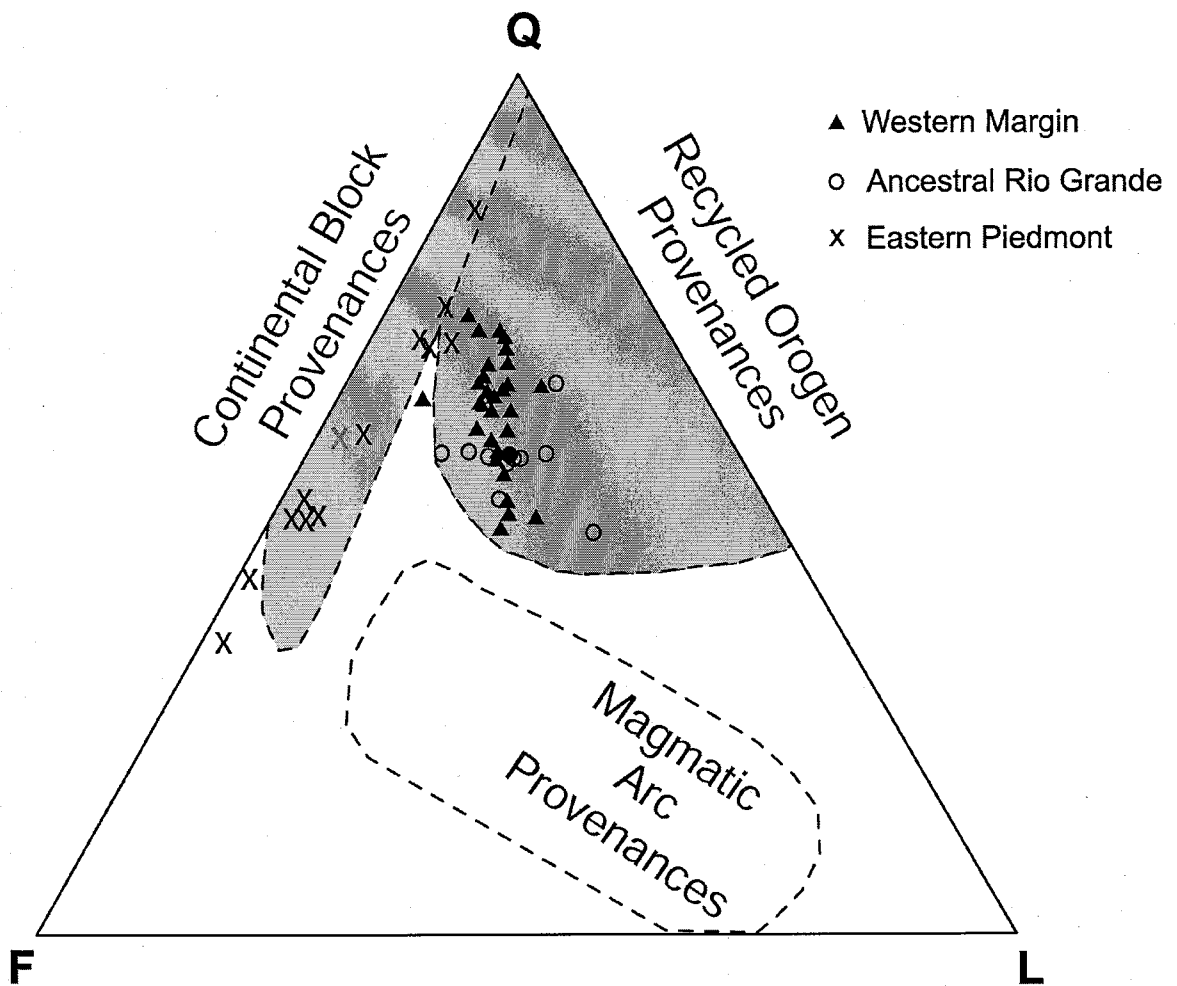


Figure 47. Ternary (quartz-feldspar-lithic) diagram of medium-grained sand and plate tectonic settings of sandstone (from Dickinson and Suczek, 1979).

areas of the ancestral Rio Puerco and ancestral Rio Grande are similar, and variations in sediment composition in these source areas are too slight to discriminate using QFL plots. Minor differences in the units are demonstrated with plots of lithic constituents, and of grain constituents, such as chert, granite, and volcanic grains (Fig. 42).

The ternary relationship among lithic fragments (LmLvLs) is widely used in petrographic analysis and provenance determination (Ingersoll and Suczek, 1979). The lithic (LmLvLs) data in this study plot near the arc-volcanic compositional field (Fig. 48), which is inconsistent with provenance interpretations using QFL relationships (Fig. 47). A study in the southern Rio Grande Rift had similar results of continental rift sediments plotted in the arc compositional field of the lithic (LmLvLs) ternary diagram (Mack, 1984). Mack suggested that this error occurs due to a transition in tectonic regime from arc-related volcanism to continental rifting, resulting in these apparently anomalous interpretations of sandstone compositions.

Depositional Environments

Most of the lithofacies components of the units studied were deposited by fluvial processes. Deposition by eolian and debris-flow or hyperconcentrated flood flow processes were also recognized, but these facies are relatively minor constituents. Based upon the amount of mud, sand, and gravel, as well as the sedimentary structures present, the depositional environments of these lithofacies assemblages can be inferred. The variation in lithofacies assemblages among the deposits of the western-margin, ancestral Rio Grande, and eastern-margin piedmont show that depositional environments varied laterally across the basin as well as vertically (Fig. 20). In the western-margin lithofacies assemblage, the planar bedded sand, low-angle cross bedded sand, and interbedded sand and mud indicate deposition by mixed-load streams and rivers. In addition, the presence

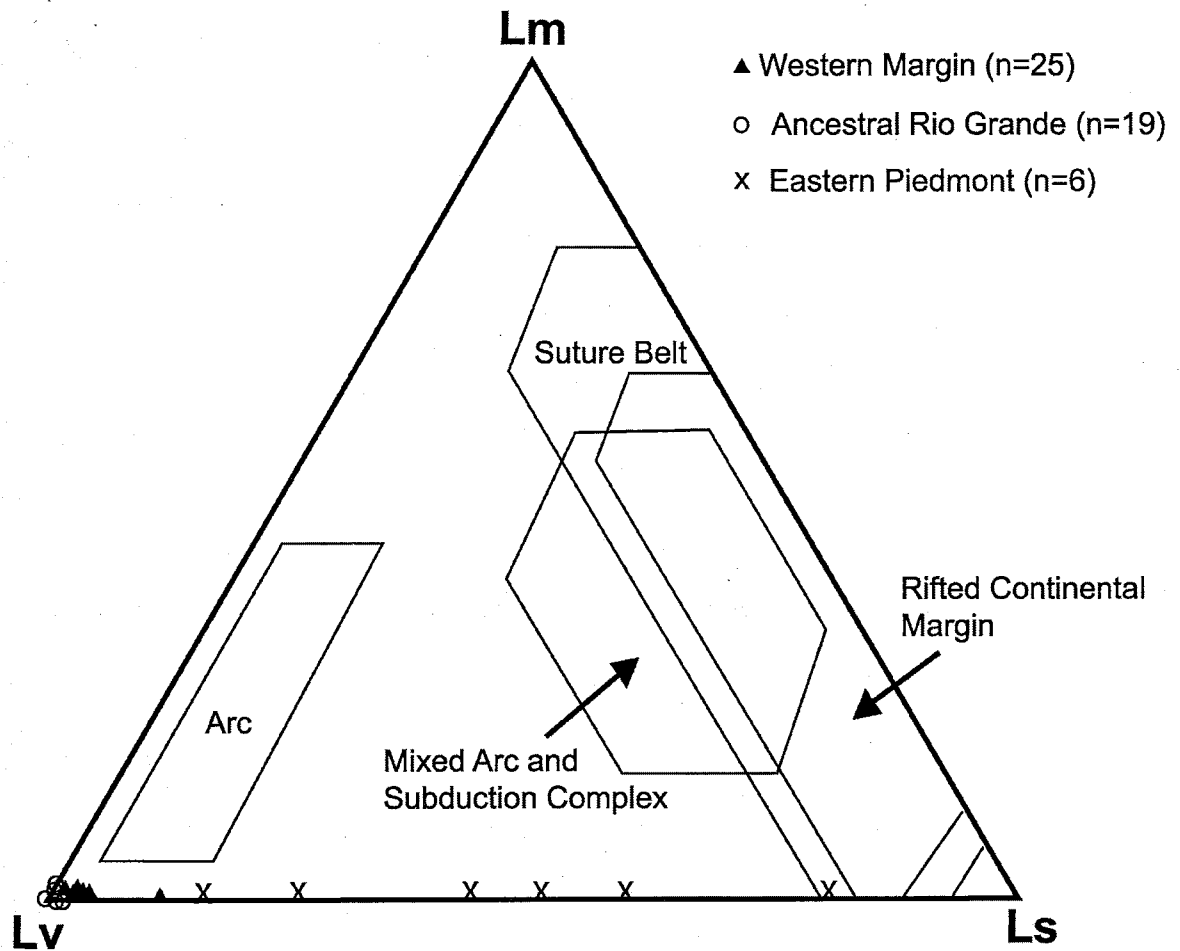


Figure 48. Ternary diagram of lithic fragments of medium-grained sand and plate tectonic settings of sandstone (from Ingersoll and Suczek, 1979).

of rhizoconcretions and paleosols indicates episodes of landscape stability and soil formation.

The Arroyo Ojito Formation (western-margin lithofacies assemblage) is associated with streams draining the western-margin of the northern Albuquerque Basin, which includes the east-tilted half grabens of the Calabacillas and southern Santo Domingo sub-basins. The Arroyo Ojito Formation contains tabular sandstone and conglomerate beds that are typically only a few meters thick at most. Sediments include gravels, planar and

cross stratified sands, as well as minor bioturbated mud. These deposits form channels with cross stratified, moderately sorted sand and gravel deposited in a fluvial environment by south-southeastward-flowing streams on faulted hangingwall-ramps of the study area sub-basins.

Gravel comprises a larger proportion of the western-margin lithofacies assemblage near the basin margin. With the exception of the Ceja Member (uppermost Arroyo Ojito Formation), which is quite coarse-grained and contains stacked channel sands and gravels that extend across much of the study area, gravel comprises a minor portion of the section towards basin depocenters to the southeast, where proportions of sand and gravel to mudstone and sandy mudstone tend to be greater. No single trunk channel system was distinguished, suggesting either deposition by contributory or distributary streams originating from the western-margin. This down-"stream" fining of sand and gravel beds suggests that the western-margin assemblage may have been deposited as a fluvial fan (e.g., Love, 1996; Miall, 1996; Mack et al., 1997); however, the lateral distribution and timing of channel facies deposition was not determined during this study. Channel deposits of the western-margin lithofacies assemblage may have braided-stream characteristics near the basin margin, but they probably do not characterize the entire western-margin fluvial system. These coarse-grained basin-margin facies become finer and may represent low-sinuosity, anastomosing, or distributary forms towards the basin depocenter.

The lack of strongly developed lateral accretionary beds and fining-upwards sequences in the western-margin lithofacies assemblage suggests deposition by low sinuosity or relatively straight channels, however, the greater scatter in paleocurrent

directions as compared to the other lithofacies assemblages (Figs. 12, 21, and 24) suggests that some of these channels might be meandering or anastomosing. The presence of distinct sand and gravel channels within the mudstone and sandstone that dominates the Arroyo Ojito Formation does not support the presence of large braided rivers, such as the Rio Grande. The western-margin lithofacies assemblage contain a considerable amount of mud and mudstone (10-35%), significantly more mud than in braided stream models, such as the Platte River sandy braided stream model of Miall (1977). Instead, low-sinuosity, sand- and gravel-bed streams on the gently sloping hangingwall ramp of the northern Albuquerque Basin may have deposited much of the western-margin lithofacies assemblage.

The fluvial system that deposited the western-margin assemblage was likely not a meandering fluvial system, despite the large amount of fine detritus deposited. Channels of meandering rivers tend to be narrow and deep, depending on sediment and water flux (Cant, 1982). Channel structures preserved in the Arroyo Ojito Formation are typically 1 to 5 meters thick and up to 80 meters in lateral extent. Meandering rivers are characterized by fining-upward trends (Boggs, 1995). The deposits of the Arroyo Ojito Formation exhibit few unambiguous fining-upwards trends. In addition, sand content in meandering rivers averages between 20 and 40% (Einsele, 1992). Deposits of the western-margin facies typically average 40 to 80% sand, significantly more than a typical meandering river. Meandering rivers are commonly interpreted as lower gradient fluvial systems (Einsele, 1992). The presence of cobbles and scattered boulders 10-15 km from the southern flank of the Sierra Nacimiento indicates that the streams were competent enough to move large detritus and likely had higher stream gradients near the basin

margins. However, braided rivers and meandering rivers are basically end member types of fluvial systems, and many fluvial systems have areas which are braided and areas that are meandering (Leeder, 1982; Boggs, 1995).

Lithofacies components of the western- and eastern-margin assemblages are similar. These lithofacies are also distinct from the braided axial-fluvial system of the ancestral Rio Grande (see below). The western-margin lithofacies assemblage may represent deposition on a laterally extensive alluvial plain coursed by south-southeastward-flowing streams.

The ancestral Rio Grande lithofacies assemblage of the Sierra Ladrones Formation is inferred to have been deposited by a braided river because deposits contain abundant open-framework gravel, abundant planar and cross-stratified gravels, planar and cross-stratified sands, and lack of fine-grained overbank deposits and soils (Miall, 1977). Thin, fine-grained sand and mud beds are present, but not common. This is consistent with braided river deposition (Cant, 1982; Einsele, 1992). This sort of gravel dominated braided river typically forms where there are rapid fluctuations in river discharge or an abundant source of coarse sediment and high rate of sediment supply. The presence of rip-up clasts of floodplain mudstone indicates incorporation of overbank deposits into the channel by scour and probably reflects deposition in an actively subsiding asymmetric or half-graben basin (Mack and James, 1993).

In the study area, the eastern-margin piedmont lithofacies assemblage of the Sierra Ladrones Formation is interpreted to have been deposited in a streamflow-dominated piedmont setting. Deposits of the piedmont assemblage in the study area commonly contain sedimentary structures indicative of fluvial deposition. For example, gravel beds

in the piedmont lithofacies assemblage are commonly cross-stratified, clast supported, and lenticular. Common sedimentary structures include planar and cross-stratified sands, indicative of upper flow-regime deposition and low-relief bar migration, respectively. Massive, matrix-supported beds are present, but make up only a small proportion of the total section. These minor conglomeratic beds were probably deposited as debris flows. Most conglomerate beds, though poorly sorted, exhibit planar bedding indicative of deposition in a longitudinal bedform of a fluvial system. Smith (2000b) suggests that such fluvially dominated piedmont sediments be classified as alluvial slope deposits, reserving the term alluvial fan deposits for sediments dominated by unconfined flow deposits.

Provenance

Gravel

Gravel in the western-margin lithofacies assemblage includes red granite, volcanic, and sedimentary rocks. Plutonic rocks are common in the Sierra Nacimiento, whereas volcanic rocks are common throughout the Jemez volcanic field. Sedimentary rocks are abundant on the Colorado Plateau and San Juan Basin. Paleocurrents measured in the western-margin lithofacies assemblage trend to the south-southeast (Fig. 12), supporting derivation from the northwest.

Connell et al. (1999) suggested that compositional differences in gravel content within the type Arroyo Ojito Formation section recorded unroofing of the southern flank of the Sierra Nacimiento. Such vertical variations in gravel composition were not

recognized at the Marillo-Zia sections. This difference could be due to input from other streams, not directly originating along the front of the Sierra Nacimiento, contributing sediments to the east of the type section of the Arroyo Ojito Formation. The Marillo-Zia section lies in a more basinward position relative to the Arroyo Ojito type section and Sierra Nacimiento. In addition, the vertical variation might not be as apparent towards basin depocenters.

Gravel of the ancestral Rio Grande deposits contain mainly rounded metaquartzite and volcanic clasts. Volcanic fields that lie to the north of the Albuquerque Basin, such as the Jemez, Ortiz-Cerillos, San Juan, and Latir volcanic fields, could be the source areas for some of the volcanic gravels. The Ortega Group of northern New Mexico (Soegaard and Eriksson, 1985) is the likely source of stratified metaquartzite gravels. A northern source is also supported by south-southwest trending paleocurrent data.

Conglomerate beds of the piedmont facies are dominated by clasts of coarse-grained pink granite and sedimentary rocks, especially limestone. Paleocurrent data and composition indicate these plutonic rocks are derived from the granite cored Sandia Mountains. The sedimentary clasts are derived from Paleozoic strata surrounding and capping the Sandia Mountains.

Sand

Sand in the western-margin lithofacies assemblage contains significant amounts of quartz, feldspar, and volcanic lithic fragments. Granite and chert grains are also present in smaller quantities. Numerous pre-rift formations in the San Juan Basin and Colorado

Plateau contain quartzose sandstones (Fig. 7) and erosion of these rocks could supply abundant quartz. The large amount of volcanic lithic fragments and the fact that plagioclase feldspars in the Arroyo Ojito Formation are commonly zoned indicates a volcanic source area. The Abiquiu Formation, a volcanoclastic sandstone exposed north of the Albuquerque Basin, probably supplied some sediment to the Arroyo Ojito Formation. Volcanic detritus could also be derived from the Jemez Volcanic Fields. Potassium-feldspar grains and granite in the western-margin lithofacies assemblage could be derived from the granitic rocks in the Sierra Nacimiento. Quartz detritus could be derived from a variety of sources, including quartzose upper Paleozoic and Mesozoic sandstone and lower Tertiary sandstones exposed on the adjacent Colorado Plateau and southern San Juan Basin (Stone et al., 1983).

Sand in the ancestral Rio Grande lithofacies assemblage is similar to that of the western-margin as it is quartz rich with significant amounts of feldspars and volcanic lithic fragments. As with western-margin deposits, quartz could be derived from a number of pre-rift quartzose sandstones. The abundant feldspar and volcanic lithic fragments in these deposits could be derived from older units containing large amounts of volcanic detritus or from volcanic centers to the north.

Piedmont sands contain much more quartz, feldspars, and granitic grains than the other lithofacies assemblages. These sediments are likely derived from Paleozoic sedimentary rocks that cap the granite core of the Sandia Mountains.

Drainage Evolution

Previous investigators (Large and Ingersoll, 1997) have postulated that the upper Santa Fe Group in the northern Albuquerque Basin is derived mostly from recycling of lower Santa Fe Group rocks such as the Zia Formation. The upward coarsening trend in deposits of the upper Santa Fe Group (Connell et al., 1998, 1999) does not support recycling of sandstone and mudstone in the Zia Formation, which contain only sparse chert gravel near the base (Gawne, 1981). The presence of Pedernal chert in the Arroyo Ojito Formation demonstrates at least partial recycling of lower Abiquiu Formation strata. The presence of red granite suggests derivation from the plutonic core of the Sierra Nacimiento. Abundant mud beds in the western-margin lithofacies assemblage suggest a source area with fine-grained rocks, most likely the extensive exposures of Mesozoic shale and sandstone in the Colorado Plateau and San Juan Basin (Stone et al., 1983). Paleocurrent data indicate that streams flowing to the south-southeast deposited the western-margin lithofacies assemblage (Arroyo Ojito Formation), supporting evidence that the source area for these sediments include the Sierra Nacimiento, San Juan Basin, and Colorado Plateau.

The evidence for a source of the Arroyo Ojito Formation in the Sierra Nacimiento and San Juan Basin, and a source of the ancestral Rio Grande sediments north of the Albuquerque Basin, supports the paleogeographic reconstruction of Connell et al. (1999), which attributes Arroyo Ojito Formation sedimentation to a south-southeasterly flowing fluvial system that is tributary to the axial-fluvial ancestral Rio Grande. In the paleogeographic reconstruction of Connell et al. (1999), the axial-fluvial deposits

interfingering with piedmont deposits, which were locally derived from the eastern structural margin of the Albuquerque Basin in the study area. The stratigraphic section measured at Arroyo San Francisco in this study document interfingering between eastern-margin piedmont and ancestral Rio Grande deposits, supporting the paleogeographic reconstruction of Connell et al. (1999) as the sole source of sediment for upper Santa Fe Group deposits.

The composition of gravel in the ancestral Rio Grande lithofacies assemblage is intermediate to the western- and eastern-margin assemblages (Figs. 26-32). The axial lithofacies constitutes the smallest proportion of the three lithofacies assemblages studied. If the axial-fluvial system of the ancestral Rio Grande transported sediments out of the basin, then compositional mixing from the western-margin and piedmont lithofacies assemblages would be expected as the ancestral Rio Grande flowed downstream. The intermediate character of the axial river gravel composition either retains its lithologic character through the study area, or that gravel content of the tributary lithofacies assemblages are easily modified by erosion and become compositionally indistinct from the axial system. Sandstone and limestone are not as durable as quartzite and chert (Abbott and Peterson, 1978). The presence of durable clasts of quartzite and chert that distinguish the western-margin and ancestral Rio Grande assemblages supports the inference that the axial river retains much of its lithologic character or that less durable gravels of the western-margin lithofacies assemblage are quickly broken down during transport within the ancestral Rio Grande assemblage.

Implications for Future Studies

This study documents petrographic distinctions among three major lithofacies assemblages of the upper Santa Fe Group in the northern Albuquerque Basin study area. Each lithofacies assemblage in the study area has a fairly distinctive petrography, both in the gravel and the sand fraction. The results of this study also show that the petrographic differences among the three lithofacies assemblages studied are pronounced in the gravel fraction of the deposits. This observation is an important implication for petrographic studies in the Albuquerque Basin. Previous studies (Lozinsky, 1994; Gillentine, 1996; Large and Ingersoll, 1997) concentrated on the petrography of the sand fraction. Dependence on medium-grained sand may not provide the most reliable basis for differentiation of the lithofacies assemblages studied. In the case of the northern Albuquerque Basin study area, the gravel fraction provides a reliable basis for differentiation of the lithofacies assemblages in the Albuquerque Basin. Weaker compositional trends in the sand fraction provide a basis for local differentiation among the lithofacies assemblages studied. Because the gravel shows significant clustering within the three lithofacies assemblages studied and the medium-grained sand shows only weak trends, the coarse- and very coarse-grained sand fractions might provide better control on differentiating sand in future subsurface studies.

CONCLUSIONS

The results of this study have several implications for ongoing studies in the Albuquerque Basin. First, integration of recent geologic mapping, stratigraphic sections, paleocurrent measurements, and sand and gravel petrography demonstrates that upper Santa Fe Group deposits in the northern Albuquerque Basin can be differentiated into at least three distinct lithofacies assemblages. The Arroyo Ojito Formation consists of sediments deposited from the western margin of the Albuquerque Basin. These sediments are derived from the San Juan Basin, Colorado Plateau, and Sierra Nacimiento and were deposited in a fluvial environment. Gravel clasts are mainly subangular to subrounded red granite, volcanic, Pedernal chert, and sedimentary rocks. Sands are mostly subarkose in composition. In addition to abundant quartz, feldspar, and volcanic grains, western margin sands contain noticeable amounts of chert and granite. Paleocurrents measured in the western margin deposits trend to the south-southeast.

The Sierra Ladrones Formation consists of sediments deposited by the ancestral Rio Grande and piedmont sediments shed off the faulted eastern margin of the Albuquerque Basin, including the rift-bounding Sandia Mountains. The ancestral Rio Grande sediments are derived from the northern New Mexico and southern Colorado and were deposited by a gravel-dominated braided river. Gravels are mainly rounded metaquartzite and volcanic rocks. Sands are subarkose that, unlike the western margin sands, do not

have significant chert. Paleocurrents measured in the ancestral Rio Grande deposits trend to the south-southwest. In the study area, piedmont deposits of the Sierra Ladrones Formation are derived from the Sandia Mountains and the eastern margin of the rift basin and were deposited in a stream-flow dominated alluvial-slope (piedmont) environment. Gravel clasts are mainly angular to subangular sedimentary rocks and pink granite clasts. Sands range from subarkose to arkose and are depleted in volcanic grains, unlike the other two facies of the basin. Paleocurrents measured in the piedmont trend to the west, and away from the eastern structural margin of the basin.

Integrated stratigraphic and petrographic (gravel and sand) analyses allows for differentiation of the three major lithofacies assemblages in the northern Albuquerque Basin. The lack of distinct vertical trends in the composition of sand and gravel and the upward coarsening trend of the deposits does not support a theory of simply recycling older basin-margin deposits of the Santa Fe Group, but rather recycling and erosion of older units outside the basin margin. This study also shows that detailed petrographic analyses of sand and gravel can be used to differentiate among the three lithofacies assemblages. In addition, though there is limited confidence in differentiating sand in the subsurface, some trends are present and may prove to be promising in differentiating units in the subsurface. Ancestral Rio Grande deposits contain abundant volcanic grains. Western-margin deposits also predominantly volcanic, but contain more granite and chert grains than the ancestral Rio Grande lithofacies assemblage deposits. Sediments of the eastern-margin piedmont lithofacies assemblage contain very few volcanic grains.

This study demonstrates the utility of gravel in determining provenance. Though the sand fraction of the lithofacies assemblages studied shows some compositional overlap,

the gravel fraction shows distinct clustering among the studied lithofacies assemblages.

This is an important observation because it demonstrates that even if the sand fraction of basin deposits appears to be compositionally similar, the coarser grained sediments can reveal important information for data analysis. Thus, in basins where gravel is present in the sediments, it is a very useful tool for provenance analysis.

REFERENCES

- Abbott, P.L., and Peterson, G.L., 1978, Effects of abrasion durability on conglomerate clast populations; examples from Cretaceous and Eocene conglomerates of the San Diego area, California: *Journal of Sedimentary Petrology*, v. 48, p. 31-42.
- Aldrich, M.J., Jr., Chapin, C.E., and Laughlin, A.W., 1986, Stress history and tectonic development of the Rio Grande rift, New Mexico: *Journal of Geophysical Research*, v. 94, p. 6199-6244.
- Anstey, R.L. and Chase, T.L., 1974, *Environments through time; a laboratory manual in the interpretation of ancient sediments and organisms*: American Geological Institute, 136 p.
- Bachman, G. O. and Mehnert, H. H., 1978, New K-Ar dates and late Pliocene to Holocene geomorphic history of the central Rio Grande region, New Mexico: *Geological Society of American Bulletin*, v. 89, p. 283-292.
- Beckner, J.R., 1996, *Cementation processes and sand petrography of the Zia Formation, Albuquerque Basin, New Mexico* [M.S. Thesis]: Socorro, New Mexico Institute of Mining and Technology, 146 p.
- Beckner, J.R., and Mozley, P.S., 1998, Origin and spatial distribution of early vadose and phreatic calcite cements in the Zia Formation, Albuquerque Basin, New Mexico, USA: *Special Publication of the International Association of Sedimentology*, v. 26, p. 27-51.
- Birkeland, P.W., 1984, *Soils and geomorphology*: New York, Oxford University Press, 372 p.
- Boggs, S., 1995, *Principles of Sedimentology and Stratigraphy*: Englewood Cliffs, Prentice Hall, 774 p.
- Bryan, K., 1938, *Geology and groundwater conditions of the Rio Grande depression in Colorado and New Mexico*, in *Natural Resources Planning Board, The Rio Grande joint investigations in the upper Rio Grande basin*: Washington, D. C., U.S. Government Printing Office, v. 1, part 2, p. 197-225.
- Bryan, K. and McCann, F.T., 1937, The Ceja del Rio Puerco-a border feature of the Basin and Range province in New Mexico, part I, stratigraphy and structure: *Journal of Geology*, v. 45, p. 801-828.

- Bryan, K. and McCann, F. T., 1938, The Ceja del Rio Puerco: a border feature of the Basin and Range province in New Mexico, Part II, geomorphology: *Journal of Geology*, v. 46, p. 1-16.
- Cant, D.J., 1982, Fluvial Facies Models *in* Scholle, P.A. and Spearing, D., eds., Sandstone Depositional Environments: American Association of Petroleum Geologists Memoir 31, p. 115-137.
- Cather, S.M., and Connell, S.D., 1998, Geology of the San Felipe Pueblo 7.5-minute quadrangle, Sandoval County, New Mexico: New Mexico Bureau of Mines and Mineral Resources, Open-File Digital Map 19, scale 1:24,000.
- Cather, S.M., Chamberlin, R.M., Chapin, C.E., and McIntosh, W.C., 1994, Stratigraphic consequences of episodic extension in the Lemitar Mountains, central Rio Grande rift: Geological Society of America, Special Paper 291, p. 157-170.
- Cather, S.M. Connell, S.D., Heynekamp, M.R. and Goodwin, L.B., 1997, Geology of the Sky Village SE (Arroyo de Las Calabacillas) 7.5-minute quadrangle, Sandoval County, New Mexico: New Mexico Bureau of Mines and Mineral Resources, Open-File Digital Geologic Map OF-DM 9, scale 1:24,000.
- Cather, S.M., Connell, S.D., and Black, B.A., 2000, Preliminary geologic map of the San Felipe Pueblo NE 7.5-Minute quadrangle, Sandoval County, New Mexico: New Mexico Bureau of Mines and Mineral Resources, Open-File Geologic Map OF-GM 37, scale 1:24,000.
- Chapin, C.E., 1979, Evolution of the Rio Grande rift--A summary, *in* Riecker, R. E., ed., Rio Grande rift: Tectonics and magmatism: Washington, D.C., American Geophysical Union, p. 1-5.
- Chapin, C.E., 1988, Axial basins of the northern and central Rio Grande rift; *in* Sloss, L.S., et al., eds., Sedimentary cover--North American Craton (U.S.) Geological Society of America, *Geology of North America*, v. D-2, p. 165-170.
- Chapin, C.E., and Cather, S.M., 1994, Tectonic setting of the axial basins of the northern and central Rio Grande rift: Geological Society of America, Special Paper 291, p. 5-25.
- Chapin, C.E. and Seager, W.R., 1975, Evolution of the Rio Grande rift in the Socorro and Las Cruces areas: New Mexico Geological Society, Guidebook 26, p. 297-321.
- Church, F.S., and Hack, J.T., 1939, An exhumed erosion surface in the Jemez Mountains: *Journal of Geology*, v. 47, p. 613-629.

- Colburn, I.P., Abbott, P.L., Minch, J., eds., 1989, Conglomerates in Basin Analysis: A Symposium Dedicated to A.O. Woodford: Pacific Section, Society of Economic Paleontologists and Mineralogists, v. 62, 312 p.
- Compton, R.R., 1985, *Geology in the field*: New York, John Wiley and Sons, 398 p.
- Connell, S.D., 1997, Geology of the Alameda 7.5-minute quadrangle, Bernalillo and Sandoval Counties, New Mexico: New Mexico Bureau of Mines and Mineral Resources, Open-File Digital Map 10, scale 1:24,000.
- Connell, S.D., 1998, Geology of the Bernalillo 7.5-minute quadrangle, Sandoval County, New Mexico: New Mexico Bureau of Mines and Mineral Resources, Open-File Digital Map 16, scale 1:24,000.
- Connell, S.D., 2001, Stratigraphy of the Albuquerque Basin, New Mexico: A progress report, *in* Connell, S.D., et al., eds., *Stratigraphy and tectonic development of the Albuquerque Basin, central Rio Grande rift, mini-papers for field trip guidebook*: New Mexico Bureau of Geology and Mineral Resources, Open-file report 454B, p. A1-A27.
- Connell, S.D., and Wells, S.G., 1999, Pliocene and Quaternary stratigraphy, soils, and tectonic geomorphology of the northern flank of the Sandia Mountains, New Mexico: implications for the tectonic evolution of the Albuquerque Basin: *New Mexico Geological Society, Guidebook 50*, p. 379-391.
- Connell, S.D., and Cather, S.M., 2001, Stratigraphy of the lower Santa Fe Group, Hagan embayment, north-central New Mexico: Preliminary results: New Mexico Bureau of Mines and Mineral Resources, Open-file report 454A, chapter H, 8 p.
- Connell, S.D., Cather, S.M., Ilg, B., Karlstrom, K.E., Menne, B., Picha, M., Andronicos, C., Read, A.S., Ilg, B., Bauer, P.W., and Johnson, P.S., 1995, Geology of the Placitas 7.5-minute quadrangle, Sandoval County, New Mexico: New Mexico Bureau of Mines and Mineral Resources, Open-File Digital Map 2, scale 1:12,000 and 1:24,000, *revised Sept. 9, 1999*.
- Connell, S.D., Allen, B.D., Hawley, J.W., and Shroba, R., 1998a, Geology of the Albuquerque West 7.5-minute quadrangle, Bernalillo County, New Mexico: New Mexico Bureau of Mines and Mineral Resources, Open-File Digital Geologic Map 17, scale 1:24,000.
- Connell, S.D., Allen, B.D., and Hawley, J.W., 1998b, Subsurface stratigraphy of the Santa Fe Group from borehole geophysical logs, Albuquerque area, New Mexico: *New Mexico Geology*, v. 20, n. 1, p. 2-7.

- Connell, S.D., Koning, D.J., and Cather, S.M., 1999, Revisions to the stratigraphic nomenclature of the Santa Fe Group, northwestern Albuquerque Basin, New Mexico: New Mexico Geological Society, Guidebook 50, p. 337-353.
- Connell, S.D., Love, D.W., Maldonado, F., Jackson, P.B., McIntosh, W.C., and Eppes, M.C., 2000, Is the top of the upper Santa Fe Group diachronous in the Albuquerque Basin? [abstract]: U.S. Geological Survey, Open-File Report 00-488, p. 18-20.
- Connell, S.D., Koning, D.J., Derrick, N.N., Love, D.W., Lucas, S.G., Morgan, G.S., Jackson-Paul, P.B., 2001, Second-day, Calabacillas sub-basin: Zia Pueblo, Rio Rancho, and Tijeras Arroyo, *in* Connell, S.D., Love, D.W., Lucas, S.G., Koning, D.J., Derrick, N.N., Maynard, S.R., Morgan, G.S., Jackson-Paul, P.B., and Chamberlin, R., trip leaders., Stratigraphy and tectonic development of the Albuquerque Basin, central Rio Grande rift, field trip guidebook: New Mexico Bureau of Geology and Mineral Resources, Open-file report 454A, p. 17-26.
- Darton, N.H., 1922, Geologic structure of parts of New Mexico: U.S. Geological Survey, Bulletin 726-E, 275 p.
- Davis, J.M., Lohmann, R.C., Phillips, F.M., Wilson, J.L. and Love, D.W., 1993, Architecture of the Sierra Ladrones Formation, central New Mexico: Depositional controls on the permeability correlation structure: Geological Society of America Bulletin, v. 105, p. 998-1007.
- Dickinson, W.R., 1970, Interpreting detrital modes of graywacke and arkose: Journal of Sedimentary Petrology, v. 40, p. 695-707.
- Dickinson, W.R., 1988, Provenance and sediment dispersal patterns in relation to paleotectonics and paleogeography of sedimentary basins, *in* Kleinspehn, K.L., and Paola, C., eds, New Perspectives in Basin Analysis: New York, Springer-Verlag, p. 3-26.
- Dickinson, W.R., and Suczek, 1979, Plate tectonics and sandstone composition: American Association of Petroleum Geologists Bulletin, v. 63, p. 2164-2182.
- Dutro, J.T., Dietrich, R.V., and Foose, R.M., *compilers*, 1989, Data sheets: Virginia, American Geological Institute, unpaginated.
- Eachran, D.B., 1991, Rosy, 2-D orientation analysis for the Macintosh, 20 p.
- Einsele, G., 1992, Sedimentary basins; evolution, facies, and sediment budget: Springer-Verlag, 628 p.

- Erskine, D.W., and Smith, G.A., 1993, Compositional characterization of volcanic products from a primarily sedimentary record: Geological Society of America Bulletin, v. 105, p. 1214-1222.
- Faulds, J.E. and Varga, R.J., 1998, The role of accommodation zones in the regional segmentation of extended terranes: Geological Society of America Special Paper 323 p. 1-45.
- Folk, R. L., 1974, Petrology of sedimentary rocks: Austin, Hemphill Publishing Company, 182 p.
- Galusha, T., 1966, The Zia Sand Formation, new early to medial Miocene beds in New Mexico: American Museum Novitates, n. 2271, p. 1-12.
- Gawne, C.E., 1981, Sedimentology and stratigraphy of the Miocene Zia Sand of New Mexico: Geological Society of America Bulletin, v. 92, part I (summary), p. 999-1007.
- Gawthorpe, R.L., and Leeder, M.R., 2000, Tectono-sedimentary evolution of active extensional basins: Basin Research, v. 12, p. 195-218.
- Gazzi, P., 1966, Le arenarie del flysch sopracretaceo dell' Appennino modenese: correlazioni con il flysch di Monghidoro: Mineralogica e Petrographica Acta, v. 12, p. 69-97 [cited in Dickinson, 1970].
- Gile, L.H., Hawley, J.W. and Grossman, R.B., 1981, Soils and geomorphology in the Basin Range area of southern New Mexico--guidebook to the Desert Project: New Mexico Bureau of Mines and Mineral Resources, Memoir 39, 222 p.
- Gillentine, J.M., 1996, Petrology and diagenesis of the middle and lower Santa Fe Group in the northern Albuquerque Basin, New Mexico: New Mexico Bureau of Mines and Mineral Resources, Open-file Report 402C, Chapter 6, 50 p., 4 app.
- Gorham, T.W. and Ingersoll, R.V., 1979, Evolution of the Eocene Galisteo Basin, north-central New Mexico: New Mexico Geological Society, Guidebook 30, p. 219-224.
- Gorham, T.W., 1979, Geology of the Galisteo Formation, Hagan basin, New Mexico [M.S. Thesis]: Albuquerque, University of New Mexico, 136 p.
- Grauch, V.J.S., Gillespie, C.L., and Keller, G.R., 1999, Discussion of new gravity maps for the Albuquerque basin area: New Mexico Geological Society, Guidebook 50, p. 119-124.

- Hawley, J.W., compiler, 1978, Guidebook to the Rio Grande rift in New Mexico and Colorado: New Mexico Bureau of Mines and Mineral Resources, Circular 163, 241 p.
- Hawley, J. W., 1996, Hydrogeologic framework of potential recharge areas in the Albuquerque Basin, central New Mexico: New Mexico Bureau of Mines and Mineral Resources, Open-file Report 402 D, Chapter 1, 68 p., appendix.
- Hawley, J.W., Kottowski, F.E., Strain, W.S., Seager, W.R., King, W.E. and LeMone, D.V., 1969, The Santa Fe Group in the south-central New Mexico border region: New Mexico Bureau of Mines and Mineral Resources, Circular 104, p. 52-76.
- Hawley, J.W., Hasse, C.S., and Lozinsky, R.P., 1995, An underground view of the Albuquerque Basin, *in* The Water Future of the Albuquerque and middle Rio Grande Basin: Water Resource Research Institute Report, p. 37-56.
- Hayden, F.V., 1869, Preliminary field report of the U.S. Geological Survey of Colorado and New Mexico: U.S. Geological Survey, 3rd Annual Report, 155 p.
- Howard, J.L. 1993, The statistics of counting clasts in rudites; a review, with examples from upper Paleogene of Southern California, U.S.A.: *Sedimentology*, v. 40, p. 157-174.
- Ingersoll, R.V., and Suczek, C.A., 1979, Petrology and provenance of Neogene sand from Nicobar and Bengal fans, DSDP sites 211 and 218: *Journal of Sedimentary Petrology*, v. 49, p. 1217-1228.
- Ingersoll, R. V., Bullard, T. F., Ford, R. L., Grimm, J. P., Pickle, J. D. and Sares, S. W., 1984, The effect of grain size on detrital modes: A test of the Gazzi-Dickinson point-counting method: *Journal of Sedimentary Petrology*, v. 54, p. 103-116.
- Ingersoll, R. V., Cavazza, W., Baldrige, W. S. and Shafiqullah, M., 1990, Cenozoic sedimentation and paleotectonics of north-central New Mexico: Implications for initiation and evolution of the Rio Grande rift: *Geological Society of America Bulletin*, v. 102, p. 1280-1296.
- Izett, G.A., Obradovich, J.D., 1994, $^{40}\text{Ar}/^{39}\text{Ar}$ age constraints for the Jaramillo Normal Subchron and the Matuyama-Brunhes geomagnetic boundary: *Journal of Geophysical Research*, v. 99, n. 2, p. 2925-2934
- Kautz, P.F., Ingersoll, R.V., Baldrige, W.S., Damon, P.E., and Shafiqullah, M., 1981, Geology of the Espinazo Formation (Oligocene), north-central New Mexico: *Geological Society of America Bulletin*, v. 92, n. 12, Part I, p. 980-983, Part II, p. 2318-2400.

- Kelley, V.C., 1977, Geology of the Albuquerque Basin, New Mexico: New Mexico Bureau of Mines and Mineral Resources, Memoir 33, 60 p.
- Kelley, V.C. and Northrop, S.A., 1975, Geology of Sandia Mountains and vicinity, New Mexico: New Mexico Bureau of Mines and Mineral Resources, Memoir 29, 136 p.
- Koning, D.J., and Personius, S.F., *in press*, Preliminary geologic map of the Bernalillo NW quadrangle, Sandoval County: U.S. Geological Survey, Miscellaneous Field Investigations Map, scale 1:24,000.
- Koning, D., Pederson, J., Pazzaglia, F.J., 1998, Geology of the Cerro Conejo (Sky Village NE), 7.5 min quadrangle, Sandoval county, New Mexico: Mexico Bureau of Mines and Mineral Resources Open-File Geologic Map OF-GM48, scale 1:24,000.
- Lambert, P.W., 1968, Quaternary stratigraphy of the Albuquerque area, New Mexico: [Ph.D. Dissertation]: Albuquerque, University of New Mexico, 329 p.
- Lane, C.L., 1989, Comparison of Arenite and Conglomerate Clast Petrology: Utility in Provenance Determination, Southern California, *in* Colburn, I.P., Abbott, P.L., and Minch, J., eds., *Conglomerates in Basin Analysis: A Symposium Dedicated to A.O. Woodford: Pacific Section SEPM*, vol. 62, p. 255-267.
- Large, E., 1995, Miocene and Pliocene sandstone petrofacies of the northern Albuquerque basin, New Mexico [M.S. Thesis]: Los Angeles, California, University of California, 113 p.
- Large, E., and Ingersoll, R.V., 1997, Miocene and Pliocene sandstone petrofacies of the northern Albuquerque Basin, New Mexico, and implications for evolution of the Rio Grande rift: *Journal of Sedimentary Research, Section A: Sedimentary Petrology and Processes*, v. 67, p. 462-468.
- Leeder, M.R., 1982, *Sedimentology*: London, George Allen and Unwin, 344 p.
- Leeder, M.R., and Gawthorpe, R.L., 1987, Sedimentary models for extensional tilt-block/half-graben basins: *Geological Society of London, Special Publication 28*, p. 139-152.
- Leeder, M.R., and Jackson, J.A., 1993, The interaction between normal faulting and drainage in active extensional basins, with examples from the western United States and central Greece: *Basin Research*, v. 5, p. 79-102.
- Leeder, M.R., Mack, G.H., and Salyards, S.L., 1996, Axial-transverse fluvial interactions in half-graben: Plio-Pleistocene Palomas Basin, southern Rio Grande rift, New Mexico, USA: *Basin Research*, v. 12, p. 225-241.

- Love, D.W., 1996, Fluvial fans and related deposits of the Mimbres drainage: *New Mexico Geology*, v. 18, n. 4, p. 81-92.
- Love, D.W., and Young, J.D., 1983, Progress report on the late Cenozoic geologic evolution of the lower Rio Puerco: *New Mexico Geological Society, Guidebook 34*, p. 277-284.
- Love, D.W., Hitchcock, C., Thomas, E., Kelson, K.I., Van Hart, D., Cather, S., Chamberlain, R., Anderson, O., Hawley, J.W., Gillentine, J., White, W., Noler, J., Sawyer, T., Nyman, M., Harrison, B., and Colpitts, R., 1996, *Geology of the Hubbell Spring 7.5-minute quadrangle, Bernalillo and Valencia Counties, New Mexico: New Mexico Bureau of Mines and Mineral Resources, Open-file Digital Map 5, scale 1:24,000.*
- Lozinsky, R.P., 1988, Stratigraphy, sedimentology, and sand petrology of the Santa Fe Group and pre-Santa Fe Tertiary deposits in the Albuquerque Basin, central New Mexico: [Ph.D. Dissertation]: Socorro, New Mexico Institute of Mining and Technology, 298 p.
- Lozinsky, R.P., 1994, Cenozoic stratigraphy, sandstone petrology, and depositional history of the Albuquerque Basin, central New Mexico: *Geological Society of America, Special Paper 291*, p. 73-82.
- Lozinsky, R.P. and Hawley, J.W., 1986, Upper Cenozoic Palomas Formation of south-central New Mexico: *New Mexico Geological Society, Guidebook 37*, p. 239-247.
- Lozinsky, R.P., and Hawley, J.W., 1991, Cenozoic structural evolution and depositional history in three Rio Grande rift basins, central and southern New Mexico [abstract]: *Geological Society of America, Abstracts with Programs*, v. 23, n. 4, p. A-44.
- Lozinsky, R.P. and Tedford, R.H., 1991, Geology and paleontology of the Santa Fe Group, southwestern Albuquerque Basin, Valencia County, New Mexico: *New Mexico Bureau of Mines and Mineral Resources, Bulletin 132*, 35 p.
- Lozinsky, R.P., Hawley, J.W. and Love, D.W., 1991, Geologic overview and Pliocene-Quaternary history of the Albuquerque Basin, central New Mexico: *New Mexico Bureau of Mines and Mineral Resources, Bulletin 137*, p. 157-162.
- Lucas, S.G., Williamson, T.E., and Sobus, J., 1993, Plio-Pleistocene stratigraphy, paleoecology, and mammalian biochronology, Tijeras Arroyo, Albuquerque area, New Mexico: *New Mexico Geology*, v. 15, p. 1-8.
- Lucas, S.G., Pazzaglia, F.J., and Connell, S.D., 1999, Albuquerque Geology- Paleozoic and Mesozoic Stratigraphy: *New Mexico Geological Society, Guidebook 50.*

- Luedke, R.G., and Smith, R.L., 1978, Map showing distribution, composition, and age of late Cenozoic volcanic centers in Arizona and New Mexico: U.S. Geological Survey, Miscellaneous Investigations Series, I-1091-A.
- Machette, M.N., 1978, Geologic map of the San Acacia Quadrangle, Socorro County, New Mexico: U.S. Geological Survey, Geologic Quadrangle Map GQ-1415, scale 1:24,000.
- Mack, G.H., 1984, Exception to the relationship between plate tectonics and sandstone composition: *Journal of Sedimentary Petrology*, vol. 54, p. 212-220.
- Mack, G.H. and Seager, W.R., 1990, Tectonic control on facies distribution of the Camp Rice and Palomas Formations (Pliocene-Pleistocene) in the southern Rio Grande rift: *Geological Society of America Bulletin*, v. 102, p. 45-53.
- Mack, G.H., and James, W.C., 1993, Control of basin symmetry on fluvial lithofacies, Camp Rice and Palomas formations (Plio-Pleistocene), southern Rio Grande rift, USA: *International Association of Sedimentologists, Special Publication 17*, p. 439-449.
- Mack, G.H., Salyards, S.L., and James, W.C., 1993, Magnetostratigraphy of the Plio-Pleistocene Camp Rice and Palomas Formations in the Rio Grande rift of southern New Mexico: *American Journal of Science*, v. 293, p. 47-77.
- Mack, G.H., McIntosh, W.C., Leeder, M.R., and Monger, H.C., 1996, Plio-Pleistocene pumice floods in the ancestral Rio Grande, southern Rio Grande rift, New Mexico, USA: *Sedimentary Geology*, v. 103, p. 1-8.
- Mack, G.A., Love, D.W., and Seager, W.R., 1997, Spillover models for axial rivers in regions of continental extension: the Rio Mimbres and Rio Grande in the southern Rio Grande rift, USA: *Sedimentology*, v. 44, p. 637-652.
- Mack, G.A., Salyards, S.L., McIntosh, W.C., and Leeder, M.R., 1998, Reversal magnetostratigraphy and radioisotopic geochronology of the Plio-Pleistocene Camp Rice and Palomas Formations, southern Rio Grande rift: *New Mexico Geological Society, Guidebook 49*, p. 229-236.
- Maldonado, F., Connell, S.D., Love, D.W., Grauch, V.J.S., Slate, J.L., McIntosh, W.C., Jackson, P.B., and Byers, F.M., Jr., 1999, Neogene geology of the Isleta Reservation and vicinity, Albuquerque Basin, New Mexico: *New Mexico Geological Society Guidebook 50*, p. 175-188.
- Manley, K., 1978, Geologic map of Bernalillo NW quadrangle, Sandoval County, New Mexico: U.S. Geological Survey Geologic, Quadrangle Map GQ 1446, scale 1:24,000.

- May, S.J., and Russell, L.R., 1994, Thickness of the syn-rift Santa Fe Group in the Albuquerque Basin and its relation to structural style *in* Keller, G.R., and Cather, S.M., eds., Basins of the Rio Grande Rift: Structure, Stratigraphy, and Tectonic Setting: Boulder, Geological Society of America Special Paper 291, p. 113-123.
- McKee, E.D., and Weir, G.W., 1953, Terminology for stratification and cross-stratification in sedimentary rocks: Geological Society of America Bulletin, v. 64, p. 381-390.
- Miall, A.D., 1977, A review of the braided river depositional environment: Earth Science Review, v. 13, p. 1-62.
- Miall, A.D., 1996, The geology of fluvial deposits: New York, Springer, 582 p.
- Moore, J.D., 2000, Tectonics and volcanism during deposition of the Oligocene-lower Miocene Abiquiu Formation in northern New Mexico [M.S. Thesis]: Albuquerque, University of New Mexico, 147 p., 3 pl.
- Morgan, G.S., and Lucas, S.G., 1999, Pliocene (Blancan) vertebrates from the Albuquerque Basin, North-central New Mexico: New Mexico Geological Society Guidebook 50, p. 363-370.
- Morgan G.S., and Lucas, S.G., 2000, Pliocene and Pleistocene vertebrate faunas from the Albuquerque Basin, New Mexico: New Mexico Museum of Natural History and Science, Bulletin 16, p. 217-240.
- Mozley, P.S., Chamberlin, R.M., Gillentine, J.M., and Lozinsky, R.P., 1992, Petrologic data, *in* Hawley, J.W., and Hasse, C.S., compilers, Hydrogeologic Framework of the northern Albuquerque Basin: New Mexico Bureau of Mines and Mineral Resources, Open-file report 387, p. IV-1 to IV-17.
- Mozley, P.S. and Davis, J.M., 1996. Relationship between oriented calcite concretions and permeability correlation in an alluvial aquifer, Sierra Ladrones Formation, New Mexico: Journal of Sedimentary Research, v. 66, p. 11-16.
- Munsell, 1992, Soil Color Chart: Kollmorgen Instruments Corp., New York, unpaginated.
- Peters, L., 2001, $^{40}\text{Ar}/^{39}\text{Ar}$ geochronology results from the Albuquerque Basin mapping project [unpubl. data]: New Mexico Geochronological Research Laboratory Internal Report NMGR-IR-157, Socorro, New Mexico Institute of Mining and Technology, 26 p.

- Perkins, M.E., Brown, F.H., Nash, W.P., McIntosh, W.C., Williams, S.K., 1998, Sequence, age, and source of silicic fallout tuffs in middle to late Miocene basins of the northern Basin and Range Province: Geological Society of America Bulletin, v. 110, p. 344-360.
- Personius, S.F., Machette, M.N., and Stone, B.D., 2000, Preliminary geologic map of the Loma Machete quadrangle, Sandoval County, New Mexico: U.S. Geological Survey, Miscellaneous Field Investigations, MF-2334, scale 1:24,000, *ver. 1.0*.
- Powers, M.C., 1953, A new roundness scale for sedimentary particles: Journal of Sedimentary Petrology, v. 23, p. 117-119.
- Rosendahl, B. R., 1987, Architecture of continental rifts with special reference to East Africa: Annual Reviews of Earth and Planetary Sciences, v. 15, p. 445-503.
- Russell, L.R., and Snelson, S., 1994, Structure and tectonic of the Albuquerque Basin segment of the Rio Grande rift: Insights from reflection seismic data: Geological Society of America, Special Paper 291, p. 83-112.
- Sloss, L.L., 1988, Tectonic evolution of the craton in Phanerozoic time, *in* Sloss, L.L. ed., Sedimentary Cover – North American Craton: Boulder, Geological Society of America, The Geology of North America, v. D-2.
- Smith, G.A., 1995, Paleogeographic, volcanologic, and tectonic significance of the upper Abiquiu Formation at Arroyo del Cobre, New Mexico: New Mexico Geological Society, Guidebook 46, p. 261-270.
- Smith, G.A., 2000a, Oligocene onset of Santa Fe Group sedimentation near Santa Fe, New Mexico [abstract]: New Mexico Geology, v. 22, p. 43.
- Smith, G.A., 2000b, Recognition and significance of streamflow-dominated piedmont facies in extensional basins: Basin Research, v. 12, p. 399-411.
- Smith, G.A., and Kuhle, A.J., 1998, Geology of the Santo Domingo Pueblo 7.5-minute quadrangle, Sandoval County, New Mexico: New Mexico Bureau of Mines and Mineral Resources, Open-file Digital Geologic Map OF-DM 15, scale 1:24,000
- Smith, G.A., and Lavine, A., 1996, What is the Cochiti Formation?: New Mexico Geological Society, Guidebook 47, p. 219-224.
- Smith, G.A., Kuhle, A.J., McIntosh, W.C., 2001, Sedimentologic and geomorphic evidence for seesaw subsidence of the Santo Domingo accommodation-zone basin, Rio Grande Rift, New Mexico: Geological Society of America Bulletin, v. 113, p. 561-574

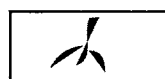
- Smith, R.L., Bailey, R.A., and Ross, C.S., 1970, Geologic map of the Jemez Mountains, New Mexico: U.S. Geological Survey, Miscellaneous Geological Investigations, I-571, scale 1:125,000.
- Soegaard, K. and Ericksson, K.A., 1985, Evidence of tide, storm, and wave interaction on a Precambrian siliciclastic shelf; the 1,700 MY Ortega Group, New Mexico: *Journal of Sedimentary Petrography*, v. 55, p. 672-684.
- Spiegel, Z., 1961, Late Cenozoic sediments of the lower Jemez River region: New Mexico Geological Society, Guidebook 12, p. 132-138.
- Spiegel, Z. and Baldwin, B., 1963, Geology and water resources of the Santa Fe area, New Mexico: U.S. Geological Survey, Water-Supply Paper 1525, 258 p.
- Stearns, C.E., 1953, Tertiary geology of the Galisteo-Tonque area, New Mexico: *Geological Society of America Bulletin*, v. 64, p. 459-508.
- Stone, W.J., Lyford, F.P., Frenzel, P.F., Mizell, N.M., and Padgett, E.T., 1983, Hydrogeology and Water Resources of the San Juan Basin, New Mexico: New Mexico Bureau of Mines and Mineral Resources, Hydrogeologic Report 6, 70 p.
- Tedford, R.H., 1981, Mammalian biochronology of the late Cenozoic basins of New Mexico: *Geological Society of America Bulletin*, Part I, v. 92, p.1008-1022.
- Tedford, R.H., and Barghoorn, S., 1997, Miocene mammals of the Española and Albuquerque Basins, north-central New Mexico: *New Mexico Museum of Natural History and Science Bulletin* 11, p. 77-95.
- Tedford, R.H., and Barghoorn, S., 1999, Santa Fe Group (Neogene), Ceja del Rio Puerco, northwestern Albuquerque Basin, Sandoval County, New Mexico: *New Mexico Geological Society, Guidebook* 50, p. 327-335.
- Woodward, L.A., 1987, Geology and mineral resources of Sierra Nacimiento and vicinity, New Mexico: New Mexico Bureau of Mines and Mineral Resources, *Memoir* 42, 84 p.
- Woodward, L.A., and Timmer, R.S., 1979, Geology of Jarosa quadrangle, New Mexico: New Mexico Bureau of Mines and Mineral Resources, *Geological Map* 34, scale 1:24,000.
- Woodward, L.A., Callender, J.F., Seager, W.R., Chapin, C.E., Gries, J.C., Shaffer, W.L., and Zilinski, R.E., 1978, Tectonic map of the Rio Grande rift region in New Mexico, Chihuahua, and Texas: New Mexico Bureau of Mines and Mineral Resources, *Circular* 163, 1 pl.

Wright, H.E., 1946, Tertiary and Quaternary geology of the lower Rio Puerco area, New Mexico: Geological Society of America Bulletin, v. 57, p. 383-456.

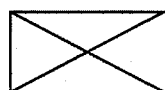
APPENDIX A

STRATIGRAPHIC SECTIONS

EXPLANATION OF SYMBOLS



rhizoconcretions and bioturbated beds



poorly exposed



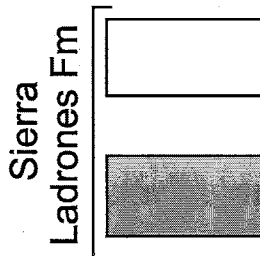
basalt flow



ash or fluviually recycled pumice



western-margin lithofacies assemblage
(Arroyo Ojito Formation)



axial fluvial lithofacies assemblage
(ancestral Rio Grande)

eastern piedmont lithofacies assemblage



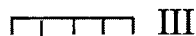
SFP-3 gravel sample (Appendix B)



SFP-3a sand sample (Appendix C)

LFC

lithofacies code (Table 3)



soil, including carbonate morphologic
stage (Birkeland, 1984)

APPENDIX A1a. Marillo measured section of the upper Cerro Conejo Member of the Zia Formation, and Navajo Draw Member of the Arroyo Ojito Formation, Bernalillo NW and Cerro Conejo 7.5-minute quadrangle, Sandoval County, New Mexico. Base of measured section at N: 3,925,858 m, E: 343,041 m (Zone 13S, NAD 83). Top at N: 3,925,790 m, E: 342,220 m. Measured upsection from unit 1 by Nathalie Brandes and Paul Brandes with Jacob Staff and Abney Level on July 25, 27, and 28, 2000. Colors measured dry. Textural abbreviations for sand include: very fine, vfL, vfU; fine fL, fU; medium, mL, mU; coarse, cL, cU; and very coarse, vcL, vcU. Numerical unit designations established upsection, but listed in descending stratigraphic order.

| Unit | Description | Thickness (m) |
|--|--|---------------|
| Arroyo Ojito Formation, Navajo Draw Member: 223 m | | |
| E. | Muddy sand with mud interbeds: yellow (2.5Y 7/6), vfU to mU, well sorted, subangular to subrounded, planar laminations, mud interbeds up to 40 cm thick are reddish brown (2.5YR 5/4) and weather to a cracked, and blocky structure. Section continues. See Zia stratigraphic section. | 6.0 |
| C-D. | Interbedded sand and mud: very pale brown (10YR 7/4), vfU to mU, moderate sorting, subangular to rounded, individual beds up to 2 m thick with indistinct internal bedding, muddier intervals are light yellowish brown to pale yellow (2.5Y 6/3 to 2.5Y 7/3), and weather to a cracked, blocky structure. | 32.8 |
| B. | Mud with interbedded sandstone: reddish brown (5YR 5/4), beds up to 60 cm thick. Interbedded very pale brown (10YR 7/3) sandstone, fL to cL, well sorted, subangular to rounded, forms cemented sandstone ledges. | 10.3 |
| A. | Sand: pale yellow (2.5Y 7/3), fL to vcU, moderate sorting, subrounded to rounded, sand beds locally exhibit fining upward sequences. Sand beds are up to 30 cm thick with internal mm-scale planar to low angle cross laminations. Pale yellow (5Y 7/3) mud interbeds are up to 6 cm thick, top of unit becomes muddier. | 24.9 |
| 18. | Sand with interbedded mud: reddish yellow (5 YR 6/6), vfU to cU, moderate sorting, subangular to subrounded, planar to cross laminations. Mud interbeds are 10-30 cm thick, red (2.5YR 4/6), and weather to a cracked popcorn-like texture. Top of the unit becomes muddier, with mud beds up to 1 m in thickness. | 20.1 |
| 17. | Sand: light yellowish brown (2.5Y 6/4), vfU to cU, moderate sorting, subangular to subrounded, millimeter-scale planar laminations. | 16.5 |
| 16. | Mud: reddish brown (5YR 4/4), weathers to a platy structure. Central 1 m of unit is very pale brown (10YR 8/4) sand, vfU to mU, well sorted, subangular to subrounded, indistinguishable bedding. Poorly exposed. | 6.6 |
| 15. | Sand: very pale brown (10 YR 7/4), fU to vcL, poor sorting, subrounded to rounded, mm-scale planar to cross laminations | 8.6 |
| 14. | Sand with interbedded mud: very pale brown (10YR 7/4), vfU to cL, moderate sorting, subangular to subrounded, beds are 10-20 cm thick with internal planar to low angle cross laminations. Very rare reddish brown (5YR 5/4) mud interbeds 2-4 mm thick are present. | 12.0 |

APPENDIX A1a. Marillo measured section (continued).

| Unit | Description | Thickness (m) |
|------|--|------------------|
| 13. | Sand with interbedded mud: yellow (10YR 7/6), fL to cL, moderate sorting, angular to subrounded, beds are 2-30 cm thick with internal planar laminations. Thin reddish brown (5YR 5/6) mudstone interbeds are present, 2-3 cm thick, weather to a platy structure. A few well cemented sandstone beds are present, ~10 cm thick, very pale brown (10YR 8/2), slightly coarser grained (mL to vcU). | 19.5 |
| 12. | Sand with mud interbeds: very pale brown (10 YR 7/4), vfL to mU, poor sorting, subangular to rounded, beds are 20-60 cm thick. Mud interbeds are 20-40 cm thick, dark reddish brown (2.5 YR 3/4), weather to a blocky and platy structure. | 8.8 |
| 11. | Sand with mud interbeds: pale yellow (2.5Y 7/4), vfU to cU, poorly sorted, subangular to rounded, 2-3 mm thick planar laminations. Mud interbeds are 5-15 cm thick, pale yellow (2.5Y 7/3), and weather to a cracked, popcorn texture. Top of the unit is an intercalated contact with the overlying reddish sand and mud. | 7.4 |
| 10. | Sand with sandstone interbeds: pale yellow (2.5Y 7/4), fL to cU, poor sorting, subrounded to rounded, planar laminations. Isolated beds 10-15 cm thick are well cemented and coarser grained (mL to vcL). | 2.7 |
| 9. | Mud with sand interbeds: pale yellow (2.5Y 7/3), mud weathers to a cracked, popcorn-like appearance. Sand interbeds are 10-20 cm thick, pale yellow (2.5 Y 7/4), vfU to cL, moderate sorting, subangular to rounded, planar laminations. | 2.5 |
| 8. | Sand with interbedded mud and sandstone: Pale yellow (2.5Y 7/3), vfL to fL, well sorted, subangular to rounded, There are a few 5-10 cm thick mud interbeds, and some 5-7 cm thick beds of well cemented, cross laminated sandstone. | 1.6 |
| 7. | Mud with sand interbeds: pale yellow (2.5Y 7/3), mud weathers to a cracked, popcorn appearance. Sand interbeds are ~20 cm thick, pale yellow (2.5Y 7/4), vfU to cL, moderate sorting, subangular to rounded, planar laminations. | 1.4 |
| 6. | Sand with interbedded mud and sandstone: Pale yellow (2.5Y 7/3), vfL to fL, well sorted, subangular to rounded, There are isolated 5-10 cm thick mud interbeds, and 5-7 cm thick beds of well cemented sandstone showing cross laminations. | 2.8 |
| 5. | Mud with sand interbeds: pale yellow (2.5Y 7/3), mud weathers to a cracked, popcorn-like appearance. Sand interbeds are 10-20 cm thick, pale yellow (2.5Y 7/4), vfU to cL, moderate sorting, subangular to rounded, weak planar laminations. | 10.3 |
| 4. | Sand: light yellowish brown (10YR 6/4), vfU to vcL, poor sorting, subrounded to rounded; indistinct bedding; poorly exposed unit. | 26.2 |
| 3. | Gravel: discontinuous gravel lenses, angular to subrounded clasts of granite, sandstone, and volcanics. Poorly exposed unit. | 1.5 |

APPENDIX A1a. Marillo measured section (continued).

| Unit | Description | Thickness (m) |
|---|---|------------------|
| Cerro Conejo Member, Zia Formation: 11 m | | |
| 2. | Sand: very pale brown (10YR 8/4), vfU to cL, moderate sorting, subangular to rounded, bedding indistinct, poorly exposed unit. | 8.3 |
| 1. | White ash: (10YR 8/1), discontinuous lens of unit thinly laminated to medium bedded (2 mm to 15 cm thick) fallout ash. Correlative to one of the middle Miocene Trapper Creek tephra of Perkins et al. (1998; Koning and Personius, <i>in review</i>). Section continues downward but not described. | 2.5 |

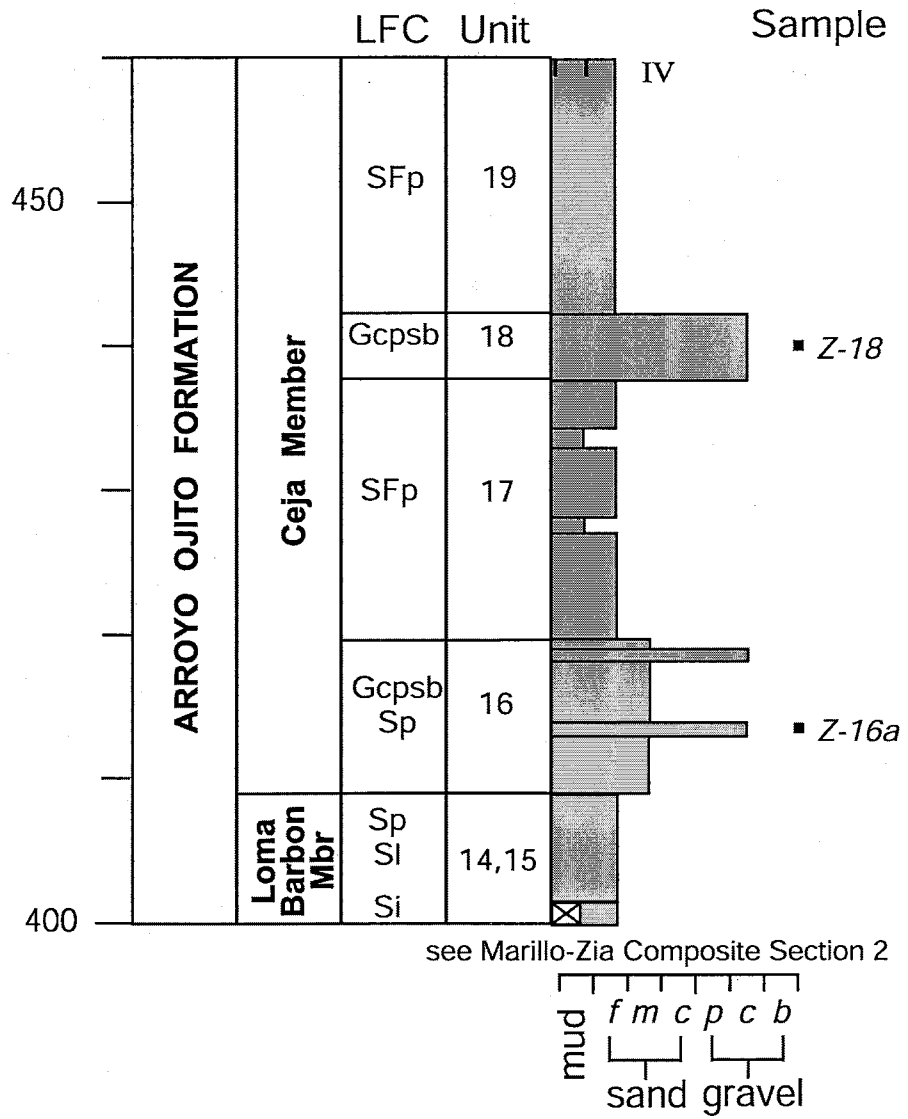
APPENDIX A2a. Zia measured section of fluvial deposits of the Arroyo Ojito Formation, Bernalillo NW and Cerro Conejo 7.5-minute quadrangle, Sandoval County, New Mexico. Base of measured section at N: 3,923,130 m, E: 341,596 m (Zone 13S, NAD 83). Measured upsection from unit 1 by Nathalie Brandes and Paul Brandes with Jacob Staff and Abney Level on July 29, 2000 and April 12, 2001. Colors measured dry. Textural abbreviations for sand include: very fine, vfL, vfU; fine fL, fU; medium, mL, mU; coarse, cL, cU; and very coarse, vcL, vcU. Numerical unit designations established upsection, but listed in descending stratigraphic order.

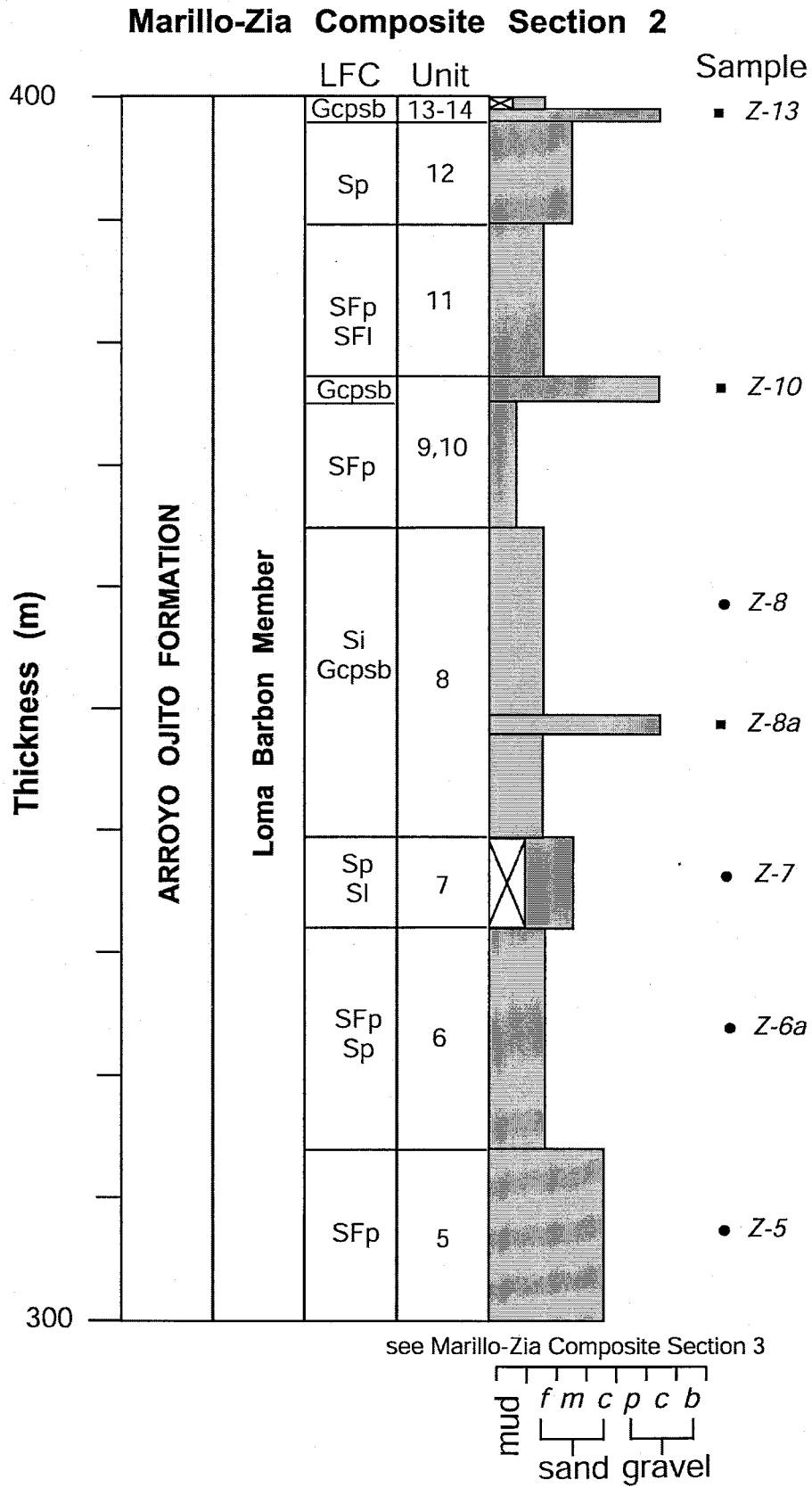
| Unit | Description | Thickness (m) |
|--|---|---------------|
| Arroyo Ojito Fm, Ceja Mbr: 51 m | | |
| 19. | Interbedded sandstone and mudstone: sandstone are vfU to cU, moderate sorting, subangular to rounded, occur in beds are up to 70 cm thick with internal planar laminations. Mudstone beds are up to 30 cm thick and weather blocks. Section ends at top of ridge on degraded remnants of the Llano de Albuquerque calcic soil. | 17.9 |
| 18. | Conglomerate: discontinuous lenses of pebble to cobble conglomerate, subangular to rounded clasts of granite, chert, and volcanic rocks, planar bedding. | 4.5 |
| 17. | Interbedded sandstone and mudstone: sandstone are vfU to mU, moderate sorting, subrounded to rounded, occur in beds up to 50 cm thick with internal planar laminations. Mudstone beds are up to 30 cm thick and weather to a blocky texture. | 17.5 |
| 16. | Interbedded sandstone and conglomerate: conglomerate beds are up to 1 m thick, pebble to cobble sized, subangular to rounded granite, volcanic, and chert, base of beds is undulatory, conglomerates are planar bedded. Sandstone is reddish yellow (7.5YR 6/6), fL to cU, moderate sorting, subangular to subrounded, individual beds are up to 1 m thick and show internal planar to cross laminations. | 10.7 |
| Arroyo Ojito Fm, Loma Barbon Mbr: 134 m | | |
| 15. | Sandstone: very pale brown (10YR 7/4), vfU to mL, moderate sorting, subangular to subrounded, planar to low angle cross laminations. | 7.5 |
| 14. | Sandstone: strong brown (7.5YR 5/6), vfU to mU, subangular to subrounded, moderate sorting, bedding indistinct, poorly exposed unit. | 2.5 |
| 13. | Conglomerate: pebble to cobble sized, subangular to rounded clasts of granite, chert, and volcanic rocks, planar bedding. Occurs as discontinuous lenses. | 1.0 |
| 12. | Sandstone: pale yellow (2.5Y 7/4), fL to cL, moderate sorting, subangular to rounded, beds up to 30 cm thick with internal planar laminations, calcium-carbonate cement, base of several beds is very coarse and beds show a fining upward sequence. | 8.2 |
| 11. | Sandstone with interbedded mudstone: pale yellow (2.5Y 7/4), vfL to mL, well sorted, subangular to rounded, calcium-carbonate cemented, beds are 1-10 cm thick with internal planar- to low-angle cross-laminations. Minor amounts of interbedded mud up to 25 cm thick. | 12.7 |
| 10. | Conglomerate: pebble to cobble sized, subangular to rounded clasts of red granite, chert, and volcanic rocks, base of unit is undulatory, crude planar bedding. | 2.0 |

| Unit | Description | Thickness (m) |
|---|---|---------------|
| 9. | Mudstone with sandstone interbeds: reddish brown (5YR 5/4), weathers into blocky texture, minor sandstone interbeds present near top of unit, sandstone well cemented with calcium-carbonate and cropping out as ledges 1-10 cm thick. | 10.3 |
| 8. | Sandstone: pale yellow (2.5Y 7/4), vFL to fL, well sorted, subrounded to rounded, indistinct bedding. At 9 m above base of unit is a discontinuous conglomerate lens about 1.5 m thick, containing subangular to subrounded pebble to cobble sized clasts of red granite, various chert, and volcanic rocks. Two boulders (reddish-brown and yellowish-brown sandstone, 60 and 90 cm maximum diameter) found about 21 m above base. | 25.2 |
| 7. | Muddy sandstone: reddish yellow (7.5YR 6/6), fL to cL, moderate sorting, subrounded to rounded, calcium-carbonate cement, planar to cross laminations. | 7.5 |
| 6. | Sandy mud: reddish brown (5YR 5/4) weathers to a cracked, blocky texture, unit becomes sandier upsection with sand beds up to 30 cm thick. Sands are pink (7.5YR 7/4), fU to mL, well sorted, subangular to subrounded. | 18.0 |
| 5. | Sand with mud interbeds: yellow (10YR 7/6), vfU to cU, moderate sorting, subangular to rounded, planar bedding, minor 3-5 cm thick mud interbeds. | 14.8 |
| 4. | Sand with mud interbeds: brownish yellow (10YR 6/6), fL to mU, moderate sorting, subangular to rounded, beds are 1-2 m thick with internal planar laminations. Mud interbeds are reddish yellow (7.5YR 6/6), 40-50 cm thick, weather into blocks. | 14.6 |
| 3. | Sand: light yellowish brown (10YR 6/4), vfU to cU, moderate sorting, subangular to rounded, indistinct bedding. | 7.1 |
| 2. | Muddy sand: light brown (7.5YR 6/4), vfU to vcL, poor sorting, subangular to rounded, indistinct bedding. | 2.2 |
| Arroyo Ojito Fm, Navajo Draw Mbr: 42 m | | |
| 1. | Sand: light gray (10YR 7/2), fL to mU, well sorted, subangular to rounded, beds are 5-20 cm thick with internal planar laminations, occasional beds of well cemented sandstone are ~5 cm thick. Upper contact is covered but inferred by a color change. Continues down-section into Marillo stratigraphic section. | 42.0 |

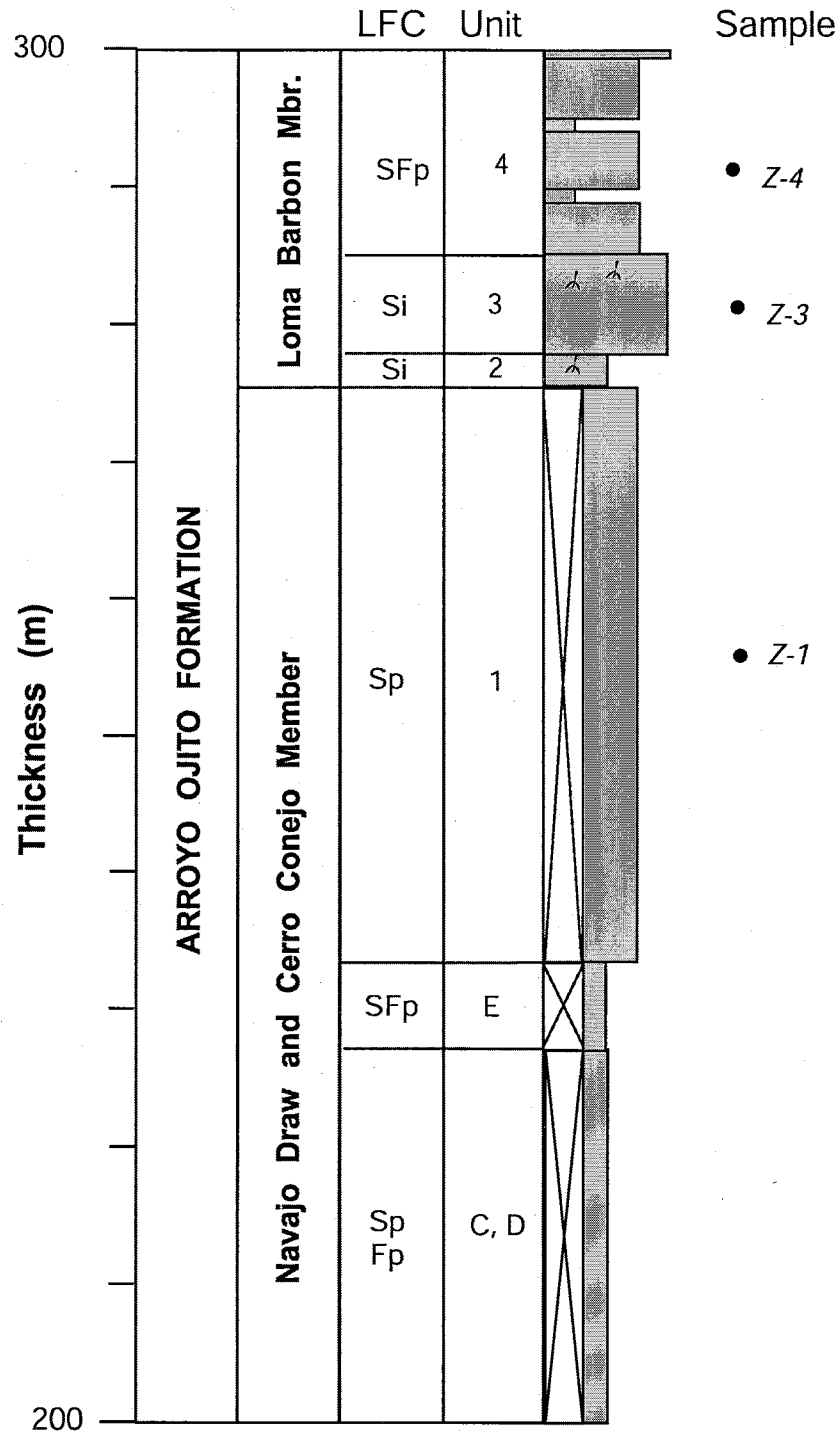
APPENDIX A2b. Graphic log of Marillo-Zia composite section.

Marillo-Zia Composite Section 1





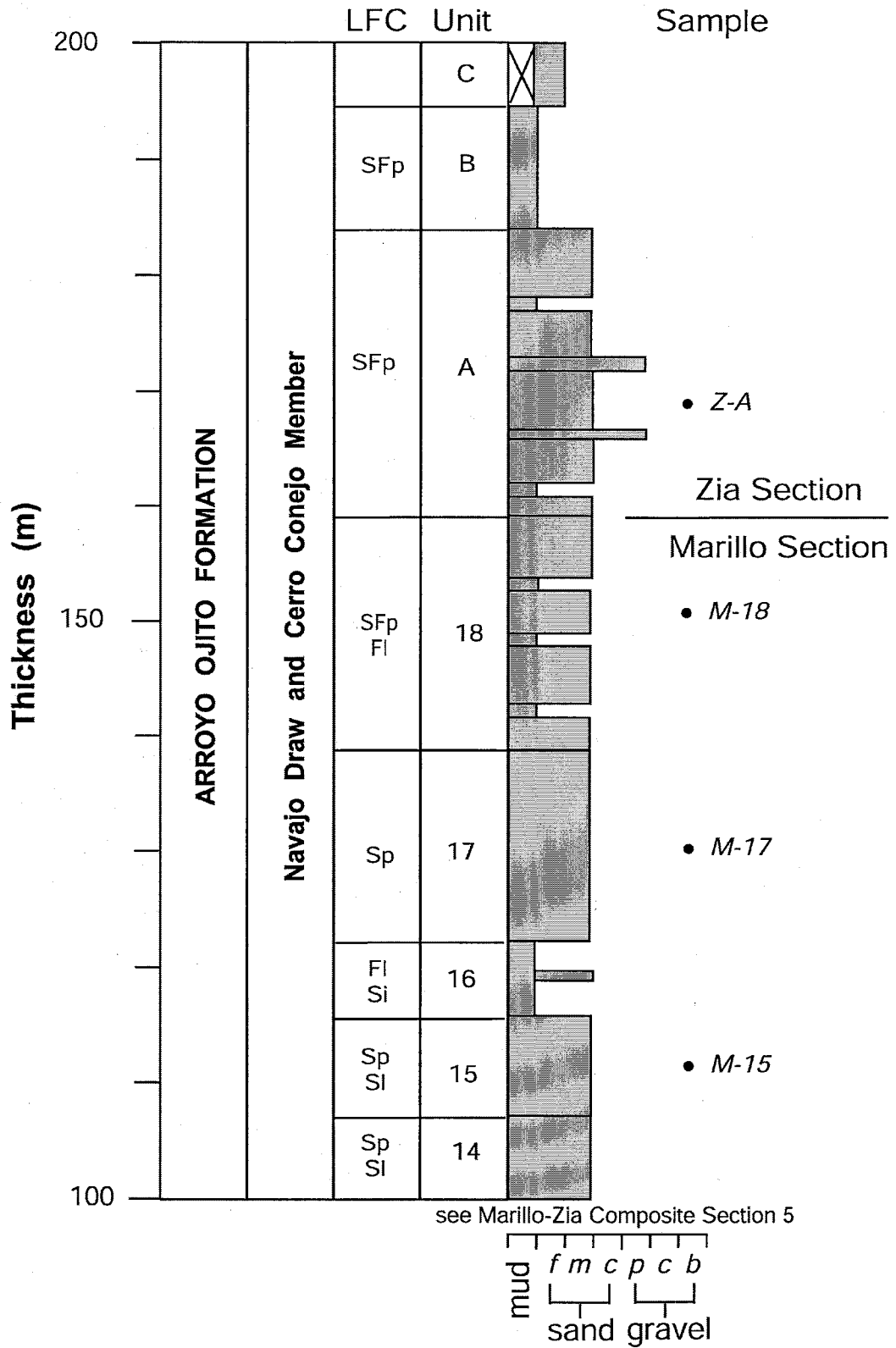
Marillo-Zia Composite Section 3



see Marillo-Zia Composite Section 4

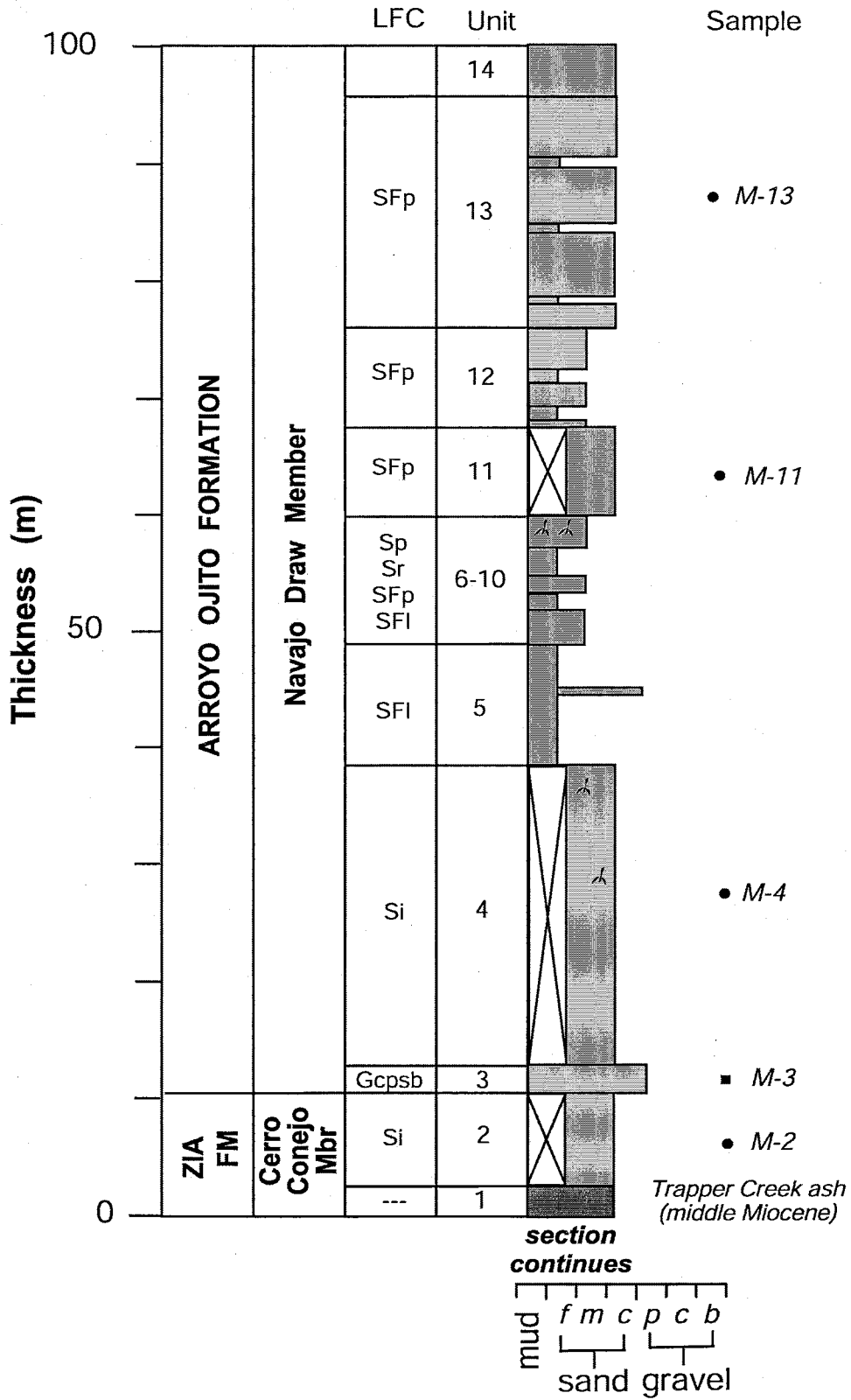
mud
 f m c p c b
 sand gravel

Marillo-Zia Composite Section 4



APPENDIX A2b. Graphic log of Marillo-Zia composite section (continued).

Marillo-Zia Composite Section 5



APPENDIX A3a. San Felipe Pueblo measured section of interfingering western fluvial deposits of the Arroyo Ojito Formation and axial-fluvial (ancestral Rio Grande) deposits of the Sierra Ladrones Formation beneath late Pliocene basalt of Santa Ana Mesa, San Felipe Pueblo 7.5-minute quadrangle, Sandoval County, New Mexico. Base of measured section at N: 3,918,355 m, E: 364,800 m (Zone 13S, NAD 83). Measured upsection from unit 1 by Nathalie Brandes and Sean Connell using Jacob Staff and Abney Level on June 16, 2000. Colors measured dry. Textural abbreviations for sand include: very fine, vFL, vfU; fine fL, fU; medium, mL, mU; coarse, cL, cU; and very coarse, vcL, vcU. Numerical unit designations established upsection, but listed in descending stratigraphic order.

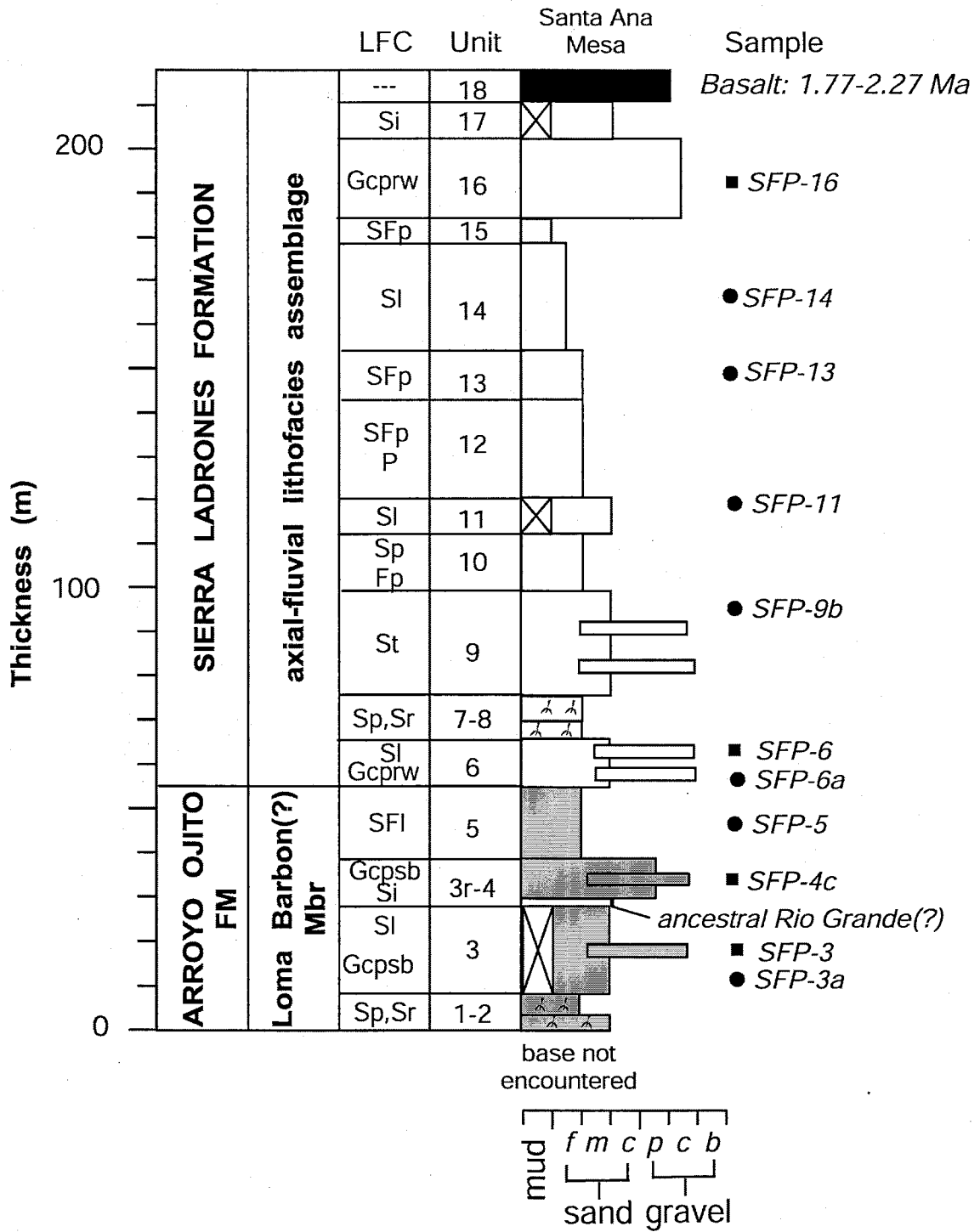
| Unit | Description | Thickness (m) |
|------|--|---------------|
| | Sierra Ladrones Fm, axial-fluvial lithofacies assemblage: 79 m | |
| 18. | Basalt at Santa Ana (San Felipe) Mesa: very dark gray (N3/), vesicular, with fine- to medium-grained plagioclase laths and olivine crystals are visible in hand specimen. Section ends at basalt capped Santa Ana (San Felipe) Mesa. Overlies fluvial deposits of unit 17 with no interbedded basaltic tephra or soil observed. Projects to unit 3 of the Tonque Arroyo section. | 3.0 |
| 17. | Sandstone: pinkish gray (5YR 6/2), mL to vcU, moderate sorting, subangular to subrounded, slightly reddened, possible baked zone at top; no basaltic tephra at upper contact, unit is very poorly exposed. Upper contact appears to be conformable with basalt and no soil is recognized. | 3.4 |
| 16. | Gravel: pebbles and cobbles, abundant rounded quartzite and volcanic clasts, clast supported, planar-cross bedding. Clasts are 3 to 12 cm in diameter. | 9.3 |
| 15. | Mud with sand interbeds: light red (5YR 5/4), medium to thickly bedded with thin to medium bedded sand interbeds that comprise ~25% of unit. | 3.0 |
| 14. | Sand and pebbly sand: pinkish gray (5YR 6/2), fL to cU, moderate sorting, subangular to subrounded, laminated to medium bedded, cross stratified, unit is poorly exposed. | 11.9 |
| 13. | Sandstone with interbedded mud: light reddish brown (5YR 6/4), fL to mU, moderate sorting, subangular to rounded, weakly cemented with calcium-carbonate, scattered medium bedded pebbly sandstone lenses present, mudstone interbeds are 2-4 cm thick, upper contact is poorly exposed. | 5.2 |
| 12. | Silty sand interbedded with mud: light reddish brown (5YR 6/4), vFL to fU, well sorted, subangular to rounded, weakly cemented with calcium-carbonate, sandy beds are 13-20 cm thick interbedded with 3-7 cm thick red (2.5YR 5/6) mudstone, culminates is a possible buried soil with Stage II carbonate morphology. | 11.0 |
| 11. | Sand and pebbly sand: pinkish gray (5YR 6/2), mL to vcU, moderate sorting, subangular to subrounded, basal 70 cm cemented with calcium-carbonate, laminated to thickly bedded, cross stratified, unit is poorly exposed. | 3.9 |

APPENDIX A3a. San Felipe Pueblo measured section (continued).

| Unit | Description | Thickness (m) |
|---|--|------------------|
| 10. | Sandstone and mudstone: pink (7.5YR 7/3), vFL to fU, well sorted, subangular to subrounded, cemented with calcium-carbonate, planar-cross beds 10-20 cm thick, about 30% of the unit is light red (2.5YR 6/8) mudstone interbeds about 2-4 cm thick. | 6.6 |
| 9. | Sandstone: pinkish gray (7.5YR 7/2), mL to vcU, well sorted, subangular to rounded, base is locally very well cemented with calcium-carbonate, distinctly cross stratified 20-25 cm thick beds. | 11.5 |
| 8. | Muddy sandstone: light brown (7.5YR 6/4), vFL to cL, moderate sorting, subangular to subrounded, medium planar-cross bedded sand, well cemented with calcium carbonate, contains root tubes 1-2 cm long with some as long as 6 cm, forming discontinuous rhizoconcretionary mats, minor beds of pebbly sandstone that fine upwards into the muddy sandstone. | 2.8 |
| 7. | Silty sandstone: very pale brown to pink (10YR 8/2 to 7.5YR 7/3), vFL to mL moderate sorting, subangular to subrounded, well cemented with calcium-carbonate, locally abundant rhizoconcretions up to 15 mm in diameter. | 1.9 |
| 6. | Sands with gravel lenses: light gray (10YR 7/2), mL to vcL, moderate sorting, subangular to subrounded, cross stratified in beds 20-30 cm thick, gravel lenses are medium planar bedded containing abundant rounded quartzite and porphyritic tuff. | 5.5 |
| Arroyo Ojito Formation, Loma Barbon(?) Mbr: 27 m | | |
| 5. | Silty sand with mud interbeds: yellowish red (5YR 5/6), vFL to cU, moderate sorting, subangular to subrounded, occurs in 15-50 cm thick planar- to cross-laminated silty sand interbedded with 10-20 cm thick reddish yellow (5YR 6/6) mud. | 7.7 |
| 4. | Conglomerate: pebble to cobble sized, subangular to subrounded, granite, volcanic tuff and rare Pedernal chert, clast supported, poorly sorted, crude planar bedding, grades finer upsection into a red to yellowish red (2.5YR 5/6 to 5YR 5/6) sandstone, fL to cU, moderate to poorly sorted, exhibits faint low angle cross stratification. | 4.7 |
| 3R. | Sand: light brown (7.5YR 6/4), fL to mU, moderately sorted, subangular to subrounded, bedding indistinct, poorly exposed unit, possibly correlative to ancestral Rio Grande deposits. | 1.0 |
| 3. | Sand: light reddish brown (5YR 6/4), fL to cU, moderate sorting, subangular to subrounded, laminated to thinly bedded, planar- to low-angle cross stratification, rare pebbly sandstone interbeds. Scattered 30-40 cm thick clast supported, pebble to cobble sized gravel lenses with granite and volcanic clasts are present. Unit is poorly exposed. | 9.5 |
| 2. | Silty sand: reddish yellow (5YR 6/6), vFL to vcL, poorly sorted, subangular to subrounded, thin planar bedding. Locally abundant 3-8 cm diameter concretions and rhizoconcretionary beds. A single 3-6 cm thick mud bed exhibits square to polygonal mud cracks. | 2.6 |
| 1. | Sandstone: reddish yellow (5YR 6/6), vFL to mU, moderate sorting, subangular to subrounded, thin planar beds, contains discontinuous thinly bedded pebbly sand. Top of unit is marked by 30-cm thick well-cemented rhizoconcretionary root mat. Base is not exposed. | 1.0 |

APPENDIX A3b. Graphic log of San Felipe Pueblo measured section.

San Felipe Pueblo Section

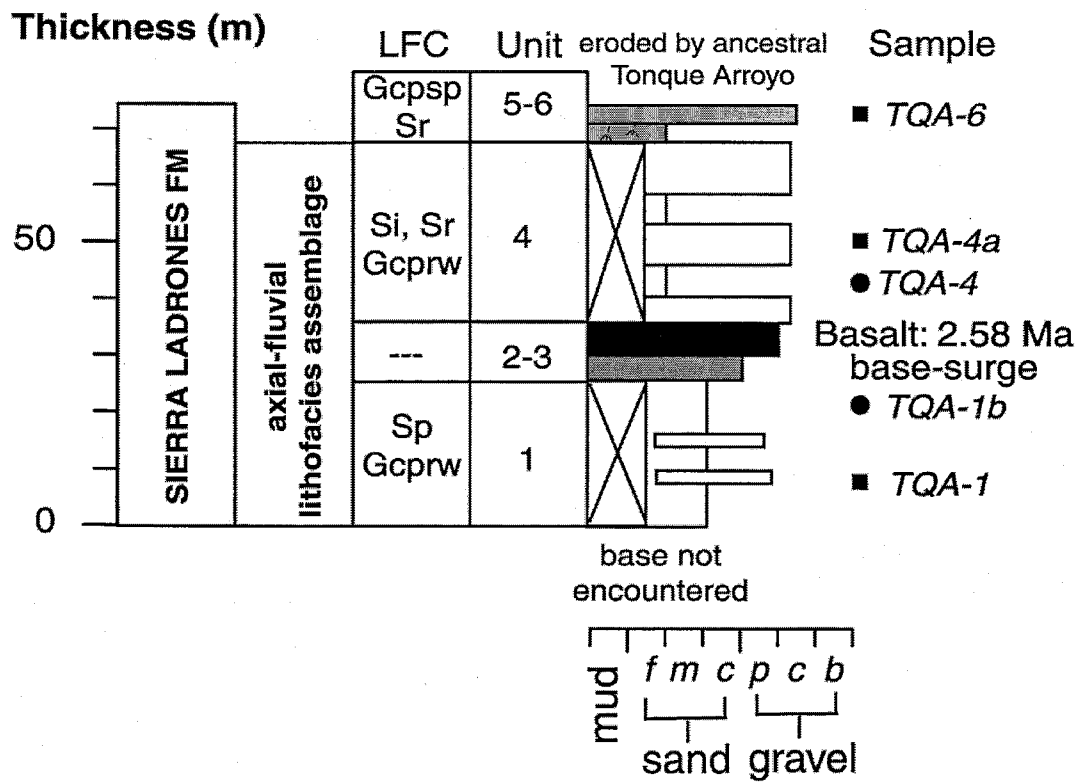


APPENDIX A4a. Tonque Arroyo measured section of axial-fluvial and piedmont deposits of the Sierra Ladrones Formation and a basalt flow at Santa Ana Mesa, San Felipe Pueblo 7.5-minute quadrangle, Sandoval County, New Mexico. Base of measured section at N: 3,920,613 m, E: 369,853 m (Zone 13S, NAD 83). Measured upsection from unit 1 by Nathalie Brandes and S.D. Connell using Jacob Staff and Abney Level on June 22, 2000. Colors measured dry. Textural abbreviations for sand include: very fine, vFL, vFU; fine fL, fU; medium, mL, mU; coarse, cL, cU; and very coarse, vcL, vcU. Numerical unit designations established upsection, but listed in descending stratigraphic order.

| Unit | Description | Thickness (m) |
|---|--|---------------|
| Sierra Ladrones Fm, piedmont lithofacies assemblage: 3 m | | |
| 6. | Gravel: pebble to cobble sized, mainly limestone clasts, bedding indistinct, poorly exposed. Top of unit is cut by gravel of Quaternary terrace deposits of the ancestral Tonque Arroyo (Cather and Connell, 1998). | 1.5 |
| 5. | Sand: light brown (7.5YR 6/4), vFL to mL, moderately sorted, subangular to subrounded, bedding is indistinct to absent. Scattered 5-15 mm in diameter, and up to 7 cm long, rhizoconcretions. Unit is poorly exposed. | 1.2 |
| Sierra Ladrones Fm, axial-fluvial lithofacies assemblage: 33 m | | |
| 4. | Gravel with sandy interbeds: gravels are pebble to cobble sized, clast supported planar bedded, predominantly well-rounded quartzite clasts. Sands are pale yellow (2.5Y 8/2) with scattered local olive yellow (2.5Y 6/8) staining, vFL to cU, poorly sorted, subangular to subrounded, bedding in the sand is indistinct. Unit is poorly exposed. | 15.7 |
| 3. | Basalt at Santa Ana (San Felipe Mesa): very dark gray (N3/), vesicular, some areas show crude columnar jointing, small plagioclase laths and olivine crystals are seen in hand specimen. Correlative to unit 18 of the SFP stratigraphic section. | 2.8 |
| 2. | Basaltic tuff: light yellowish brown to light reddish brown (10YR 6/4 to 5YR 6/3), reddish color occurs near the top, top of unit marked by undulatory surface beneath basalt flow. Represents base-surge deposits associated with basalt flow of unit 3. Base not exposed. | 1.8 |
| 1. | Sand with interbedded gravel: light brownish gray (2.5Y 6/2), mU to vcU, moderate sorting, subangular to subrounded, planar bedding. Gravel lenses are pebble to cobble sized, clast supported, consist primarily of well rounded quartzite and volcanic clasts. Gravel ranges from 3 to 10 cm. Unit is poorly exposed, but appears to be conformably overlain by unit 2. No soil is observed at the upper contact. Base is not exposed. | 12.9 |

APPENDIX A4b. Graphic log of Tonque Arroyo section.

Tonque Arroyo Section



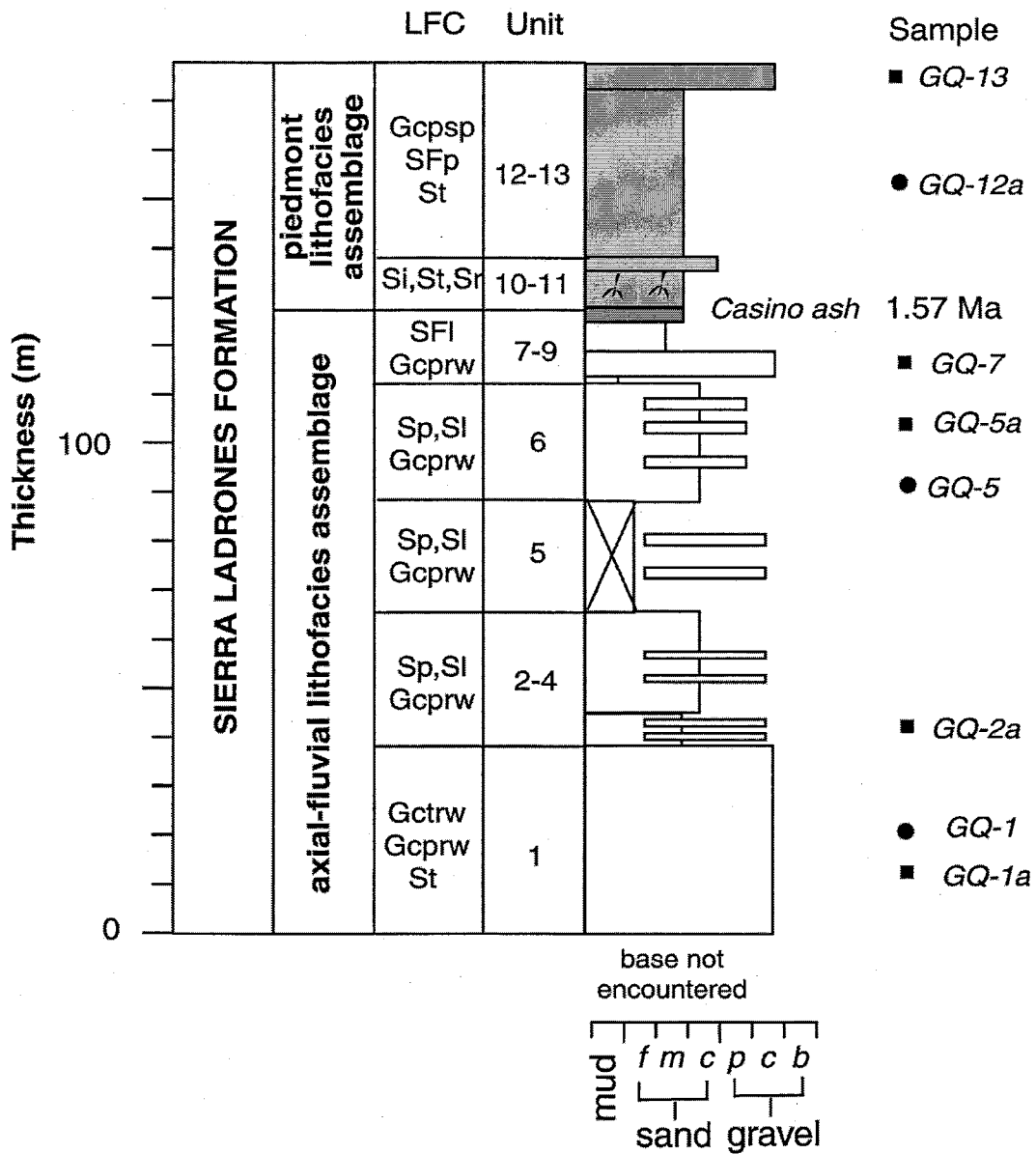
APPENDIX A5a. San Felipe gravel quarry measured section of interfingering axial-fluvial (ancestral Rio Grande) and piedmont deposits of the Sierra Ladrones Formation, San Felipe Pueblo 7.5-minute quadrangle, Sandoval County, New Mexico. Units 1-4 described in gravel quarry. Base of measured section at N: 3,918,765 m, E: 370,523 m (Zone 13S, NAD 83). Top at N: 3918727 m, E: 372100 m. Measured upsection from unit 1 by Nathalie Brandes and Sean Connell using a differentially corrected GPS unit, and Jacob Staff and Abney Level on June 22 and 27, 2000. Colors measured dry. Textural abbreviations for sand include: very fine, vfL, vfU; fine fL, fU; medium, mL, mU; coarse, cL, cU; and very coarse, vcL, vcU. Numerical unit designations established upsection, but listed in descending stratigraphic order.

| Unit | Description | Thickness (m) |
|------|--|---------------|
| | Sierra Ladrones Fm, piedmont lithofacies assemblage: 29 m | |
| 13. | Gravel: pebble to cobble sized, subangular to subrounded, mainly limestone clasts, clast supported, planar bedding. Section ends at top of narrow ridge that may represent a remnant of a local constructional top of the Sierra Ladrones Fm. Clasts are 3 to 10 cm in diameter. | 2.9 |
| 12. | Sandstone with mudstone interbeds: reddish yellow (7.5YR 6/6), fL to vcU, moderately sorted, subangular to subrounded, weakly cemented with calcium-carbonate, predominantly planar centimeter-scale bedding with local areas of cross stratification. Mud occurs in the unit as 7-10 cm interbeds between sandstone beds. | 16.9 |
| 11. | Sandstone: very pale brown (10YR 7/4), mU to vcL, well sorted, subangular to subrounded, cemented with calcium-carbonate. Unit has distinct cross stratification 3-5 cm thick. Pebble lenses mark the base of the unit and the top of the unit is capped by 6-10 cm interval of rhizoconcretions about 0.5 cm in diameter. | 1.3 |
| 10. | Muddy sandstone with mud interbeds: very pale brown (10YR 7/4), vfU to cL, moderate sorting, subangular to rounded, bedding is indistinct, possibly due to bioturbation. A discontinuous 2-3-cm thick interval of rhizoconcretionary sandstone is within unit, rhizoconcretions are less than 1 cm in diameter. Light brown (7.5YR 6/4) mud are present as 4-6 cm thick interbeds throughout the unit. | 3.5 |
| 9. | Casino Ash: white (10YR 8/1), weathers to pink (7.5YR 7/3). Most of unit is fine grained with 2-5 mm diameter lapilli in distinct beds. Sample taken from ash along the southern margin of Tonque Arroyo yielded a $^{40}\text{Ar}/^{39}\text{Ar}$ date of 1.57 ± 0.06 Ma (NMGRL 9749, sample SF23-acs; Cather and Connell, 1998). Sample taken at section (SF-acs3) is geochemically similar to the Cerro Toledo Rhyolite (N. Dunbar, 2001, written commun.). | 1.2 |
| 8. | Sand with mud interbeds: very pale brown (10YR 7/3), vfU to mL, well sorted, well rounded, sand beds are about 35 cm thick with internal cross stratification. Pale yellow (5Y 8/2) mud interbeds about 15 cm thick that weather into blocks. | 2.7 |

APPENDIX A5a. San Felipe gravel quarry measured section (continued).

| Unit | Description | Thickness (m) |
|---|--|------------------|
| Sierra Ladrones Fm, axial-fluvial lithofacies assemblage: 58 m | | |
| 7. | Gravel: pebble to cobble sized, well rounded quartzite and volcanic clasts, clast supported, 1-2 m thick planar beds. Base of unit is marked by a 70 cm thick reddish-brown mudstone that pinches out to the west. Clasts are 2 to 10 cm in diameter. | 2.9 |
| 6. | Sand with gravel interbeds: olive yellow to yellowish brown (2.5Y 6/8 to 10YR 5/8), mL to vcL, moderately sorted, angular to subangular, laminated to thinly bedded, planar to low angle cross stratification. Gravels interbeds are pebble to cobble sized, well rounded quartzite and volcanic clasts, clast supported, beds are up to 1 m in thickness. | 11.3 |
| 5. | Sand: light gray to olive yellow (2.5Y 7/2 to 5Y 6/6). vfL to cU, poorly sorted, subangular to subrounded, laminated to thinly bedded, planar to low and cross stratification. Scattered pebble to cobble gravel beds containing of rounded quartzite and volcanic rocks, clast supported, planar bedding. Poorly exposed. | 11.7 |
| 3-4. | Sand with gravel interbeds: yellowish brown to pale yellow (10YR 5/8 to 5Y 7/3), mL to vcL, moderately sorted, subangular to subrounded, laminated to thinly bedded with planar to low angle cross stratification. Pebble to cobble sized gravels of well rounded quartzite and volcanic clasts in discontinuous 50 cm thick clast supported lenses. Cobble to small boulders composed of rounded mudballs are present as in distinct layers and probably represent fluviually recycled floodplain material. Unit 4 is a gravelly lens within unit 3. Clasts are 4 to 12 cm in diameter. | 10.1 |
| 2. | Interbedded sand and gravel: pale yellow to yellowish brown (5Y 8/2 to 10YR 5/8), unit is approximately half sand. Sands are fL to cU, poorly sorted, angular to subrounded, thinly bedded to thickly laminated, low angle cross stratification. Gravels are well rounded, mostly quartzite and volcanic clasts, clast supported, planar bedding. | 3.2 |
| 1. | Gravel with interbedded sand: pebble to cobble sized, well rounded quartzite and volcanic clasts, clast supported, thickly bedded planar and cross stratified, some beds are lenticular and appear to scour older beds. Gravel ranges from 4 to 11 cm. Sand is light gray (2.5Y 7/2), vfU to vcL, poorly sorted, angular to subrounded, 50-100 cm thick lenses that exhibit internal centimeter-scale cross stratification. Well exposed in highwall of gravel quarry. Base not exposed. | 18.9 |

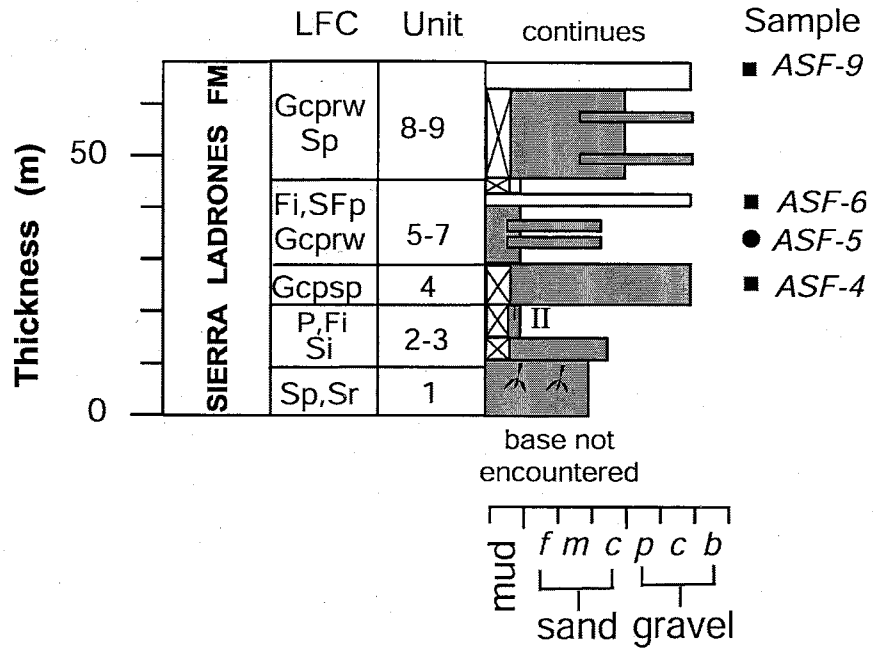
San Felipe Gravel Quarry Section



APPENDIX A6a. Arroyo San Francisco measured section near Arroyo San Francisco of interfingering axial-fluvial and piedmont deposits of the Sierra Ladrones Formation, San Felipe Pueblo 7.5-minute quadrangle, Sandoval County, New Mexico. Base of measured section at N: 3,917,608 m, E: 371,811 m (Zone 13S, NAD 83). Measured upsection from unit 1 by Nathalie Brandes and Paul Brandes with Jacob Staff and Abney Level on July 19, 2000. Colors measured dry. Textural abbreviations for sand include: very fine, vFL, vFU; fine fL, fU; medium, mL, mU; coarse, cL, cU; and very coarse, vcL, vcU. Numerical unit designations established upsection, but listed in descending stratigraphic order.

| Unit | Description | Thickness (m) |
|---------------------------------|--|------------------|
| Sierra Ladrones Fm: 33 m | | |
| 9. | Gravel: pebble to cobble size, well rounded quartzite and volcanic clasts, clast supported, 50-cm thick planar bedding; ancestral Rio Grande deposits. | 2.7 |
| 8. | Sand with interbedded gravels: pale yellow (2.5Y 7/3), mL to vcU, poor sorting, subangular to subrounded. Isolated meter-scale pebble to cobble sized, clast supported, planar bedded gravel lenses are present. Unit is poorly exposed. | 8.6 |
| 7. | Mud: reddish brown (5YR 5/4), no visible bedding, and weathers to a blocky texture, very poorly exposed; ancestral Rio Grande deposits. | 1.4 |
| 6. | Conglomerate: pebble to cobble sized, well rounded quartzite and volcanic clasts, clast supported, planar bedding; ancestral Rio Grande deposits. Base of unit is undulatory. | 1.0 |
| 5. | Mud with sandstone interbeds: reddish yellow (7.5YR 6/6), finely laminated, contains some pink (7.5YR 7/4) sandstone interbeds about 6-10 cm thick. Sandstone is fU to mU, well sorted, subangular to subrounded, cemented with calcium-carbonate, beds contain internal planar laminations. | 5.3 |
| 4. | Conglomerate: pebble to cobble sized, subangular to rounded, contains abundant limestone and red sandstone, clast supported, 50-cm thick, crude planar bedding; piedmont deposits. Gravel ranges from 4 to 15 cm. | 3.6 |
| 3. | Mud: yellowish red (5YR 5/6), bedding is indistinguishable, rhizoconcretions are present, 1-2 cm long, and 2 mm in diameter. Top of unit marked by a possible weakly developed calcic soil with Stage II carbonate morphology. | 3.4 |
| 2. | Sand: pale yellow (2.5Y 8/2), mL to vcU, poor sorting, subangular to subrounded, bedding indistinct due to poor exposure. | 2.0 |
| 1. | Sand and Sandstone: sand is interbedded with well cemented sandstone, beds are 15-50 cm thick with internal planar laminations ~1-2 mm thick. Sandstone is cemented with calcium-carbonate. Sand is reddish yellow (7.5YR 6/6), fL to mL, moderate sorting, subrounded to rounded. Sandstone is pink (5YR 7/3), mL to cL, moderate sorting, subrounded to rounded. Base not exposed. | 5.4 |

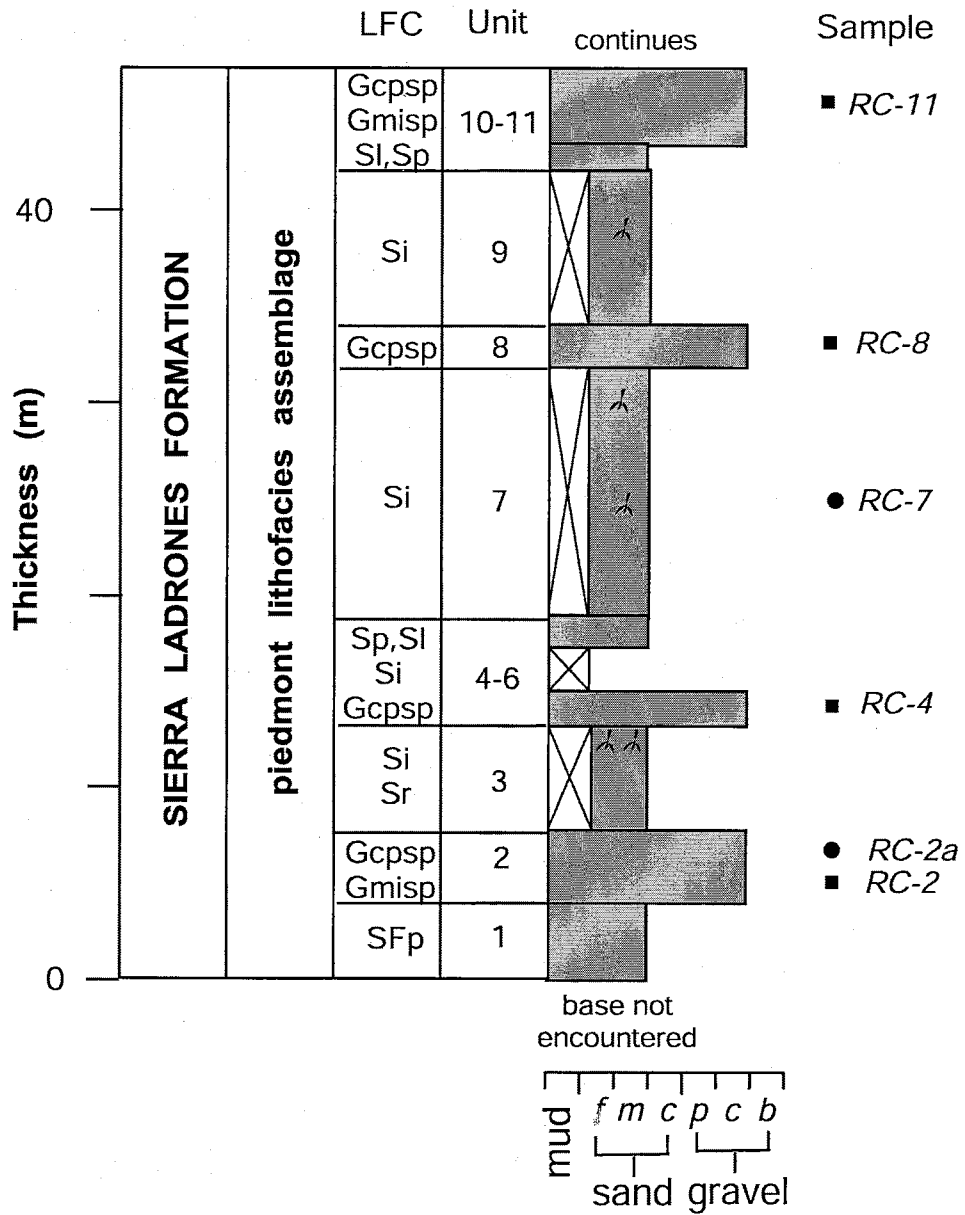
Arroyo San Francisco Section



APPENDIX A7a. Red Cliffs measured section, Arroyo San Francisco. Piedmont deposits of the Sierra Ladrones Formation, San Felipe Pueblo 7.5-minute quadrangle, Sandoval County, New Mexico. Base of measured section at N: 3,916,755 m, E: 372,331 m (Zone 13S, NAD 83). Measured upsection from unit 1 by Nathalie Brandes and Paul Brandes with Jacob Staff and Abney Level on July 20, 2000. Colors measured dry. Textural abbreviations for sand include: very fine, vfL, vfU; fine fL, fU; medium, mL, mU; coarse, cL, cU; and very coarse, vcL, vcU. Numerical unit designations established upsection, but listed in descending stratigraphic order.

| Unit | Description | Thickness (m) |
|--|--|---------------|
| Sierra Ladrones Fm, piedmont lithofacies assemblage: 46 m | | |
| 11. | Conglomerate with sandstone interbeds: pebble to cobble sized clasts, abundant sedimentary clasts, clast supported, 25-50 cm thick planar bedding. Sandstone in 5-10 cm thick interbeds with internal low angle cross stratification. | 3.6 |
| 10. | Sandstone: pink (7.5YR 7/3), fL to cL, moderate sorting, subangular to rounded, beds are 10cm thick, planar stratification. | 1.3 |
| 9. | Sand: reddish yellow (7.5YR 6/6), vfU to cL, subangular to subrounded, moderately sorted, indistinct bedding. Unit is poorly exposed. | 8.2 |
| 8. | Conglomerate: pebble to cobble sized, abundant sedimentary clasts (limestone), clast supported, distinct 50 cm thick planar bedding, | 2.0 |
| 7. | Sand: yellowish red (5YR 5/6), vfL to vcU, poor sorting, subangular to rounded, bedding indistinct. Unit is poorly exposed. | 13.1 |
| 6. | Sandstone: pink (7.5YR 7/3), vfU to cL, moderate sorting, subangular to subrounded, planar to low angle cross laminations, cemented with calcium-carbonate. | 1.0 |
| 5. | Muddy sand: light reddish brown (5YR 6/4), mL to mU, well sorted, subangular to subrounded, bedding indistinct. Unit is poorly exposed. | 2.5 |
| 4. | Conglomerate: pebble to cobble sized, abundant sedimentary clasts(limestone), clast supported, distinct planar beds. Base is undulatory. Isolated sandstone beds contain mm-scale cross laminations. | 1.1 |
| 3. | Sand: yellowish red (5YR 5/6), vfL to mU, poorly sorted, angular to subrounded, some parts of the unit are bioturbated as shown by randomly scattered pebbles and rare small (2 mm diameter) rhizoconcretions. Top meter of unit contains small matrix supported pebble lenses that contain abundant limestone. Poorly exposed unit. | 6.0 |
| 2. | Conglomerate: pebble to cobble sized, subangular to rounded, abundant limestone, clast and matrix supported, crude m-scale planar bedding. Base of unit is undulatory, grades upward to a very pale brown (10YR 8/3) sandstone, fU to mU, moderate sorting, subangular to subrounded, bedding indistinguishable. | 3.4 |
| 1. | Sandstone with interbedded mud: yellowish red (5YR 5/6), fU to cL, poor sorting, subangular to subrounded, 20-cm thick planar beds. Mud occurs as 2-4 cm thick interbeds. Base not exposed. | 4.0 |

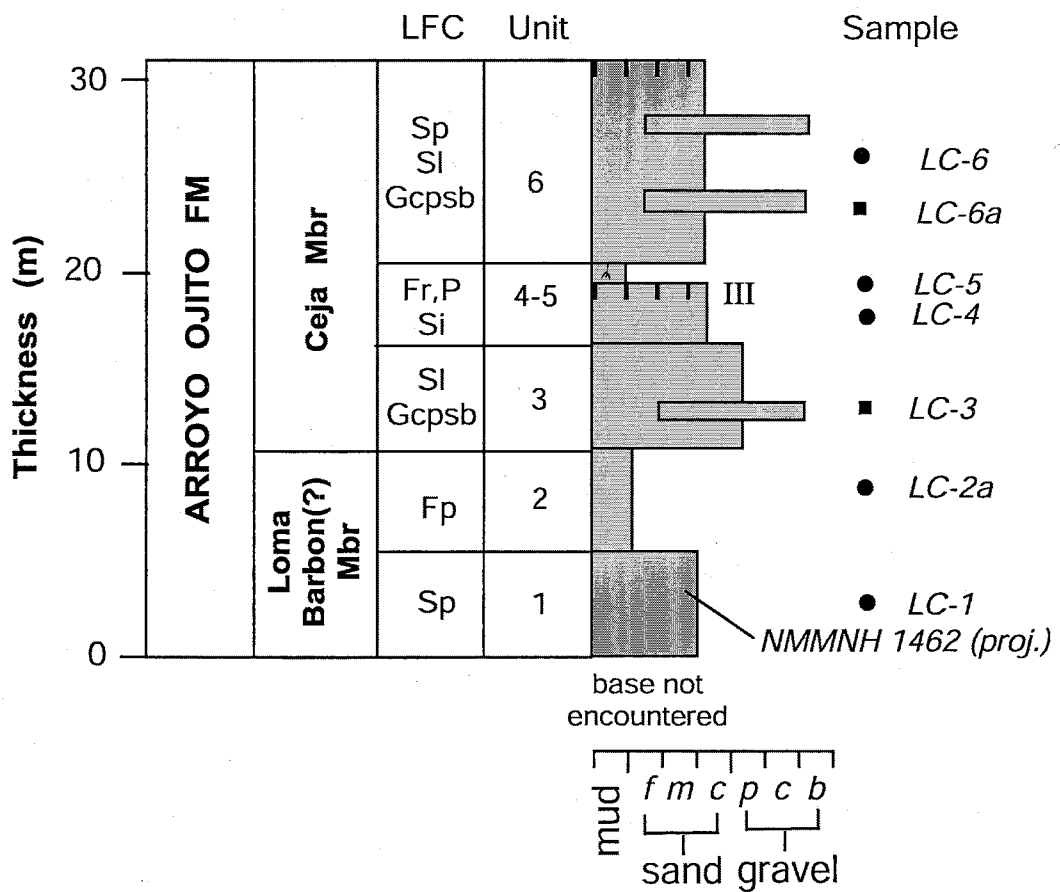
Red Cliffs Section



APPENDIX A8a. Loma Colorado de Abajo measured section, north of Rio Rancho High School, of fluvial deposits of the Arroyo Ojito Formation, Loma Machette 7.5-minute quadrangle, Sandoval County, New Mexico. Base of measured section at N: 3,903,964 m, E: 348,180 m (Zone 13S, NAD 83). Measured upsection from unit 1 by Nathalie Brandes and Paul Brandes with Jacob Staff and Abney Level on October 14, 2000. Colors measured dry. Textural abbreviations for sand include: very fine, vfL, vfU; fine fL, fU; medium, mL, mU; coarse, cL, cU; and very coarse, vcL, vcU. Numerical unit designations established upsection, but listed in descending stratigraphic order.

| Unit | Description | Thickness (m) |
|---|--|---------------|
| Arroyo Ojito Fm, Ceja Mbr: 19 m | | |
| 6. | Sand with interbedded gravels: light gray (10YR 7/2), fU to mU, angular to subrounded, planar laminations to low-angle cross laminations. Gravel lenses present, planar bedding, clast supported, contain abundant volcanic rocks and chert. Clasts range in size from 3 to 7 cm. Section end at top of hill. Projected top of the Llano de Albuquerque is about 60-90 m above section (estimated elevations from topographic map). | 10.1 |
| 5. | Sandy mudstone: very pale brown (10YR 7/3), massive, rhizoconcretions present, uppermost 10 cm is white (10YR 8/1) calcic soil. | 0.4 |
| 4. | Sandstone: pink (7.5YR 7/3), fL to mU, angular to subrounded, no bedding visible, and bioturbated. Locally abundant pumice clasts up to 10 mm in diameter. | 3.1 |
| 3. | Sandstone: very pale brown (10YR 7/3), fU to cU, subangular to rounded, thinly bedded, low-angle cross stratification. Locally present very well cemented beds are generally coarser grained, containing granules up to 2 mm in diameter. Isolated conglomerate lenses are present, planar bedded, clast supported, contain abundant volcanic rocks and chert. Gravel sample LC-3 contains a greater amount of quartzite than average western-margin deposits. This may be due to mixing of ancestral Rio Grande sediments and western-margin sediments or it may be a quartzite-rich channel in the Arroyo Ojito Formation. | 5.4 |
| Arroyo Ojito Fm, Loma Barbon Mbr: 11 m | | |
| 2. | Mudstone with sandstone interbeds: very pale brown (10YR 8/3), mud are laminated. Thinly bedded sandstone, cemented with calcium carbonate, trough cross-stratified. Locally contains <6-mm diameter, fluviually recycled pumice gravel. | 5.1 |
| 1. | Sand and sandstone: reddish yellow (5YR 6/6), vfU to mU, subangular to rounded, planar bedding 1-30 cm thick. Well cemented sandstone beds make up ~20% of the unit. NMMNHS Locality 1462 (unit 5 of Morgan and Lucas, 2000) projects into section. Base is not observed. | 5.4 |

Loma Colorada de Abajo Section



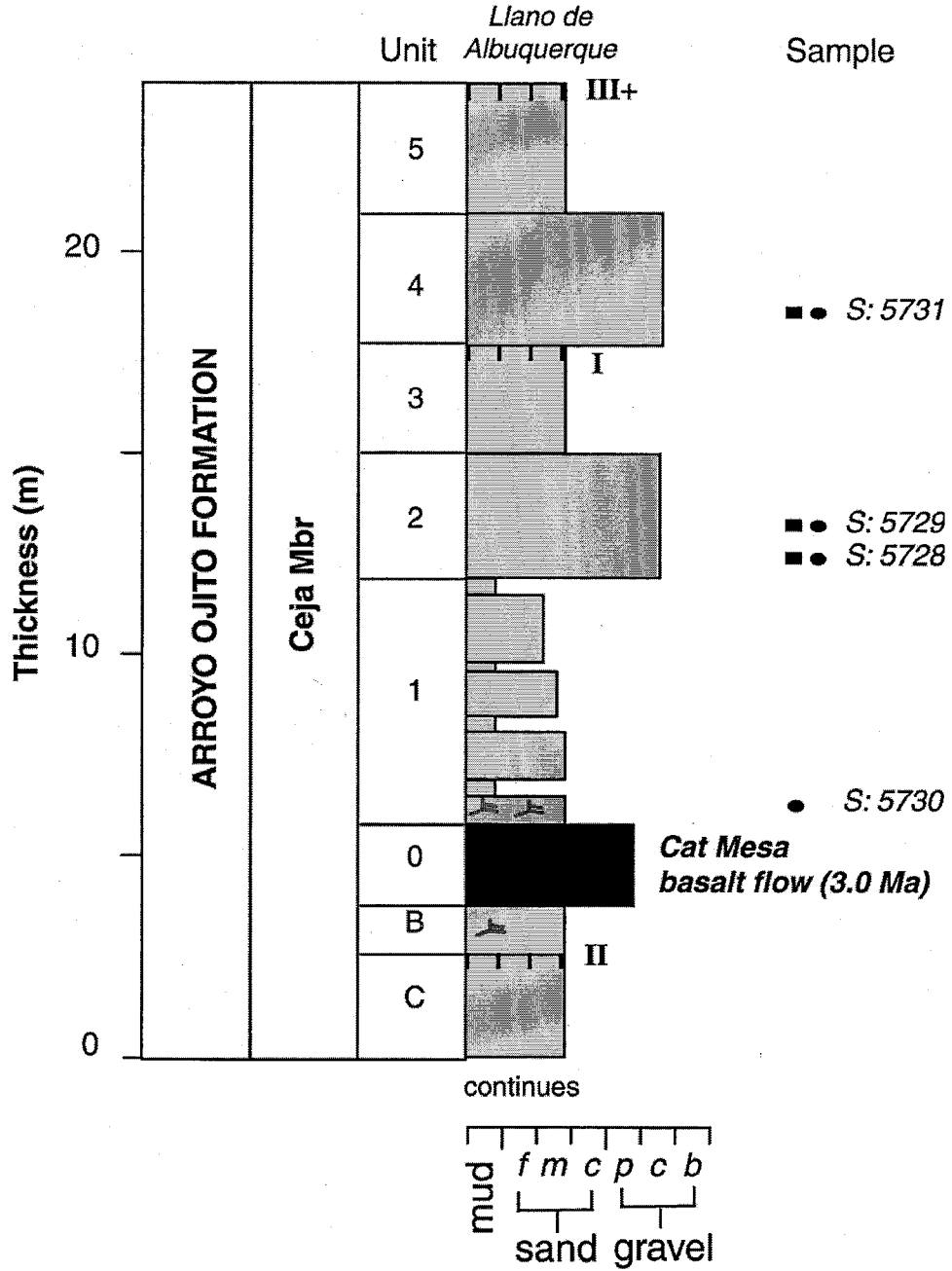
APPENDIX A9a. Cat Mesa measured section of upper Santa Fe Group sediments along southern Ceja del Rio Puerco escarpment, Rio Puerco 7.5-minute quadrangle. Top of unit 0 at E: 321,535 m; N: 3,858,635 m (UTM zone 13S, NAD 1983). Measured upsection from unit C by S.D. Connell, D.W. Love, and F. Maldonado on November 30, 1999 using an Abney level and Jacob staff. Colors are dry unless otherwise noted. Textural abbreviations include: very fine, vfl, vfU; fine, fL, fU, medium, mL, mU, coarse, cL, cU, and very coarse, vcL, vcU. Numerical unit designations were established upsection for measured section, but are listed in descending stratigraphic order.

| Unit | Description | Thickness (m) |
|------|---|------------------|
| | Arroyo Ojito Fm (QTui, Maldonado et al., 1999): 25 m | |
| 5. | Sand: white to reddish-yellow (N8/0 to 7.5YR 6/6), moderately sorted, fine-to medium-grained sand; strongly developed soil with degraded Stage III+ carbonate morphology at top of unit. Pebbles are generally absent or comprise <5% of unit. | 3.3 |
| 4. | Pebbly sand: very pale-brown (10YR 7/4 and 8/4), poorly sorted, very fine- to very coarse-grained (silt-vcU), matrix supported pebbly sand; 20-40% gravel. Gravel size distribution is generally bimodal, containing mostly subrounded to subangular fine pebbles up to 3 cm diameter with scattered (<15%) 10 cm diameter clasts. Unit is consolidated but not generally cemented by calcium-carbonate. Forms slope at top of section. Medium to thickly bedded, lenticular, moderately sorted, fine- to medium-grained (fL-mU), sand lens. | 3.4 |
| 3. | Silty sand: pale-brown (10YR 6/3), poorly sorted, fine-grained (mostly fU), silty sand. Grades upsection to pink (7.5YR 7/3-7/4) silty sand with scattered pebbles (<5%) and cylindrical calcium-carbonate nodules. Matrix is slightly cemented with calcium carbonate. | 2.8 |
| 2. | Pebbly sand and sand: light brownish-gray (10YR 6/2), poorly sorted, coarse-grained (vfL-cL), cross stratified, medium to very thickly bedded, matrix and clast supported pebbly sand, pebble gravel (15-45% gravel), and sand. Gravel composed of fine- to medium-diameter, rounded to subangular pebbles with scattered subangular cobbles of Cat Mesa basalt up to 15 cm diameter. Clast size distribution is bimodal with abundant fine pebbles up to 3 cm diameter and scattered pebbles up to 15 cm diameter. Moderately consolidated but not cemented with calcium carbonate. Basal 30 cm contains local pebble and cobble gravel that forms sharp, scoured contact with unit 1. | 3.2 |
| 1. | Silty sand and mud: reddish-yellow (7.5YR 7/6), well sorted, massive to tabular, thickly bedded, fine-grained (fL) sand with interbedded light yellowish-brown (10YR 6/4 to 2.5Y 6/4), silty clay with selenite crystals up to 1 cm long. Base of clay is sharp; upper contact is gradational with sand. Sand contains little or no calcium-carbonate cement; clay contains calcium-carbonate cement. Sand contains scattered, hard carbonate nodules up to 4 cm diameter. Top of unit Tssi of Maldonado et al. (1999). | 6.0 |

APPENDIX A9a. Cat Mesa measured section (continued).

| Unit | Description | Thickness (m) |
|------|---|------------------|
| 0. | Basalt at Cat Mesa: Dark gray to grayish black (N3/0-N2/0), coarse-grained, locally vesiculated, porphyritic basaltic flow with dyxitaxitic texture. Groundmass is coarsely microgranular and composed of plagioclase, olivine, clinopyroxene, magnetite(?), and ilmenite(?) (Maldonado and Atencio, 1998b). Dated at 3.00 ± 0.01 Ma using $^{40}\text{Ar}/^{39}\text{Ar}$ method (Maldonado et al., 1999). | 2.0 |
| B. | Silty sand: upper 35 cm to upper contact with Cat Mesa basalt (unit 0) is very pale-brown (10YR 6/4) very poorly sorted sand with cinders, rounded fine pebbles, and subangular pebbles of cemented Santa Fe Group sandstone. Middle of unit is composed of yellowish-red (5YR 5/6), moderately sorted, fine-grained (fL) sand with <5% scattered calcium-carbonate nodules. Lower portion is light-brown (7.5YR 6/4), fine-grained silty sand. Top of unit T1s1 of Maldonado et al. (1999). | 1.3 |
| C. | Slightly pebbly sand: very pale-brown (10YR 7/4-8/4), poorly sorted, massive, very fine- to coarse-grained (vfL-cL) sand. upper 60-80 cm is hard and contains scattered cylindrical calcium-carbonate nodules and possible Stage II carbonate morphology. Texture is similar to unit 3. Lower 2 m composed of light brown to light yellowish-brown (7.5YR-10YR 6/4), poorly sorted, massive to medium bedded, very fine- to medium-grained (vfL-mL) slightly pebbly sand with 5-10% scattered subrounded to subangular pebbles. Section continues but not measured. | 4.8 |

Cat Mesa Section

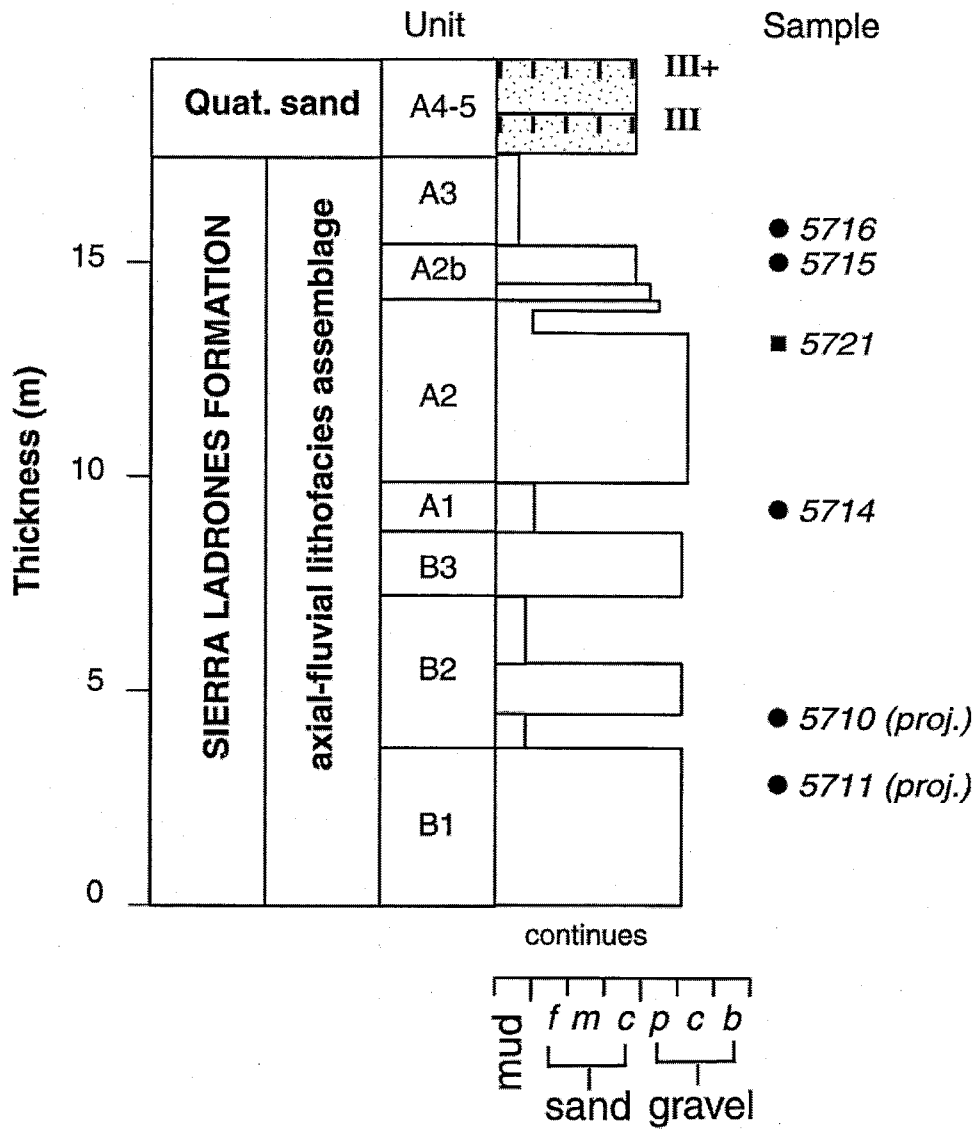


APPENDIX A10a. Isleta upper powerline road measured section of Santa Fe Group sediments east of powerline road, Isleta 7.5-minute quadrangle. Measured upsection from unit 1 by S.D. Connell, D.W. Love, and P.B. Jackson on November 9, 1999 using an Abney level and Jacob staff. Colors are dry unless otherwise noted. Textural abbreviations include: very fine, vfl, vfU; fine, fL, fU, medium, mL, mU, coarse, cL, cU, and very coarse, vcL, vcU. Numerical unit designations were established upsection for measured section, but are listed in descending stratigraphic order. Section contains approximately 30% silt and clay, and 70% sand and gravel.

| Unit | Description | Thickness (m) |
|---|--|------------------|
| Sierra Ladrones Fm, axial-fluvial lithofacies assemblage: 21 m | | |
| A5. | Sand: surface soil forming degraded top of the Sunport geomorphic surface. Overlain by <0.5 m thick fine- to medium-grained eolian sand sheets. | 1.3 |
| A4. | Sand: Two buried soils exhibiting stage III and III+ pedogenic carbonate morphology. | 1.0 |
| A3. | Claystone: lower 70 cm is a light reddish-brown (5YR 6/3) thinly to medium bedded claystone. Overlain by 64 cm thick, light olive-gray (5Y 6/2) silty clay with sand-sized muscovite flakes, mottled with <2 cm diameter soft white carbonate nodules. Overlain by 93 cm thick, reddish-brown, massive slightly silty clay containing thin shelled planispiral and conispiral snails. Grades upward into clayey sand containing prismatic soil structure. | 2.3 |
| A2a. | Sand: light brownish-gray (10YR 6/2), moderately sorted, subangular, fine- to very coarse-grained (mostly cL), quartz and lithic rich sand with scattered fine pebbles (5%); loose and uncemented; local brownish-yellow (10YR 6/8) staining. | 1.3 |
| A2. | Pebbly sand: light brownish-gray (10YR 6/2), poorly sorted, fine- to coarse-grained (dominantly cU), matrix supported pebbly sand. coarse-grained sand is subangular to subrounded and contains abundant lithic fragments. Clasts are rounded to subrounded, fine-pebble to small cobbles containing quartzite, volcanic rocks, and very rare Pedernal chert, obsidian, and limestone. Scattered very pale brown (10YR 7/3), medium bedded silty sand interbeds (<10% of unit). Grades upsection into sand of units A2a. | 4.7 |
| A1. | Siltstone: very pale-brown (10YR 7/3), poorly sorted, slightly sandy siltstone. | 1.2 |
| B3. | Pebbly sand: Pumiceous pebbly sand | 1.6 |
| B2. | Siltstone: pink (7.5YR 7/4) finely laminated, slightly sandy silt; bed thins to the east. | 1.8 |
| B1. | Pebbly sand and siltstone: pumiceous pebbly sand with 80 cm thick sandy silt bed about 4 m above base of unit. Base rests on Arroyo Ojito Formation. | 6.1 |

APPENDIX A10b. Graphic log of Isleta upper powerline section.

Isleta Upper Powerline Section



APPENDIX A11a. Hell Canyon Wash measured section of Santa Fe Group sediments along the middle reach of Hell Canyon, Hubbell Springs 7.5-minute quadrangle. Base of measured section at E: 3,862,690 m; N: 355,430 m (UTM zone 13S, NAD 1983). Measured upsection from unit 1 by S.D. Connell, and D.W. Love on November 5, 1999, using an Abney level and Jacob staff. Colors are dry unless otherwise noted. Textural abbreviations include: very fine, vfl, vfU; fine, fL, fU, medium, mL, mU, coarse, cL, cU, and very coarse, vcL, vcU. Numerical unit designations were established upsection for measured section, but are listed in descending stratigraphic order.

| Unit | Description | Thickness (m) |
|---|---|------------------|
| Sierra Ladrones Fm, piedmont lithofacies assemblage: 9 m | | |
| 9c. | Pebbly conglomerate: white (N8/0) moderately to poorly sorted, clast-supported pebble conglomerate. Well cemented with micritic calcium-carbonate cement and locally forms cliffs. Limestone clasts are weathered and exhibit relatively deep (0.1-1.5 cm deep) pendants formed by dissolution of limestone; thick pedogenic carbonate rinds exposed on about 25% of clasts. | 2.2 |
| 9b. | Sand and pebble conglomerate: light-brown (10YR 6/4), medium-to fine-grained (mL-vfL) slightly silty sand with scattered carbonate nodules and lenticular thinly to medium bedded pebbly sand interbeds. | 1.4 |
| 9a2. | Slightly silty sand with scattered pebbles: light-brown (10YR 6/4), moderately to poorly sorted, medium- to very fine-grained (mL-vfL, mostly fU), slightly silty sand with scattered and medium bedded, lensoidal pebbly sand interbeds and scattered carbonate nodules. | 2.7 |
| 9a1. | Pebble gravel: light-brown (10YR 6/4), moderately sorted pebble conglomerate; clasts are 85% limestone, 6% greenstone, 4% gneiss and schist, 4% yellowish-brown sandstone, and 1% chert; clasts are generally <50 cm diameter; matrix is <15% silty sand; interbedded lensoidal silty sand. | 2.7 |
| Sierra Ladrones Fm, axial-fluvial lithofacies assemblage: 28 m | | |
| 8. | Sand and pebbly sand: reddish-yellow (7.5YR 7/6), poorly sorted, very fine- to very coarse-grained (vfL-vcU, mostly fL) sand and scattered pebbles (about 10%); three weakly developed, brown to pink (7.5YR 5/4-7/1) paleosols in upper 3 m. | 6.2 |
| 7. | Sand and clay: yellow (10YR 7/6), well sorted and rounded, thinly to medium-bedded, fine-grained (fL) sand interbedded with thinly bedded, reddish-brown (5YR 4/4) clay. Upper contact is gradational, interfingers with unit 8, and is placed at lowest occurrence of limestone-bearing gravel. | 2.4 |
| 6. | Silty sand: yellow (10YR 7/6), moderately sorted, massive, silty sand with thinly bedded pink (7.5YR 8/3) <1-cm diameter, irregular-shaped concretions and nodules, which are common on the ground surface. Base is marked by ca. 1-m thick, reddish-brown (5YR 4/4) clay. Upper contact is poorly exposed, gradational, interfingers with unit 7 and is placed at the lowest thinly bedded reddish-brown clay. | 2.6 |

APPENDIX A11a. Hell Canyon Wash measured section (continued).

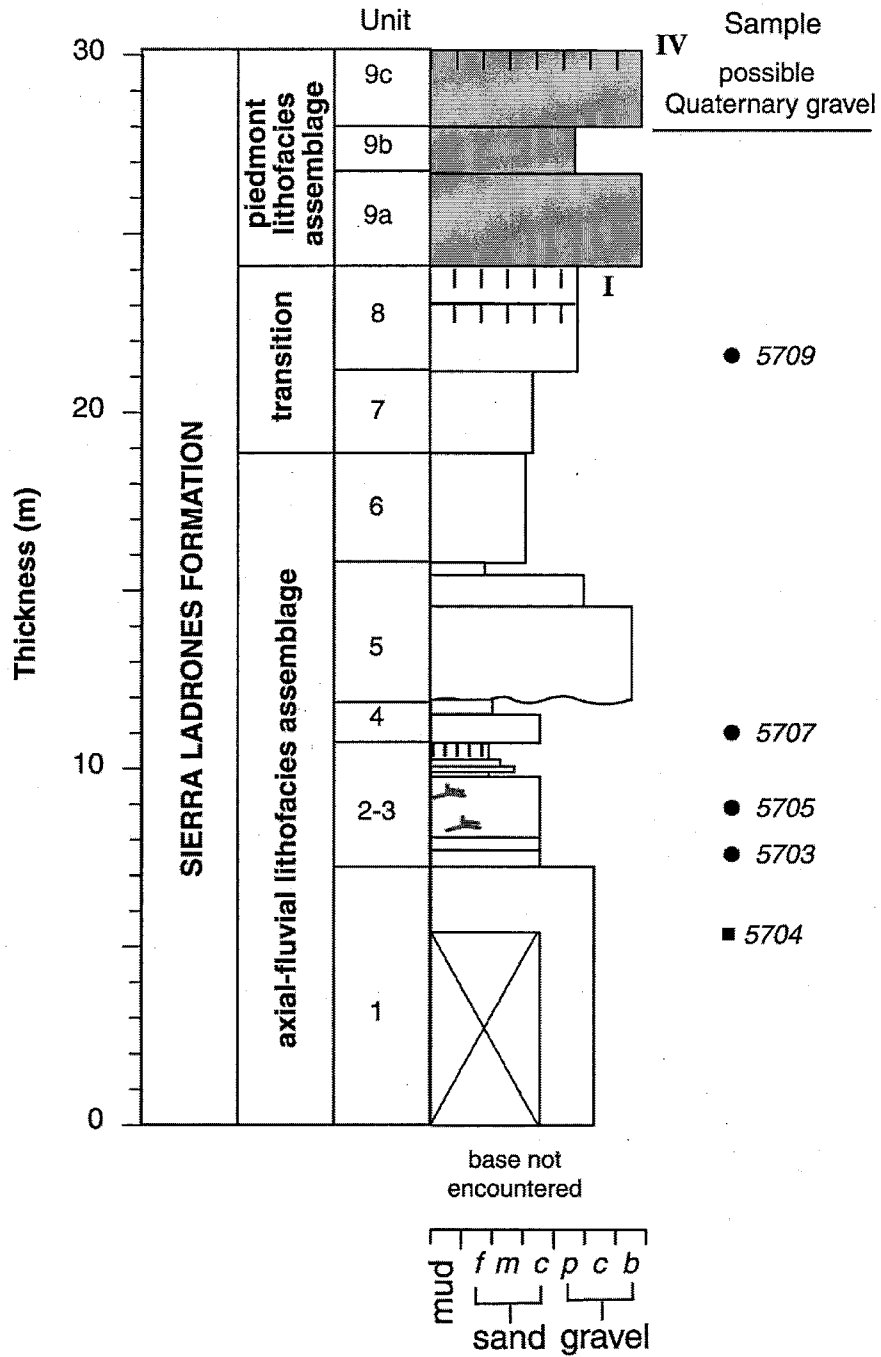
| Unit | Description | Thickness (m) |
|------|---|------------------|
| 5. | Pebble conglomerate and sandstone: light brownish-gray, well cemented (sparry calcium carbonate), moderately sorted, medium- to coarse-grained (mU-vcU), cross bedded sandstone (40%) and pebble conglomerate (60%). Pebbles are subrounded to rounded and clast supported; a single small cobble of limestone is present at base. Pumice-rich beds are common near base. Trough cross beds are common and up to 60-cm high. Abundant torpedo-shaped, calcium-carbonate cemented concretions. paleocurrent directions taken on scour directions (5) and trough cross sets (1). Bedding: N50E, 2SE. Grades upsection to uncemented pebbly sand about 1 m below top. Upper contact is poorly exposed and gradational with placed at the lowest ca. 1m thick reddish-brown (5YR 4/4) clay bed. | 4.7 |
| 4b. | Sandy silt: pink (7.5YR 8/4), well sorted, medium bedded silty to fine-grained (silt-fL) sandy silt with abundant fine, calcium-carbonate cemented root tubes. Upper contact is sharp and scoured; carbonate nodules are common near top. Discontinuous white siltstone about 40 cm below top. | 0.6 |
| 4a. | Slightly silty sand: pink (7.5YR 7/4), moderately sorted, silty to coarse-grained (fL-cU) slightly silty sand with scattered, thinly bedded, lenticular very coarse-grained sand and very fine pebbly sand (vcU-3 cm); gravel locally comprises ca. 10-25% of pebbly sand beds and are angular-subangular and dominantly matrix supported with rare, thin clast-supported lenses. Nodular and disseminated carbonate. Upper contact is gradational. | 0.6 |
| 3. | Silty clay: very pale-yellow (5Y 7/3) silty clay; upper 10-20 cm is reddish-brown; nodular carbonate and scattered Mn-oxide stains suggests subaerial exposure and minor soil formation. B: N30E, 2SE | 0.5 |
| 2c. | Silty sand: very pale-brown (10YR 7/3), thinly to medium bedded silty clay and fine-grained (fL-silt) silty sand. Silty clay forms thinly bedded, lenticular beds with abundant vertical fractures. Upper contact is sharp, irregular with 5-20 cm of relief, and marked by thinly bedded white (N8/0) zone of hard nodular carbonate. | 0.5 |
| 2b. | Silty sand: very pale-brown (10YR 7/4), massive fU sand with minor cU-vcL biotite grains. Contains thinly bedded white (N8/0), hard calcium-carbonate nodules. | 1.8 |

APPENDIX A11a. Hell Canyon Wash measured section (continued).

| Unit | Description | Thickness (m) |
|------|---|------------------|
| 2a. | <p>Silty sand: very pale-brown (10YR 7/3-8/2); moderately sorted, very fine- to fine-grained (vfU-fU) silty sand. Lower 40 cm contains thinly bedded and locally low-angle silty sand with discontinuous, low-angle cross laminations with a single medium-grained pumice pebble at base of unit. Upper 40 cm contains massive, silt to very fine-grained (vfU) silty sand with 1-2 cm thick carbonate-cemented sandstone nodules. Upper massive silty sand is similar in texture and composition to Unit 4a. Forms ledge; disseminated calcium-carbonate cement. Unit 1 and 2a may form a single upward-fining sequence. Upper contact is abrupt and marked by a 10-cm thick brown (7.5YR 5/4), plastic clay with scattered very pale-brown (10YR 7/3-8/2) silty sand pebbles. Top forms a west-thickening wedge of clay balls with rare rip-up clasts of silty sandstone.</p> | 0.8 |
| 1. | <p>Sand and pebbly sand: light-gray (10YR 7/2), well to moderately sorted, thinly to medium bedded sand with thinly bedded lenticular, matrix-supported fine pebbly sand interbeds and pumiceous cross-stratified fine pebbly sand; uncemented to very weakly cemented with calcium-carbonate; clasts are rounded; grains are mU-vcU and subrounded to subangular; commonly forms slope; upper contact is sharp; partly covered with colluvium up to 3 m below top. Base not exposed.</p> | 7.2 |

APPENDIX A11b. Graphic log of Hell Canyon section.

Hell Canyon Section



Appendix B1. Detrital modes of >8-mm diameter gravel from the Arroyo Ojito Formation, including Navajo Draw (Ton), Loma Barbon (Tob), and Ceja (Toc) members, and the Cerro Conejo Member (Tzc) of the Zia Formation. See Table 2 for description of compositional abbreviations.

| Sample | Q | Qw | Qp | Qg | Qb | Ql | Qcb | Qcg | Qcr | Qcp | Qcl | Vfg | Vtt | Vtw | Vtr | Vb | Va | Vr |
|-----------------|---|----|----|----|----|----|-----|-----|-----|-----|-----|-----|-----|-----|-----|----|----|----|
| SFP-3 | 0 | 18 | 5 | 0 | 3 | 0 | 7 | 7 | 3 | 95 | 0 | 256 | 0 | 6 | 0 | 73 | 4 | 0 |
| SFP-4c | 0 | 16 | 4 | 1 | 1 | 0 | 0 | 12 | 0 | 62 | 0 | 211 | 0 | 0 | 0 | 38 | 5 | 0 |
| M-3 | 0 | 13 | 2 | 5 | 2 | 0 | 4 | 2 | 0 | 13 | 3 | 64 | 4 | 2 | 0 | 4 | 2 | 0 |
| Z-8a | 0 | 10 | 4 | 3 | 0 | 0 | 3 | 3 | 0 | 9 | 3 | 159 | 9 | 6 | 0 | 0 | 4 | 5 |
| Z-10 | 0 | 6 | 0 | 3 | 0 | 0 | 1 | 1 | 0 | 17 | 2 | 127 | 7 | 4 | 0 | 0 | 8 | 0 |
| Z-13 | 0 | 8 | 0 | 3 | 2 | 0 | 0 | 2 | 1 | 16 | 0 | 144 | 3 | 3 | 0 | 1 | 0 | 0 |
| Z-16a | 0 | 10 | 0 | 0 | 0 | 0 | 4 | 3 | 0 | 17 | 0 | 142 | 6 | 3 | 0 | 4 | 0 | 0 |
| LC-3 | 0 | 27 | 11 | 7 | 10 | 0 | 62 | 5 | 7 | 71 | 37 | 87 | 6 | 0 | 0 | 7 | 0 | 0 |
| LC-6a | 0 | 41 | 16 | 28 | 50 | 0 | 24 | 0 | 17 | 99 | 52 | 130 | 0 | 4 | 0 | 20 | 47 | 4 |
| Cat Mesa 5729 | 0 | 13 | 1 | 6 | 3 | 0 | 18 | 21 | 0 | 26 | 10 | 183 | 7 | 16 | 0 | 19 | 0 | 0 |
| ER-2 | 0 | 24 | 7 | 3 | 5 | 0 | 25 | 32 | 4 | 42 | 11 | 171 | 3 | 1 | 0 | 6 | 0 | 0 |
| Rio Bravo | 0 | 21 | 6 | 11 | 23 | 0 | 23 | 30 | 7 | 30 | 15 | 163 | 12 | 8 | 0 | 0 | 0 | 0 |
| Casino South U1 | 0 | 8 | 1 | 4 | 4 | 0 | 8 | 7 | 1 | 18 | 1 | 110 | 4 | 5 | 0 | 1 | 0 | 0 |
| Casino South U4 | 0 | 9 | 4 | 5 | 3 | 0 | 17 | 18 | 4 | 21 | 6 | 144 | 12 | 3 | 1 | 0 | 0 | 0 |
| Ceja 5 | 0 | 8 | 5 | 2 | 4 | 0 | 7 | 6 | 1 | 28 | 5 | 51 | 0 | 5 | 0 | 1 | 0 | 0 |
| Ceja 7 | 0 | 18 | 6 | 5 | 10 | 0 | 17 | 12 | 3 | 26 | 13 | 70 | 3 | 1 | 0 | 1 | 0 | 0 |
| Ceja 9 | 0 | 18 | 3 | 6 | 5 | 0 | 4 | 3 | 2 | 28 | 2 | 64 | 0 | 3 | 0 | 1 | 0 | 0 |
| Ceja 10 | 0 | 11 | 0 | 5 | 2 | 0 | 3 | 6 | 0 | 14 | 2 | 57 | 0 | 0 | 0 | 0 | 0 | 0 |
| Ceja 15 | 0 | 46 | 10 | 18 | 4 | 1 | 3 | 5 | 2 | 17 | 0 | 74 | 0 | 5 | 2 | 2 | 2 | 0 |

Appendix B1. Detrital modes of >8-mm diameter gravel from the Arroyo Ojito Formation, including Navajo Draw (Ton), Loma Barbon (Tob), and Ceja (Toc) members, and the Cerro Conejo Member (Tzc) of the Zia Formation. See Table 2 for description of compositional abbreviations. (Continued)

| Sample | Ssg | Ssr | Ssy | Sir | Sc | Sw | SI | PMgr | PMgw | PMgsp | PMn | PMs | PMd | U | Total |
|-----------------|-----|-----|-----|-----|----|----|----|------|------|-------|-----|-----|-----|----|-------|
| SFP-3 | 27 | 3 | 0 | 0 | 0 | 0 | 1 | 48 | 26 | 265 | 2 | 0 | 0 | 9 | 858 |
| SFP-4c | 46 | 6 | 0 | 0 | 0 | 0 | 0 | 30 | 16 | 145 | 2 | 0 | 0 | 9 | 604 |
| M-3 | 44 | 2 | 19 | 0 | 1 | 0 | 1 | 23 | 4 | 55 | 1 | 0 | 0 | 7 | 277 |
| Z-8a | 46 | 1 | 23 | 0 | 1 | 0 | 1 | 121 | 2 | 115 | 0 | 0 | 0 | 11 | 539 |
| Z-10 | 33 | 5 | 30 | 0 | 4 | 0 | 2 | 52 | 2 | 52 | 3 | 0 | 0 | 9 | 368 |
| Z-13 | 53 | 0 | 17 | 0 | 0 | 0 | 0 | 91 | 1 | 79 | 4 | 0 | 0 | 4 | 432 |
| Z-16a | 41 | 5 | 10 | 1 | 0 | 0 | 0 | 54 | 2 | 43 | 3 | 0 | 0 | 5 | 353 |
| LC-3 | 187 | 4 | 22 | 0 | 0 | 0 | 0 | 21 | 2 | 61 | 0 | 0 | 3 | 9 | 646 |
| LC-6a | 200 | 4 | 17 | 0 | 0 | 3 | 0 | 8 | 2 | 24 | 1 | 0 | 0 | 7 | 798 |
| Cat Mesa 5729 | 101 | 6 | 24 | 0 | 2 | 2 | 0 | 8 | 3 | 14 | 0 | 0 | 0 | 8 | 491 |
| ER-2 | 80 | 1 | 8 | 0 | 0 | 2 | 0 | 21 | 0 | 31 | 0 | 0 | 0 | 6 | 483 |
| Rio Bravo | 54 | 4 | 23 | 0 | 1 | 1 | 0 | 17 | 2 | 33 | 1 | 0 | 0 | 9 | 494 |
| Casino South U1 | 50 | 0 | 5 | 0 | 0 | 0 | 0 | 0 | 0 | 11 | 0 | 0 | 0 | 1 | 239 |
| Casino South U4 | 32 | 0 | 13 | 0 | 0 | 0 | 0 | 11 | 1 | 12 | 1 | 0 | 0 | 6 | 324 |
| Ceja 5 | 55 | 4 | 3 | 0 | 1 | 0 | 0 | 19 | 0 | 8 | 0 | 0 | 0 | 5 | 218 |
| Ceja 7 | 39 | 5 | 3 | 0 | 1 | 3 | 0 | 17 | 0 | 14 | 0 | 0 | 0 | 4 | 271 |
| Ceja 9 | 34 | 3 | 4 | 0 | 0 | 1 | 0 | 32 | 0 | 22 | 0 | 0 | 0 | 1 | 236 |
| Ceja 10 | 36 | 4 | 4 | 0 | 0 | 1 | 0 | 19 | 0 | 15 | 0 | 0 | 0 | 3 | 182 |
| Ceja 15 | 44 | 7 | 10 | 0 | 2 | 1 | 0 | 16 | 0 | 2 | 0 | 0 | 0 | 3 | 274 |

Appendix B2. Detrital modes of >8-mm diameter gravel from the axial-fluvial (ancestral Rio Grande) facies of the Sierra Ladrones Formation, northern Albuquerque Basin study area. See Table 2 for description of compositional abbreviations.

| Sample | Q | Qw | Qp | Qg | Qb | Ql | Qcb | Qcg | Qcr | Qcp | Qcl | Vtg | Vtt | Vtr | Vb | Va | Vr |
|-------------------|---|-----|----|----|----|----|-----|-----|-----|-----|-----|-----|-----|-----|----|-----|----|
| SFP-6 | 0 | 131 | 18 | 33 | 30 | 12 | 7 | 3 | 1 | 8 | 0 | 174 | 11 | 0 | 0 | 111 | 0 |
| SFP-16 | 0 | 46 | 12 | 12 | 8 | 3 | 2 | 0 | 0 | 1 | 0 | 81 | 16 | 0 | 0 | 46 | 0 |
| TQA-1 | 0 | 82 | 19 | 17 | 24 | 3 | 9 | 0 | 1 | 0 | 0 | 159 | 24 | 0 | 0 | 11 | 66 |
| TQA-4a | 0 | 73 | 13 | 26 | 20 | 5 | 1 | 1 | 0 | 0 | 0 | 140 | 17 | 11 | 0 | 5 | 2 |
| GQ-1a | 0 | 69 | 18 | 40 | 35 | 4 | 1 | 0 | 0 | 0 | 0 | 246 | 36 | 12 | 0 | 1 | 45 |
| GQ-2a | 0 | 156 | 27 | 48 | 39 | 4 | 1 | 0 | 0 | 6 | 3 | 261 | 16 | 8 | 0 | 3 | 75 |
| GQ-6a | 0 | 98 | 22 | 24 | 45 | 7 | 0 | 1 | 0 | 4 | 0 | 246 | 10 | 3 | 0 | 0 | 38 |
| GQ-7 | 0 | 76 | 14 | 19 | 48 | 5 | 3 | 4 | 0 | 1 | 0 | 184 | 48 | 6 | 0 | 1 | 47 |
| ASF-6 | 0 | 61 | 7 | 16 | 18 | 3 | 0 | 0 | 1 | 4 | 0 | 73 | 5 | 1 | 0 | 2 | 21 |
| ASF-9 | 0 | 54 | 9 | 26 | 36 | 3 | 0 | 0 | 0 | 0 | 0 | 210 | 26 | 6 | 0 | 0 | 50 |
| PL-U UA2 5721 | 0 | 119 | 13 | 17 | 26 | 10 | 2 | 3 | 0 | 3 | 2 | 298 | 27 | 6 | 0 | 1 | 15 |
| LL-2 U4 | 0 | 38 | 10 | 9 | 19 | 6 | 1 | 0 | 0 | 2 | 0 | 140 | 13 | 4 | 0 | 0 | 15 |
| Hell Canyon 5704 | 0 | 17 | 2 | 1 | 15 | 3 | 0 | 1 | 0 | 0 | 0 | 90 | 5 | 4 | 0 | 0 | 3 |
| S. Powerline 5713 | 0 | 66 | 15 | 7 | 10 | 0 | 0 | 5 | 0 | 7 | 1 | 410 | 10 | 3 | 0 | 8 | 14 |

Appendix B2. Detrital modes of >8-mm diameter gravel from the axial-fluvial (ancestral Rio Grande) facies of the Sierra Ladrones Formation, northern Albuquerque Basin study area. See Table 2 for description of compositional abbreviations. (Continued)

| Sample | Ssg | Ssr | Ssy | Sir | Sc | Sw | Sl | PMgr | PMgw | PMgp | PMn | PMs | PMd | U | Total |
|-------------------|-----|-----|-----|-----|----|----|----|------|------|------|-----|-----|-----|----|-------|
| SFP-6 | 4 | 3 | 0 | 6 | 0 | 0 | 0 | 4 | 20 | 73 | 8 | 0 | 41 | 7 | 705 |
| SFP-16 | 0 | 1 | 0 | 0 | 1 | 0 | 0 | 1 | 5 | 22 | 3 | 0 | 26 | 4 | 290 |
| TQA-1 | 0 | 0 | 0 | 0 | 3 | 0 | 0 | 2 | 4 | 22 | 0 | 2 | 9 | 10 | 467 |
| TQA-4a | 3 | 0 | 1 | 0 | 0 | 0 | 0 | 2 | 4 | 6 | 0 | 0 | 8 | 7 | 380 |
| GQ-1a | 4 | 0 | 4 | 3 | 0 | 0 | 0 | 0 | 0 | 20 | 7 | 0 | 12 | 5 | 566 |
| GQ-2a | 1 | 0 | 2 | 5 | 0 | 0 | 0 | 3 | 4 | 37 | 9 | 4 | 5 | 8 | 725 |
| GQ-6a | 0 | 0 | 3 | 0 | 0 | 0 | 0 | 10 | 7 | 18 | 6 | 2 | 5 | 8 | 561 |
| GQ-7 | 1 | 0 | 6 | 0 | 0 | 0 | 0 | 4 | 0 | 8 | 3 | 1 | 11 | 7 | 497 |
| ASF-6 | 0 | 2 | 2 | 0 | 0 | 0 | 3 | 10 | 7 | 40 | 4 | 0 | 1 | 2 | 289 |
| ASF-9 | 1 | 0 | 3 | 0 | 1 | 0 | 0 | 3 | 1 | 13 | 3 | 1 | 1 | 6 | 454 |
| PL-U UA2 5721 | 5 | 0 | 3 | 0 | 0 | 0 | 0 | 18 | 1 | 26 | 3 | 1 | 0 | 8 | 610 |
| LL-2 U4 | 2 | 1 | 4 | 0 | 0 | 0 | 1 | 5 | 3 | 26 | 1 | 0 | 5 | 5 | 311 |
| Hell Canyon 5704 | 1 | 0 | 0 | 0 | 0 | 0 | 0 | 0 | 6 | 10 | 0 | 0 | 3 | 2 | 163 |
| S. Powerline 5713 | 12 | 0 | 3 | 1 | 3 | 0 | 0 | 30 | 5 | 49 | 0 | 1 | 0 | 9 | 669 |

Appendix B3. Detrital modes of >8-mm diameter gravel from the eastern-margin piedmont facies of the Sierra Ladrones Formation, northern Albuquerque Basin study area. See Table 2 for description of compositional abbreviations.

| Sample | Q | Qw | Qp | Qg | Qb | Ql | Qcb | Qcg | Qcr | Qep | Qcl | Vtg | Vtt | Vtr | Vb | Va | Vr |
|--------|----|----|----|----|----|----|-----|-----|-----|-----|-----|-----|-----|-----|----|----|----|
| TQA-6 | 47 | 0 | 0 | 4 | 0 | 0 | 0 | 32 | 0 | 0 | 0 | 0 | 6 | 0 | 4 | 0 | 0 |
| GQ-13 | 55 | 0 | 10 | 11 | 3 | 0 | 4 | 25 | 0 | 0 | 0 | 0 | 9 | 3 | 5 | 0 | 5 |
| ASF-4 | 59 | 0 | 2 | 5 | 3 | 0 | 0 | 16 | 0 | 0 | 0 | 0 | 9 | 0 | 4 | 0 | 19 |
| RC-2 | 18 | 0 | 3 | 0 | 0 | 0 | 0 | 4 | 0 | 0 | 3 | 3 | 0 | 0 | 0 | 0 | 5 |
| RC-4 | 30 | 0 | 3 | 3 | 1 | 0 | 0 | 5 | 0 | 0 | 0 | 4 | 0 | 0 | 0 | 0 | 7 |
| RC-8 | 26 | 0 | 0 | 2 | 0 | 0 | 0 | 2 | 0 | 0 | 1 | 19 | 1 | 15 | 0 | 0 | 26 |
| RC-11 | 15 | 0 | 0 | 0 | 0 | 0 | 0 | 2 | 0 | 0 | 0 | 4 | 2 | 8 | 0 | 0 | 20 |

| Sample | Ssg | Ssr | Ssy | Sir | Sc | Sw | Sl | PMgr | PMgw | PMgp | PMIn | PMs | PMD | U | Total |
|--------|-----|-----|-----|-----|----|----|-----|------|------|------|------|-----|-----|---|-------|
| TQA-6 | 10 | 21 | 12 | 0 | 0 | 0 | 260 | 0 | 0 | 64 | 54 | 14 | 6 | 9 | 543 |
| GQ-13 | 21 | 20 | 50 | 0 | 0 | 0 | 229 | 7 | 0 | 51 | 12 | 4 | 0 | 4 | 528 |
| ASF-4 | 14 | 22 | 8 | 0 | 0 | 0 | 278 | 9 | 0 | 35 | 34 | 3 | 0 | 5 | 525 |
| RC-2 | 9 | 20 | 13 | 1 | 0 | 0 | 245 | 1 | 3 | 43 | 29 | 9 | 0 | 4 | 413 |
| RC-4 | 20 | 24 | 17 | 0 | 2 | 0 | 270 | 3 | 4 | 39 | 75 | 12 | 0 | 6 | 525 |
| RC-8 | 12 | 22 | 23 | 2 | 0 | 0 | 201 | 3 | 1 | 31 | 56 | 8 | 0 | 7 | 459 |
| RC-11 | 9 | 11 | 14 | 0 | 0 | 0 | 76 | 0 | 0 | 9 | 16 | 1 | 0 | 6 | 193 |

Appendix B4. Percent normalized detrital parameters of gravel, Arroyo Ojito Fm.

| Sample | Q | Qw | Qp | Qg | Qb | Ql | Qcb | Qcg | Qcr | Qcp | Qcl | Vtg | Vtt | Vtw | Vtr | Vb | Va | Vr |
|--------------------|---|-----------|-----------|-----------|-----------|----|-----------|-----------|-----------|-----------|-----------|------------|-----------|-----------|-----|-----------|-----------|----|
| SFP-3 | 0 | 2 | 1 | 0 | 0 | 0 | 1 | 1 | 0 | 11 | 0 | 30 | 0 | 1 | 0 | 8 | 0 | 0 |
| SFP-4c | 0 | 3 | 1 | 0 | 0 | 0 | 0 | 2 | 0 | 10 | 0 | 35 | 0 | 0 | 0 | 6 | 1 | 0 |
| M-3 | 0 | 5 | 1 | 2 | 1 | 0 | 1 | 1 | 0 | 5 | 1 | 24 | 1 | 1 | 0 | 1 | 1 | 0 |
| Z-8a | 0 | 2 | 1 | 1 | 0 | 0 | 1 | 1 | 0 | 2 | 1 | 30 | 2 | 1 | 0 | 0 | 1 | 1 |
| Z-10 | 0 | 2 | 0 | 1 | 0 | 0 | 0 | 0 | 0 | 5 | 1 | 35 | 2 | 1 | 0 | 0 | 2 | 0 |
| Z-13 | 0 | 2 | 0 | 1 | 0 | 0 | 0 | 0 | 0 | 4 | 0 | 34 | 1 | 1 | 0 | 0 | 0 | 0 |
| Z-16a | 0 | 3 | 0 | 0 | 0 | 0 | 1 | 1 | 0 | 5 | 0 | 41 | 2 | 1 | 0 | 1 | 0 | 0 |
| LC-3 | 0 | 4 | 2 | 1 | 2 | 0 | 10 | 1 | 1 | 11 | 6 | 14 | 1 | 0 | 0 | 1 | 0 | 0 |
| LC-6a | 0 | 5 | 2 | 4 | 6 | 0 | 3 | 0 | 2 | 13 | 7 | 16 | 0 | 1 | 0 | 2 | 6 | 1 |
| Cat Mesa 5729 | 0 | 3 | 0 | 1 | 1 | 0 | 4 | 4 | 0 | 5 | 2 | 38 | 1 | 3 | 0 | 4 | 0 | 0 |
| ER-2 | 0 | 5 | 1 | 1 | 1 | 0 | 5 | 7 | 1 | 9 | 2 | 36 | 1 | 0 | 0 | 1 | 0 | 0 |
| Rio Bravo | 0 | 4 | 1 | 2 | 5 | 0 | 5 | 6 | 1 | 6 | 3 | 34 | 2 | 2 | 0 | 0 | 0 | 0 |
| Casino South U1 | 0 | 3 | 0 | 2 | 2 | 0 | 3 | 3 | 0 | 8 | 0 | 46 | 2 | 2 | 0 | 0 | 0 | 0 |
| Casino South U4 | 0 | 3 | 1 | 2 | 1 | 0 | 5 | 6 | 1 | 7 | 2 | 45 | 4 | 1 | 0 | 0 | 0 | 0 |
| Ceja 5 | 0 | 4 | 2 | 1 | 2 | 0 | 3 | 3 | 0 | 13 | 2 | 24 | 0 | 2 | 0 | 2 | 0 | 0 |
| Ceja 7 | 0 | 7 | 2 | 2 | 4 | 0 | 6 | 4 | 1 | 10 | 5 | 26 | 1 | 0 | 0 | 0 | 0 | 0 |
| Ceja 9 | 0 | 8 | 1 | 3 | 2 | 0 | 2 | 1 | 1 | 12 | 1 | 27 | 0 | 1 | 0 | 0 | 0 | 0 |
| Ceja 10 | 0 | 6 | 0 | 3 | 1 | 0 | 2 | 3 | 0 | 8 | 1 | 32 | 0 | 0 | 0 | 0 | 0 | 0 |
| Ceja 15 | 0 | 17 | 4 | 7 | 1 | 0 | 1 | 2 | 1 | 6 | 0 | 27 | 0 | 2 | 1 | 1 | 0 | 0 |
| Mean $\pm 1\sigma$ | 0 | 5 ± 3 | 1 ± 1 | 2 ± 2 | 2 ± 2 | 0 | 3 ± 3 | 2 ± 2 | 1 ± 1 | 8 ± 3 | 2 ± 2 | 31 ± 9 | 1 ± 1 | 1 ± 1 | 0 | 2 ± 2 | 1 ± 1 | 0 |

Appendix B4. Percent normalized detrital parameters of gravel, Arroyo Ojito Fm. (Continued)

| Sample | Ssg | Ssr | Ssy | Sir | Sc | Sw | SI | PMgr | PMgw | PMgp | PMn | PMs | PMd |
|-----------------|------|-----|-----|-----|----|----|----|------|------|------|-----|-----|-----|
| SFP-3 | 3 | 0 | 0 | 0 | 0 | 0 | 0 | 6 | 3 | 31 | 0 | 0 | 0 |
| SFP-4c | 8 | 1 | 0 | 0 | 0 | 0 | 0 | 5 | 3 | 24 | 0 | 0 | 0 |
| M-3 | 16 | 1 | 7 | 0 | 0 | 0 | 0 | 9 | 1 | 20 | 0 | 0 | 0 |
| Z-8a | 9 | 0 | 4 | 0 | 0 | 0 | 0 | 23 | 0 | 22 | 0 | 0 | 0 |
| Z-10 | 9 | 1 | 8 | 0 | 1 | 1 | 0 | 14 | 1 | 14 | 1 | 0 | 0 |
| Z-13 | 12 | 0 | 4 | 0 | 0 | 0 | 0 | 21 | 0 | 18 | 1 | 0 | 0 |
| Z-16a | 12 | 1 | 3 | 0 | 0 | 0 | 0 | 16 | 1 | 12 | 1 | 0 | 0 |
| LC-3 | 29 | 1 | 3 | 0 | 0 | 0 | 0 | 3 | 0 | 10 | 0 | 0 | 0 |
| LC-6a | 25 | 1 | 2 | 0 | 0 | 0 | 0 | 1 | 0 | 3 | 0 | 0 | 0 |
| Cat Mesa 5729 | 21 | 1 | 5 | 0 | 0 | 0 | 0 | 2 | 1 | 3 | 0 | 0 | 0 |
| ER-2 | 17 | 0 | 2 | 0 | 0 | 0 | 0 | 4 | 0 | 6 | 0 | 0 | 0 |
| Rio Bravo | 11 | 1 | 5 | 0 | 0 | 0 | 0 | 4 | 0 | 7 | 0 | 0 | 0 |
| Casino South U1 | 21 | 0 | 2 | 0 | 0 | 0 | 0 | 0 | 0 | 5 | 0 | 0 | 0 |
| Casino South U4 | 10 | 0 | 4 | 0 | 0 | 0 | 0 | 3 | 0 | 4 | 0 | 0 | 0 |
| Ceja 5 | 26 | 0 | 1 | 0 | 0 | 0 | 0 | 9 | 0 | 4 | 0 | 0 | 0 |
| Ceja 7 | 15 | 2 | 1 | 0 | 0 | 0 | 1 | 6 | 0 | 5 | 0 | 0 | 0 |
| Ceja 9 | 14 | 1 | 2 | 0 | 0 | 0 | 0 | 14 | 0 | 9 | 0 | 0 | 0 |
| Ceja 10 | 20 | 2 | 2 | 0 | 0 | 0 | 1 | 11 | 0 | 8 | 0 | 0 | 0 |
| Ceja 15 | 16 | 3 | 4 | 0 | 1 | 0 | 0 | 6 | 0 | 1 | 0 | 0 | 0 |
| Mean ± 1σ | 16±7 | 1±1 | 3±2 | 0 | 0 | 0 | 0 | 8±7 | 1±1 | 11±9 | 0 | 0 | 0 |

Appendix B5. Percent normalized detrital parameters of gravel, ancestral Rio Grande.

| Sample | Q | Qw | Qp | Qg | Qb | Ql | Qcb | Qcg | Qcr | Qcp | Qcl | V ^{ig} | V ^{tt} | V ^{tw} | V ^{tr} | V _b | V _a | V _r |
|-------------------|---|------|-----|-----|-----|-----|-----|-----|-----|-----|-----|-----------------|-----------------|-----------------|-----------------|----------------|----------------|----------------|
| SFP-6 | 0 | 19 | 3 | 5 | 4 | 2 | 1 | 0 | 0 | 1 | 0 | 25 | 2 | 0 | 0 | 16 | 0 | 0 |
| SFP-16 | 0 | 16 | 4 | 4 | 3 | 1 | 1 | 0 | 0 | 0 | 0 | 28 | 6 | 0 | 0 | 16 | 0 | 0 |
| TQA-1 | 0 | 18 | 4 | 4 | 5 | 1 | 2 | 0 | 0 | 0 | 0 | 35 | 5 | 0 | 0 | 2 | 14 | 0 |
| TQA-4a | 0 | 20 | 3 | 7 | 5 | 1 | 0 | 0 | 0 | 0 | 0 | 38 | 5 | 3 | 1 | 1 | 9 | 0 |
| GQ-1a | 0 | 12 | 3 | 7 | 6 | 1 | 0 | 0 | 0 | 0 | 0 | 44 | 6 | 2 | 0 | 0 | 8 | 1 |
| GQ-2a | 0 | 22 | 4 | 7 | 5 | 1 | 0 | 0 | 1 | 1 | 0 | 36 | 2 | 1 | 0 | 0 | 10 | 0 |
| GQ-6a | 0 | 18 | 4 | 4 | 8 | 1 | 0 | 0 | 1 | 0 | 0 | 44 | 2 | 1 | 0 | 0 | 7 | 1 |
| GQ-7 | 0 | 16 | 3 | 4 | 10 | 1 | 1 | 1 | 0 | 0 | 0 | 38 | 10 | 1 | 0 | 0 | 10 | 0 |
| ASF-6 | 0 | 21 | 2 | 6 | 6 | 1 | 0 | 0 | 1 | 0 | 0 | 25 | 2 | 0 | 0 | 1 | 7 | 2 |
| ASF-9 | 0 | 12 | 2 | 6 | 8 | 1 | 0 | 0 | 0 | 0 | 0 | 47 | 6 | 1 | 0 | 0 | 11 | 0 |
| PL-UUA2 5721 | 0 | 20 | 2 | 3 | 4 | 2 | 0 | 0 | 0 | 0 | 0 | 50 | 4 | 1 | 0 | 2 | 0 | 0 |
| LL-2 U4 | 0 | 12 | 3 | 3 | 6 | 2 | 0 | 0 | 1 | 0 | 0 | 46 | 4 | 1 | 0 | 0 | 5 | 0 |
| Hell Canyon 5704 | 0 | 11 | 1 | 1 | 9 | 2 | 0 | 1 | 0 | 0 | 0 | 56 | 3 | 2 | 0 | 0 | 2 | 0 |
| S. Powerline 5713 | 0 | 10 | 2 | 1 | 2 | 0 | 0 | 1 | 0 | 1 | 0 | 62 | 2 | 0 | 0 | 1 | 2 | 0 |
| Mean ± 1σ | 0 | 16±4 | 3±1 | 4±2 | 6±2 | 1±1 | 0 | 0 | 0 | 0 | 0 | 41±11 | 4±2 | 1±1 | 0 | 3±6 | 6±5 | 0 |

Appendix B5. Percent normalized detrital parameters of gravel, ancestral Rio Grande. (Continued)

| Sample | Ssg | Ssr | Ssy | Sir | Sc | Sw | Sl | PMgr | PMgw | PMgp | PMn | PMs | PMd |
|--------------------|-----|-----|-----|-----|----|----|----|------|------|------|-----|-----|-----|
| SFP-6 | 1 | 0 | 0 | 1 | 0 | 0 | 0 | 1 | 3 | 10 | 1 | 0 | 6 |
| SFP-16 | 0 | 0 | 0 | 0 | 0 | 0 | 0 | 0 | 2 | 8 | 1 | 0 | 9 |
| TQA-1 | 0 | 0 | 0 | 0 | 1 | 0 | 0 | 0 | 1 | 5 | 0 | 0 | 2 |
| TQA-4a | 1 | 0 | 0 | 0 | 0 | 0 | 0 | 1 | 1 | 2 | 0 | 0 | 2 |
| GQ-1a | 1 | 0 | 1 | 1 | 0 | 0 | 0 | 0 | 0 | 4 | 1 | 0 | 2 |
| GQ-2a | 0 | 0 | 0 | 1 | 0 | 0 | 0 | 0 | 1 | 5 | 1 | 1 | 1 |
| GQ-6a | 0 | 0 | 1 | 0 | 0 | 0 | 0 | 2 | 1 | 3 | 1 | 0 | 1 |
| GQ-7 | 0 | 0 | 1 | 0 | 0 | 0 | 0 | 1 | 0 | 2 | 1 | 0 | 2 |
| ASF-6 | 0 | 1 | 1 | 0 | 0 | 1 | 0 | 3 | 2 | 14 | 1 | 0 | 0 |
| ASF-9 | 0 | 0 | 1 | 0 | 0 | 0 | 0 | 1 | 0 | 3 | 1 | 0 | 0 |
| PL-U UA2 5721 | 1 | 0 | 0 | 0 | 0 | 0 | 0 | 3 | 0 | 4 | 0 | 0 | 0 |
| LL-2 U4 | 1 | 0 | 1 | 0 | 0 | 0 | 0 | 2 | 1 | 8 | 0 | 0 | 2 |
| Hell Canyon 5704 | 1 | 0 | 0 | 0 | 0 | 0 | 0 | 0 | 4 | 6 | 0 | 0 | 2 |
| S. Powerline 5713 | 2 | 0 | 0 | 0 | 0 | 0 | 0 | 5 | 1 | 7 | 0 | 0 | 0 |
| Mean $\pm 1\sigma$ | 0 | 0 | 0 | 0 | 0 | 0 | 0 | 1±1 | 1±1 | 6±4 | 1±1 | 0 | 2±3 |

Appendix B6. Percent normalized detrital parameters of gravel, piedmont facies.

| Sample | Q | Qw | Qp | Qg | Qb | Ql | Qcb | Qcg | Qcr | Qcp | Qcl | Vfg | Vtt | Vtw | Vtr | Vb | Va | Vr |
|-----------|-----|----|-----|-----|----|----|-----|-----|-----|-----|-----|-----|-----|-----|-----|----|-----|----|
| TQA-6 | 9 | 0 | 0 | 1 | 0 | 0 | 0 | 6 | 0 | 0 | 0 | 0 | 1 | 0 | 1 | 0 | 0 | 0 |
| GQ-13 | 10 | 0 | 2 | 2 | 1 | 0 | 1 | 5 | 0 | 0 | 0 | 2 | 1 | 1 | 1 | 0 | 0 | 1 |
| ASF-4 | 11 | 0 | 0 | 1 | 1 | 0 | 0 | 3 | 0 | 0 | 0 | 2 | 0 | 1 | 0 | 0 | 0 | 4 |
| RC-2 | 4 | 0 | 1 | 0 | 0 | 0 | 0 | 1 | 0 | 0 | 1 | 1 | 0 | 0 | 0 | 0 | 0 | 1 |
| RC-4 | 6 | 0 | 1 | 1 | 0 | 0 | 0 | 1 | 0 | 0 | 0 | 1 | 0 | 0 | 0 | 0 | 0 | 1 |
| RC-8 | 6 | 0 | 0 | 0 | 0 | 0 | 0 | 0 | 0 | 0 | 0 | 4 | 0 | 3 | 0 | 0 | 0 | 6 |
| RC-11 | 8 | 0 | 0 | 0 | 0 | 0 | 0 | 1 | 0 | 0 | 0 | 2 | 1 | 4 | 0 | 0 | 0 | 11 |
| Mean ± 1σ | 8±3 | 0 | 1±1 | 1±1 | 0 | 0 | 0 | 2±2 | 0 | 0 | 0 | 2±1 | 0 | 1±2 | 0 | 0 | 3±4 | 0 |

| Sample | Ssg | Ssr | Ssy | Sir | Sc | Sw | Sl | PMgr | PMgw | PMgp | PMn | PMs | PMd |
|-----------|-----|-----|-----|-----|----|------|----|------|------|------|-----|-----|-----|
| TQA-6 | 2 | 4 | 2 | 0 | 0 | 49 | 0 | 0 | 0 | 12 | 10 | 3 | 1 |
| GQ-13 | 4 | 4 | 10 | 0 | 0 | 44 | 0 | 1 | 0 | 10 | 2 | 1 | 0 |
| ASF-4 | 3 | 4 | 2 | 0 | 0 | 53 | 0 | 2 | 0 | 7 | 7 | 1 | 0 |
| RC-2 | 2 | 5 | 3 | 0 | 0 | 60 | 0 | 0 | 1 | 11 | 7 | 2 | 0 |
| RC-4 | 4 | 5 | 3 | 0 | 0 | 52 | 0 | 1 | 1 | 8 | 14 | 2 | 0 |
| RC-8 | 3 | 5 | 5 | 0 | 0 | 44 | 0 | 1 | 0 | 7 | 12 | 2 | 0 |
| RC-11 | 5 | 6 | 7 | 0 | 0 | 41 | 0 | 0 | 0 | 5 | 9 | 1 | 0 |
| Mean ± 1σ | 3±1 | 5±1 | 5±3 | 0 | 0 | 49±7 | 0 | 1±1 | 0 | 8±3 | 9±4 | 2±1 | 0 |

Appendix B7. Recalculated detrital parameters (in percent) for gravel of the western lithofacies assemblage (Arroyo Ojito Formation) in the northern Albuquerque Basin study area. Recalculated from point count data in Appendix B2 (n=19).

| Sample | %O | QFL | | %Lm | LvLvLs | | QcQq | | QcQqPm | | QcQqV | | QcQqS | | | | |
|------------------|--------------|--------------|-------------|----------|--------------|--------------|-------------|------------|--------------|--------------|--------------|--------------|-------------|--------------|--------------|-------------|--------------|
| | | %F | %L | | %Lv | %Ls | %Qc | %Qq | %Qc | %Qq | %Qc | %Qq | %V | %Qc | %Qq | | |
| SFP-3 | 16 | 70 | 44 | 0 | 89 | 8 | 13 | 3 | 23 | 5 | 71 | 23 | 5 | 71 | 66 | 15 | 18 |
| SFP-4c | 16 | 32 | 52 | 0 | 81 | 17 | 12 | 4 | 26 | 8 | 67 | 21 | 6 | 73 | 50 | 15 | 35 |
| M-3 | 16 | 30 | 54 | 0 | 51 | 45 | 8 | 8 | 17 | 17 | 65 | 18 | 18 | 63 | 20 | 20 | 60 |
| Z-8a | 7 | 44 | 49 | 0 | 69 | 27 | 3 | 3 | 7 | 6 | 87 | 8 | 8 | 84 | 17 | 16 | 67 |
| Z-10 | 8 | 30 | 62 | 0 | 64 | 32 | 6 | 2 | 15 | 6 | 78 | 12 | 5 | 83 | 20 | 9 | 71 |
| Z-13 | 7 | 41 | 52 | 0 | 67 | 31 | 4 | 3 | 9 | 6 | 85 | 10 | 7 | 83 | 19 | 13 | 69 |
| Z-16a | 10 | 29 | 61 | 0 | 71 | 26 | 7 | 3 | 18 | 7 | 75 | 13 | 5 | 82 | 26 | 11 | 63 |
| LC-3 | 37 | 13 | 50 | 0 | 31 | 66 | 28 | 9 | 56 | 17 | 27 | 54 | 16 | 30 | 40 | 12 | 47 |
| LC-6a | 41 | 4 | 55 | 0 | 47 | 51 | 24 | 17 | 53 | 37 | 10 | 36 | 25 | 39 | 35 | 25 | 41 |
| Cat Mesa 5729 | 20 | 5 | 75 | 0 | 61 | 37 | 15 | 5 | 61 | 19 | 20 | 23 | 7 | 70 | 32 | 10 | 58 |
| ER-2 | 32 | 11 | 58 | 0 | 65 | 33 | 24 | 8 | 56 | 19 | 25 | 34 | 12 | 54 | 47 | 16 | 37 |
| Rio Bravo | 34 | 11 | 56 | 0 | 67 | 30 | 21 | 12 | 48 | 28 | 24 | 30 | 17 | 52 | 42 | 24 | 33 |
| Casino | 22 | 5 | 74 | 0 | 68 | 31 | 15 | 7 | 56 | 27 | 17 | 20 | 10 | 70 | 33 | 16 | 51 |
| South U1 | | | | | | | | | | | | | | | | | |
| Casino | 27 | 8 | 65 | 0 | 76 | 21 | 20 | 7 | 59 | 19 | 22 | 27 | 9 | 65 | 50 | 16 | 34 |
| South U4 | | | | | | | | | | | | | | | | | |
| Ceja 5 | 30 | 12 | 59 | 0 | 46 | 50 | 22 | 9 | 51 | 20 | 29 | 37 | 15 | 48 | 38 | 15 | 47 |
| Ceja 7 | 41 | 11 | 57 | 0 | 58 | 39 | 26 | 14 | 50 | 28 | 22 | 38 | 21 | 41 | 44 | 24 | 32 |
| Ceja 9 | 30 | 23 | 48 | 0 | 61 | 38 | 17 | 14 | 31 | 26 | 43 | 28 | 23 | 49 | 35 | 28 | 37 |
| Ceja 10 | 24 | 19 | 47 | 0 | 54 | 43 | 14 | 10 | 32 | 23 | 44 | 25 | 18 | 57 | 28 | 20 | 51 |
| Ceja 15 | 39 | 7 | 55 | 0 | 55 | 43 | 10 | 29 | 22 | 64 | 15 | 14 | 42 | 44 | 16 | 46 | 38 |
| Mean±1σ | 24±12 | 20±13 | 56±8 | 0 | 62±13 | 35±13 | 15±8 | 9±7 | 36±19 | 20±14 | 44±27 | 25±12 | 14±9 | 61±17 | 35±13 | 19±9 | 47±15 |

Appendix B8. Recalculated detrital parameters (in percent) for gravel of the axial-fluvial (ancestral Rio Grande) lithofacies assemblage (Sierra Ladrones Formation) in the northern Albuquerque Basin study area. Recalculated from point count data in Appendix B3 (n=14).

| Sample | %Q | QFL %F | %L | %Lm | LvLvLs %Lv | LvLvLs %Lv | QcQq %Qc | QcQq %Qc | QcQqPm %Qc | %Pm | QcQqV %Qc | %V | QcQqS %Qc | %S | | | |
|-------------------|-------------|------------|-------------|----------|---------------|---------------|-------------|-------------|---------------|--------------|--------------|------------|--------------|-------------|------------|-------------|------------|
| SFP-6 | 35 | 15 | 51 | 0 | 83 | 4 | 3 | 32 | 5 | 58 | 38 | 4 | 42 | 55 | 7 | 88 | 5 |
| SFP-16 | 29 | 11 | 60 | 0 | 82 | 1 | 1 | 28 | 2 | 57 | 40 | 1 | 36 | 63 | 3 | 94 | 2 |
| TQA-1 | 33 | 6 | 61 | 1 | 92 | 1 | 2 | 31 | 5 | 75 | 20 | 2 | 35 | 63 | 6 | 92 | 2 |
| TQA-4a | 37 | 3 | 60 | 0 | 92 | 2 | 1 | 36 | 1 | 86 | 13 | 1 | 39 | 30 | 1 | 96 | 3 |
| GQ-1a | 30 | 5 | 66 | 0 | 92 | 3 | 0 | 29 | 0 | 81 | 19 | 0 | 32 | 37 | 1 | 93 | 6 |
| GQ-2a | 39 | 7 | 54 | 1 | 94 | 2 | 1 | 38 | 3 | 79 | 18 | 2 | 42 | 56 | 3 | 94 | 3 |
| GQ-6a | 36 | 7 | 57 | 1 | 94 | 1 | 1 | 35 | 2 | 79 | 19 | 1 | 39 | 60 | 2 | 96 | 1 |
| GQ-7 | 34 | 3 | 63 | 0 | 92 | 2 | 2 | 33 | 4 | 82 | 14 | 2 | 36 | 63 | 5 | 92 | 4 |
| ASF-6 | 38 | 21 | 41 | 0 | 92 | 6 | 2 | 36 | 3 | 61 | 36 | 2 | 48 | 50 | 4 | 90 | 6 |
| ASF-9 | 28 | 4 | 67 | 0 | 96 | 2 | 0 | 28 | 0 | 85 | 15 | 0 | 30 | 70 | 0 | 96 | 4 |
| PL-U UA2 5721 | 32 | 8 | 60 | 0 | 95 | 2 | 2 | 15 | 7 | 50 | 43 | 2 | 18 | 80 | 10 | 75 | 15 |
| LL-2 U4 | 27 | 11 | 61 | 0 | 91 | 4 | 2 | 30 | 4 | 76 | 20 | 2 | 34 | 64 | 5 | 91 | 4 |
| Hell Canyon 05704 | 24 | 10 | 66 | 0 | 94 | 1 | 1 | 26 | 2 | 66 | 32 | 1 | 32 | 67 | 3 | 88 | 9 |
| S. Powerline 5713 | 17 | 13 | 71 | 0 | 94 | 4 | 1 | 23 | 2 | 66 | 33 | 1 | 27 | 72 | 3 | 95 | 3 |
| Mean±1σ | 31±6 | 9±5 | 60±7 | 0 | 92±4 | 3±1 | 1±1 | 30±6 | 3±2 | 71±12 | 26±11 | 1±1 | 35±7 | 64±8 | 4±3 | 91±5 | 5±3 |

Appendix B9. Recalculated detrital parameters for (in percent) gravel of the eastern-margin piedmont lithofacies assemblage (Sierra Ladrones Formation) in the northern Albuquerque Basin study area. Recalculated from point count data in Appendix B4 (n=7).

| Sample | %Q | QFL | | %Lm | LvLvLs | | QcQq | | QcQqPm | | QcQqV | | QcQqS | | | | |
|----------------|-------------|-------------|-------------|------------|------------|-------------|------------|------------|------------|--------------|--------------|--------------|--------------|--------------|------------|-------------|-------------|
| | | %F | %L | | %Lv | %Ls | %Qc | %Qq | %Qc | %Qq | %V | %Qc | %Qq | %S | | | |
| TQA-6 | 15 | 22 | 63 | 4 | 3 | 89 | 6 | 9 | 14 | 23 | 62 | 34 | 55 | 11 | 8 | 13 | 78 |
| GQ-13 | 21 | 13 | 66 | 1 | 6 | 91 | 5 | 15 | 16 | 43 | 41 | 22 | 61 | 17 | 7 | 18 | 75 |
| ASF-4 | 16 | 15 | 69 | 1 | 9 | 89 | 3 | 13 | 10 | 42 | 49 | 14 | 59 | 27 | 4 | 17 | 79 |
| RC-2 | 7 | 18 | 75 | 3 | 3 | 93 | 2 | 5 | 6 | 19 | 75 | 19 | 58 | 22 | 2 | 7 | 91 |
| RC-4 | 8 | 23 | 69 | 3 | 3 | 92 | 1 | 7 | 3 | 21 | 76 | 9 | 70 | 21 | 1 | 10 | 89 |
| RC-8 | 7 | 20 | 73 | 2 | 18 | 77 | 1 | 6 | 2 | 22 | 76 | 3 | 30 | 67 | 1 | 10 | 89 |
| RC-11 | 9 | 13 | 78 | 1 | 23 | 73 | 1 | 8 | 5 | 35 | 60 | 4 | 29 | 67 | 2 | 12 | 87 |
| Mean±1σ | 11±6 | 17±4 | 72±6 | 3±2 | 9±8 | 87±8 | 3±2 | 9±4 | 8±5 | 29±10 | 63±14 | 15±11 | 52±16 | 33±24 | 4±3 | 12±4 | 84±6 |

Appendix C1. Detrital modes of medium-grained sand for the Arroyo Ojito Formation (To), including the Navajo Draw (Ton), Loma Barbon (Tob) and Ceja (Toc) members, and Cerro Conejo Member (Tzc) of the Zia Formation, northern Albuquerque Basin study area. See Table 1 for description of compositional abbreviations.

| Unit | Sample | Qm | Qp | P | K | gn | Qv | Pv | Vg | Qs | Qc | Fs | Sc | S | M | Opg | U | Total |
|------|--------|-----|----|----|----|----|----|----|----|----|----|----|----|---|----|-----|---|-------|
| Tob | SFP-3a | 225 | 16 | 32 | 62 | 21 | 0 | 4 | 25 | 0 | 4 | 0 | 0 | 3 | 2 | 2 | 4 | 400 |
| Tob | SFP-5 | 266 | 8 | 35 | 42 | 0 | 0 | 1 | 25 | 0 | 1 | 0 | 0 | 0 | 4 | 14 | 4 | 400 |
| Tob | SFP-12 | 225 | 5 | 29 | 45 | 10 | 0 | 4 | 55 | 0 | 11 | 0 | 0 | 0 | 10 | 4 | 2 | 400 |
| Tob | SFP-13 | 243 | 15 | 15 | 49 | 17 | 0 | 1 | 39 | 0 | 15 | 0 | 0 | 0 | 1 | 2 | 3 | 400 |
| Tzcc | M-2 | 230 | 14 | 18 | 50 | 12 | 0 | 5 | 50 | 1 | 19 | 0 | 0 | 1 | 0 | 0 | 0 | 400 |
| Ton | M-4 | 226 | 12 | 24 | 32 | 15 | 1 | 8 | 62 | 0 | 18 | 0 | 0 | 0 | 0 | 1 | 1 | 400 |
| Ton | M-11 | 230 | 7 | 14 | 53 | 18 | 2 | 5 | 49 | 1 | 15 | 0 | 0 | 1 | 0 | 3 | 2 | 400 |
| Ton | M-13 | 210 | 9 | 17 | 48 | 13 | 5 | 6 | 61 | 0 | 27 | 0 | 0 | 0 | 0 | 2 | 2 | 400 |
| Ton | M-15 | 236 | 15 | 24 | 41 | 6 | 3 | 5 | 52 | 0 | 16 | 0 | 0 | 1 | 0 | 0 | 1 | 400 |
| Ton | M-17 | 232 | 15 | 23 | 29 | 13 | 5 | 9 | 58 | 1 | 12 | 0 | 0 | 0 | 0 | 2 | 1 | 400 |
| Ton | M-18 | 203 | 15 | 28 | 38 | 10 | 2 | 7 | 71 | 1 | 20 | 0 | 0 | 1 | 0 | 3 | 1 | 400 |
| Ton | Z-A | 227 | 17 | 36 | 34 | 8 | 3 | 7 | 49 | 0 | 13 | 0 | 0 | 1 | 1 | 3 | 1 | 400 |
| Ton | Z-1 | 227 | 4 | 36 | 41 | 8 | 1 | 1 | 51 | 0 | 23 | 0 | 0 | 0 | 0 | 4 | 4 | 400 |
| Tob | Z-3 | 196 | 16 | 31 | 52 | 15 | 1 | 4 | 59 | 0 | 21 | 0 | 0 | 1 | 0 | 1 | 3 | 400 |
| Tob | Z-4 | 209 | 12 | 29 | 52 | 14 | 0 | 3 | 68 | 1 | 8 | 0 | 0 | 1 | 0 | 1 | 2 | 400 |
| Tob | Z-5 | 219 | 10 | 30 | 48 | 9 | 0 | 6 | 52 | 0 | 21 | 0 | 0 | 1 | 1 | 1 | 2 | 400 |
| Tob | Z-6a | 171 | 11 | 36 | 51 | 11 | 1 | 11 | 86 | 2 | 13 | 0 | 0 | 3 | 2 | 0 | 2 | 400 |
| Tob | Z-7 | 204 | 14 | 28 | 50 | 11 | 0 | 3 | 74 | 0 | 13 | 0 | 0 | 0 | 0 | 2 | 1 | 400 |
| Tob | Z-8 | 230 | 6 | 20 | 41 | 5 | 1 | 1 | 77 | 0 | 13 | 0 | 0 | 0 | 4 | 2 | 0 | 400 |
| Tob | LC-1 | 196 | 13 | 35 | 50 | 8 | 1 | 9 | 71 | 3 | 10 | 0 | 0 | 1 | 0 | 2 | 1 | 400 |
| Tob | LC-2a | 173 | 5 | 37 | 44 | 14 | 2 | 13 | 86 | 2 | 10 | 0 | 0 | 3 | 4 | 3 | 4 | 400 |
| Toc | LC-4 | 188 | 16 | 48 | 32 | 18 | 0 | 7 | 72 | 0 | 13 | 0 | 0 | 1 | 1 | 1 | 3 | 400 |
| Toc | LC-5 | 183 | 12 | 37 | 42 | 18 | 3 | 9 | 81 | 0 | 13 | 0 | 0 | 0 | 1 | 1 | 3 | 400 |
| Toc | LC-6 | 174 | 14 | 44 | 44 | 12 | 2 | 8 | 87 | 0 | 9 | 0 | 0 | 0 | 2 | 1 | 3 | 400 |

Appendix C1. Detrital modes of medium-grained sand for the Arroyo Ojito Formation (To), including the Navajo Draw (Ton), Loma Barbon (Tob) and Ceja (Toc) members, and Cerro Conejo Member (Tzc) of the Zia Formation, northern Albuquerque Basin study area. See Table 1 for description of compositional abbreviations. (Continued)

| Unit | Sample | Qm | Qp | P | K | gn | Qv | Pv | Vg | Qs | Qc | Fs | Sc | S | M | Opq | U | Total |
|------|----------|-----|----|----|----|----|----|----|----|----|----|----|----|---|---|-----|---|-------|
| Toc | CM1-U2 | 221 | 16 | 26 | 62 | 7 | 0 | 1 | 52 | 0 | 10 | 0 | 0 | 0 | 1 | 2 | 2 | 400 |
| Toc | MDC 0090 | 173 | 14 | 57 | 36 | 11 | 0 | 16 | 76 | 0 | 11 | 0 | 0 | 1 | 0 | 2 | 3 | 400 |
| Toc | MDC 0180 | 198 | 8 | 46 | 33 | 12 | 4 | 8 | 62 | 0 | 11 | 0 | 0 | 0 | 1 | 11 | 6 | 400 |
| Toc | MDC 0310 | 241 | 22 | 25 | 45 | 8 | 0 | 2 | 37 | 0 | 14 | 1 | 0 | 0 | 0 | 2 | 3 | 400 |
| Tob | MDC 0950 | 231 | 18 | 35 | 33 | 14 | 1 | 1 | 48 | 0 | 14 | 1 | 0 | 1 | 0 | 1 | 2 | 400 |
| Tob | MDC 1230 | 253 | 11 | 23 | 38 | 8 | 0 | 1 | 46 | 0 | 16 | 0 | 0 | 0 | 0 | 1 | 3 | 400 |
| Tob | MDC 1670 | 240 | 8 | 22 | 39 | 7 | 0 | 5 | 54 | 2 | 17 | 0 | 0 | 1 | 0 | 3 | 2 | 400 |
| Tob | MDC 1990 | 252 | 7 | 27 | 35 | 7 | 0 | 2 | 47 | 1 | 18 | 0 | 0 | 1 | 0 | 0 | 3 | 400 |
| Toc | ER-1 | 174 | 3 | 58 | 49 | 4 | 1 | 7 | 89 | 0 | 8 | 0 | 0 | 1 | 1 | 1 | 4 | 400 |

Appendix C2. Detrital modes of medium-grained sand for the ancestral Rio Grande deposits (QTsa) of the Sierra Ladrones Formation, northern Albuquerque Basin study area. See Table 1 for description of compositional abbreviations.

| Unit | Sample | Qm | Qp | P | K | gn | Qv | Pv | Vg | Qs | Qc | Fs | Sc | S | M | Opq | U | Total |
|-------|----------|-----|----|----|----|----|----|----|-----|----|----|----|----|---|---|-----|---|-------|
| QTsa | SFP-6a | 198 | 14 | 25 | 48 | 9 | 0 | 19 | 70 | 0 | 2 | 0 | 0 | 0 | 4 | 6 | 5 | 400 |
| QTsa | SFP-9b | 200 | 15 | 34 | 53 | 8 | 6 | 16 | 60 | 0 | 3 | 0 | 0 | 0 | 0 | 3 | 2 | 400 |
| QTsa | SFP-11 | 200 | 14 | 27 | 39 | 3 | 1 | 28 | 80 | 0 | 2 | 0 | 0 | 0 | 2 | 0 | 4 | 400 |
| QTsa | SFP-14 | 230 | 8 | 20 | 32 | 2 | 0 | 3 | 77 | 0 | 7 | 0 | 0 | 0 | 7 | 11 | 3 | 400 |
| QTsa | TQA-1b | 192 | 21 | 19 | 34 | 8 | 0 | 19 | 88 | 0 | 5 | 0 | 0 | 3 | 2 | 5 | 4 | 400 |
| QTsa | TQA-4 | 157 | 12 | 34 | 31 | 5 | 4 | 8 | 128 | 0 | 5 | 0 | 0 | 0 | 9 | 4 | 3 | 400 |
| QTsa | GQ-1 | 217 | 22 | 42 | 29 | 5 | 0 | 8 | 62 | 0 | 1 | 0 | 0 | 0 | 2 | 1 | 2 | 400 |
| QTsa | GQ-5 | 206 | 17 | 57 | 51 | 4 | 0 | 9 | 50 | 0 | 1 | 0 | 0 | 0 | 2 | 1 | 2 | 400 |
| QTsa | LL-2-U4 | 230 | 10 | 31 | 41 | 10 | 2 | 4 | 60 | 0 | 9 | 0 | 0 | 0 | 1 | 0 | 1 | 400 |
| QTsa | HC-L1-U1 | 198 | 16 | 20 | 53 | 11 | 1 | 7 | 80 | 0 | 5 | 0 | 0 | 1 | 2 | 1 | 5 | 400 |
| QTsa | 05703 | 199 | 8 | 36 | 43 | 5 | 1 | 14 | 78 | 1 | 6 | 0 | 0 | 0 | 3 | 3 | 3 | 400 |
| QTsa | 05704 | 190 | 8 | 38 | 57 | 6 | 0 | 10 | 83 | 0 | 2 | 0 | 0 | 0 | 2 | 1 | 3 | 400 |
| QTsa | 05707 | 189 | 8 | 40 | 57 | 4 | 2 | 7 | 79 | 0 | 6 | 0 | 0 | 0 | 2 | 4 | 2 | 400 |
| QTsa | 05709 | 193 | 7 | 39 | 48 | 8 | 1 | 4 | 87 | 0 | 6 | 0 | 0 | 0 | 0 | 2 | 5 | 400 |
| QTsa | 5710 | 197 | 5 | 43 | 42 | 8 | 2 | 9 | 82 | 0 | 9 | 0 | 0 | 0 | 0 | 0 | 3 | 400 |
| QTsa | 5711 | 197 | 5 | 46 | 48 | 3 | 2 | 4 | 80 | 0 | 7 | 0 | 0 | 1 | 2 | 1 | 4 | 400 |
| QTsa | 5714 | 194 | 9 | 35 | 31 | 6 | 3 | 7 | 98 | 2 | 8 | 0 | 0 | 0 | 2 | 1 | 4 | 400 |
| QTsa | 5715 | 198 | 13 | 34 | 51 | 7 | 0 | 4 | 88 | 0 | 2 | 0 | 0 | 0 | 0 | 2 | 1 | 400 |
| QTsa | PV-2b | 206 | 8 | 30 | 42 | 5 | 1 | 4 | 85 | 1 | 8 | 0 | 0 | 0 | 3 | 2 | 5 | 400 |
| QTsa? | MAT 1335 | 255 | 5 | 29 | 42 | 12 | 0 | 0 | 45 | 0 | 5 | 0 | 0 | 0 | 2 | 0 | 4 | 400 |
| QTsa? | MAT 1390 | 238 | 11 | 36 | 44 | 1 | 0 | 2 | 57 | 0 | 4 | 0 | 0 | 0 | 0 | 3 | 3 | 400 |
| QTsa? | MAT 1420 | 206 | 4 | 33 | 53 | 8 | 1 | 3 | 82 | 0 | 6 | 0 | 0 | 0 | 0 | 1 | 3 | 400 |
| QTsa? | MAT 1545 | 207 | 9 | 50 | 44 | 6 | 0 | 9 | 66 | 0 | 2 | 0 | 0 | 0 | 1 | 3 | 3 | 400 |

Appendix C3. Detrital modes of medium-grained sand for the piedmont deposits (QTsp) of the Sierra Ladrones Formation, northern Albuquerque Basin study area. See Table 1 for description of compositional abbreviations.

| Unit | Sample | Qm | Qp | P | K | gn | Qv | Pv | Vg | Qs | Qc | Fs | Sc | S | M | Opq | U | Total |
|------|----------|-----|----|-----|----|-----|----|----|----|----|----|----|----|----|----|-----|---|-------|
| QTsp | GQ-12a | 245 | 20 | 41 | 26 | 21 | 0 | 0 | 16 | 0 | 5 | 0 | 0 | 12 | 2 | 8 | 4 | 400 |
| QTsp | ASF-5 | 216 | 21 | 42 | 33 | 58 | 0 | 0 | 9 | 1 | 8 | 1 | 0 | 3 | 0 | 5 | 3 | 400 |
| QTsp | RC-2a | 224 | 32 | 41 | 26 | 35 | 0 | 0 | 7 | 0 | 11 | 0 | 0 | 10 | 8 | 3 | 3 | 400 |
| QTsp | RC-7 | 305 | 23 | 13 | 10 | 27 | 0 | 0 | 2 | 0 | 0 | 0 | 0 | 8 | 1 | 10 | 1 | 400 |
| QTsp | PV-5b | 153 | 11 | 81 | 54 | 33 | 0 | 0 | 7 | 5 | 3 | 0 | 0 | 0 | 39 | 8 | 6 | 400 |
| QTsp | AS-1b | 246 | 7 | 29 | 32 | 20 | 0 | 0 | 7 | 9 | 13 | 1 | 0 | 7 | 2 | 21 | 6 | 400 |
| QTsp | MAT 0040 | 112 | 15 | 101 | 54 | 103 | 0 | 0 | 0 | 2 | 0 | 0 | 0 | 0 | 6 | 0 | 7 | 400 |
| QTsp | MAT 0090 | 169 | 2 | 70 | 69 | 28 | 0 | 0 | 2 | 0 | 3 | 0 | 0 | 0 | 34 | 19 | 4 | 400 |
| QTsp | MAT 0145 | 169 | 12 | 80 | 74 | 35 | 0 | 0 | 3 | 0 | 1 | 0 | 0 | 0 | 13 | 8 | 5 | 400 |
| QTsp | MAT 0270 | 173 | 3 | 93 | 70 | 22 | 0 | 0 | 3 | 0 | 1 | 0 | 0 | 1 | 8 | 22 | 4 | 400 |
| QTsp | MAT 0320 | 177 | 4 | 72 | 72 | 37 | 0 | 0 | 4 | 0 | 2 | 0 | 2 | 0 | 10 | 16 | 4 | 400 |
| QTsp | MAT 0630 | 161 | 3 | 101 | 54 | 39 | 0 | 0 | 0 | 0 | 0 | 0 | 0 | 0 | 31 | 7 | 4 | 400 |
| QTsp | MAT 0790 | 174 | 4 | 83 | 66 | 38 | 0 | 0 | 5 | 0 | 5 | 0 | 0 | 1 | 8 | 11 | 5 | 400 |
| QTsp | MAT 1050 | 254 | 8 | 37 | 39 | 29 | 0 | 0 | 18 | 0 | 8 | 0 | 0 | 0 | 2 | 1 | 4 | 400 |

Appendix C4. Percent normalized detrital modes of medium-grained sand for the ancestral Rio Grande (QTsa) and piedmont (QTsp) deposits of the Sierra Ladrones Formation, Arroyo Ojito Formation (To), including the Navajo Draw (Ton), Loma Barbon (Tob) and Ceja (Toc) members, and Cerro Conejo Member (Tzc) of the Zia Formation.

| Unit | Sample | Qm | Qp | P | K | gn | Qv | Pv | Vg | Qs | Qc | Fs | Sc | S | M | Opq |
|-----------------------|---------|-------------|------------|------------|-------------|------------|----------|------------|-------------|----------|------------|----------|----------|----------|----------|------------|
| Toc | ER-1 | 44 | 1 | 15 | 12 | 1 | 0 | 2 | 22 | 0 | 2 | 0 | 0 | 0 | 0 | 0 |
| Toc | LC-4 | 47 | 4 | 12 | 8 | 5 | 0 | 2 | 18 | 0 | 3 | 0 | 0 | 0 | 0 | 0 |
| Toc | LC-5 | 46 | 3 | 9 | 11 | 4 | 1 | 2 | 20 | 0 | 3 | 0 | 0 | 0 | 0 | 0 |
| Toc | LC-6 | 44 | 4 | 11 | 11 | 3 | 1 | 2 | 22 | 0 | 2 | 0 | 0 | 0 | 1 | 0 |
| Toc | CM1-U2 | 56 | 4 | 7 | 16 | 2 | 0 | 0 | 13 | 0 | 3 | 0 | 0 | 0 | 0 | 1 |
| Toc | MDC0090 | 44 | 4 | 14 | 9 | 3 | 0 | 4 | 19 | 0 | 3 | 0 | 0 | 0 | 0 | 1 |
| Toc | MDC0180 | 50 | 2 | 12 | 8 | 3 | 1 | 2 | 16 | 0 | 3 | 0 | 0 | 0 | 0 | 3 |
| Toc | MDC0310 | 61 | 6 | 6 | 11 | 2 | 0 | 1 | 9 | 0 | 4 | 0 | 0 | 0 | 0 | 1 |
| Tob | SFP-3a | 57 | 4 | 8 | 16 | 5 | 0 | 1 | 6 | 0 | 1 | 0 | 0 | 1 | 1 | 1 |
| Tob | SFP-5 | 67 | 2 | 9 | 11 | 0 | 0 | 0 | 6 | 0 | 0 | 0 | 0 | 0 | 1 | 4 |
| Tob | SFP-12 | 57 | 1 | 7 | 11 | 3 | 0 | 1 | 14 | 0 | 3 | 0 | 0 | 0 | 3 | 1 |
| Tob | SFP-13 | 61 | 4 | 4 | 12 | 4 | 0 | 0 | 10 | 0 | 4 | 0 | 0 | 0 | 0 | 1 |
| Tob | Z-3 | 49 | 4 | 8 | 13 | 4 | 0 | 1 | 15 | 0 | 5 | 0 | 0 | 0 | 0 | 0 |
| Tob | Z-4 | 53 | 3 | 7 | 13 | 4 | 0 | 1 | 17 | 0 | 2 | 0 | 0 | 0 | 0 | 0 |
| Tob | Z-5 | 55 | 3 | 8 | 12 | 2 | 0 | 2 | 13 | 0 | 5 | 0 | 0 | 0 | 0 | 0 |
| Tob | Z-6a | 43 | 3 | 9 | 13 | 3 | 0 | 3 | 22 | 1 | 3 | 0 | 0 | 1 | 1 | 0 |
| Tob | Z-7 | 51 | 4 | 7 | 13 | 3 | 0 | 1 | 19 | 0 | 3 | 0 | 0 | 0 | 0 | 1 |
| Tob | Z-8 | 58 | 2 | 5 | 10 | 1 | 0 | 0 | 19 | 0 | 3 | 0 | 0 | 0 | 1 | 1 |
| Tob | LC-1 | 49 | 3 | 9 | 13 | 2 | 0 | 2 | 18 | 1 | 3 | 0 | 0 | 0 | 0 | 1 |
| Tob | LC-2a | 44 | 1 | 9 | 11 | 4 | 1 | 3 | 22 | 1 | 3 | 0 | 0 | 1 | 1 | 1 |
| To? | LL-2-U4 | 58 | 3 | 8 | 10 | 3 | 1 | 1 | 15 | 0 | 2 | 0 | 0 | 0 | 0 | 0 |
| Tob | MDC0950 | 58 | 5 | 9 | 8 | 4 | 0 | 0 | 12 | 0 | 4 | 0 | 0 | 0 | 0 | 0 |
| Tob | MDC1230 | 64 | 3 | 6 | 10 | 2 | 0 | 0 | 12 | 0 | 4 | 0 | 0 | 0 | 0 | 0 |
| Tob | MDC1670 | 60 | 2 | 6 | 10 | 2 | 0 | 1 | 14 | 1 | 4 | 0 | 0 | 0 | 0 | 1 |
| Tob | MDC1990 | 63 | 2 | 7 | 9 | 2 | 0 | 1 | 12 | 0 | 5 | 0 | 0 | 0 | 0 | 0 |
| Ton | M-4 | 57 | 3 | 6 | 8 | 4 | 0 | 2 | 16 | 0 | 5 | 0 | 0 | 0 | 0 | 0 |
| Ton | M-11 | 58 | 2 | 4 | 13 | 5 | 1 | 1 | 12 | 0 | 4 | 0 | 0 | 0 | 0 | 1 |
| Ton | M-13 | 53 | 2 | 4 | 12 | 3 | 1 | 2 | 15 | 0 | 7 | 0 | 0 | 0 | 0 | 1 |
| Ton | M-15 | 59 | 4 | 6 | 10 | 2 | 1 | 1 | 13 | 0 | 4 | 0 | 0 | 0 | 0 | 0 |
| Ton | M-17 | 58 | 4 | 6 | 7 | 3 | 1 | 2 | 15 | 0 | 3 | 0 | 0 | 0 | 0 | 1 |
| Ton | M-18 | 51 | 4 | 7 | 10 | 3 | 1 | 2 | 18 | 0 | 5 | 0 | 0 | 0 | 0 | 1 |
| Ton | Z-A | 57 | 4 | 9 | 9 | 2 | 1 | 2 | 12 | 0 | 3 | 0 | 0 | 0 | 0 | 1 |
| Ton | Z-1 | 57 | 1 | 9 | 10 | 2 | 0 | 0 | 13 | 0 | 6 | 0 | 0 | 0 | 0 | 1 |
| Tzcc | M-2 | 58 | 4 | 5 | 13 | 3 | 0 | 1 | 13 | 0 | 5 | 0 | 0 | 0 | 0 | 0 |
| Mean (n= 33) ± | | 54±6 | 3±1 | 8±3 | 11±2 | 3±1 | 0 | 1±1 | 15±4 | 0 | 3±1 | 0 | 0 | 0 | 0 | 1±0 |
| 1σ | | | | | | | | | | | | | | | | |

Appendix C4. . Percent normalized detrital modes of medium-grained sand for the ancestral Rio Grande (QTsa) and piedmont (QTsp) deposits of the Sierra Ladrones Formation, Arroyo Ojito Formation (To), including the Navajo Draw (Ton), Loma Barbon (Tob) and Ceja (Toc) members, and Cerro Conejo Member (Tzc) of the Zia Formation. (Continued)

| Unit | Sample | Qm | Qp | P | K | gn | Qv | Pv | Vg | Qs | Qc | Fs | Sc | S | M | Opg |
|-------|-----------------|-------------|------------|------------|-------------|------------|----------|------------|-------------|----------|------------|----------|----------|----------|------------|------------|
| QTsa | SFP-6a | 50 | 4 | 6 | 12 | 2 | 0 | 5 | 18 | 0 | 1 | 0 | 0 | 0 | 1 | 2 |
| QTsa | SFP-9b | 50 | 4 | 9 | 13 | 2 | 2 | 4 | 15 | 0 | 1 | 0 | 0 | 0 | 0 | 1 |
| QTsa | SFP-11 | 50 | 4 | 7 | 10 | 1 | 0 | 7 | 20 | 0 | 1 | 0 | 0 | 0 | 1 | 0 |
| QTsa | SFP-14 | 58 | 2 | 5 | 8 | 1 | 0 | 1 | 19 | 0 | 2 | 0 | 0 | 0 | 2 | 3 |
| QTsa | TQA-1b | 48 | 5 | 5 | 9 | 2 | 0 | 5 | 22 | 0 | 1 | 0 | 0 | 1 | 1 | 1 |
| QTsa | TQA-4 | 40 | 3 | 9 | 8 | 1 | 1 | 2 | 32 | 0 | 1 | 0 | 0 | 0 | 2 | 1 |
| QTsa | GQ-1 | 55 | 6 | 11 | 7 | 1 | 0 | 2 | 16 | 0 | 0 | 0 | 0 | 0 | 1 | 0 |
| QTsa | GQ-5 | 52 | 4 | 14 | 13 | 1 | 0 | 2 | 13 | 0 | 0 | 0 | 0 | 0 | 1 | 0 |
| QTsa | HC-L1U1 | 50 | 4 | 5 | 13 | 3 | 0 | 2 | 20 | 0 | 1 | 0 | 0 | 0 | 1 | 0 |
| QTsa | 5703 | 50 | 2 | 9 | 11 | 1 | 0 | 4 | 20 | 0 | 2 | 0 | 0 | 0 | 1 | 1 |
| QTsa | 5704 | 48 | 2 | 10 | 14 | 2 | 0 | 3 | 21 | 0 | 1 | 0 | 0 | 0 | 1 | 0 |
| QTsa | 5707 | 47 | 2 | 10 | 14 | 1 | 1 | 2 | 20 | 0 | 2 | 0 | 0 | 0 | 1 | 1 |
| QTsa | 5709 | 48 | 2 | 10 | 12 | 2 | 0 | 1 | 22 | 0 | 2 | 0 | 0 | 0 | 0 | 1 |
| QTsa | 5710 | 49 | 1 | 11 | 11 | 2 | 1 | 2 | 21 | 0 | 2 | 0 | 0 | 0 | 0 | 0 |
| QTsa | 5711 | 49 | 1 | 12 | 12 | 1 | 1 | 1 | 20 | 0 | 2 | 0 | 0 | 0 | 1 | 0 |
| QTsa | 5714 | 49 | 2 | 9 | 8 | 2 | 1 | 2 | 25 | 1 | 2 | 0 | 0 | 0 | 1 | 0 |
| QTsa | 5715 | 50 | 3 | 9 | 13 | 2 | 0 | 1 | 22 | 0 | 1 | 0 | 0 | 0 | 0 | 1 |
| QTsa | PV-2b | 52 | 2 | 8 | 11 | 1 | 0 | 1 | 21 | 0 | 2 | 0 | 0 | 0 | 1 | 1 |
| QTsa? | MAT1335 | 65 | 1 | 7 | 11 | 3 | 0 | 0 | 11 | 0 | 1 | 0 | 0 | 0 | 1 | 0 |
| QTsa? | MAT1390 | 60 | 3 | 9 | 11 | 0 | 0 | 1 | 14 | 0 | 1 | 0 | 0 | 0 | 0 | 1 |
| QTsa? | MAT1420 | 52 | 1 | 8 | 13 | 2 | 0 | 1 | 21 | 0 | 2 | 0 | 0 | 0 | 0 | 0 |
| QTsa? | MAT1545 | 52 | 2 | 13 | 11 | 2 | 0 | 2 | 17 | 0 | 1 | 0 | 0 | 0 | 0 | 1 |
| | Mean | 52±5 | 3±1 | 9±2 | 11±2 | 2±1 | 0 | 2±2 | 19±4 | 0 | 1±1 | 0 | 0 | 0 | 1±1 | 1±1 |
| | (n=22) ± | | | | | | | | | | | | | | | |
| | 1σ | | | | | | | | | | | | | | | |

Appendix C4. . Percent normalized detrital modes of medium-grained sand for the ancestral Rio Grande (QTsa) and piedmont (QTsp) deposits of the Sierra Ladrones Formation, Arroyo Ojito Formation (To), including the Navajo Draw (Ton), Loma Barbon (Tob) and Ceja (Toc) members, and Cerro Conejo Member (Tzc) of the Zia Formation. (Continued)

| Unit | Sample | Qm | Qp | P | K | gn | Qv | Pv | Vg | Qs | Qc | Fs | Sc | S | M | Opq |
|------|-------------------|------------|------------|-----------|-------------|------------|----------|----------|------------|----------|------------|----------|----------|------------|------------|------------|
| QTsp | GQ-12a | 62 | 5 | 10 | 7 | 5 | 0 | 0 | 4 | 0 | 1 | 0 | 0 | 3 | 1 | 2 |
| QTsp | ASF-5 | 54 | 5 | 11 | 8 | 15 | 0 | 0 | 2 | 0 | 2 | 0 | 0 | 1 | 0 | 1 |
| QTsp | RC-2a | 56 | 8 | 10 | 7 | 9 | 0 | 0 | 2 | 0 | 3 | 0 | 0 | 3 | 2 | 1 |
| QTsp | RC-7 | 76 | 6 | 3 | 3 | 7 | 0 | 0 | 1 | 0 | 0 | 0 | 0 | 2 | 0 | 3 |
| QTsp | PV-5b | 39 | 3 | 20 | 14 | 8 | 0 | 0 | 2 | 1 | 1 | 0 | 0 | 0 | 10 | 2 |
| QTsp | AS-1b | 62 | 2 | 7 | 8 | 5 | 0 | 0 | 2 | 2 | 3 | 0 | 0 | 2 | 1 | 5 |
| QTsp | MAT0040 | 28 | 4 | 25 | 14 | 26 | 0 | 0 | 0 | 1 | 0 | 0 | 0 | 0 | 2 | 0 |
| QTsp | MAT0090 | 43 | 1 | 18 | 17 | 7 | 0 | 0 | 1 | 0 | 1 | 0 | 0 | 0 | 9 | 5 |
| QTsp | MAT0145 | 43 | 3 | 20 | 19 | 9 | 0 | 0 | 1 | 0 | 0 | 0 | 0 | 0 | 3 | 2 |
| QTsp | MAT0270 | 44 | 1 | 23 | 18 | 6 | 0 | 0 | 1 | 0 | 0 | 0 | 0 | 0 | 2 | 6 |
| QTsp | MAT0320 | 45 | 1 | 18 | 18 | 9 | 0 | 0 | 1 | 0 | 1 | 0 | 1 | 0 | 3 | 4 |
| QTsp | MAT0630 | 41 | 1 | 25 | 14 | 10 | 0 | 0 | 0 | 0 | 0 | 0 | 0 | 0 | 8 | 2 |
| QTsp | MAT0790 | 44 | 1 | 21 | 17 | 10 | 0 | 0 | 1 | 0 | 1 | 0 | 0 | 0 | 2 | 3 |
| QTsp | MAT1050 | 64 | 2 | 9 | 10 | 7 | 0 | 0 | 5 | 0 | 2 | 0 | 0 | 0 | 1 | 0 |
| | Mean | 50± | 3±2 | 16 | 12±5 | 9±5 | 0 | 0 | 1±1 | 0 | 1±1 | 0 | 0 | 1±1 | 3±3 | 3±2 |
| | (n=14) ±1σ | 13 | | | ±7 | | | | | | | | | | | |

Appendix C5. Recalculated detrital parameters (in percent) of medium-grained sand, Arroyo Ojito Formation (n=32).

| Sample | QFL | | | LmLvLs | | | QcGnV | | |
|----------------|-------------|-------------|-------------|----------|-------------|------------|-------------|-------------|-------------|
| | %Q | %F | %L | %Lm | %Lv | %Ls | %Qc | %Gn | %V |
| SFP-3a | 62 | 30 | 8 | 0 | 89 | 11 | 8 | 42 | 50 |
| SFP-5 | 72 | 20 | 8 | 0 | 100 | 0 | 4 | 0 | 96 |
| SFP-12 | 62 | 23 | 15 | 0 | 100 | 0 | 14 | 13 | 72 |
| SFP-13 | 69 | 21 | 11 | 0 | 100 | 0 | 21 | 24 | 55 |
| M-4 | 64 | 20 | 16 | 0 | 100 | 0 | 19 | 16 | 65 |
| M-11 | 64 | 23 | 13 | 0 | 98 | 2 | 18 | 22 | 60 |
| M-13 | 63 | 21 | 16 | 0 | 100 | 0 | 27 | 13 | 60 |
| M-15 | 68 | 19 | 14 | 0 | 98 | 2 | 22 | 8 | 70 |
| M-17 | 67 | 19 | 15 | 0 | 100 | 0 | 14 | 16 | 70 |
| M-18 | 61 | 21 | 18 | 0 | 99 | 1 | 20 | 10 | 70 |
| Z-A | 66 | 22 | 13 | 0 | 98 | 2 | 19 | 11 | 70 |
| Z-1 | 64 | 22 | 14 | 0 | 100 | 0 | 28 | 10 | 62 |
| Z-3 | 59 | 26 | 16 | 0 | 98 | 2 | 22 | 16 | 62 |
| Z-4 | 58 | 25 | 18 | 0 | 99 | 1 | 9 | 16 | 76 |
| Z-5 | 63 | 23 | 14 | 0 | 98 | 2 | 26 | 11 | 63 |
| Z-6a | 50 | 27 | 23 | 0 | 97 | 3 | 12 | 10 | 78 |
| Z-7 | 58 | 23 | 19 | 0 | 100 | 0 | 13 | 11 | 7 |
| Z-8 | 64 | 17 | 20 | 0 | 100 | 0 | 14 | 5 | 81 |
| LC-1 | 56 | 26 | 18 | 0 | 99 | 1 | 11 | 9 | 80 |
| LC-2a | 49 | 28 | 24 | 0 | 97 | 3 | 9 | 13 | 78 |
| LC-4 | 55 | 26 | 19 | 0 | 99 | 1 | 13 | 17 | 70 |
| LC-5 | 53 | 26 | 21 | 0 | 100 | 0 | 12 | 16 | 72 |
| LC-6 | 50 | 27 | 23 | 0 | 100 | 0 | 8 | 11 | 81 |
| CM1-U2 | 62 | 24 | 14 | 0 | 100 | 0 | 14 | 10 | 75 |
| MDC 0090 | 50 | 26 | 28 | 0 | 99 | 1 | 11 | 11 | 78 |
| MDC 0180 | 57 | 26 | 18 | 0 | 100 | 0 | 13 | 14 | 73 |
| MDC 0310 | 70 | 20 | 10 | 0 | 100 | 0 | 24 | 14 | 63 |
| MDC 0950 | 66 | 21 | 13 | 0 | 98 | 2 | 18 | 18 | 63 |
| MDC 1230 | 70 | 18 | 12 | 0 | 100 | 0 | 23 | 11 | 66 |
| MDC 1670 | 67 | 18 | 14 | 0 | 98 | 2 | 22 | 9 | 69 |
| MDC 1990 | 70 | 18 | 13 | 0 | 98 | 2 | 25 | 10 | 65 |
| ER-1 | 47 | 30 | 24 | 0 | 99 | 1 | 8 | 4 | 88 |
| Mean±1σ | 61±7 | 23±4 | 16±5 | 0 | 99±2 | 1±2 | 16±6 | 13±7 | 70±9 |

Appendix C6. Recalculated detrital parameters (in percent) of medium-grained sand, ancestral Rio Grande deposits, Sierra Ladrones Formation (n=23).

| Sample | QFL | | | LmLvLs | | | QcGnV | | |
|----------------|-------------|-------------|-------------|----------|--------------|----------|------------|------------|-------------|
| | %Q | %F | %L | %Lm | %Lv | %Ls | %Qc | %Gn | %V |
| SFP-6a | 55 | 26 | 19 | 0 | 100 | 0 | 2 | 11 | 86 |
| SFP-9b | 56 | 28 | 16 | 0 | 100 | 0 | 4 | 11 | 85 |
| SFP-11 | 55 | 24 | 21 | 0 | 100 | 0 | 2 | 4 | 94 |
| SFP-14 | 64 | 15 | 21 | 0 | 100 | 3 | 8 | 2 | 90 |
| TQA-1b | 56 | 20 | 24 | 0 | 97 | 0 | 5 | 8 | 87 |
| TQA-4 | 46 | 20 | 34 | 0 | 100 | 0 | 4 | 4 | 93 |
| GQ-1 | 61 | 22 | 17 | 0 | 100 | 0 | 1 | 7 | 91 |
| GQ-5 | 56 | 31 | 13 | 0 | 100 | 1 | 2 | 7 | 91 |
| HC-L1-U1 | 55 | 23 | 22 | 0 | 99 | 0 | 5 | 11 | 83 |
| LL2-U4 | 63 | 22 | 16 | 0 | 100 | 0 | 11 | 13 | 76 |
| 05703 | 55 | 25 | 21 | 0 | 100 | 0 | 7 | 6 | 88 |
| 05705 | 50 | 28 | 22 | 0 | 100 | 0 | 2 | 7 | 91 |
| 05707 | 52 | 27 | 21 | 0 | 100 | 0 | 7 | 4 | 89 |
| 05709 | 52 | 25 | 23 | 0 | 100 | 0 | 6 | 8 | 86 |
| 5710 | 54 | 24 | 21 | 0 | 100 | 0 | 9 | 8 | 83 |
| 5711 | 54 | 24 | 21 | 0 | 99 | 1 | 8 | 3 | 89 |
| 5714 | 56 | 21 | 23 | 0 | 100 | 0 | 7 | 5 | 88 |
| 5715 | 54 | 24 | 22 | 0 | 100 | 0 | 2 | 7 | 91 |
| PV-2b | 56 | 20 | 23 | 0 | 100 | 0 | 8 | 5 | 87 |
| MAT 1335 | 67 | 21 | 12 | 0 | 100 | 0 | 8 | 19 | 73 |
| MAT 1390 | 64 | 21 | 15 | 0 | 100 | 0 | 6 | 2 | 92 |
| MAT 1420 | 54 | 24 | 21 | 0 | 100 | 0 | 6 | 8 | 85 |
| MAT 1545 | 55 | 28 | 17 | 0 | 100 | 0 | 3 | 8 | 89 |
| Mean±1σ | 56±5 | 24±3 | 20±5 | 0 | 100±1 | 0 | 7±3 | 7±4 | 87±5 |

Appendix C7. Recalculated detrital parameters (in percent) of medium-grained sand, piedmont deposits, Sierra Ladrone Formation (n=14).

| Sample | QFL | | | LmLvLs | | | QcGnV | | |
|----------------|--------------|--------------|------------|----------|--------------|--------------|------------|--------------|--------------|
| | %Q | %F | %L | %Lm | %Lv | %Ls | %Qc | %Gn | %V |
| GQ-12a | 69 | 23 | 8 | 0 | 57 | 43 | 12 | 50 | 38 |
| ASF-5 | 62 | 34 | 4 | 0 | 75 | 25 | 11 | 77 | 12 |
| RC-2a | 69 | 26 | 5 | 0 | 41 | 59 | 21 | 66 | 13 |
| RC-7 | 84 | 13 | 3 | 0 | 20 | 80 | 0 | 93 | 7 |
| PV-5b | 49 | 48 | 4 | 0 | 100 | 0 | 7 | 77 | 16 |
| AS-1b | 73 | 22 | 5 | 0 | 50 | 50 | 33 | 50 | 18 |
| MAT 0040 | 33 | 65 | 2 | 0 | 0 | 0 | 0 | 100 | 0 |
| MAT 0090 | 50 | 48 | 2 | 0 | 100 | 0 | 9 | 85 | 6 |
| MAT 0145 | 48 | 50 | 2 | 0 | 100 | 0 | 3 | 90 | 8 |
| MAT 0270 | 48 | 50 | 2 | 0 | 75 | 25 | 4 | 85 | 12 |
| MAT 0320 | 49 | 48 | 2 | 0 | 100 | 0 | 5 | 86 | 9 |
| MAT 0630 | 45 | 64 | 1 | 0 | 0 | 0 | 0 | 100 | 0 |
| MAT 0790 | 48 | 49 | 3 | 0 | 83 | 17 | 10 | 79 | 10 |
| MAT 1050 | 68 | 26 | 6 | 0 | 100 | 0 | 15 | 53 | 33 |
| Mean±1σ | 57±14 | 40±16 | 3±2 | 0 | 64±37 | 21±27 | 9±9 | 78±17 | 13±11 |

APPENDIX D

GRAVEL AND SAND SAMPLE LOCATIONS

Appendix D. Universal Transverse Mercator (UTM, Zone 13S, North American Datum of 1983 (NAD 83)) locations of gravel (G) and sand (S) samples from the Arroyo Ojito Formation (To) and axial-fluvial deposits of the Sierra Ladrones Formation (QTsa). Drillhole data from Metropolitan Detention Center (MDC) and Matheson Park (MAT). Asterisk (*) indicates locations based on North American Datum of 1927 (NAD 27).

| Unit | Sample | Type | Quadrangle (7.5 min.) | UTM (m) |
|-----------|----------------|------|----------------------------|------------------------------|
| To | ER-1, 2 | G, S | La Mesita Negra | N: 3,881,780 E: 329,290 |
| To | Rio Bravo | G | Albuquerque West | N: 3,876,815 E: 350,690 |
| To | Ceja 5 | G | La Mesita Negra | N: 3,884,020 E: 328,825 |
| To | Ceja 7 | G | La Mesita Negra | N: 3,884,090 E: 329,035 |
| To | Ceja 9 | G | The Volcanoes | N: 3,902,445 E: 330,390 |
| To | Ceja 10 | G | Arroyo de las Calabacillas | N: 3,904,830 E: 329,890 |
| To | Ceja 15 | G | Arroyo de las Calabacillas | N: 3,916,060 E: 330,285 |
| QTsa | LL-2 U4 (5726) | G, S | Los Lunas | N: 3,859,175 E: 348,220 |
| QTsa | HC-L1-U1 | S | Hubbell Spring | N: 3,863,740* E: 353,770* |
| To | MDC | S | La Mesita Negra | N: 3,875,100* E: 361,400* |
| QTsp/QTsa | MAT | S | Albuquerque East | N: 3,886,600* E: 361,400* |
| QTsa/QTsp | PV-2b, 5b | S | Placitas | N: 3,908,400* E: 362,500* |
| QTsp | AS-1b | S | Placitas | N: 3,909,400 E: 364,650 |

APPENDIX E: PALEOCURRENT DATA

Appendix E1. Paleocurrent azimuths measured during this study from imbricated clasts in gravel and conglomerate deposits from western margin (*To*, n=34), ancestral Rio Grande (*QTsa*, n=14), and eastern piedmont (*QTsp*, n=14) lithofacies assemblages. Orientations are rounded to the nearest 5°.

| Rio Bravo site | El Rincon site | Marillo- Zia section | Placitas Vista site | Gravel Quarry section | Arroyo San Francisco section | Red Cliffs section |
|-------------------------------|-------------------------------|-------------------------------------|------------------------------------|--------------------------------------|---|-----------------------------------|
| <i>To</i> | <i>To</i> | <i>To</i> | <i>QTsa</i> | <i>QTsa</i> | <i>QTsp</i> | <i>QTsp</i> |
| 180 | 195 | 180 | 230 | 130 | 265 | 250 |
| 170 | 175 | 140 | 240 | 140 | 300 | 265 |
| 160 | 170 | 155 | 225 | 155 | 290 | 285 |
| 165 | 190 | 165 | 210 | 165 | 310 | 290 |
| 160 | --- | 135 | --- | 165 | 260 | 295 |
| 175 | --- | 140 | --- | 180 | 260 | 330 |
| 175 | --- | 135 | --- | 180 | 305 | --- |
| 165 | --- | 160 | --- | 185 | --- | --- |
| 180 | --- | 175 | --- | 200 | --- | --- |
| 195 | --- | 160 | --- | 230 | --- | --- |
| 155 | --- | 145 | --- | --- | --- | --- |
| 150 | --- | 160 | --- | --- | --- | --- |
| 185 | --- | 170 | --- | --- | --- | --- |
| 160 | --- | 170 | --- | --- | --- | --- |
| --- | --- | 180 | --- | --- | --- | --- |
| --- | --- | 165 | --- | --- | --- | --- |

Appendix E2. Paleocurrent azimuths measured from geologic maps for western margin (To), ancestral Rio Grande (QTsa), and eastern piedmont (QTsp) lithofacies assemblages. Geologic maps used are the Albuquerque West, Arroyo de las Calabacillas, Bernalillo, Cerro Conejo, Hubbell Spring, Placitas, and San Felipe Pueblo, San Felipe Pueblo NE 7.5-minute quadrangles (Cather and Connell, 1998; Cather et al., 1997, 2001; Connell, 1998; Connell et al., 1995, 1998a; Koning et al., 1998; Koning and Personius, *in review*; Love et al., 1996). Orientations are rounded to the nearest 5°.

| To | To | To | QTsa | QTsp |
|-----|-----|-----|------|------|
| 15 | 135 | 170 | 90 | 0 |
| 60 | 135 | 170 | 135 | 15 |
| 75 | 135 | 170 | 145 | 155 |
| 80 | 140 | 172 | 145 | 165 |
| 80 | 140 | 175 | 150 | 170 |
| 85 | 140 | 180 | 190 | 170 |
| 90 | 140 | 180 | 205 | 175 |
| 90 | 140 | 180 | 205 | 185 |
| 100 | 145 | 188 | 205 | 205 |
| 103 | 145 | 190 | 215 | 210 |
| 105 | 150 | 195 | 215 | 220 |
| 107 | 150 | 195 | 215 | 250 |
| 110 | 150 | 195 | 215 | 255 |
| 115 | 150 | 200 | 225 | 255 |
| 115 | 155 | 200 | 225 | 255 |
| 120 | 155 | 200 | 225 | 255 |
| 123 | 155 | 220 | 225 | 270 |
| 125 | 155 | 223 | 235 | 270 |
| 125 | 155 | 225 | 235 | 270 |
| 125 | 160 | 230 | 245 | 270 |
| 125 | 160 | 248 | 245 | 270 |
| 125 | 165 | 250 | 245 | 275 |
| 130 | 165 | 260 | 245 | 295 |
| 130 | 170 | 265 | 250 | 295 |
| 130 | 170 | 298 | 255 | 315 |
| 135 | 170 | 305 | 260 | 320 |
| 135 | 170 | --- | 345 | 335 |
| 135 | 170 | --- | --- | 345 |

Appendix E3. Summary of paleocurrent statistics, classed in 10° intervals, determined using software program *Rosy* for Macintosh, version 2.1 (Eachran, 1991).

| Unit | Number | Vector mean azimuth | Resultant (R) |
|------|--------|------------------------|------------------|
| To | 116 | 157±8° | 0.77 |
| QTsa | 41 | 209±14° | 0.74 |
| QTsp | 42 | 271±15° | 0.69 |

$$R = (x^2 + y^2)^{1/2} / N$$

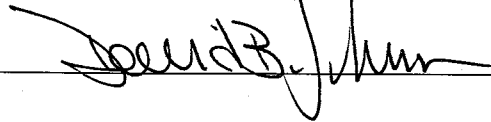
where: $x = \sum \cos \theta_i$
 $y = \sum \sin \theta_i$
 $N = \text{number of measurements}$

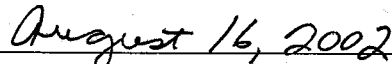
This thesis is accepted on behalf of the
Faculty of the Institute by the following committee:



Advisor

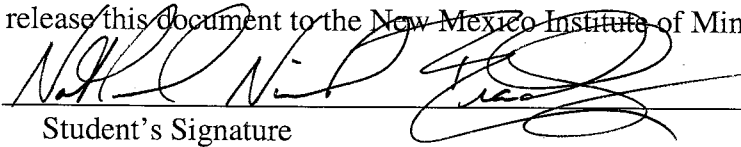




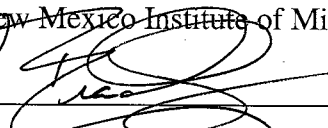


Date

I release this document to the New Mexico Institute of Mining and Technology.



Student's Signature


15 JULY 2002
Date